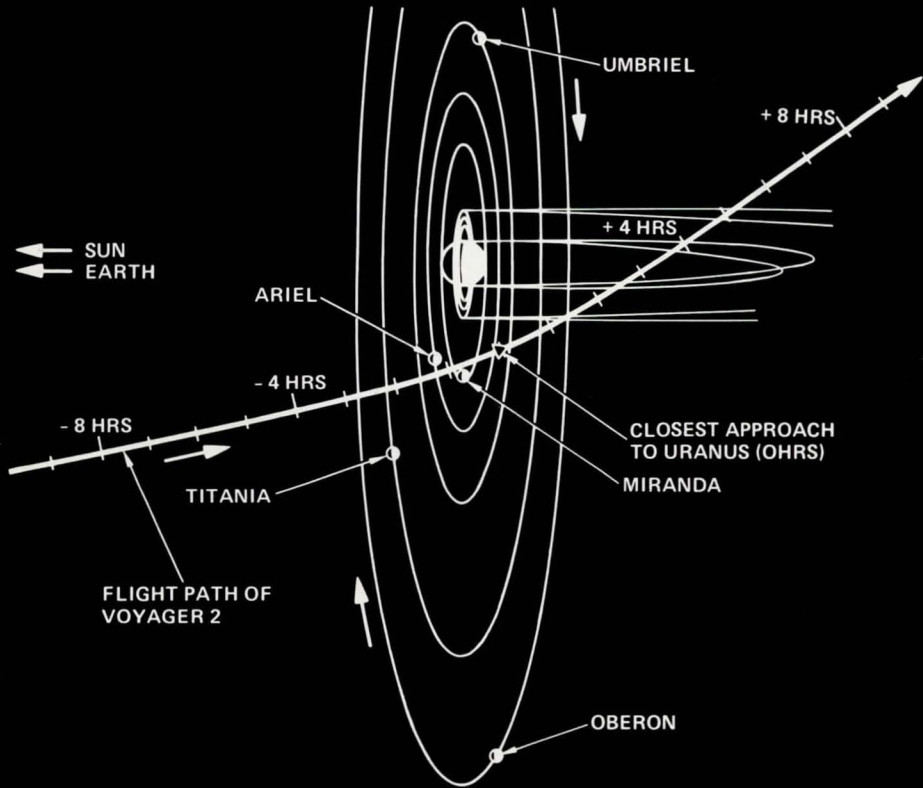


NASA Tech Briefs

National
Aeronautics and
Space
Administration

March/April 1986
Volume 10 Number 2

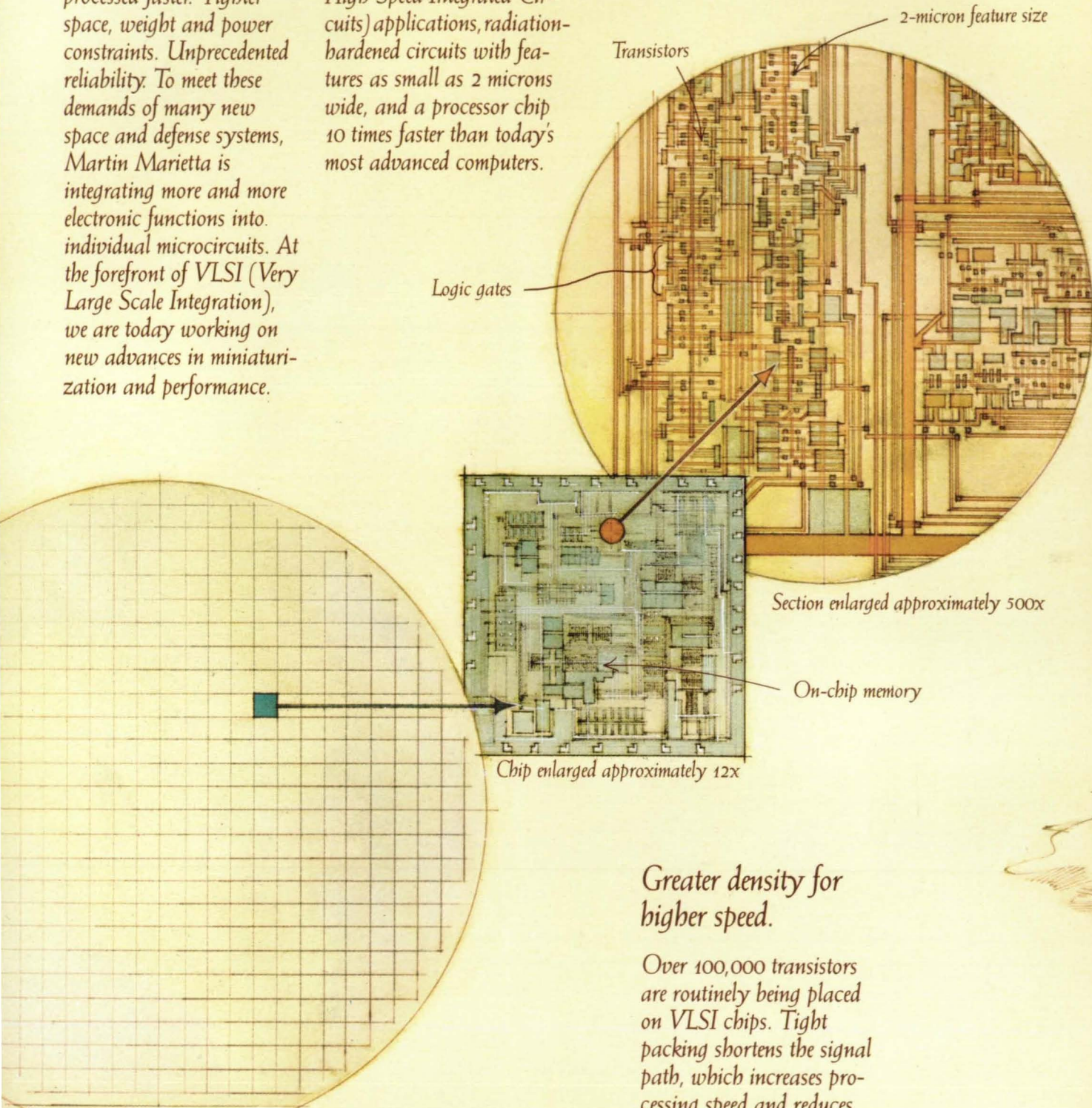
Pushing Back the Frontier: Voyager 2's Flight Past Uranus



VLSI circuits. More brainpower in less space.

Floods of data to be processed faster. Tighter space, weight and power constraints. Unprecedented reliability. To meet these demands of many new space and defense systems, Martin Marietta is integrating more and more electronic functions into individual microcircuits. At the forefront of VLSI (Very Large Scale Integration), we are today working on new advances in miniaturization and performance.

These include VHSIC (Very High Speed Integrated Circuits) applications, radiation-hardened circuits with features as small as 2 microns wide, and a processor chip 10 times faster than today's most advanced computers.



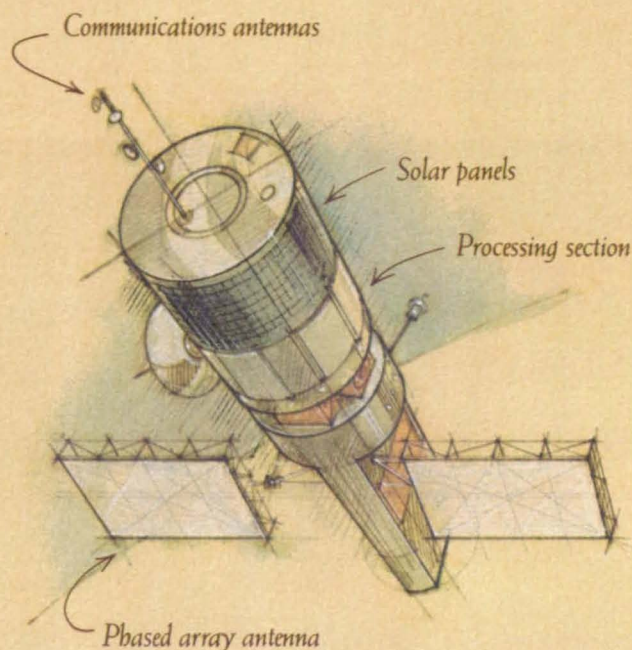
5" dia. wafer containing 430 VLSI chips

Greater density for higher speed.

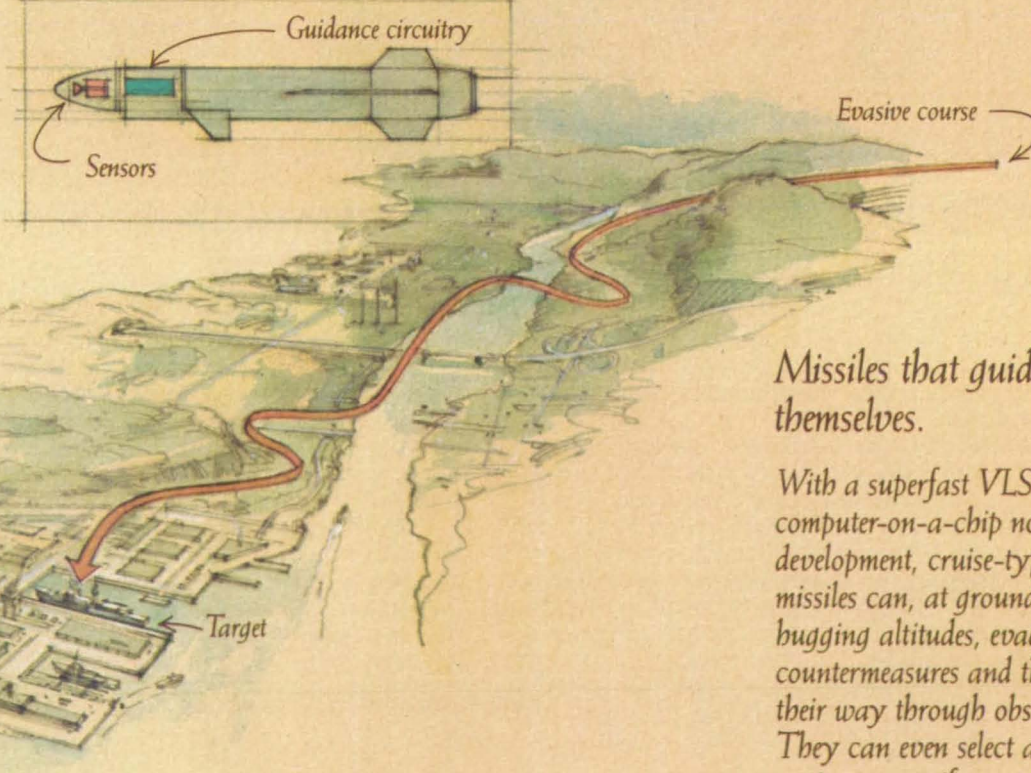
Over 100,000 transistors are routinely being placed on VLSI chips. Tight packing shortens the signal path, which increases processing speed and reduces power needs.

Defense satellites with brains.

To identify, track and inventory thousands of objects in space, satellites will need radiation-hardened circuits capable of billions of operations per second. They'll be vital for such functions as battle management, communications, damage assessment, aiming and pointing.



Smart cruise missile



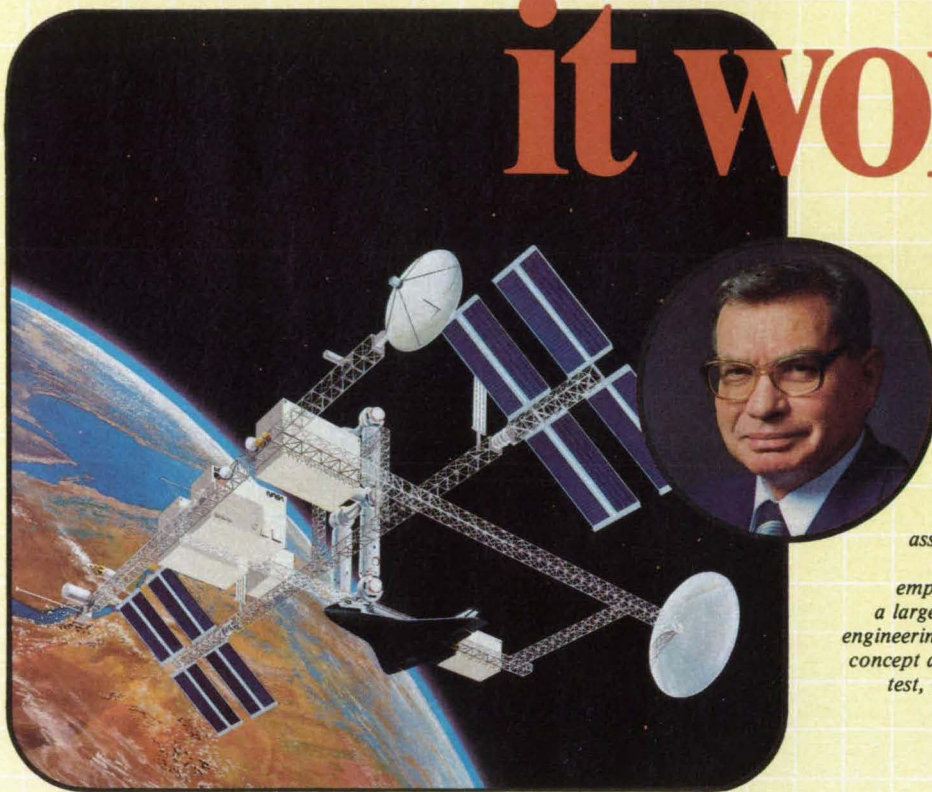
Missiles that guide themselves.

With a superfast VLSI computer-on-a-chip now in development, cruise-type missiles can, at ground-bugging altitudes, evade countermeasures and thread their way through obstacles. They can even select alternative targets if necessary.

MARTIN MARIETTA

Martin Marietta Corporation
6801 Rockledge Drive, Bethesda, Maryland 20817, USA

Making sure it works



"We provide the engineering and management assistance required for successful space operations. With 6,000 employees worldwide, we comprise a large experience base for aerospace engineering and operations, from system concept and design through integration, test, launch, and mission support."

Harry Clark
Space Operations Manager

The Space Transportation System must! Vitro Aerospace Systems Engineering

This Vitro experience accounts for much of our success in helping NASA meet the complex demands of the space transportation system and space station.

The Vitro staff has the experience, knowledge, skill, and familiarity with space systems hardware, software, management, and operations to provide effective overall program integration. Their aerospace engineering, management, and operations experience includes commercial and government space launch vehicles, payloads, and launch and mission operations systems and facilities.

In addition to expertise in aerospace engineering, management, and operations, Vitro has developed a comprehensive array of supporting technical skills. These include software development, maintenance and maintainability planning, information management, and logistic support.

Vitro meets mission requirements on time and within budget. We stand ready to meet your aerospace needs with our experience, teamwork, flexibility, and rapid response...to continue a tradition of engineering excellence.

Vitro Turning Today's
Technologies
Into Tomorrow's Systems
CORPORATION

14000 Georgia Avenue, Silver Spring, Maryland 20910
For information call our Marketing Manager, (301) 231-1300

A Unit of the Penn Central Federal Systems Company

Circle Reader Action No. 394

NASA Tech Briefs

National Aeronautics and
Space Administration

MARCH/APRIL 1986
Volume 10 Number 2



Special Features and Departments

10.....Editorial Notebook

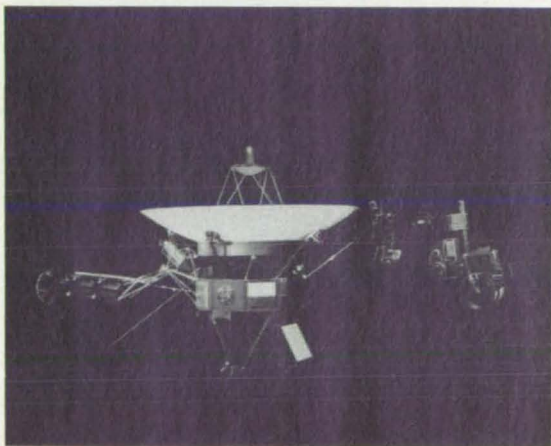
Jet Propulsion Laboratory:
14.....From Rockets to Robotics

154.....Letters

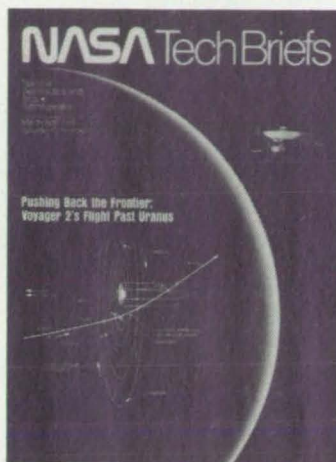
Advertising
155.....Index

156.....About This Publication

157.....Mission Accomplished



The Voyager is the most sophisticated robotic spacecraft ever to have flown. It carries scientific instruments and two cameras, and is governed by three sets of twin computers. The Voyager project is managed by NASA's Jet Propulsions Laboratory...page 14.



ON THE FRONT COVER:

This wide-angle image of Uranus was recorded by Voyager 2 on January 25, 1986, as the spacecraft left the planet behind and set forth on its journey to Neptune



NASA research on self-contained ecosystems led to the development of the EcoSphere®, an ecologically balanced system capable of sustaining plant and animal life...page 157.

Technical Section Thumb Index

28.....NASA TU
Services



22.....New
Product
Ideas



32...Electronic
Components
and Circuits



50.....Electronic
Systems



64.....Physical
Sciences



78.....Materials



94.....Computer
Programs



108.....Mechanics



118.....Machinery



138....Fabrication
Technology



146.....Mathematics and
Information
Sciences



148.....Life
Sciences



150.....Subject
Index



Thumb Index
Technical Section

This document was prepared under the sponsorship of the National Aeronautics and Space Administration. Neither Associated Business Publications, Inc., nor anyone acting on behalf of Associated Business Publications, Inc., nor the United States Government nor any person acting on behalf of the United States Government assumes any liability resulting from the use of the information contained in this document, or warrants that such use will be free from privately owned rights. The U.S. Government does not endorse any commercial product, process, or activity identified in this publication.

NASA Tech Briefs, ISSN 0145-319X, copyright © 1986 in U.S., is published bi-monthly by Associated Business Publications, Inc., 41 E. 42nd St., New York, NY 10017-5391. The copyrighted information does not include the individual Tech Briefs which are supplied by NASA. Editorial, sales, production and circulation offices at 41 E. 42nd Street, New York, NY 10017-5391. Subscriptions for non-qualified subscribers in the U.S., Panama Canal Zone, and Puerto Rico, \$50.00 for 1 year; \$100.00 for 2 years; \$150 for 3 years. Single copies \$15.00. Remit by check, draft, postal or express orders. Other remittances at sender's risk. Address all communications for subscriptions or circulation to NASA Tech Briefs, 41 E. 42nd Street, New York, NY 10017-5391. Application to mail at second-class postage rates is pending at New York, NY 10017 and additional mailing offices.

POSTMASTER: please send address changes to NASA Tech Briefs, 41 E. 42nd Street, Suite 921, New York, NY 10017-5391.

SYSTEMS INTEGRATION OF MIXING APPLICATIONS



TION: THE SCIENCE S AND ORANGES

We've been doing it successfully for over 15 years

Grumman Data Systems approaches information processing problems with a single goal: to develop integrated systems that deliver the best performance at the lowest life-cycle cost, while remaining as simple and user-friendly as state-of-the-art technology allows.

It's a difficult task, at best. But it's one to which we bring years of experience, and the objective viewpoint that only a hardware-independent system integrator can provide.

In C³I systems, management information systems, computerized test systems, engineering and scientific systems, and integrated manufacturing systems, we've built a record of success that any company would envy.

To maintain that record, we've invested substantially in research and

development. That's why our name is so often linked to new advances in networking, computer graphics, machine intelligence, command support systems, fault tolerant systems and the Ada software language.

We're also a total service company, not one that simply installs a system and walks away. We have facilities nationwide. And we support our customers with information processing services, multi-vendor hardware and software maintenance, training, data base publishing and facilities management.

Our ability to effectively mix apples and oranges has made us the fastest growing division of the Grumman Corporation. For further information about any of our capabilities, contact Wesley R. Stout, Director, Technical Services at (516) 682-8500.

CUSTOM SOLUTIONS
for Managing Information

Grumman Data Systems

Circle Reader Action No. 363

® A registered trademark of Grumman Corporation

GRUMMAN


ENHANCE YOUR PRODUCT RELIABILITY!

Manufacturers nationwide rely on the high quality and timely delivery of Aurora Bearing Company products. Select from a complete family of general purpose, economy, extra strength and heavy-duty rod ends to 2" bore size. Quality 1-piece race, swaged construction, precision ground balls for maximum trouble-free performance. Aurora Bearing, THE MOTION TRANSFER SPECIALISTS, will customize units to your special materials and linkage requirements.

Aurora Bearing is an OEM supplier of rod ends and special linkages to the following industries:

- HEAVY TRUCKING & TRANSPORTATION
- PRINTING EQUIPMENT
- AUTOMATION & PACKAGING MACHINERY
- AIRCRAFT—AEROSPACE
- OFF-HIGHWAY CONSTRUCTION EQUIPMENT
- FARM MACHINERY AND EQUIPMENT
- RACING CARS OF ALL TYPES
- AND MANY MORE...

Let Aurora Bearing apply its manufacturing, application, and design expertise to your needs. Call or write today for technical assistance, price and delivery on your rod end and special linkage applications.

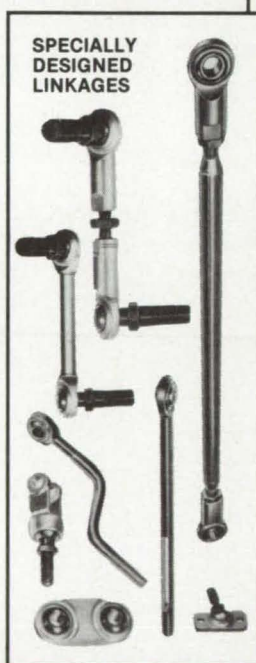


**WRITE FOR
CURRENT
CATALOG**

**TELEX: 280079 AUR BRGS
THE MOTION-TRANSFER SPECIALISTS**



**STANDARD
ROD ENDS**



**SPECIALLY
DESIGNED
LINKAGES**



AURORA BEARING COMPANY
970 South Lake Street
Aurora, IL 60506 • Phone (312) 859-2030

NASA Tech Briefs:

Published by **Associated Business Publications**
Editor-in-Chief/Publisher **Bill Schnirring**
Managing Editor **R.J. Laer**
Associate Editor **Judith Mann**
Assistant Editor **Elena Nacanthier**
Technical Advisor **Dr. Robert E. Waterman**
Creative Director **Michael Renchiwich**
Art Director **Melanie Gottlieb**
Production Manager **Rita Nothhaft**
Traffic Manager **Karen Galindo**
Circulation Manager **Anita Weissman**
Fulfillment Manager **Elizabeth Kuzio**
Controller **Neil B. Rose**

Technical Staff:

Briefs prepared for National Aeronautics and Space Administration by **Logical Technical Services Corp.**
Technical Editor **Jay Kirschenbaum**
Art Director **Ernest Gillespie**
Managing Editor **Ted Selinsky**
Administrator **Elizabeth Texeira**
Chief Copy Editor **Pamela Touboul**
Staff Editors **James Boyd, Theron Cole, Jr., Larry Grunberger, Jordan Randjelovich, George Watson**
Graphics **Kenneth Blasko, Luis Martinez, Huburn Proffitt**
Editorial & Production **Walter J. Pawlowski, Trudy Cavallo, Lorne Bullen, Frank Ponce, Joe Renzler, Ivonne Valdes**

NASA:

NASA Tech Briefs are provided by the National Aeronautics and Space Administration, Technology Transfer Division, Washington, DC:

Acting Administrator **Dr. William R. Graham**
Assistant Administrator for Commercial Programs **Isaac T. Gilliam IV**
Acting Director Technology Utilization Division **Henry J. Clarks**
Publications Manager **Leonard A. Ault**

Associated Business Publications

**41 East 42nd Street, Suite 921
New York, NY 10017-5391
(212) 490-3999**

President **Bill Schnirring**
Executive Vice President **Frank Nothhaft**
Vice President—Sales **Wayne Pierce**
Vice President **Patricia Neri**

Advertising:

New York Office: (212) 490-3999

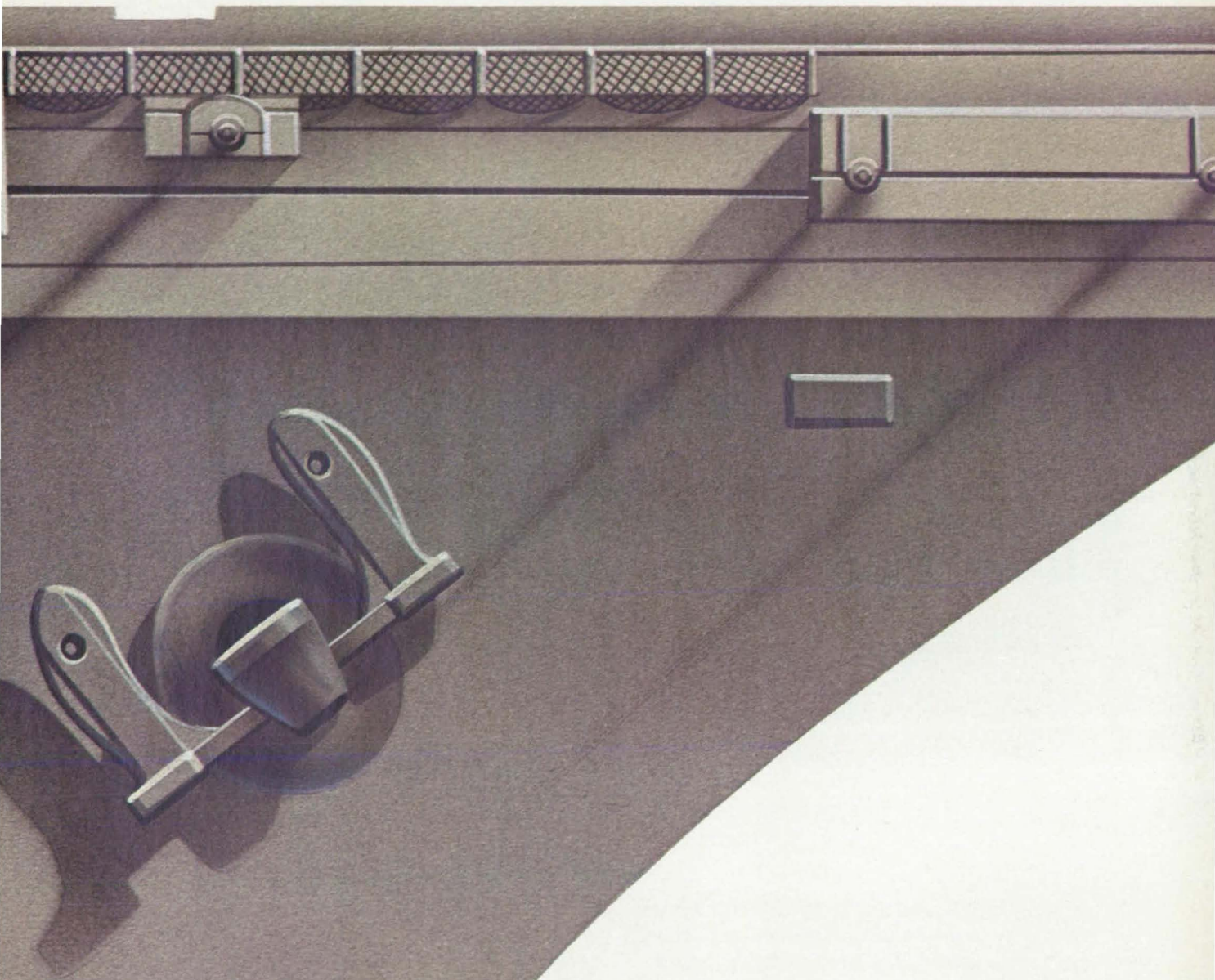
Vice President—Sales **Wayne Pierce**
Sales Manager **Robin DuCharme**
Account Executive **Dick Soule**
Advertising Assistant **Erving Dockery, Jr.**

Chicago Office: (312) 848-8144

Account Executive **Irene Froehlich**

Los Angeles Office: (213) 477-5866

Account Executive **Robert Bruder**



Power in a pinch.

When the nuclear reactor needs support, General

Electro-Motive Division is a source of reliable, efficient diesel-electric technology.

Six carriers in the *Nimitz* class. Electro-Motive Division generator sets are installed on each ship. It's not a record contract, but the responsibilities are monumental: supply back-up electrical power for America's premier strategic influence. Power for lights and ventilation. For air and sea communications. A fast start is imperative, and these General Motors diesels deliver.



Simplicity breeds reliability. Every GM generator set is based on the uncomplicated power of a GM two-stroke cycle diesel engine. Units configured with 8, 12, 16, or 20 cylinders deliver power outputs from 1000 to 4000 HP. The straightforward design results in a generator that starts fast, makes maintenance easy, and lasts. The service life of an EMD engine is typically 20 years or more.

Technology enhances performance. Continued research and development has taken a time-tested performer and given it an evolutionary edge. An engine-driven turbocharger that delivers the necessary air for fast engine response in the critical low-rev range. An improved injector. Redesigned pistons and relocated rings. And cylinder liners hardened in the world's largest industrial laser operation. In all, technological refinements have improved the fuel economy of our engines by ten percent in the past five years.

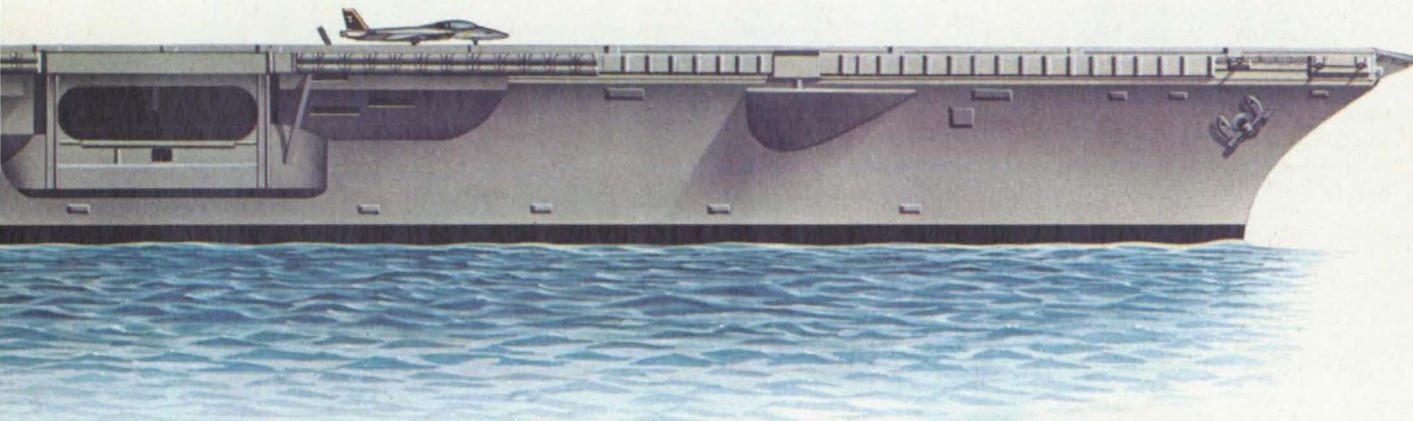
in a Nimitz-class carrier Motors diesels react.

The Electro-Motive Division of General Motors has a long history of turning its production capacity and innovative abilities toward the defense community. During World War II, many U.S. Navy fleet submarines were driven by GM engines. We also delivered thousands of diesel engines for LSTs in the rapid build-up of our nation's landing forces.

For the Korean conflict, EMD designed and built a diesel-electric locomotive that was capable of operat-

ing on any gauge track. More recently, we developed portable generator sets for rugged duty in Southeast Asia. That they are still in the Army's inventory is a tribute to their flexibility and durability.

Electro-Motive diesel locomotives are controlled by a microprocessor. And the generator sets on the *Nimitz*-class are tested to "Hi-shock" standards for combat sea duty.



General Motors is always proud to qualify a commercial product for military service. This aggressive policy, combined with our defense experience, is the reason we enjoy such broad acceptance today. We provide primary power for Coast Guard cutters and buoy tenders. We supply stand-by generators for Navy submarine bases. We power submarine docking vessels as well as U.S. Navy LSTs. We propel a fleet of harbor tugs for the U.S. Army. We are even active in the export military market.

Electro-Motive Division. It's just one of the many resources at GM that are committed to providing the latest in tactical and strategic technology—on time and on cost. General Motors Defense. We're your ultimate ally in the fight for dependable, affordable defense. To enlist our aid, write to our Washington, D.C. office: General Motors, 1911 North Fort Myer Drive, Suite 800, Rosslyn, Virginia 22209.

THE ULTIMATE ALLY



GENERAL MOTORS DEFENSE

Editorial Notebook

The New and the Noteworthy

Henry Clarks, the acting director of NASA's Technology Utilization Division, recently called a Technology Utilization conference together in Washington and invited *NASA Tech Briefs'* editors to attend. It was an excellent conference. As editor and publisher of *NTB*, the primary medium for NASA technology transfer, I gained new insight into the involvement of the different members of the NASA Technology Utilization team. Out of the learning process and the discussions came several new ideas for improving *NTB*.

The most immediate need we saw for *NTB* was a better editorial explanation of the technology transfer process, and part and parcel of that was a clear-cut explanation of how you, the reader, can go that step beyond *NTB* and its Technical Support Packages to consultation with NASA's Industrial Applications Centers (IACs) to solve current problems and investigate new opportunities.

There are 9 IACs that are funded in part by NASA as part of its technology

transfer effort. These IACs have the ability of not just searching literally hundreds of data bases, but also of editing that material and offering suggestions on ideas and processes. The problems that the 9 IACs have solved number in the thousands.

What they can do for you may be limited only by your ability to ask the right question. The IACs have done searches for hundreds of Fortune 500 companies. Probably the only reason they haven't done more is because of the difficulty that exists in explaining and marketing their product—information. NASA's huge storehouse of knowledge, including all the tech briefs ever published, is at the IACS, waiting for American industry to avail itself of it.

Effective with this issue, we've attempted to better explain the IACS, how and whom to contact for future ideas and details, by redesigning the Technology Utilization pages that are found in every issue. In this issue, they're on pages 28 and 29.

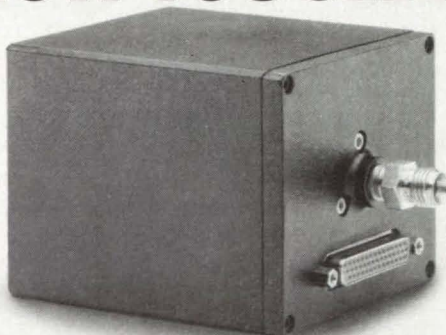
Also in this issue, you'll find a new

tech brief category: Computer Programs. Previously, new computer programs described in *NTB* could be found at the end of whatever tech brief category they referred to, whether physical sciences, mechanics or the like. While the programs will still be referenced under these categories, the actual descriptions of new computer programs will now be grouped together in a separate section. We hope this makes it easier for you to access NASA software and easier for you to utilize *NASA Tech Briefs*.

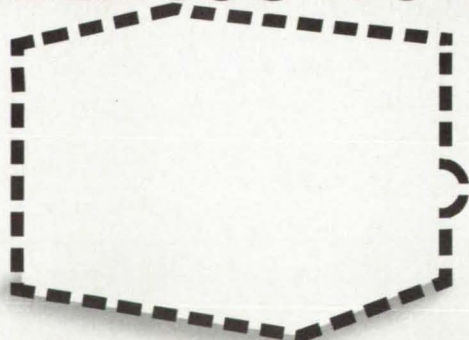
We've had myriad compliments since we commercialized *NTB*. We appreciate the compliments, but feel we can continue to improve our product. As always, comments and suggestions are not only welcomed, they're solicited. □

Brie Schuring

NOW YOU SEE IT.



LATER YOU WON'T.



Put the Sonix™ digital pressure sensor into your application and you may never see it again.

With $\pm 0.01\%$ per year guaranteed stability, this smart transducer is truly "Fit and Forget." What's more, its internal microcomputer compensates for systematic and thermal errors and outputs data in corrected engineering units.

The Sonix is rugged enough to fly on board jet fighters, and accurate for the most demanding applications.

For more information, call or write PSI...the leaders in digital pressure measurement technology.

- $\pm 0.01\%$ FS accuracy/stability
- Corrected digital output
- Applications include metrology, flight test and calibration
- New display option now available



PRESSURE SYSTEMS

34 Research Drive, Hampton, VA 23666
804/865-1243

Product/Research Developments®

Second of a series

General

To help you keep up-to-date on what is available to you from 3M, we offer this new series of summaries.

This represents only a small part of the 3M line of more than 40,000 diverse and innovative products, many of which are covered by government contracts.

So chances are whatever you need to get the job done better and more efficiently, you can get it from 3M . . . the company that hears you.

A versatile discovery

3M Glass Bubbles are hollow microscopic spheres, composed of water-insoluble, chemically stable glass. They are unicellular, and average less than 70 microns—one-fourth the size of a grain of salt.

Originally developed to displace more expensive filler materials, such as resin, 3M Glass Bubbles were found to greatly improve the performance of end products.

Lower weight and density, and smoother and less porous surfaces are among attributes that make this product ideal in aerospace and hydrospace applications—as well as more traditional fields, including construction, and automotive manufacturing and repair.

The use of 3M Glass Bubbles as a sensitizer in explosives is one of many specialized applications that have been discovered recently.

3M engineers can help research any special product use you may envision. And the Federal Systems Department will make it easy for you to work with them.

Surer footing

This time of year, in many parts of the country, there is more need than ever to look to 3M for floor matting.

Nomad Matting is recommended for use inside building entrances, in hallways, and in other areas where dirt tracking is a problem.

It is available in six colors and four sizes. One style is designed for outdoor use where oil, grease, or hard chemicals may be present, and still another is designed to cope with snow and slush.

Matting can be ordered with the following official seals and logos:

GSA	U.S. Navy
Postal Service	U.S. Marine Corps
Veterans Administration	U.S. Coast Guard
U.S. Air Force	Air National Guard
U.S. Army	Express Mail

(Contract number: GS-00F-76304)

Electronic protection

A low-cost, flame-retardant, quick-curing powdered resin is now available to provide a coating that will insulate, seal, and protect radial lead film capacitors, ceramic disc capacitors, tantalum capacitors, printed circuits, and other electronic components without adversely affecting their performance.

Called *Scotchcast* Brand Electrical Resins 5300 Series, these products are designed to conformally coat and environmentally protect electronic components.

Information retrieval system

Available immediately from 3M is the newly announced MFB 1100, multi-format plain paper reader-printer.

This unit represents the eleventh generation of microfilm retrieval units from 3M.

Handling all formats, the unit will provide positive prints from both positive and negative microfilm, and will accommodate all reduction ratios from 9× to 47×. The MFB 1100 features a 13×11½-inch screen, 360-degree image rotation, and manual or automatic film advance.

The unit delivers high-quality, inexpensive plain-bond prints from all microforms.

Conclusion

When you need help, think of 3M.

In particular, think of the Federal Systems Department/3M, the organization established nearly two years ago to better serve people in the U.S. Government.

As our name implies, we are dedicated to understanding *your* mission, and *your* particular needs.

Those of us on field assignment are thoroughly trained in government procurement procedures, and are charged with facilitating and expediting your contact with 3M product specialists, research and development scientists, and staff experts who may be able to serve you.

For more information on how to work with the Federal Systems Department/3M, or on these or any of the more than 40,000 products currently available from 3M, write, or call toll-free 800-328-1684 (or in Minnesota 800-792-1072).

Descriptive literature will be mailed to you without cost or obligation. Or, if you wish, a 3M representative will call you for an appointment at your convenience to discuss your particular needs.

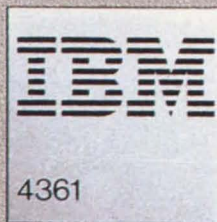
Just call **800-328-1684**

(In Minnesota 800-792-1072)

Scotchcast and *Nomad* are registered trademarks of 3M.

3M hears you . . .

Here's one supermini that's



gonna knock your socks off.

It's the IBM 4361.

And it's setting new standards for cost-performance. IBM? Supermini? For computational processing? You bet. It'll knock the socks off a centipede.

Speed. The 4361 features a high-speed cache buffer. It has a separate floating-point processor to handle multiplication. And it executes the 70 most-used instructions in the hardware. No wonder the 4361 will turn in a Whetstone that will knock your.... You get the idea.

Precision and accuracy. The 4361 has advanced 32/64-bit architecture. It can handle 31-decimal-digit precision. And as for accuracy, IBM's high-accuracy arithmetic facility (ACRITH) includes 22 special floating-point instructions that can be used to process iterative calculations accurately. The ACRITH program notifies you if the accuracy you need can't be maintained.

Ease of use. The 4361 needs no pampering. Install it almost anywhere—in a corner of your office, for example. And the 4361 can run unattended, with no onsite DP specialist.

To make life easier yet, there's the IBM Engineering/Scientific Support System (E/S³)—a consistent, menu-driven interface for interactive users. E/S³ is rich in function and offers an open architecture so you can add applications easily. It handles graphics, text and data manipulation. And it supports a wide range of administrative applications.

Attachability. What would you like to attach to your IBM 4361? Lab instruments? Personal computers? ASCII-oriented devices? Are they Multibus* or Unibus**-oriented? Or do they use a serial digital interface? The 4361 welcomes them all. It attaches to IBM and non-IBM devices of all kinds.

Growth path. The 4361 protects your investment. It can be upgraded on your premises over a processing power range of three to one. At low cost and in small steps. If you out-grow even the biggest 4361, you can move up to the IBM 4381 or one of the large 308X or 3090 processors.

There's much, much more. In technology, architecture, service and support. The 4361 is an engineering/scientific computer from head to toe. But hold our feet to the fire. Demand answers to all your questions.

To receive brochures on the 4361 and E/S³, or to have an IBM marketing representative call, return the coupon.



IBM DRM Dept. LQ/710 101 Paragon Drive Montvale, NJ 07645	3-86
<input type="checkbox"/> Please send me information on the IBM 4361 supermini and E/S ³ .	
<input type="checkbox"/> Please have an IBM marketing representative call.	
Name _____	
Title _____	
Company _____	
Address _____	
City _____	State _____ Zip _____
Phone _____	

*Multibus is a trademark of Intel Corporation./**Unibus is a trademark of Digital Equipment Corporation.

Jet Propulsion Laboratory: From Rockets to Robotics

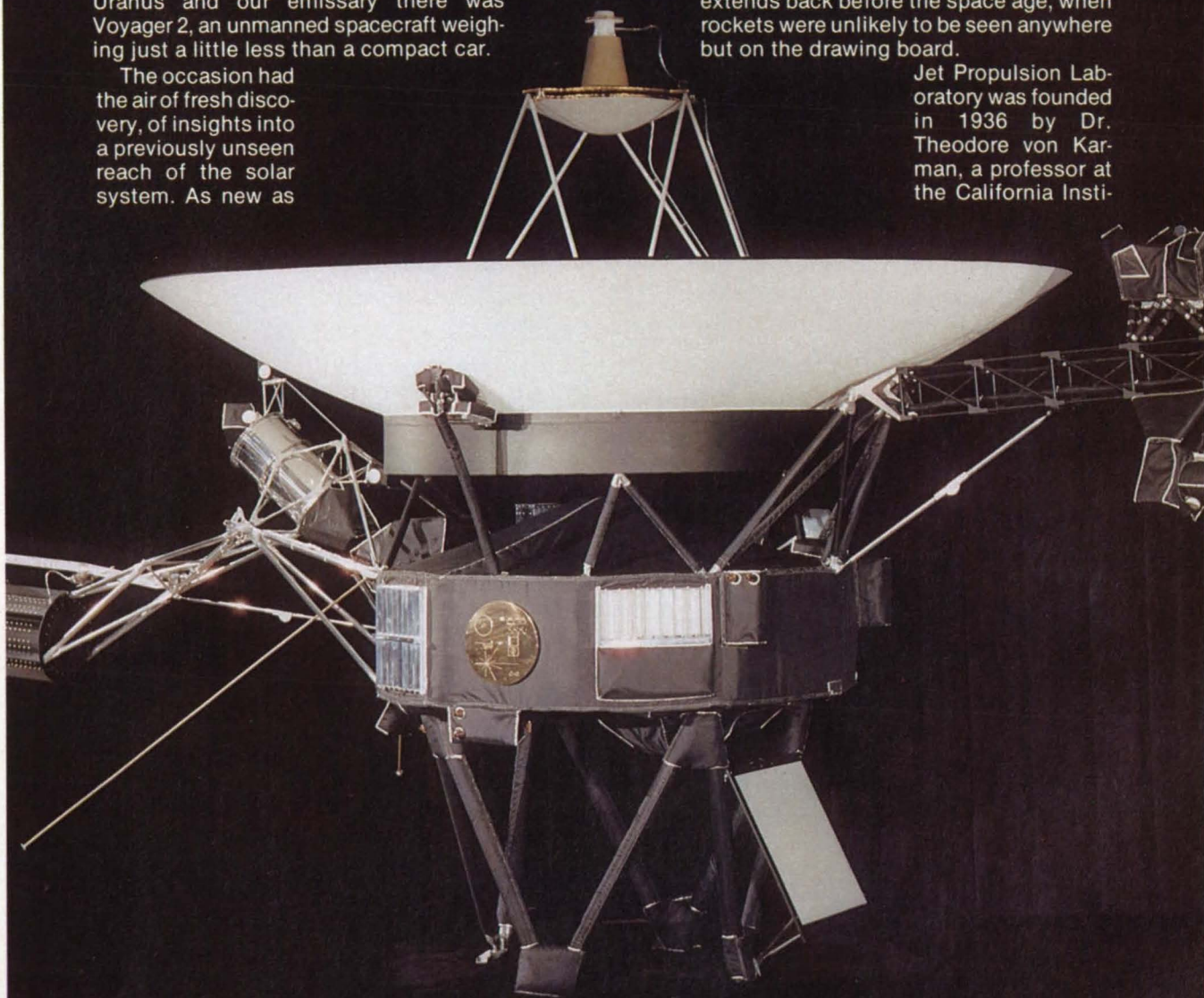
For a few days this past January, Pasadena, California, was host to an international gathering reminiscent of the 1984 Summer Olympics in nearby Los Angeles. Scientists, journalists and VIPs from around the world—video crews from Japan and writers from Scandinavia—gathered there to take in the first close views of a new world nearly two billion miles away. The new world was Uranus and our emissary there was Voyager 2, an unmanned spacecraft weighing just a little less than a compact car.

The occasion had the air of fresh discovery, of insights into a previously unseen reach of the solar system. As new as

the discoveries were, however, the event had become a common scene at what has been a Pasadena institution for half a century: Jet Propulsion Laboratory.

As NASA's lead center for the unmanned exploration of the solar system, Jet Propulsion Laboratory, better known as JPL, has a long history of designing and building automated spacecraft to probe the mysteries of the planets. But JPL's history extends back before the space age, when rockets were unlikely to be seen anywhere but on the drawing board.

Jet Propulsion Laboratory was founded in 1936 by Dr. Theodore von Karman, a professor at the California Insti-



Performance That's Out Of This World.



For Real World Applications.

Performance—Mainframe, multi-user performance in an office-compatible package. That's what Celerity Computing's distributed Superminicomputer Systems bring to you. They redefine the way compute-intensive tasks are accomplished in the engineering design environment.

Real world application software—ANSYS, PATRAN II, NASTRAN, MARC, MENTAT, SINDA, ADAMS, DYNA and others.

Productivity, Economy, Flexibility: Available NOW from Celerity Computing.

CELERITY COMPUTING

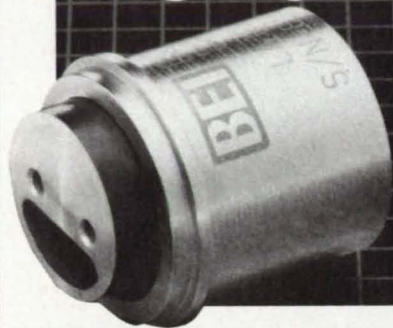


Corporate Headquarters: 9692 Via Excelencia, San Diego, CA 92126 (619) 271-9940.

ANSYS, PATRAN, NASTRAN, MARC AND MENTAT, and ADAMS are registered trademarks of SWANSON ANALYSIS SYSTEMS, INC., PDA ENGINEERING, NATIONAL AERONAUTICS AND SPACE ADMINISTRATION, MARC ANALYSIS RESEARCH CORPORATION and MECHANICAL DYNAMICS, INC., respectively.

Circle Reader Action No. 352

LINEAR AND ROTARY ACTUATORS



THE KEY TO PRECISE POSITIONING SYSTEMS

Using state-of-the-art electro-magnetic technology, BEI-KIMCO produces highly responsive and controllable actuators. BEI actuators produce a force or torque proportionate to current with zero friction, and with outstanding linearity and controllability. The key to precise positioning systems.

BEI actuators feature...

- Compact Linear and Rotary Designs
- Peak Force of .6 oz. to 500 lbs.
- Peak Torque of 10 oz. to 110 oz. in.
- Linear Actuator Stroke Ranges of $\pm .01$ in. to ± 2.25 in.
- Rotary Actuator Stroke Ranges of $\pm 5^\circ$ to $\pm 30^\circ$

Find BEI actuators in precision systems such as...

- Laser Mirror Positioning
- Satellite Truss Dampening
- Optical Bench Stabilizer
- Zoom Lens Actuation
- Stabilizing of Optical Sight

Call BEI for the key to your precise positioning system.



**BEI MOTION
SYSTEMS COMPANY**
KIMCO DIVISION

P.O. BOX 1626, SAN MARCOS, CA 92069 (619) 744-5671

Circle Reader Action No. 312



DISCOVERY

JPL. Discover us. A unique team of engineers and scientists. A free exchange of innovative ideas and opinions. High involvement. Creativity.

JPL. Discover inspiration. A special place to work. Modern laboratory facilities on a 173-acre park-like setting. The scenic foothills of the San Gabriel Mountains north of Los Angeles.

JPL. Discover impact. Projects and experiments of tremendous scientific importance. Space projects, like the Galileo mission that will take us back to Jupiter. Studies of Earth resources, the oceans, atmosphere, and environment. Imaging technologies. Medical diagnostics.

Discover our opportunities for professionals in the following disciplines: Electrical Engineering, Communications Systems, Computer Science, Computer-Aided Design, Physics and Math.

JPL is discovery. Please write us at: **Professional Staffing, Jet Propulsion Laboratory, Department T54, 4800 Oak Grove Drive, Pasadena, CA 91109.** An Equal Opportunity Employer M/F.

"There's only one..."



Jet Propulsion Laboratory
California Institute of Technology

JPL

tute of Technology, and a group of his students and colleagues. At a deserted site just north of Pasadena, they erected a few simple shacks in which they built rudimentary rocket systems. This pioneering work earned the attention of the U.S. government, and in 1938 the CalTech laboratory, later JPL, was awarded the first federal contract for rocket studies.

Early work at the laboratory resulted in the development of solid- and liquid-fueled rockets, and a jet-assisted take-off application for Army aircraft. During the '50s, JPL researchers focused on the development of guided missile systems for the U.S. Army. When NASA was created in 1958, federal jurisdiction over JPL was transferred from the Army to the new civilian agency. Under a NASA contract with, CalTech, JPL was assigned to lead the nation's unmanned exploration of the solar system.

Moving into Space

JPL's history of space-related accomplishments begins with the first U.S. satellite, Explorer 1, which was launched in early 1958. It detected the Van Allen radiation belts that surround the Earth. The Ranger and Surveyor missions of the 1960s mapped and probed the lunar surface, in part to determine the feasibility of landing. These missions ultimately led to the successful Apollo missions and the manned exploration of the lunar surface. JPL's Mariner missions explored the inner solar system and returned images of Earth's nearest neighbors, Mars, Venus, and Mercury. The Viking Mars orbiters and landers of the late '70s transmitted startling images of the red planet's surface and searched for signs of life in the Martian soil. In 1977, JPL's most sophisticated robotic spacecraft, Voyagers 1 and 2, were launched. The twin Voyagers encountered Jupiter in 1979 and Saturn in late 1980 and early 1981, transmitting a wealth of data concerning these two giant planets, their rings and their satellites.

Following the Saturn flyby, Voyager 1 set off on an upward course that will eventually take it out of the solar system toward the star Rigel (Alpha Ophiuchus). Voyager 2 was originally to have flown directly out of the solar system as well, but mission planners decided to reroute the spacecraft to accomplish a "grand tour" of the planets. As Voyager 2 swung around Saturn in August 1981, it was deflected into a trajectory that would take it past Uranus in January 1986 and past Neptune in August 1989.

An approximate alignment of Jupiter, Saturn, Uranus and Neptune that occurs only once every 176 years made the addition of Uranus and Neptune to Voyager 2's itinerary a theoretical possibility. Technical developments and spacecraft modifications made the extension of Voyager 2's mission a practical feasibility.

As Voyager 2 set off on its five-year journey from Saturn to Uranus, engineers and scientists at JPL's mission control facility began customizing the spacecraft's systems for the Uranian encounter. New techniques for collecting, processing and transmitting data were developed to compensate for the vastly increasing distance between the spacecraft and its tracking and control stations on Earth.

One of the spacecraft's onboard computers was programmed to preprocess all imaging data before transmitting it to Earth. This innovation involved a JPL-developed form of data compression, which resulted in a 60% reduction in the level of data needed to create images of the Uranian system. It also reduced the time required to transmit the data, allowing more images to be generated and transmitted to Earth.

Another technique, image motion compensation, countered the effects of Voyager 2's 45,000 miles per hour velocity.

When the challenge is handling propellants in space...



Fairchild Control Systems Company has the answers

Fairchild Control Systems Company has provided disconnects for every major space program requiring storable propellants, cryogenics, and gases. Our reliability and safety record is second to none.

If your system requires light weight, long life, low leakage, self-alignment, minimal pressure drop, manual or remote actuation, give the challenge to Fairchild Control Systems Company. Go with the leader in fluid transfer technology... with more QD's in

space than all other competitors combined.

Fairchild's fluid transfer couplings used aboard:

- VOYAGER (Hypergolic)
- SATURN/APOLLO (Cryogenic)
- LUNAR MODULE (Oxygen and EGW)
- TITAN (Hypergolic)
- SPACE SHUTTLE (Hypergolic, Cryogenic, Pneumatic)
- SHUTTLE/CENTAUR (Cryogenic)

Fairchild Control Systems Company... meeting the aerospace challenges of today and tomorrow.



FAIRCHILD
CONTROL SYSTEMS COMPANY

Fairchild Control Systems Company
1800 Rosecrans Avenue
Manhattan Beach, California 90266
Tel.: (213) 643-9222
Telex: 910-325-6216



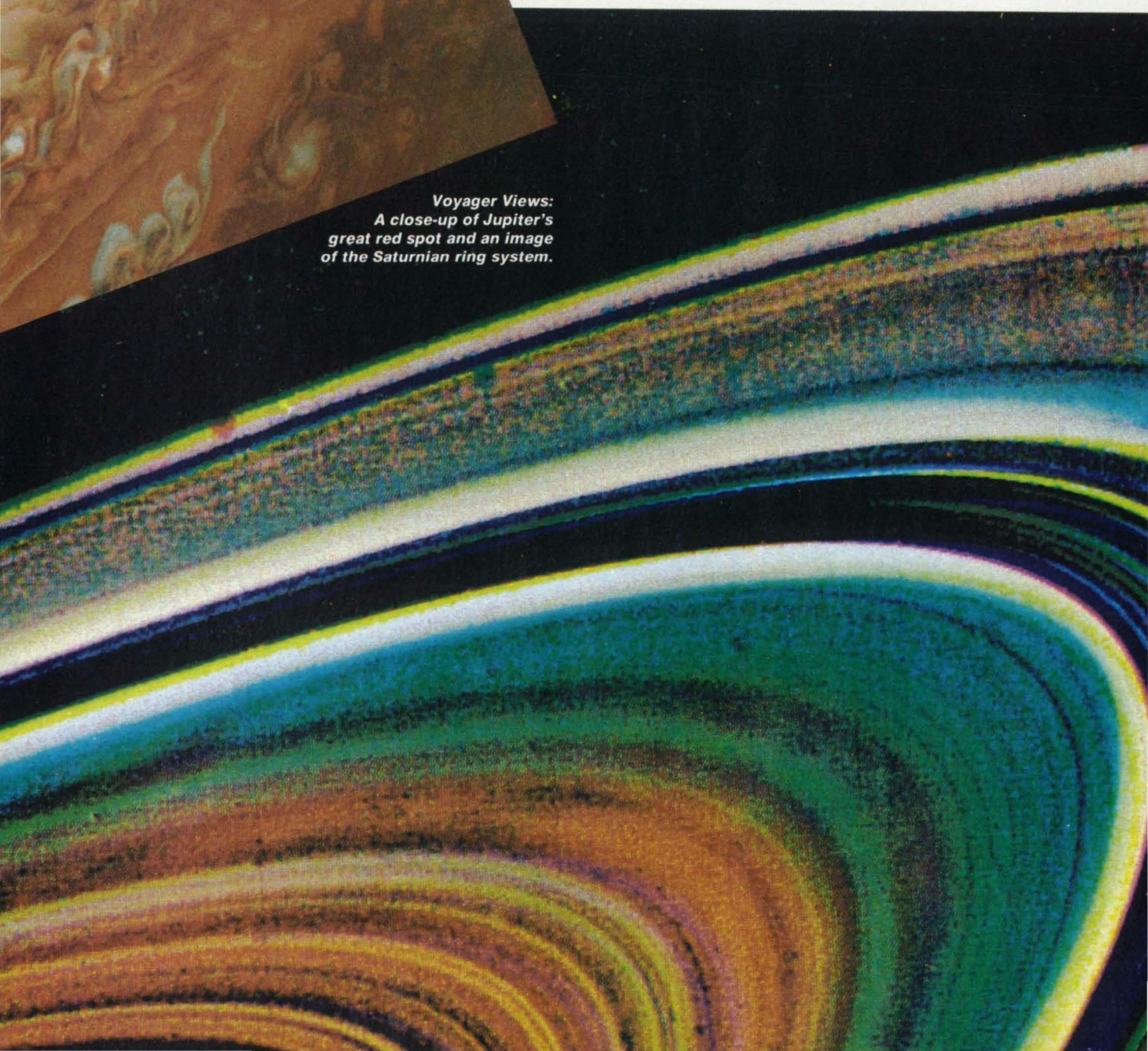
JPL

city and low levels of sunlight illumination during the encounter to allow the spacecraft's two cameras increased exposure times without causing image smearing. By rotating the spacecraft itself, at rates approaching 1/30th of a degree per second, the cameras were able to obtain clear, close-up images of the Uranian moons.

Finally, a technique called arraying was developed to enhance the strength of Voyager 2's signals and the rate of data transmission. Arraying involved electronically linking the antennas at each of the

NASA Deep Space Network sites, thereby increasing the strength and quality of the received signals. (The Deep Space Network consists of three tracking stations: one at Goldstone, near Barstow in the Mojave Desert of California, and the others in Robledo, near Madrid, Spain, and Canberra, Australia. All three are equipped with one 210-ft. diameter antenna and two 85-ft. antennas, plus associated receivers and transmitters. JPL operates NASA's Deep Space Network, which provides receiving and tracking information and controls transmissions to all unmanned, deep space missions.)

By all accounts, Voyager 2's encounter with Uranus was an unprecedented success. The challenges of extremely low light levels (Uranus receives 1/400th as much light from



Voyager Views:
A close-up of Jupiter's great red spot and an image of the Saturnian ring system.

the sun as Earth does) and long transmission distances (Uranus is 2 billion miles from Earth) were overcome through technical innovation.

The discovery of ten new moons and at least one additional ring at Uranus were among the initial results of the Voyager 2 encounter. Detailed analysis of the data may take as long as ten years, and a number of other discoveries can be expected. In the meantime, though, JPL's engineers and scientists have a number of other deep space exploration missions in the works.

Planetary Preview

The Galileo mission will send an orbiter around Jupiter to explore the planet and its four large moons. Galileo will also drop an instrumented probe into the Jovian atmosphere. The

probe will penetrate about 60 miles into the dense cloud cover of the planet, and its instruments will radio back to the orbiter data on the atmosphere, its structure and dynamics. The orbiter will continue to study the stormy clouds of Jupiter and will make extensive photographic and scientific studies of the planet and its moons over an extended period. Like the Voyagers, Galileo was designed, built and tested in-house at JPL.

JPL is also managing the American portion of the joint NASA-European Space Agency Ulysses mission. Ulysses, formerly called the International

Solar Polar Mission, will use a boost from the gravity of Jupiter to propel itself over the poles of the sun, probing the poles and the interstellar space that surrounds them. Like Galileo, Ulysses was originally scheduled for a May 1986 shuttle launch. The launch schedules for both spacecraft have been delayed, tentatively until June-July 1987, due to the suspension of the shuttle program.

JPL's Magellan spacecraft, scheduled for a 1988 launch, will orbit Venus and obtain detailed radar images of almost 90% of the planet's sur-

(continued on page 31)

FAIRCHILD WESTON... The Name To Know For Quality Instrumentation Data Recorders

Unrivalled Range and Versatility



Fairchild Weston products illustrated above include:

- MODEL 10 - Microprocessor controlled, 16" reel laboratory recorder/reproducer.
- EDCS - Error Detection and Correction System with Monitor.
- MODEL 12-B (AN/USH-33(V)) - High Environmental 10 1/2" reel recorder, monitor/reproducer.
- MODEL 9 - Transportable 15" reel, microprocessor controlled, very high versatility recorder/reproducer.
- ANALOG MULTIPLEXER/DEMULTIPLEXER - 16 Channels of Analog Data on 1 Channel of any tape recorder.
- MODEL 15 - High environmental 15" reel, microprocessor controlled, high versatility recorder/reproducer.
- MODEL 80 - Portable 14" reel, low cost recorder/reproducer.
- MODEL 80TA - Tempest qualified 14" reel, microprocessor controlled high versatility recorder/reproducer.
- MODEL 85 - Portable 14" reel, microprocessor controlled, high versatility recorder/reproducer.
- All models to IRIG (RCC) specifications.



FAIRCHILD WESTON SYSTEMS INC.

DATA SYSTEMS DIVISION
P.O. Box 3041, Sarasota, Florida 33578
(813) 371-0811 • Telex: 4947160

In 1992, we set sail for a New World.

In 1492, a Genoese navigator and an intrepid crew crossed uncharted waters in search of a west passage to India. In the process, they uncovered the vast resources of two continents. And they opened up a new base for exploration, progress, and the hopes of mankind.

In 1992, coincident with the 500th anniversary of Columbus's voyage, we plan to set sail for another New World. That year, or shortly thereafter, the United States and the world will begin benefiting from the first manned Space Station. The Station will be more than another giant step for mankind. It will be our stepping stone to living in new realms, and it will result in thousands of discoveries that will benefit earth.



This New World, free from gravity and atmospheric impurity, will provide that ideal environment for experimentation and production that is impossible on earth. Simultaneously we will have a permanent station for scanning the earth and the heavens — an unparalleled vantage point for predicting weather, aiding agriculture, and understanding the universe.

Of course, like Columbus, we cannot foresee all the benefits ahead. But we do know that we will have a new arena in which to conquer disease, transform the materials of earth, and generate precious energy. The resulting knowledge from countless discoveries will come down to earth for our well-being.

But, unlike Columbus, our craft will be in constant contact with the Old World. Harris Aerospace, as a member of the Rockwell, Grumman and Sperry team, is responsible for the Space Station's communications and tracking system. We are totally committed to this great endeavor, and we bring to the challenge the capabilities and experience necessary for success.

Harris has had 27 years of successful involvement with the kind of space communications and tracking required for the manned Space Station. Our space experience includes programs from Telstar to the Tracking and Data Relay Satellite as well as the manned programs of Apollo, Lunar Module, and Space Shuttle. We are also a leader in the architecture and design of large communication networks.

Now Harris is ready for the Space Station. Over the next years and centuries, the scope of scientific, commercial and technological opportunities and breadth of results are sure to exceed our wildest expectations.

For in 1992, we, too, will be very much like Columbus: carrying the sum of our knowledge into the unknown. And, like him, we, too, shall return with the bountiful gifts of a New World.

**HARRIS**

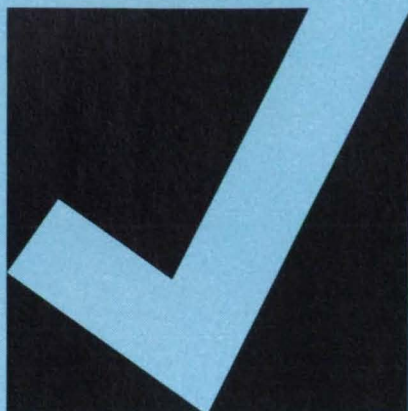
Circle Reader Action No. 410

For your information,



our name is Harris.

New Product Ideas

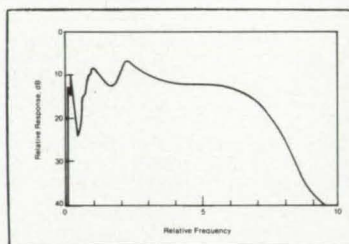


New Product Ideas are just a few of the many innovations described in this issue of *NASA Tech Briefs* and having promising commercial applications. Each is discussed further on the referenced page in the appropriate section in this issue. If you are interested in developing a product from these or other NASA innovations, you can receive further technical information by requesting the TSP referenced at the end of the full-length article or by writing the Technology Utilization Office of the sponsoring NASA center (see page 29). NASA's patent-licensing program to encourage commercial development is described on page 29.

Broadband Ultrasonic Transducers

The accuracy of sonar and ultrasonic imaging equipment can be improved through the use of a piezoelectric transducer with a greatly increased bandwidth; this increase is achieved by fabricating the transducer of nonuniform thickness. The transducer can be shaped to respond uniformly over a predetermined band of frequencies and to attenuate strongly the frequencies outside the band (see figure for the frequency response curve of a transducer in which one side of the crystal disk is planar and the other concave). The new transducers may thus make it unnecessary to use signal-processing circuits to compensate for the transducer frequency response or to use auxiliary circuits to modify the frequency spectrum of the voltage applied to the crystal.

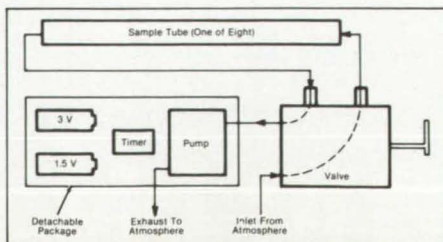
(See page 47.)



Solid-Sorbent Air Sampler

Volatile organic compounds in air are collected for analysis by a portable, self-contained sampling apparatus in which a pump draws air at a rate of 0.1 to 0.5 cm³/min through glass-lined, stainless-steel sample tubes filled with a porous polymer of 2,3-diphenyl-p-phenylene oxide. When each of the eight sample tubes is placed in the collecting position, high-boiling-point organic compounds are adsorbed onto the polymer, while low-boiling-point organics, O₂, N₂, Ar, CO₂, CO, and H₂O pass through. At the end of the sampling period, the operator turns the valve handle to the next position, thereby exposing a new sample while isolating and protecting the previous sample(s). For analysis, the sample tubes remain in place and are connected through the valve to a standard gas-chromatographic/mass-spectrometric system.

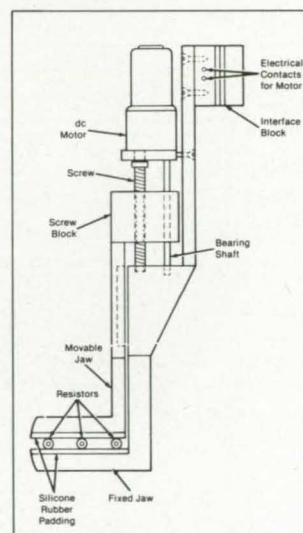
(See page 68.)



Gentle End Effector for Robots

And end effector, designed for use with a Puma (or equivalent) robot arm, handles delicate small parts firmly but gently. It grips such electronic components as resistors, capacitors, and transistors without damaging them and holds them during soldering or other processing. The end effector is driven by a dc motor instead of the usual pneumatic drive. The motor is mounted on the fixed jaw of the effector and drives the movable jaw through a screw block. The jaws are made of steel, and their gripping surfaces are lined with silicone rubber to cushion and, therefore, further reduce the chance of damaging the components. The jaws withstand soldering temperatures greater than 500 °F (260 °C).

(See page 128.)



Ball-and-Socket Mount for Instruments

A ball-and-socket mounting mechanism holds a scientific instrument securely, allows the instrument to be oriented, and minimizes the conduction of heat to and from the instrument. The mechanism includes a stationary base containing part of the spherical socket surface, two jaws that contain the rest of the socket surface, and an adjusting screw. A ball on the instrument sits in the spherical socket formed by the opposing jaws and base. Counterclockwise rotation of the screw closes the socket around the mounting ball. Clockwise screw rotation opens the mechanism by sliding the jaws outward on a dovetail track on the base. The instrument ball can then be disengaged from the open socket, allowing the instrument to be removed.

(See page 78.)

CONSISTENT QUALITY IS COST-EFFECTIVE.

IT'S IN A YELLOW BOX. CONSISTENTLY.

© Eastman Kodak Company, 1986

Consistent quality in an x-ray film means the radiographs will be right—time after time. And there's nothing in the world of NDT more cost-effective than that. Because there's nothing less cost-effective than having to repeat the job. Which is why we make Kodak Industrex film to our most exacting standards of quality and consistency. For details, call the Kodak Government Systems Division at (703) 558-8500, or visit the Kodak Imaging Systems Center at 1300 N. 17th St., Arlington, VA 22209.

Kodak Industrex film. Can you afford anything less?





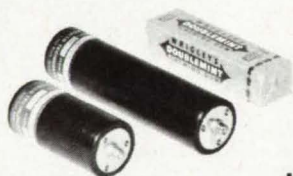
LASER SIMULATOR (eye-safe)



CS100

These convenient, easy to use laser simulators are compact and self-contained. They provide a pulsed 1.06 micron infrared signal source simulating a YAG laser. Because of their portability, they are ideally suited to laboratory or field testing of laser rangefinders, and simulation of laser designators.

LASER DIODE PULSERS



ILC

The ILC produces more average output power for driving laser diodes at 7 to 200ns pulse widths than avalanche or SCR pulsed. Models are available for pulse currents of 1 through 100A. Fast rise and fall times, with internal clock for pulse rates of 1 through 10,000 PPS.

LASER DIODE ARRAY PULSER



ILM

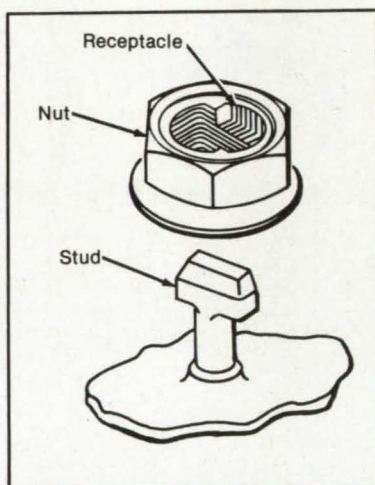
The ILM Series Laser Diode Pulser is designed to drive the ITT Ls 7711 or Laser Diode Labs LDT 350 Series Fiber Coupled laser arrays. An internal power supply allows operation from any available D.C. voltage between 10 and 28 volts.

POWER TECHNOLOGY, INC.
P.O. Box 9769
Little Rock, Arkansas 72219
Phone 501/568-1995
TWX 910/722-7313

Quick-Connect Heavy-Duty Fastener

A fastener consisting of two mating parts—a T-shaped stud and a receptacle with an external thread and nut—combines the best features of quarter-turn fasteners and threaded fasteners. Like quarter-turn attaching devices, it can be connected and disconnected quickly; like threaded devices, it can be adjusted to a desired preload, withstand high loads, and accommodate a wide range of grip lengths. Used to attach pads to the tracks of tracked vehicles, the fastener prevents pad separation under tension loads and resists loosening under compression loads. It establishes the required prestress within fairly narrow bounds (± 25 percent), despite the wide variations of the grip length that is caused by variation in the dimensions of the pad plate (a stamping) and the track shoe (a forging).

(See page 108.)

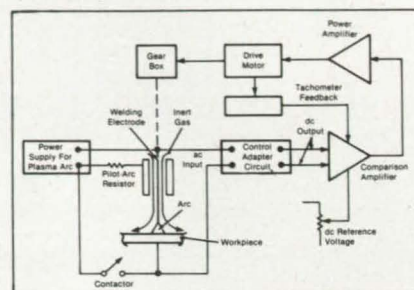


Controlling Arc Length in Plasma Welding

A control adapter circuit maintains a constant arc length during the plasma arc welding of irregularly contoured parts. The addition of this circuit to a plasma arc welding machine requires just a few wiring changes. Compared with unmodified machines, plasma arc welders containing the adapter circuit produce welds that are cleaner and require less rework. The circuit samples the ac arc voltage, then half-wave rectifies and filters it to reduce the ripple. The resulting dc measurement signal is applied to a comparison amplifier, which compares it to a reference voltage that represents the commanded arc length. The amplified comparison signal is applied to a power amplifier that drives a motor and gear train to adjust the elec-

trode position and therefore the arc length.

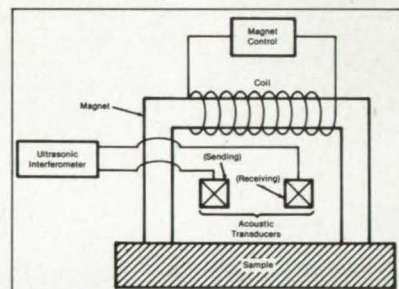
(See page 141.)



Acoustic/Magnetic Stress Sensor

A portable high-resolution acoustic/magnetic stress sensor measures compressive or tensile stresses and stress gradients in steel members quickly and nondestructively. The sensor includes a precise high-resolution acoustic interferometer, transmitting and receiving acoustic transducers, an electromagnet coil and core, a power supply, and a magnetic-field measuring device such as a Hall probe. The stress measurement depends on the shift in acoustic velocity that accompanies the stress-induced change in the magnetic-domain structure.

(See page 112.)



Adjustable Headband for Earphones

A headband, consisting of a pair of cushioned, steel head-clamping spring strips joined by a tensioning screw, holds an earphone and microphone on the wearer's head securely and comfortably. The headband contacts the head lightly but firmly at only two points, eliminating the headaches and soreness caused by conventional models, which clamp on the head over a wide arc. While wearing the headband, the wearer can adjust its width for maximum comfort by tightening or loosening the tensioning screw. The headband accommodates a standard microphone, attached to the first earphone, and a second earphone or an ear mute, either of which would replace the side support, as shown in the figure.

(See page 32.)

Precision Metal Products Engineered to Your Design Needs.

Designing the aircraft of tomorrow means solving complex systems requirements today. At Belfab we design and manufacture precision metal products that meet your requirements, while providing the durability and reliability features so critical to aircraft performance.

Capability.

Since the dawn of the space age Belfab products have been aboard our nation's most advanced commercial and military aircraft as well as the space shuttle, satellites and missiles. These products usually incorporate a bellows assembly, either edge welded or formed. Often, the bellows is only one of many components in the assembly and may serve any number of applications where there is a need for motion, flexibility, pressure sensing, fluid containment and zero leakage, while meeting limited space and weight restrictions.



Mechanical Seal



Flexible Coupling Fuel Drain Assembly



Flexible Hose

In addition, our capability to stamp, form, weld, machine, heat-treat, assemble and test, allows us to build your entire product in-house.



Durability.

Belfab products deliver benefits over and above a piece of hardware that simply meets your specifications. You receive a product engineered from the finest quality metals and alloys. A product that delivers long life while withstanding



Valve

extreme temperatures, pressures, and highly corrosive media.

Reliability. Delivering precision performance under demanding conditions has been the trademark of Belfab products the past 30 years. Delivering free engineering support up front to help design a cost effective assembly has led customers to rely on our expertise to provide custom designs



Pressure Sensor/Actuator



Temperature Sensor/Actuator

that deliver top performance. And, delivering orders with a 90% on time record keeps our customers coming back time and again.

Free Application Analysis and Design.

Whether you are developing new aircraft or improving existing models, Belfab stands ready to help with precision metal products. To determine which product best suits your needs, our applications engineers will work with you at the outset of your project - at no charge or obligation - to analyze your performance requirements and to recommend solutions. To get started or to simply find out more about our capabilities, just call or write. We'll send you our free bellows design manual today . . . to help make it fly tomorrow.



Valve Stem Seal



Volume Compensator



Thrust Control Bellows Assembly

East Coast: 305 Fentress Blvd. • P.O. Box 9370 • Daytona Beach, FL 32020

• Phone (904) 253-0628 • Telex 56-4355

West Coast: 9778 Katella Avenue • Suite 201 • Anaheim, CA 92804

• Phone (714) 530-1321 • Telex 18-3084

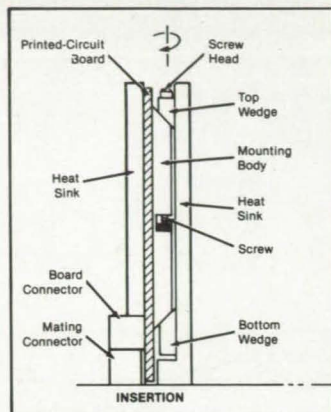
Circle Reader Action No. 301

PACIFIC SCIENTIFIC **BELFAB**
DIVISION

Ejection Mechanism for Circuit Boards

A mechanism attached to a printed-circuit board partially ejects it from an electronics assembly. The board can then be removed or replaced without using a pulling tool, which could damage circuit patterns and components. Turning a screw in the mechanism produces a jacking force parallel to the connector pins so that they do not become bent or broken as the board is disengaged from its mating connector.

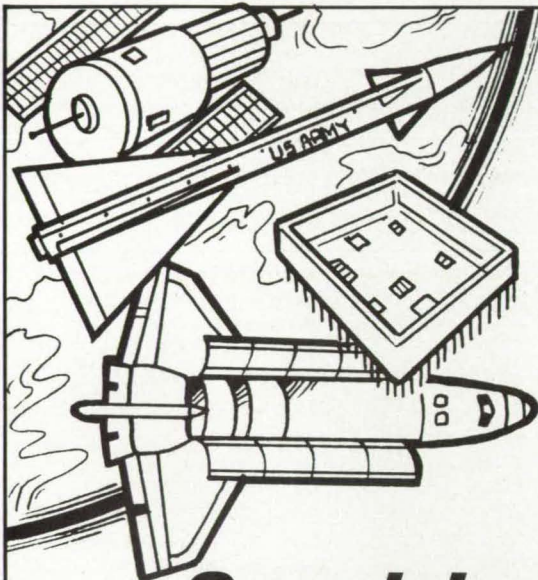
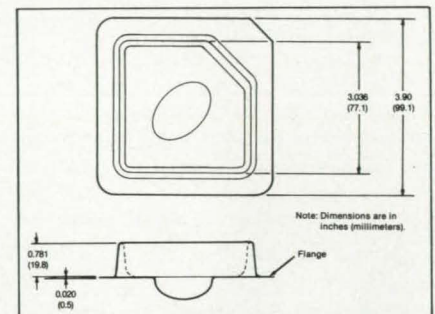
(See page 46.)



Void-Free Lid for Food Packaging

A folded, flexible plastic lid allows rigid plastic containers holding different levels of food to be sealed at the precise fill level. This lid eliminates air or vacuum pockets above the food and therefore keeps the food fresh and allows compact stacking of partially filled containers. In the sealing operation, the center of the lid is pushed into a rigid plastic cup containing the food to be preserved. As this is done, the lid unfolds and clings to the inside surface of the cup. The rim of the lid is then heat-sealed to the cup. Developed originally for packing dehydrated food for the Space Shuttle missions, this lid might be useful for home food storage and commercial food packaging.

(See page 143.)



- Clean Rooms
- Laminar Flow Benches
- Desiccator Cabinets
- Tables, Chairs
- HEPA Filters
- Precision Packaging Materials
- Glove Boats®
- Many More Clean Room Accessories

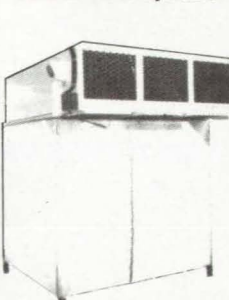
*All products tested as per required specification...
Processed and packaged
in our class 100 clean
rooms.*

Supplying the Aerospace Industry with Quality Clean Room Supplies Since 1968

Finger Cots



Laminar Flow Systems



Gloves



HEPA
Filtration Vacuum



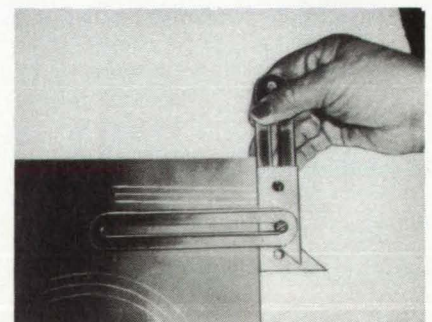
Advanced Purification Systems, Inc.
80 Raynor Ave., Ronkonkoma, NY 11779 (516) 467-2301
US toll free: 1-800-233-APSI Telex: 475-8154

"From Our Clean Room To Yours"™

Multipurpose Scribing and Drawing Tool

A multipurpose tool speeds up the laying out of patterns on sheet metal, wood, plastic, and paper. The tool consists of two elongated, flat, slotted parts with winglike protuberances that serve as cutters, pencil holders, and supports. It can be carried in a pocket, then quickly assembled for service as a height gauge, pair of dividers, protractor, surface gauge, or square (see figure). The parts are held together by a pair of screws and wingnuts in various configurations, depending on the function required of the tool. The user can thus easily and quickly change the configuration. The tool can be used as a scribe or with a pencil, depending on the material to be marked.

(See page 119.)



SQUARE

LEADER



Sometimes it's hard to go back for a scope!

60-MHz full-function field-service Attache Case Oscilloscope is so light and small it will be taken everywhere, every time.

LBO-325 packs all the power and performance of a cumbersome, backbreaking, 60-MHz workbench oscilloscope into an easy-to-carry, ultra-compact, featherweight unit. Although its 3½-inch CRT is as big and clear as screens on large field-service scopes—LBO-325 weighs only 9 lbs. So it won't weigh field-technicians down, no matter how far afield they go! LBO-325 is so small it fits inside a 3-inch deep attache case with room to spare for a multimeter, service manuals and some tools. The ideal full-function scope for a cramped work area or crowded bench.

Reduces the cost of service calls.

Time is money. A scope left in the vehicle takes time to retrieve. One kept in the shop causes repeat service calls. The LBO-325

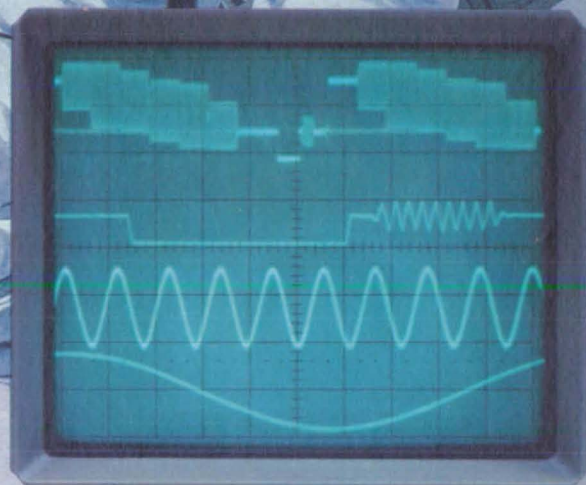
Attache Case Oscilloscope is so easy to carry and use, techs will take it everywhere, every time. And the time saved translates into extra profits for years to come.

Outperforms all other portables:

- 60 MHz • Dual channel • ALT TIME BASE simultaneously displays main waveform and any expanded portion
- ALT TRIG for stable display of 2 asynchronous signals • Bright, sharp 12-kV trace • Large 3½-inch PDA CRT • Illuminated graticule
- Comprehensive triggering • TV-V and TV-H sync separators • Variable trigger hold-off • Delay line shows sharp leading edges • CH-1 output drives low-sensitivity instruments
- Measures only 3 x 9 x 11½ inches • Weighs 9 lbs.

Two-year warranty.

Built tough to provide long use, LBO-325 is backed by Leader's 30-year reputation for reliability and by factory service depots on both coasts.



LBO-325 CRT is shown actual size.

Call toll-free
(800) 645-5104
In NY State
(516) 231-6900

Request an evaluation sample, our latest Test Instrument Catalog with over 100 outstanding products, the name and address of your nearest "Select" Leader Distributor, or additional information.

For professionals
who know the
difference.

LEADER
Instruments Corporation

380 Oser Avenue
Hauppauge, New York 11788
Regional Offices: Chicago, Dallas
Los Angeles, Boston, Atlanta
In Canada call Omnitronix Ltd.
(514) 337-9500

For Product Demonstration Circle RAC No. 443
For Product Information Circle RAC No. 444



HOW YOU CAN BENEFIT FROM NASA'S TECHNOLOGY UTILIZATION SERVICES



If you're a regular reader of TECH BRIEFS, then you're already making use of one of the low- and no-cost services provided by NASA's Technology Utilization (TU) Network. But a TECH BRIEFS subscription represents only a fraction of the technical information and applications/engineering services offered by the TU Network as a whole. In fact, when all of the components of NASA's Technology Utilization Network are considered, TECH BRIEFS represents the proverbial tip of the iceberg.

On the following pages, we've outlined NASA's TU Network—named the participants, described their services, and listed the individuals you can contact for more information relating to your specific needs. We encourage you to make use of the information, access, and applications services offered by NASA's Technology Utilization Network. You can save time and money by doing so.

HOW YOU CAN UTILIZE NASA'S **Industrial Applications Centers**

A nationwide network offering a broad range of technical services, including computerized access to over 100 million documents worldwide.

You can contact NASA's network of Industrial Applications Centers (IACs) for assistance in solving a specific technical problem or meeting your information needs. The "user friendly" IACs are staffed by technology transfer experts who provide computerized information retrieval from one of the world's largest banks of technical data. Nearly 500 computerized data bases, ranging from NASA's own data base to Chemical Abstracts and INSPEC, are accessible through the nine IACs, which are located throughout the nation. The IACs also offer technical consultation services and/or linkage with other experts in the field.

You can obtain more information about these services by calling or writing the nearest IAC. User fees are charged for IAC information services.

Aerospace Research Applications Center (ARAC)

Indianapolis Center for Advanced Research
611 N. Capitol Avenue
Indianapolis, IN 46204
John M. Ulrich, Director
(317) 262-5003

Kerr Industrial Applications Center (KIAC)

Southeastern Oklahoma State University
Station A, Box 2584
Durant, OK 74701
Tom J. McRorey, Director
(405) 924-6822

NASA Industrial Applications Center

823 William Pitt Union
University of Pittsburgh
Pittsburgh, PA 15260
Paul A. McWilliams, Executive Director
(412) 624-5211

NASA/Southern Technology Applications Center

State University System of Florida
307 Weil Hall
Gainesville, FL 32611
J. Ronald Thornton, Director
(904) 392-6760

NASA/UK Technology Applications Program

University of Kentucky
109 Kinkead Hall
Lexington, KY 40506-0057
William R. Strong, Program Director
(606) 257-6322

NERAC, Inc.

Mansfield Professional Park
Storrs, CT 06268
Daniel U. Wilde, President
(203) 429-3000

North Carolina Science and Technology Research Center (NC/STRC)

Post Office Box 12235
Research Triangle Park, NC 27709
James E. Vann, Director
(919) 549-0671

Technology Application Center (TAC)

University of New Mexico
Albuquerque, NM 87131
Stanley A. Morain, Director
(505) 277-3622

NASA Industrial Applications Center (WESRAC)

University of Southern California
Research Annex
3716 South Hope Street
Room 200
Los Angeles, CA 90007
Robert Mixer, Director
(213) 743-6132
(800) 642-2872 (CA only)
(800) 872-7477 (toll-free US)

Technology Application Team

Research Triangle Institute
P.O. Box 12194
Research Triangle Park, NC 27709
Doris Rouse, Director
(919) 541-6980

If you represent a public sector organization with a particular need, you can contact NASA's Application Team for technology matching and problem solving assistance. Staffed by professional engineers from a variety of disciplines, the Application Team works with public sector organizations to identify and solve critical problems with existing NASA technology.

A SHORTCUT TO SOFTWARE:

COSMIC®

An economical source of computer programs developed by NASA & other gov't. agencies.

Software developed by the U.S. government may be applicable to your needs. To tap this valuable resource, contact COSMIC, NASA's Computer Software Management and Information Center. Approximately 1600 computer programs and related documentation comprise the current library. New programs are announced in NASA Tech Briefs' Computer Programs section, a new tech brief category that premieres in this issue.

More information about COSMIC's services can be found on page 94, at the beginning of this section, or contact:

COSMIC®
Computer Services Annex
University of Georgia
Athens, GA 30602
John A. Gibson, Director
(404) 542-3265

HOW YOU CAN ACCESS TECHNOLOGY TRANSFER SERVICES AT NASA FIELD CENTERS:

Technology Utilization Officers & Patent Counsels

Each NASA Field Center has designated a Technology Utilization Officer and a Patent Counsel to facilitate technology transfer between NASA and the private sector.

If you need further information about new technologies presented in NASA Tech Briefs, you should request the Technical Support Package (TSP) that accompanies the brief. In the event that a TSP is not available, you can contact the Technology Utilization Officer at the NASA Field Center that sponsored the research. He can arrange for expert assistance in applying the technology by putting you in touch with the people who developed it.

If you want additional information about the patent status of a particular technology or are interested in licensing a NASA invention, contact the Patent Counsel at the NASA Field Center that sponsored the research. Be sure to refer to the NASA reference number at the end of the tech brief.

Ames Research Center

Technology Utilization Officer:

Laurance A. Milov
Mail Code 204.10
Moffett Field, CA 94035
(415) 694-5761

Patent Counsel:

Darrell G. Brekke
Mail Code: 200-11A
Moffett Field, CA 94035
(415) 694-5104

Goddard Space Flight Center

Technology Utilization Officer:

Donald S. Friedman
Mail Code 702.1
Greenbelt, MD 20771
(301) 344-6242

Patent Counsel:

John O. Tresansky
Mail Code: 204
Greenbelt, MD 20771
(301) 344-7351

Lyndon B. Johnson Space Center

Technology Utilization Officer:

William Chmylak
Mail Code AL32
Houston, TX 77058
(713) 483-3809

Patent Counsel:

Marvin F. Matthews
Mail Code: AL3
Houston, TX 77058
(713) 483-4871

John F. Kennedy Space Center

Technology Utilization Officer:

Thomas M. Hammond
Mail Stop: PT-TPO-A
Kennedy Space Center, FL 32899
(305) 867-3017

Patent Counsel:

James O. Harrell
Mail Code: PT-PAT
Kennedy Space Center, FL 32899
(305) 867-2544

Langley Research Center

Technology Utilization Officer:

John Samos
Mail Stop 139A
Hampton, VA 23665
(804) 865-3281

Patent Counsel:

Howard J. Osborn
Mail Code: 279
Hampton, VA 23665
(804) 865-3725

Lewis Research Center

Technology Utilization Officer:

Daniel G. Soltis
Mail Stop 7-3
21000 Brookpark Road
Cleveland, OH 44135
(216) 433-5567

Patent Counsel:

Gene E. Shook
Mail Code: 60-2
21000 Brookpark Road
Cleveland, OH 44135
(216) 433-5753

Jet Propulsion Laboratory

Technology Utilization Manager:

Norman L. Chalfin
Mail Stop 201-110
4800 Oak Grove Drive
Pasadena, CA 91109
(818) 354-2240

NASA Resident Office-JPL

Technology Utilization Officer:

Gordon S. Chapman
Mail Stop 180-801
4800 Oak Grove Drive
Pasadena, CA 91109
(818) 354-4849

Patent Counsel:

Paul F. McCaul
Mail Code: 180-801
4800 Oak Grove Drive
Pasadena, CA 91109
(818) 354-2734

George C. Marshall Space Flight Center

Technology Utilization Officer:

Ismail Akbay
Code AT01
Marshall Space Flight Center,
AL 35812
(205) 453-2223

Patent Counsel:

Leon D. Wofford, Jr.
Mail Code: CC01
Marshall Space Flight Center,
AL 35812
(205) 453-0020

National Space Technology Laboratories

Technology Utilization Officer:

Robert M. Barlow
Code GA-10
NSTL Station, MS 39529
(601) 388-1929

NASA Headquarters

Technology Utilization Officer:

Leonard A. Ault
Code IU
Washington, DC 20546
(202) 453-1920

*Assistant General Counsel for
Patent Matters: Robert F. Kempf*
Code GP
Washington, DC 20546
(202) 453-2424

IF YOU HAVE A QUESTION...

NASA Scientific & Technical Information Facility

If you have a general or specific question about NASA's Technology Utilization Network or its services and documents, you can contact the STI facility for assistance. The STI staff can answer your questions, supply documents and provide referrals to meet your needs. You can use the feedback card in this issue to contact STI directly.

NASA Scientific and Technical Information Facility

Technology Utilization Office
P.O. Box 8757
BWI Airport, MD 21240
Walter M. Heiland, Manager
(301) 859-5300, Ext. 242, 243

In Mathematical and Statistical FORTRAN Programming

IMSL Gets You to the Solution **Faster**

There is a faster way to get from problem to solution. A way to reduce development time, simplify maintenance, improve accuracy. A way to measurably increase productivity by selecting from hundreds of complete, fully tested mathematical and statistical FORTRAN subprograms:

IMSL subroutine libraries

Comprehensive, economical, and supported by the world's leading supplier of FORTRAN libraries for mathematics and statistics.

Calling a routine from an IMSL library is faster than writing it. It's a simple fact, but it can mean a big improvement in the productivity of both people and computers. It's why professional problem solvers in more than 60 countries have chosen IMSL libraries as their standard resource for FORTRAN programming. **IMSL libraries get you to the solution faster.**

Broad Scope.

IMSL libraries provide the most comprehensive selection of mathematical and statistical FORTRAN subprograms available. In almost any numerical programming application, IMSL libraries will meet your current and future needs with over 700 high-quality subprograms.

Standard User Interface.

Uniform calling conventions and documentation for all supported computer environments make IMSL libraries easy to learn and easy to use. Programs developed using IMSL libraries are much simpler to debug and maintain than programs containing undocumented, non-standard or unverified code.

Wide Compatibility.

IMSL libraries are affordably priced and compatible with most computing environments, from supercomputers to personal computers. Making IMSL libraries available on all of your computer systems can expand development flexibility and enhance application portability in your multiple-computer environment.

Comprehensive Support.

IMSL product support includes expert consultation, regular software enhancement, and maintenance. These services are performed entirely by IMSL personnel to ensure quality and consistency. IMSL's systematic, comprehensive support is the best way to protect the value of your software investment.

Accuracy and Reliability.

IMSL subroutines are designed, and exhaustively tested, for accuracy and reliability—and continually verified through thousands of hours of computation by customers around the world. Using IMSL libraries not only increases productivity, but can also enhance the accuracy and robustness of your programs and applications.

Return this coupon to:

IMSL Sales Division
2500 ParkWest Tower One
2500 CityWest Boulevard
Houston, Texas 77042-3020, USA.

Telephone: (713) 782-6060

Telex: 791923 IMSL INC HOU

**In the U.S. (outside Texas) call toll-free
1-800-222-IMSL.**

- ☐ The IMSL Library ☐ MATH/PC-LIBRARY
☐ SFUN/LIBRARY ☐ STAT/PC-LIBRARY

Name _____

Department _____

Title _____

Organization _____

Address _____

City _____

State _____

Postal Code _____

Area Code/Phone _____

Telex _____

Computer Type _____

NTB8603

IMSL®

Problem-Solving Software Systems

The IMSL Library **MATH/PC-LIBRARY**

STAT/PC-LIBRARY

SFUN/LIBRARY

Over 500 mathematical and statistical subroutines
Subroutines for mathematical applications (for IBM personal computers)
Subroutines for statistical analysis (for IBM personal computers)
Subprograms for evaluating special functions

(continued from page 19)

face. Using a synthetic aperture radar system, Magellan will, in effect, see through Venus' thick sulfuric acid and carbon dioxide cloud cover to produce photograph-like images of the surface with a resolution as fine as 1 km. As part of a trend toward reducing the cost of building scientific spacecraft, Magellan will incorporate spare parts from other JPL-built spacecraft, including the Viking orbiters, the Voyagers and Galileo.

A number of other space and planetary exploration missions are on deck at JPL, among them the Extreme Ultraviolet Explorer, which will conduct an all-sky survey of sources of extreme ultraviolet radiation. The Mars Observer mission will be the first installment in a series of low-cost Planetary Observer missions that use existing spacecraft designs and instrument technology to follow up on the investigations conducted by the Mariner, Pioneer and Viking spacecraft. The Mars Observer will focus on the Martian climate and soil.

Still in the planning stages at JPL is the Mariner Mark II-Comet Rendezvous/Asteroid Flyby (CRAF) mission.

Mariner Mark II denotes the next generation of NASA's exploratory spacecraft, which will allow the cost-effective study of objects in the outer solar system. Mariner Mark II spacecraft will adhere to a standard yet flexible design that accommodates a variety of instruments and a variety of mission objectives. The CRAF mission, when funded, will utilize a Mariner Mark II spacecraft to rendezvous with Comet Temple II, and then fly alongside it as the comet orbits the sun.

Diversity in Action

While JPL's primary function is deep space exploration—designing and building spacecraft, then tracking and controlling their missions—these are not the only activities in progress there. As its name implies, and as the tech briefs generated by JPL research and development projects testify, a great deal of innovative activity goes on across a broad spectrum of disciplines at the laboratory.

Much of the technology developed in connection with JPL's planetary exploration program is finding secondary applications in the fields of biomedicine, solar energy and robotics. For example, the computer image processing techniques used to generate the enhanced images of the planets

are being applied in medical diagnostics. The photovoltaic cells that were developed to provide electric power for orbiting spacecraft have been applied to the generation of electric energy on Earth. The technology associated with automated spacecraft systems has formed a base from which industrial and scientific applications of robotics and machine intelligence can be developed.

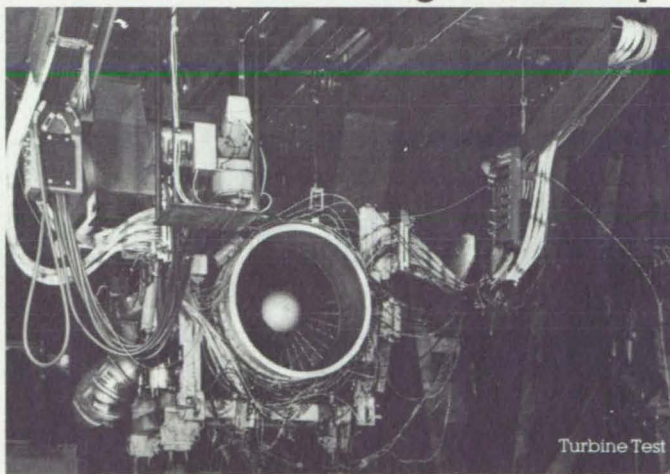
As a contractor facility, JPL is something of an anomaly among NASA's field centers. While the U.S. government owns, funds and monitors the facility, it is administered and staffed by CalTech employees, 5000 in all. About 75% of the laboratory's human resources are applied to NASA projects, with the remaining 25% allocated to specific projects coordinated through JPL's Defense and Civil Programs Office, which manages the biomedical- and energy-related research, as well as coordinating programs for the Department of Defense.

As diverse as the laboratory is, its most memorable accomplishments are undoubtedly those relating to its planetary exploration projects. Twenty-five years, 7 planets and 43 satellites later, JPL has introduced Earth to its neighbors near and far: Mercury, Venus, Mars, Jupiter, Saturn and now Uranus. Next stop, Neptune. □

Scanivalve Corporation: 30 Years of Pressure Scanning Leadership



Scanivalve Corporation has been the leading supplier of multiple point pressure scanning systems to the most advanced aerospace research facilities for nearly 30 years. Scanivalves are in use worldwide providing 0.06% accuracy while scanning 20 pressures per second for as little as \$50.00 per point. Many of our Scanivalve Systems have been in continuous operation for over 200,000 hours without failure, an outstanding record. Scanivalves are configured to automatically calibrate the transducer during each data scan. This provides the most accurate data possible, while at the same time eliminating the costly down time associated with manual recalibration of multiple dedicated transducers.



For applications that require very high speed pressure data, Scanivalve Corp. pioneered the design and manufacture of electronic pressure scanners. Features unique to our electronic pressure scanners include integral valving which allows calibration data to be obtained on demand, purging of input lines, and internal leak checks. These systems are capable of scanning up to 50,000 pressures per second, allowing virtually simultaneous pressure data "snap-shots" to be taken at any time during dynamic testing.

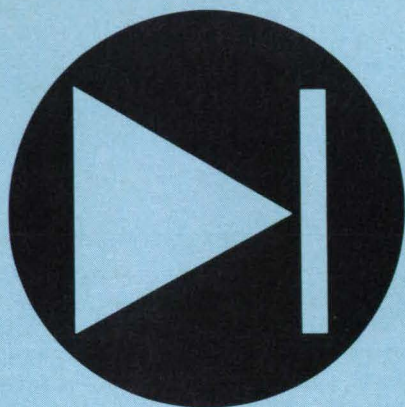
Scanivalve's pressure scanning systems have been imitated, but never equalled. For all of your pressure scanning needs, contact the originator of pressure scanning technology, SCANIVALVE CORPORATION.



Scanivalve Corporation

10222 San Diego Mission Rd / PO Box 20005 / San Diego, CA USA 92120 / (619) 283-5851 / Tlx 695023

Electronic Components & Circuits



Hardware, Techniques, and Processes

- 32 Adjustable Headband for Earphones
- 34 Linear Phase Modulator
- 38 Cross-Array Antenna With Switched Steering
- 40 Positive-Index Guiding in CDH-LOC Lasers
- 40 Bidirectional dc-to-dc Power Converter
- 42 Video Processor for Transponder Pulses
- 43 Lithium-Counterdoped Solar Cells
- 46 Ejection Mechanism for Circuit Boards
- 47 Broadband Ultrasonic Transducers
- 47 Correcting for Nonlinearity in a Photodetector
- 48 Improved High/Low Junction Silicon Solar Cell
- 49 A 25-kW Series-Resonant Power Converter

Adjustable Headband for Earphones

A new handband is designed for comfort and convenience.

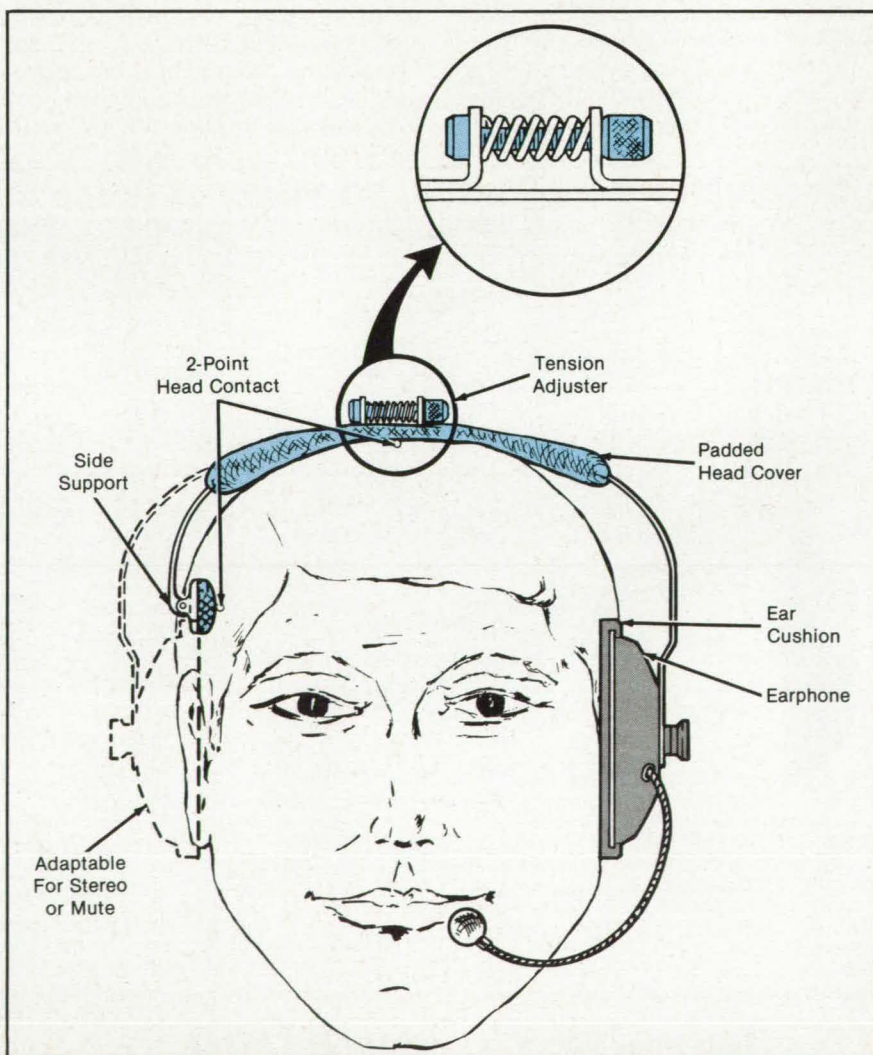
John F. Kennedy Space Center, Florida

A new headband holds an earphone and microphone on the wearer's head securely and comfortably. A wearer can easily adjust it for his or her own head size and can readily readjust it for greater comfort without removing it.

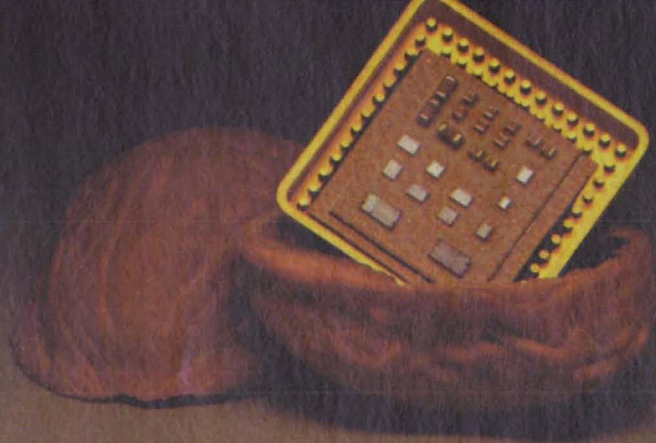
Unlike conventional headbands, which are essentially springs that clamp on the head over in an arc, the new headband contacts the head, lightly but firmly, at only two points, eliminating the headaches and soreness often caused by the conventional models. Moreover, the new headband can be adjusted more precisely to the individual's needs. Whereas a

wearer would adjust the width of a conventional headband in a coarse way by bending it, the new headband can be adjusted finely by a tensioning device.

The new band consists of a pair of steel head-clamping spring strips joined by the tensioning screw (see figure). A cushioned side support is mounted on the end of one strip, and a cushioned earphone and the microphone are mounted on the end of the second strip. The band is reversible; that is, the earphone can be worn on either the left or the right ear. The side support can be replaced by a second earphone for stereo listening or by an ear



The **Headband Contacts the Head** at only two points; at the top and above one ear and at the padded side support. It accommodates standard earphones and microphones.



IN A NUTSHELL, BOEING CAN HELP WITH MILITARY/AEROSPACE ELECTRONICS.

Last year alone, Boeing Electronics Company supplied over a quarter billion dollars worth of high quality electronics. We can handle the toughest electronics assignments in the industry.

For instance, we've produced some of the most sophisticated microcircuits available. Including thick-film hybrids and thin-film circuits.

We can provide everything from concept develop-

ment to packaging and design. And Boeing delivers what it promises — on time.

If you have a special requirement for micro-circuits, power supplies, ceramic circuit boards, controllers or avionics, give us a call.

Contact Boeing Electronics Company, P.O. Box 3707, M/S 9A-10, Seattle, WA 98124.

Or call (206) 575-5755.

Boeing Electronics Company
Reliability By Design

Circle Reader Action No. 414

mute for use in noisy surroundings.

The wearer adjusts the tension, tightening or loosening the knurled-head screw. This screw and a small, compressed coil spring cooperate to slide the head-clamping springs toward or away from each other. The wearer adjusts it while it is still on the head by turning the knurled

head, thereby compressing or loosening the spring. Various alternatives to the coil-spring adjuster are available, such as a bidirectional rotatable cylinder on a threaded shaft, a thumbscrew on sliding strips, or a rack-and-pinion arrangement.

This work was done by Pierce C. Toole, Howard E. Chalson, and Stephen Bussey

of Kennedy Space Center. For further information, Circle 104 on the TSP Request Card.

Inquiries concerning rights for the commercial use of this invention should be addressed to the Patent Counsel, Kennedy Space Center [see page 29]. Refer to KSC-11322.

Linear Phase Modulator

The circuit suppresses the AM component while providing a matched input impedance.

Lyndon B. Johnson Space Center, Houston, Texas

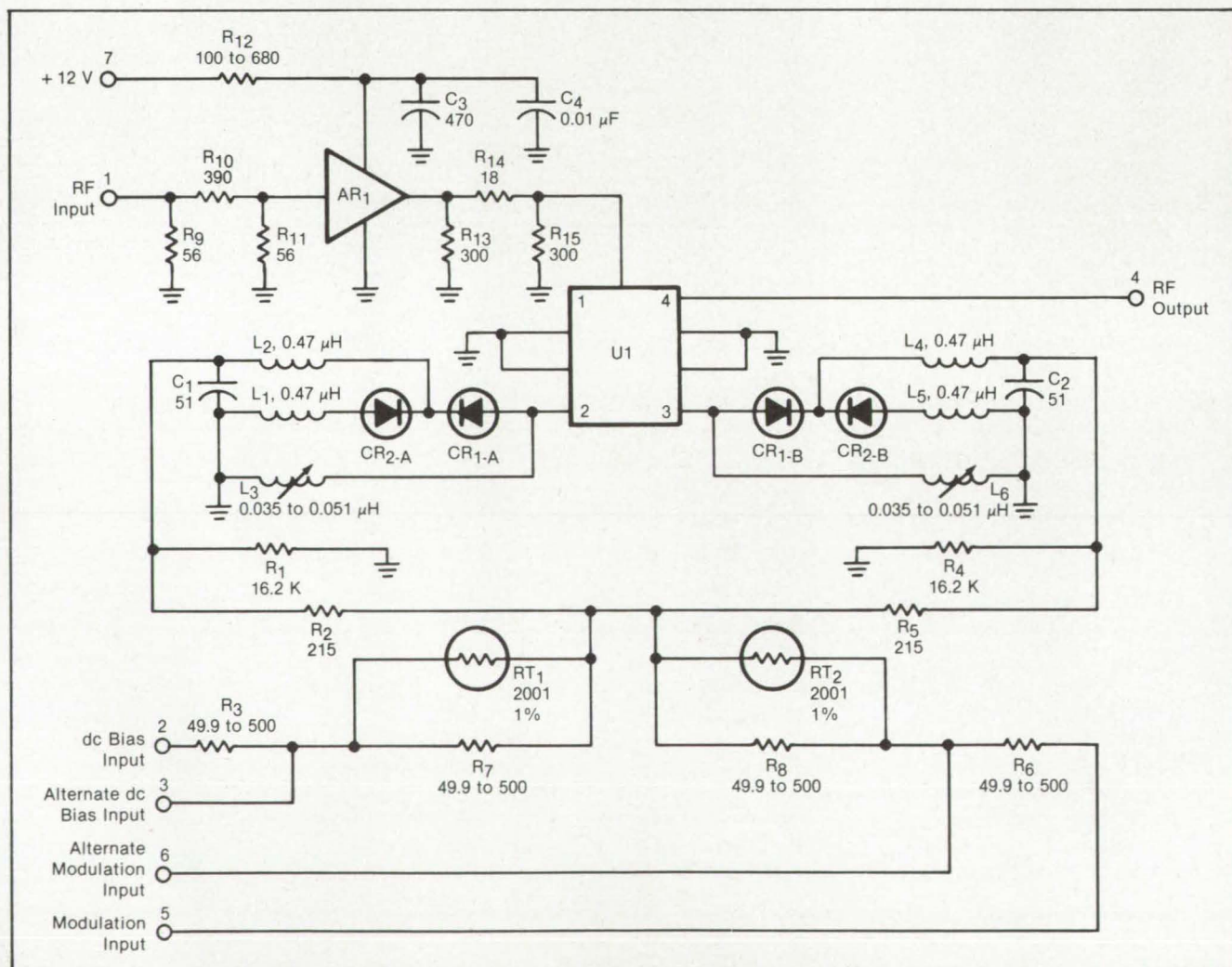
A linear phase modulator combines two shorted resonant circuits with a quadrature hybrid coupler to produce a matched input impedance and eliminate the amplitude-modulation (AM) component. Previous designs created a large AM component along with the phase-modulation component. The circuit, which was used in the payload integrator of the Space Shuttle S-band

communications and tracking equipment, should find application in other communications and tracking equipment.

The new phase modulation shown in the figure uses the reflective properties of a series resonant tank to reflect all of the signal except for a small amount in the unloaded Q of the coils and varactor diode. The circuit was designed to meet the follow-

ing requirements: operation at 320 MHz with the capability of modulating $\pm 36^\circ$ within ± 10 percent of the best-fit straight line with an AM component of less than 0.5 percent.

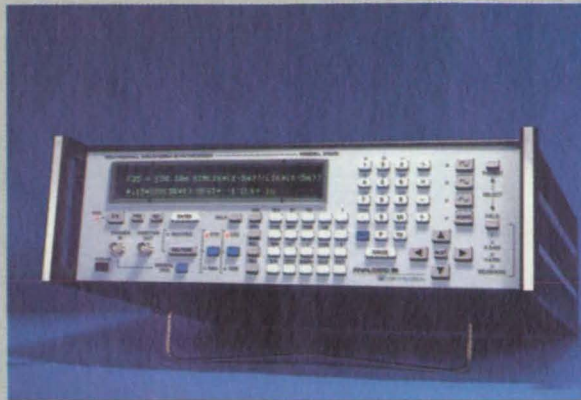
This work was done by Robert H. Hesse of TRW, Inc., for Johnson Space Center. For further information, Circle 33 on the TSP Request Card. MSC-20555



The 320-MHz Phase Modulator provides $\pm 36^\circ$ modulation while suppressing the AM component. The circuit also eliminates the input mismatch problems because of the matching capabilities of the balanced design using a quadrature coupler.



DATA 6000 Waveform Analyzer



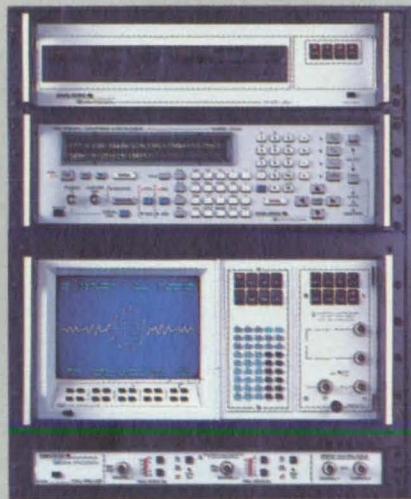
DATA 2020 Waveform Generator

Rule the Waves

Coming... or Going.

The DATA 6000 Universal Waveform Analyzer offers the ultimate in signal acquisition and on-board waveform analysis in one unit—without programming. Front panel commands are available for complex waveform operations, such as FFT and Correlation as well as scalar parameters such as Max., Min., Width, Rise, or PK-PK, using the display cursor and crosshair. For specialized measurements, the 6000 can also store analytical routines internally.

- Digitizing Plug-Ins from millihertz to 100MHz sample rates.
- An ultra-high dynamic range digitizing plug-in: 1MHz at 16 bits.
- Simultaneous multi-channel sampling with pre- and post-trigger transient capture.
- FFT (Magnitude and Phase), Convolution, Correlation, Waveform Average, Amplitude Histogram, etc.
- Direct plotter drive for HP-GL compatible plotters.
- Companion Model 681 Flexible Disk Drive for waveform and program storage.
- Full Programmability for ATE via IEEE-488 or RS-232 interface.



Combining the DATA 2020 and DATA 6000 yields an unbeatable system for signal acquisition, analysis and regeneration. Capture actual signals with the DATA 6000. They can then be modified or combined with other waveforms and down-loaded into the 2020 for regeneration. What was transient can become repetitive, available on call. Shown above, from top to bottom, are the 681 Flexible Disk, the DATA 2020, DATA 6000 and D-1000 Pre-Amplifier: products which give you the power to rule the waves both coming and going.

The DATA 2020 Polynomial Waveform Synthesizer provides an unprecedented ability to emulate real world signals, creating desired waveforms from mathematical definitions. Modify the ideal waveforms to add distortion, noise or glitches. Simulate degraded rise times, phase shifts . . . test the limits. Your systems and products must live in the real world. Emulate it with the 2020.

- Direct front panel or remote entry of mathematical equations of the form $Y=f(t)$.
- High-speed waveform generation—up to 25 megapoints per second at 12 bits (100 megapoints at 12 bits, optional).
- Large waveform output memory—up to 512K points, combined with non-volatile storage of hundreds of waveform equations.
- Standard Functions—sine, square, triangle with variable symmetry, plus white noise which can be summed with any signal.
- Arbitrary Mode including point entry, scope draw, and down-loading of the waveform memory.
- Full Programmability for ATE via IEEE-488 or RS-232 interface.

ANALOGIC®

DATA PRECISION®

HEADQUARTERS: DATA PRECISION, Division of Analogic Corporation, Electronics Avenue, Danvers, MA 01923. Tel: 617-246-1600. Telex: 6817144.

ANALOGIC Ltd., The Center, Weybridge, Surrey, England KT138BN. Tel: 0932-56011. Telex: 928030 ANALOG G.

ANALOGIC GmbH, Daimlering 2, 6200 Wiesbaden-Nordenstadt, W. Germany. Tel: 06122-4071. Telex: 4182587 ANA D.

See us at Southcon Show, Booth No. 1211

For additional information Circle RAC No. 432

For a demonstration Circle RAC No. 433



THE SKY WAS THE LIMIT.

AT&T has shattered the information barrier—with a beam of light.

Recently, AT&T Bell Laboratories set the world record for transmission capacity of a lightwave communications system—20 billion pulses of light per second. The equivalent of 300,000 conversations, sent 42 miles, on a hair-thin fiber of super-transparent glass. But that's really getting ahead of the story.

Actually, the 20-gigabit record is only one of a series of AT&T achievements in the technology of lightwave communications.

But what does that record mean?

The Light Solution To A Heavy Problem

All of us face a major problem in this Information Age: too much data and too little information. The 20-gigabit lightwave record means AT&T is helping to solve the problem.

For data to become useful information, it must first be quickly, accurately and securely moved to a data transformer—a computer, for instance. Getting there, however, hasn't always been half the fun.

Metallic pathways have a limited transmission speed, sensitivity to electrical interference and potential for interception—factors that reduce the effectiveness of today's powerful computers. Factors that are eliminated by lightwave communications technology.

Ten Goes Into One 20 Billion Times

Three primary components make up any lightwave communications system. On the transmitting end, a laser or light-emitting diode; on the receiving end, a highly sensitive photodetector; and in the middle, super-transparent glass fibers we call lightguides.

Installing these fibers is a major cost of a lightwave communications

system. So, once installed they should stay put—increased capacity should come from fibers carrying more, rather than from more fibers.

Which brings us to the 20-billion bit-per-second story—about experimental technology that has the potential to upgrade installed fiber to meet any foreseeable capacity needs.

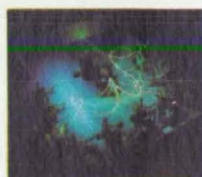
Using new, sophisticated lightwave system components, we multiplexed (combined) the outputs from 10 slightly different colored 2-billion bit-per-second laser beams into a single 20-billion bit-per-second data stream.

Playing Both Ends Against The Middle

But, let's start at the beginning—the 10 distributed feedback laser transmitters.

These powerful semiconductor lasers can be grown to produce light of different, but very precise, wavelengths. The lasers we used transmitted in the 1.55 micron (infrared) range, with only minuscule fractions of a micron between their wavelengths. The purity and stability of the beams let us pack their ten colors into the most efficient transmitting region of our single-mode, silica-core fiber.

To make the original 10 beams into one, a fiber from each laser was fed into a new lightwave multiplexer—a



20-gigabit
multiplexer

prism-like grating that exactly aimed each beam into the single transmission fiber. Over 42 miles later, a second grating fanned the beam back into its original 10 colors for delivery to 10 exceptionally sensitive avalanche photodetectors—receivers that convert the light pulses back into electrical signals and amplify them many times.

A similar avalanche photodetector

was the receiver when AT&T Bell Laboratories set the world record for unboosted lightwave transmission—125 miles at 420 million bits per second.

From Sea To Shining Sea

System capacity is important. But system reliability is vital. Especially when the system is going under 10 thousand miles of water—and is expected to last for 25 years.

AT&T is going to build the first lightwave communications system under the Atlantic Ocean. A similar system is planned for the Pacific. In 1988, laser beams traveling through two pairs of glass fibers will carry the equivalent of 37,800 simultaneous conversations overseas, underwater, from the U.S. to Europe and the Far East.

AT&T has manufactured and installed lightwave systems—as large as the 780-mile Northeast Corridor and as small as single-office local area networks—containing enough fiber to stretch to the moon and back. And the capacity of each network is tailored to meet the unique needs of its users.

Systems being installed in 1985 will be able to grow from 6,000 up to 24,000 simultaneous conversations on a single pair of fibers.

AT&T is meeting today's needs with lightwave systems that are growable, flexible and ultra-reliable. And anticipating tomorrow's needs with a whole spectrum of leading-edge lightwave communications technologies.



AT&T

The right choice.

Cross-Array Antenna With Switched Steering

Selected phase shifting of the feeds to antenna elements aims the antenna beam.

Lyndon B. Johnson Space Center, Houston, Texas

The aiming direction of a S-band cross-array antenna proposed for Space Shuttle use would be controlled in two dimensions by double-pole, double-throw switches in the antenna feeds. The switches would control the phasing of the antenna elements by transposing transmission-line delay elements between the feeds to pairs of elements located on opposite sides of the antenna.

The figure shows a 5-element antenna with 4 switches, capable of 16 different beam directions. The two switches in the feeds to antenna elements A and B control the horizontal component of the beam direction; the switches in the feeds to C and D, the vertical.

The angular separation between aim directions is determined by the spacing between the antenna elements and the amount

of phase shift from element to element at the operating frequency. Except for a small correction due to the directionality of the radiation pattern of the individual elements, the maximum gain of the antenna would occur in the direction in which all the elements contribute in phase. By turning off either or both of the outer pairs of elements, the beam pattern can be broadened along one or both axes.

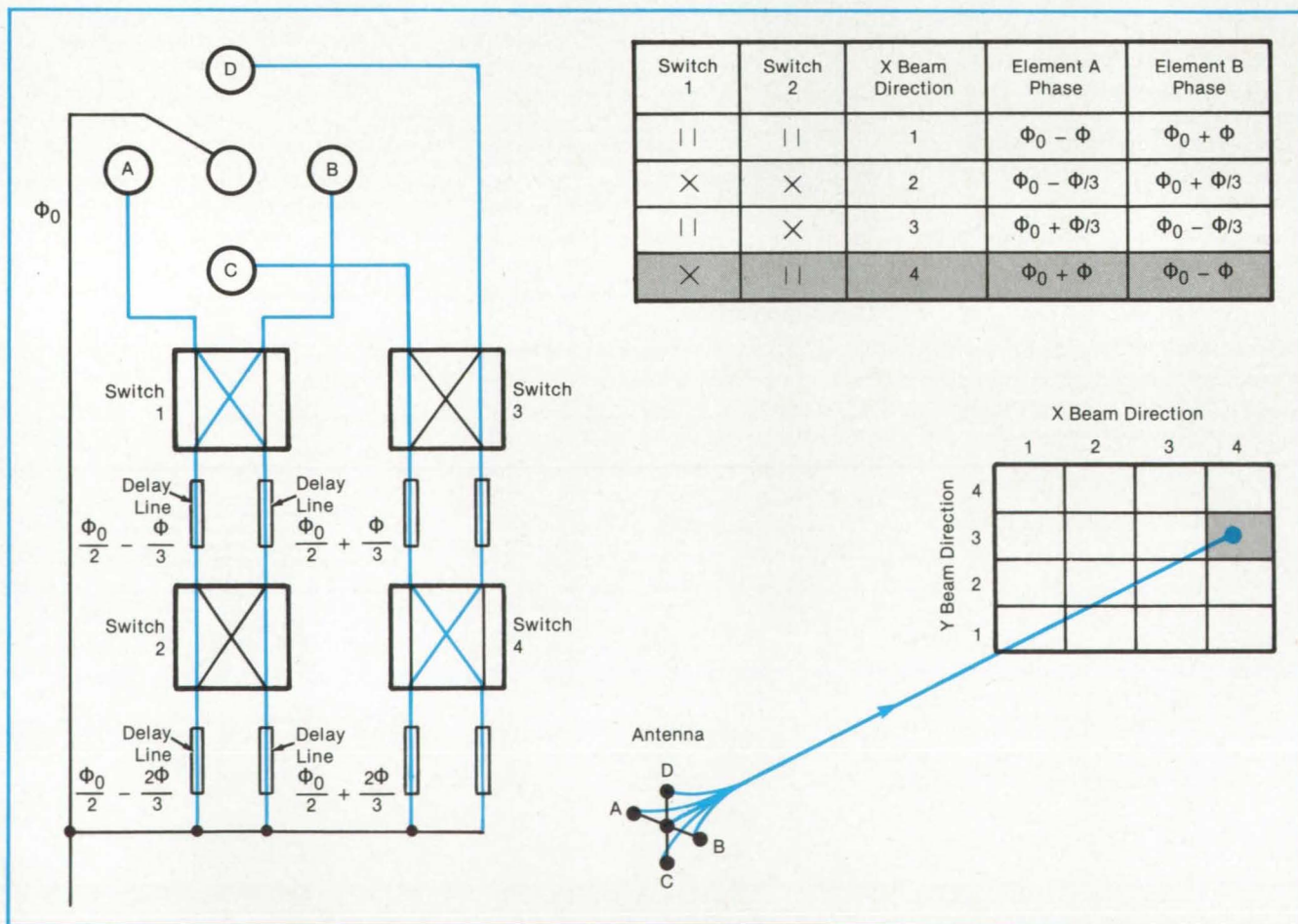
Each of the phase-changing switches has a 0.2-dB insertion loss. Since only the phase differences between the elements (but not the absolute phases) are significant, one element may be fed directly. Therefore, the total power loss is minimized by feeding the center element directly, since this element receives the feed of highest amplitude.

The number of switches and delay

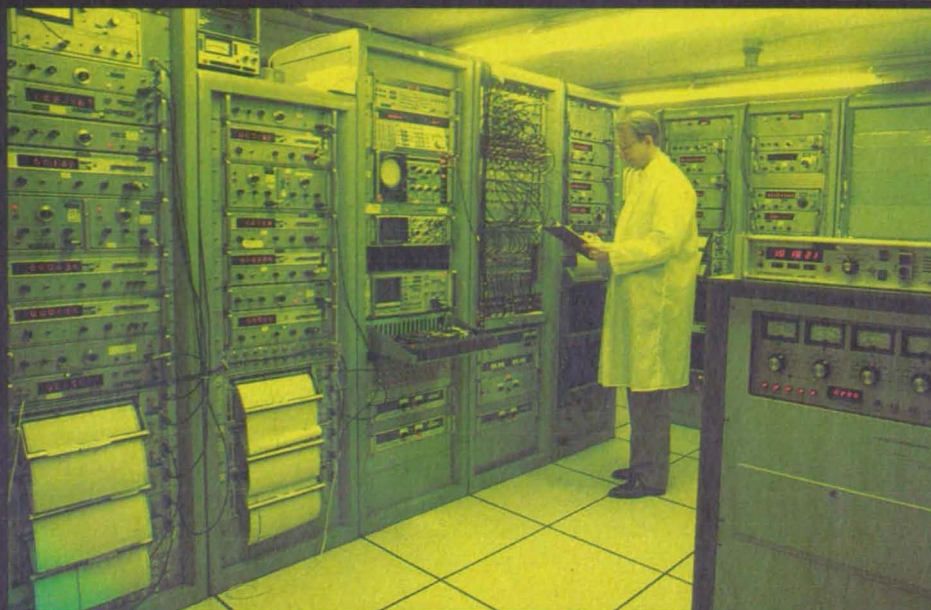
lines determines the number of different aim directions that will be available. For n switches, there can be up to 2^n aim directions, provided that appropriate delays are selected. While the example of the figure uses two switches in each feed axis, more or fewer than two can be used. Similarly, the same principles can be applied to antennas with additional elements along each axis.

For a configuration with n switches, an n -bit binary number suffices to specify the aim direction: Each bit represents the setting of one switch. A microprocessor could be used to control the switches.

This work was done by Richard S. Iwasaki of Axiomatrix for Johnson Space Center. For further information, Circle 55 on the TSP Request Card. MSC-20889



The **Five-Element Cross-Array Antenna** is shown in a 4-switch configuration. The table shows the phases (ϕ 's) obtained at elements A and B by setting switches 1 and 2. A similar table applies to switches in the feeds to elements C and D. For the switch settings shown in color, the antenna aims toward the shaded region in the perspective drawing.



AFFORDABLE CESIUM CLOCK ACCURACY ANYWHERE, ANYTIME.

Collins NAVCORE I™ GPS receiver today offers laboratories Coordinated Universal Time (UTC) calibration accuracy within 100 nanoseconds. • The low-cost NAVCORE I™ GPS receiver is designed to be integrated into a variety of time-based systems—making precision equipment calibration much more affordable than an expensive cesium clock. NAVCORE I™ receiver eliminates the need for periodic off-site synchronization or waiting for an outside calibration service. • The Collins single-channel NAVCORE I™ receiver uses the currently available Navstar GPS coarse/acquisition (C/A) code to instantly deliver precise time and frequency at any site. Today GPS time signals are available from 16-20 hours daily worldwide. Contact your time-frequency equipment supplier for information on how the NAVCORE I™ GPS receiver can fit your specific time or frequency needs, or for a list of manufacturers offering NAVCORE I™ receivers contact Collins Industrial GPS Products, Rockwell International, Cedar Rapids, Iowa 52498, U.S.A. (319) 395-3234, Telex 464-421.

COLLINS GPS



**Rockwell
International**

...where science gets down to business

Aerospace / Electronics / Automotive
General Industries / A-B Industrial Automation

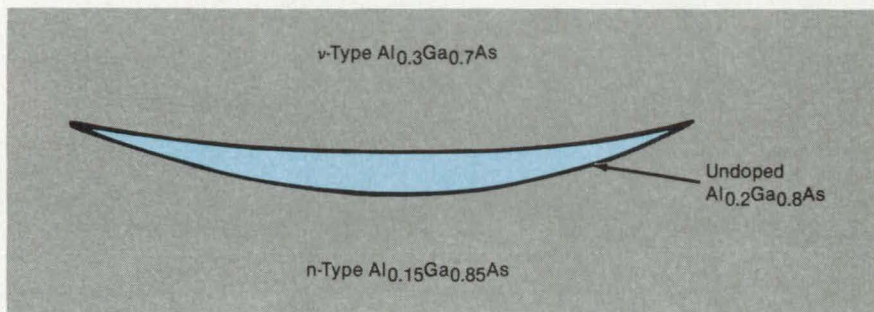
Positive-Index Guiding in CDH-LOC Lasers

A nonabsorbing passive region has beam-guiding capability.

Langley Research Center, Hampton, Virginia

A previous approach to a non-absorbing-mirror (NAM) constricted-double-heterojunction, large-optical-cavity (CDH-LOC) laser involved passive regions formed by etching and regrowth. Lateral mode control was to be provided in the passive region by lateral thickness variations of the guide layer. However, if the guide layer has the same shape in the passive region as in the active region (i.e., minimum thickness in its middle tapering laterally to larger thicknesses), light will be quickly dispersed in the passive region since the result is essentially an antiguiding structure without gain.

A new technique for providing positive-index guiding in the passive sections of NAM-CDH-LOC lasers consists of having two layers regrown: (1) a convex-shaped layer of an index of refraction close to that of the guide layer and of material that does not absorb the light generated in the active portion of the CDH-LOC structure and (2) the ν -type $\text{Al}_{0.3}\text{Ga}_{0.7}\text{As}$ burying material (see figure). The convex-lens-shaped $\text{Al}_{0.2}\text{Ga}_{0.8}\text{As}$ layer (see figure) provides positive-index guiding in the passive region. That occurs while the guide layer keeps the same shape in both the active and passive regions. By varying the Al concentration and thickness of the



The **Convex-Lens-Shaped Layer** has a refractive index higher than that of the surrounding material so that it serves as an optical waveguide.

regrown convex-lens-shaped layer, beam shaping can be achieved. The convex-lens-shaped layer could be of any material (for example, AlGaAs or InGaAsP) as long as its index of refraction is close to that of the guide layer so as to allow light spreading from the guide layer into the convex layer and as long as it does not absorb the light generated in the active section.

A semiconductor laser incorporating these principles was fabricated by sequential liquid-phase epitaxy deposition onto the surface of an n^+ -GaAs substrate wafer. After chemical etching and regrowth of the appropriate layers to obtain the convex-lens-shaped configura-

tion shown, individual laser chips were formed from the substrate wafer by cleaving through the burying region. A maximum output power of about 1.5 W was obtained with 100-ns pulses at a 1-kHz rate. This is about four times more power than is achieved for devices of this type not incorporating the passive region.

This work was done by Dan Botez of RCA Corp. for Langley Research Center. For further information, Circle 100 on the TSP Request Card.

Title to this invention has been waived under the provisions of the National Aeronautics and Space Act [42 U.S.C. 2457(f)], to the RCA Corp., Princeton, NJ 08540. LAR-13312

Bidirectional dc-to-dc Power Converter

A solid-state, series-resonant converter would use high-voltage thyristors.

Marshall Space Flight Center, Alabama

A conceptual solid-state, series-resonant dc-to-dc power converter would be used either to convert high-voltage, low-current dc power to low-voltage, high-current power or the reverse. It takes advantage of newly-available high-voltage thyristors to provide better reliability and efficiency than do traditional converters that use vacuum tubes as power switches: Vacuum tubes have short lifetimes, and the power required to heat their filaments reduces conversion efficiency. The new circuit uses no rotating ma-

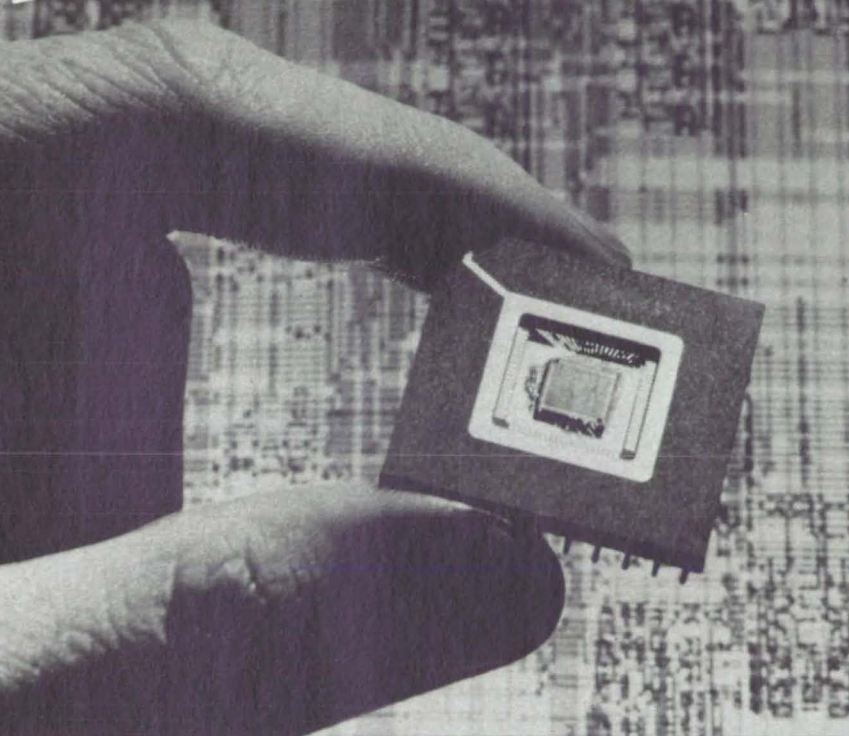
chinery, such as the motor/generator sets used in some converters. Having neither moving parts nor vacuum tubes, the new converter should be essentially maintenance free and should provide greatly increased mean time between failures. Converters of the new type should be attractive in industrial applications whether or not bidirectional capability is required.

The converter would be built of ten modules in parallel, each carrying a tenth of the total power. Except for the need to use pairs of thyristors in series on the

high-voltage side, the high- and low-voltage sides of the circuit are topologically equivalent (see figure). The only other things that distinguish the two sides of the circuit are the asymmetry in the turns ratios of the two transformers and, of course, the voltage and current ratings of the components.

In one mode, the converter would transmit power from the high-voltage side (4,000 to 5,240 V) to the low-voltage side (140 V). The converter could deliver as much as 120 kW to the low-voltage side in

**FOR THE WAR AGAINST
TIME AND SPACE**



HUGHES MILITARY VLSI PRODUCTS

HCMOS GATE ARRAYS

Three HCMOS array families distinguished by 3-micron, 2-micron, and VHSIC compatible processes featuring...

■ Wide ranging gate complexity:

H-Series 1.2k to 8k gates

V-Series 1.2k to 8k gates

U-Series 1k to 40k gates

■ Maximum 248 TTL or CMOS Input/output pins and over 16 mA drive capability per I/O.

■ Advanced design tools to accommodate easy placement and routing of advanced channelless structures.

■ Mentor or Daisy workstation support for efficient design development and convenient interface.

MILITARY PRODUCTS AND SERVICES

STANDARD PRODUCTS/SERVICES

EPROMs CMOS EPROMs originated at Hughes. Electrically erasable/programmable non-volatile memory, low-power operation and in-circuit programming.

ROMs Full range of high density, mask programmable CMOS ROMs. Single voltage supply, low quiescent operating power. Industry standard and 1802 compatible control architectures.

800 SERIES Full range of low-power microprocessors and peripherals.

LCD DRIVERS Industry's widest choice of CMOS liquid crystal drivers for both direct drive and multiplexed applications.

CUSTOMER-OWNED TOOLING Full service foundry. CMOS and PMOS processes. More than 25 variations. Select proximity, projection or DSW alignment techniques.

CUSTOM CIRCUITS

At the forefront of CMOS technology since the late 1960s, Hughes offers multiple CMOS processes, all available for custom circuit designs. Unique combinations of digital, analog and EPROM may be included in a single chip. In-house capabilities include design, layout, mask making, wafer fabrication, assembly, test and screening.

FOR QUICK ANSWERS AND COMPLETE INFORMATION,

write or call Hughes Semiconductor Division, 500 Superior Avenue, Box H, Newport Beach, CA 92658-8903; (714) 759-2727; TWX 910/596-1374.

Circle Reader Action No. 449

HUGHES

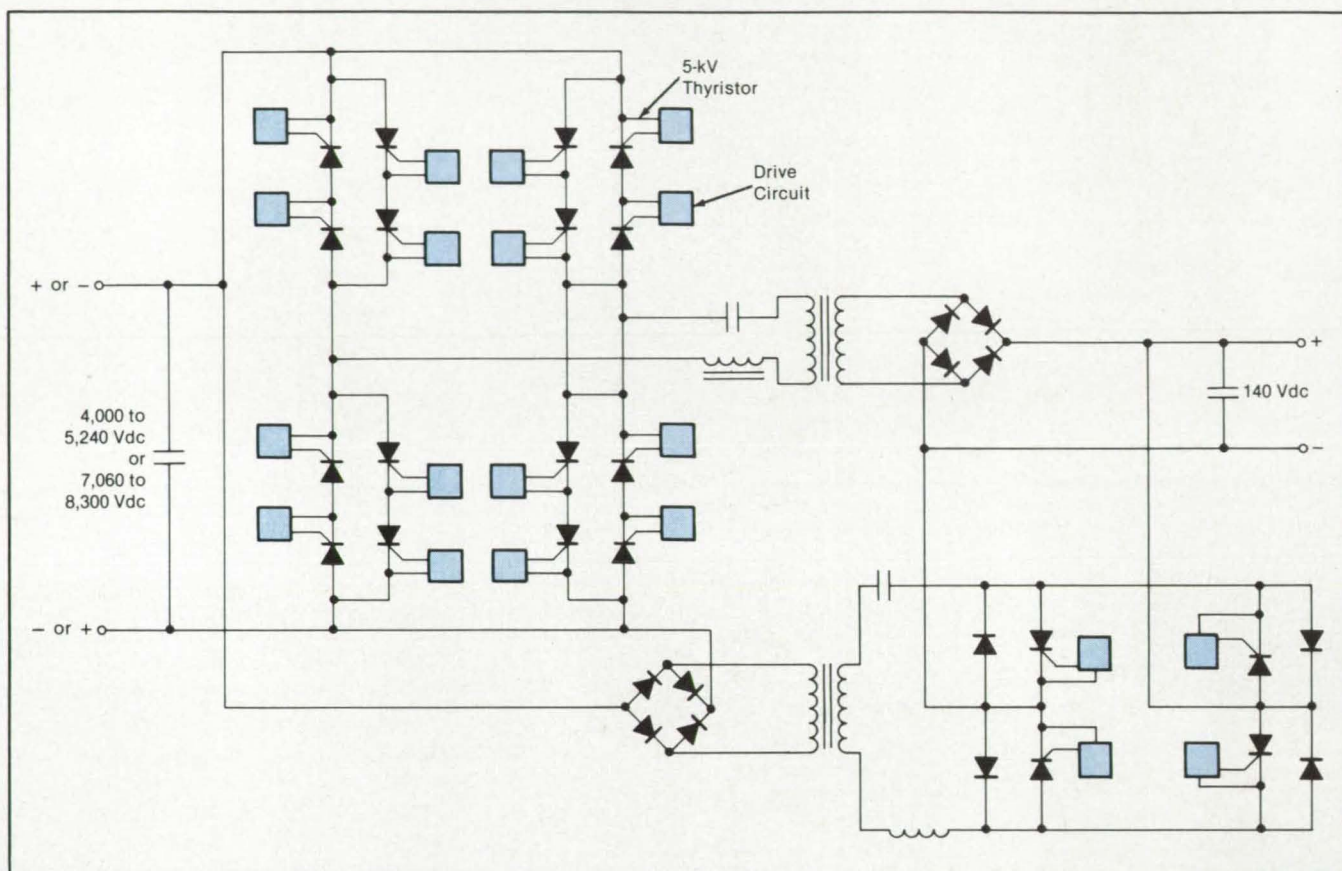
AIRCRAFT COMPANY

SEMICONDUCTOR DIVISION
Industrial Electronics Group

this mode. In the opposite mode, the converter would transfer power from the low- to the high-voltage side, delivering as much as 331 kW at 7,060 to 8,300 V. The anticipated conversion efficiency is 94 per-

cent. The transition between the two modes would be gradual; that is, the amount of power transferred in either direction would be continuous from one extreme to the other.

This work was done by Carl R. Griesbach of Martin Marietta Corp. for Marshall Space Flight Center. No further documentation is available.
MFS-28095



A Bidirectional dc-to-dc Power Converter with no moving parts or vacuum tubes can be constructed using newly-available high-voltage thyristors.

Video Processor for Transponder Pulses

A circuit helps determine whether pulses are from the main lobe of a radar beam.

John F. Kennedy Space Center, Florida

A circuit detects interrogation signals from an air-traffic-control station and helps to determine whether the transponder of an airplane should respond. The circuit examines the relative magnitudes of the first two pulses in the three-pulse sequence of an interrogation signal. On the basis of the relative magnitudes, the circuit decides whether the main lobe of the interrogating radar beam has been received (and a response should be generated) or whether only a side lobe has been received (and the interrogation should therefore be ignored). The circuit differs from previous circuits for distinguishing the main lobe from the side lobe in that it is simple and inexpensive.

The new circuit is used in conjunction with a scheme for reducing clutter on the radar screens viewed by air-traffic controllers. The ground radar transmits a special side-lobe suppression pulse with other pulses during interrogation. An interrogation pulse train consists of a sequence of three pulses: P_1 , P_2 , and P_3 . Pulses P_1 and P_3 are transmitted by a directional antenna, and the side-lobe suppression pulse P_2 is transmitted by an omnidirectional antenna.

If P_2 is greater than or about equal to P_1 , the transponder should not reply, since it has received only a side lobe of the interrogating beam. When pulse P_1 is at least 9 decibels greater than P_2 , how-

ever, the transponder has been directly addressed by the beam and should reply.

An intermediate-frequency transformer converts the received signals to levels suitable for driving a diode in a detector (see figure). The detector generates positive pulses for all pulses received from the ground station. The detected pulses are fed to the base of a transistor Q_1 .

Pulse P_1 turns on this transistor, thereby turning on transistor Q_2 , which is connected by its base to the collector of Q_1 . When Q_2 turns on, it applies a dc voltage to resistor R_4 , thereby charging capacitor C_4 to about the voltage of P_1 and sending an output pulse to the logic circuitry

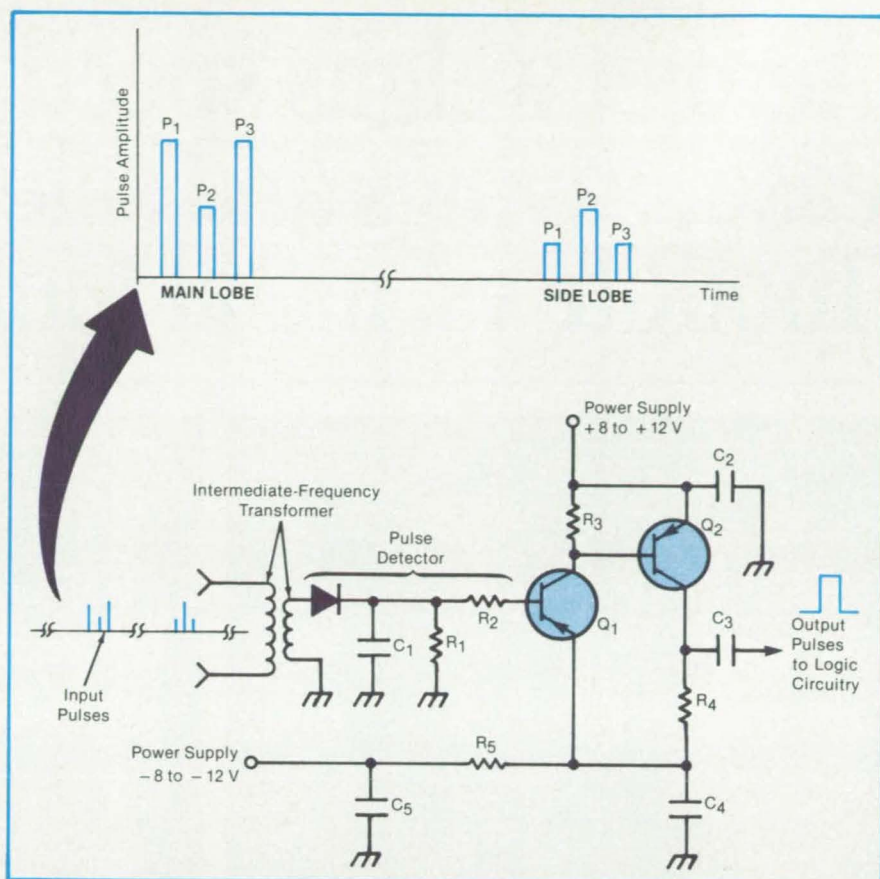
through capacitor C_3 .

At the end of P_1 , the transistors return to their off state, while C_4 slowly discharges through resistor R_5 , with a time constant considerably greater than the interval between the pulses in one sequence. Pulse P_2 arrives shortly but does not activate Q_1 unless the pulse amplitude exceeds the voltage remaining on the capacitor from P_1 . Thus, if P_2 is less than P_1 (indicating the main lobe), the transistors remain off, and a second pulse is not sent to the logic circuitry. The logic circuitry interprets the lack of a second pulse as an instruction to transmit the response code.

If, however, P_2 is greater than the capacitor voltage remaining from P_1 (indicating a side lobe), it turns on Q_1 , which then produces a second output pulse. The logic circuitry interprets the two-pulse sequence as an instruction not to transmit the response code.

This work was done by Frank Byrne of Kennedy Space Center. For further information, Circle 78 on the TSP Request Card.

This invention has been patented by NASA (U.S. Patent No. 4,540,986). Inquiries concerning nonexclusive or exclusive license for its commercial development should be addressed to the Patent Counsel, Kennedy Space Center [see page 29]. Refer to KSC-11155.



The **Pulse-Processing Circuit** determines whether the amplitude of pulse P_2 exceeds that of pulse P_1 . If so, the circuit puts out a double pulse that a logic circuit interprets to mean that a valid interrogation signal has not been received.

Lithium-Counterdoped Solar Cells

Resistance to damage by energetic electrons is increased.

Lewis Research Center, Cleveland, Ohio

Future space missions will require increased end-of-life output power from solar-cell arrays. To achieve this goal, researchers have been seeking ways to minimize the degrading effects of space radiation on solar cells. A new technique has been demonstrated using an n^+p silicon solar cell with a boron-doped p -type base counterdoped with lithium. Lithium is an n dopant in silicon. However, in the present case, the lithium is introduced in small enough quantities so that the cell base remains p -type. The purpose is to increase the radiation resistance of the silicon cells currently used to supply electrical power to spacecraft. Since cell performance can be partially restored after radiation damage, by annealing, a second purpose is to reduce the annealing temperature substantially lower than that currently required to restore performance in

conventional n^+p silicon solar cells.

The prior-art lithium-doped p^+n silicon solar cells have shown no improvement in radiation resistance, over conventional n^+p silicon cells, when exposed to 1-MeV electron irradiations. Such irradiations are the industry laboratory standard utilized to test solar cells for use in space. Also, the prior-art conventional n^+p boron-doped silicon solar cells have the disadvantage of requiring annealing temperatures of 400°C or higher. At this temperature, irreversible damage to solar-cell-array components occurs. This precludes the possibility of in situ annealing in space, which, if it were possible, would extend the useful space lifetime of solar-cell arrays in space.

It has long been recognized, by workers in space photovoltaics, that p -type silicon is innately more radiation-

resistant than n -type silicon. Since most of the radiation damage occurs in the cell base region, the present n^+p lithium-counterdoped silicon solar cell retains the increased-radiation-resistance feature of the p -type base with the added advantage offered by lithium, which tends to increase further the radiation resistance of the cell. Hence, the present invention is more radiation-resistant than the conventional n^+p boron-doped silicon cell currently used in space. This is demonstrated in the figure, where the lithium-counterdoped cells can be seen to produce more output power than the presently-used, conventional n^+p silicon cells, after irradiation by MeV electrons.

In addition to possessing increased radiation resistance, the lithium-counterdoped silicon solar cells show significant performance restoration when

Aerojet weighs speed, ease, savings and safety of ToolRite vs. metal tooling



17 lbs.

This ToolRite fixture simplifies handling, permits snap curing.



980 lbs.

Parts on this heavy steel tool take almost 40% longer to cure.

Steel tooling can put a burden on a development schedule, and on the corporate bankroll, as well as on the people who have to lug the heavy fixtures in and out of an autoclave.

This is what Aerojet Strategic Propulsion Company is finding as it studies the advantages of a new prepreg composite tooling system—the ToolRite System, from Fiberite.

Its study is part of an ongoing effort—as a primary contractor of solid propellant rocket motors—to maintain leadership in the use of advanced composite materials.



For components such as this flexseal shim for a rocket motor exit cone, Aerojet projects faster prototype development and greater dimensional stability—in addition to tool room, production floor and capital cost advantages.

"We're looking at tooling methods and materials more compatible with the materials we design for and the components we produce," says Paul Vasterling, in charge of advanced tooling concepts at Aerojet.

"We're looking at tooling that's more compatible with the materials we design for and produce."

*Paul Vasterling
Manager
Advanced Tooling Concepts*

Potential benefits of the ToolRite System include lower scrap rate, easier validation, and averting the need for an additional autoclave.

ToolRite: the new way to mold prepregs— with a tool made from prepregs

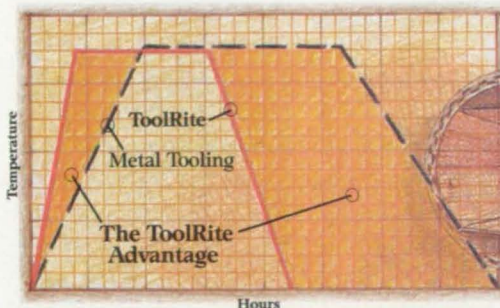
"But, looking at the big picture, from the drawing board to the finished part," says Ritch Hollingsworth, Senior Manufacturing Engineer, "the main advantage is speed."

First, by allowing Aerojet to build tooling for its prototype parts on plastic-faced plaster masters, the ToolRite System helps trim down the waiting time for tooling late in the project schedule. "It's nice to be able to get a tool 3 or 4 weeks quicker," Hollingsworth says.

*"Looking at the big picture
...the main advantage
is speed."*

Ritch Hollingsworth
Senior Manufacturing
Engineer

Reducing tool mass 98%, compared with the steel tooling, allows Aerojet to greatly reduce its ramping and curing times, opening the opportunity for snap cure resin systems. Snap curing brings a tool and part very rapidly up to a critical temperature, at which the system will cure quickly. Steel tools, slow to heat up because of their mass, prolong the exposure of the resin system to lower temperatures and allow it to degrade.



ToolRite System prepreg composite fixtures absorb heat quickly and evenly. This permits snap curing, not possible with steel tools. Shorter cure cycles save on tool inventory, make better use of work force, and may avert the need for an additional autoclave.



The ToolRite System permits low temperature cure on a plastic-faced master and free-standing post-cure. Part validation covers the tool and plaster master as well.

As a result of shorter cure cycles—perhaps as much as 40% shorter—you can get your tools back into use faster, and not tie up the autoclave so long.

Then there is the money ToolRite saves you in handling equipment—carts and cranes. The added safety of lighter tools. And easier, more efficient storage.

For rate production, you can pull additional tools from the ToolRite plaster-faced master economically, with fewer validation steps than when you have to re-machine a new metal tool. (Free-standing post-cure, possible with ToolRite, preserves your plaster master for repeated use.)

Dimensional stability compared with metal tooling is another big advantage. Because the ToolRite

System prepregs follow the same heat-up/cool-down curves as the parts curing on them, you can virtually eliminate parts distortion and cure stress.

Compared with wet lay-up, ToolRite prepreg composite tooling means: less labor, less mess and hazardous fumes, greater control of resin content and fiber placement, longer open time, and improved vacuum integrity for up to 500% longer tool life.

Using the ToolRite System is a thoroughly documented procedure, backed by complete factory support from Fiberite. May we arrange a technical briefing for your management, and a shop floor demonstration? Call Kris Ralph at (714) 639-2050 and describe your project. Or send this coupon.

☐ Please send me a copy of your brochure showing step-by-step tool fabrication procedures using ToolRite Prepreg System. I am considering ToolRite materials for the following areas:

- | | |
|--|---|
| <input type="checkbox"/> Commercial Aircraft | <input type="checkbox"/> Missiles/Rockets |
| <input type="checkbox"/> Military Aircraft | <input type="checkbox"/> Recreational |
| <input type="checkbox"/> Helicopters | <input type="checkbox"/> Thermoforming |
| <input type="checkbox"/> Satellites/Space Vehicles | <input type="checkbox"/> Other _____ |

Name _____

Title _____

Firm _____

Address _____

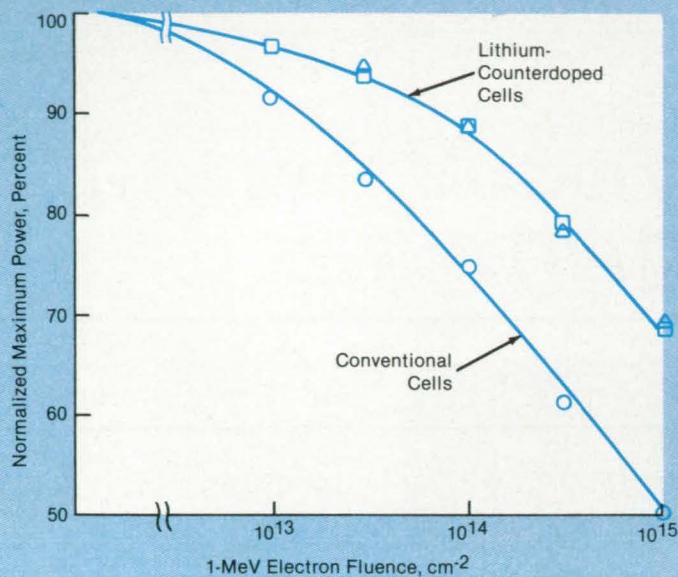
City, State, Zip _____

Telephone _____ / _____

Application _____

Mail to: Michael A. Edwards,
Fiberite, 501 West 3rd Street,
Winona, MN 55987

FIBERITE®
AN ICI COMPANY



The Performances of Lithium-Counterdoped and Conventional cells are compared after irradiation with 1-MeV electrons.

annealed at a temperature of 100° C. The conventional silicon cells now used in space require annealing temperatures of 400° C, or higher, to remove the radiation-induced degradation. Components of solar-cell arrays now used in space, such as adhesives, degrade irreversibly at this high temperature and will not degrade at 100° C. Thus, the present lithium-counterdoped solar cell offers the potential for in situ annealing in space, a process that would increase the electrical power available from the solar-cell array during its use in space missions subject to the degrading particulate environment of space.

This work was done by Irving Weinberg and Henry Brandhorst of **Lewis Research Center**. Further information may be found in "Increased Radiation Resistance in Lithium Counterdoped Silicon Solar Cells." To obtain a copy, Circle 6 on the TSP Request Card.

Inquiries concerning rights for the commercial use of this invention should be addressed to the Patent Counsel, Lewis Research Center [see page 29]. LEW-14177

Ejection Mechanism for Circuit Boards

Damage to connectors is reduced and special tools are not needed.

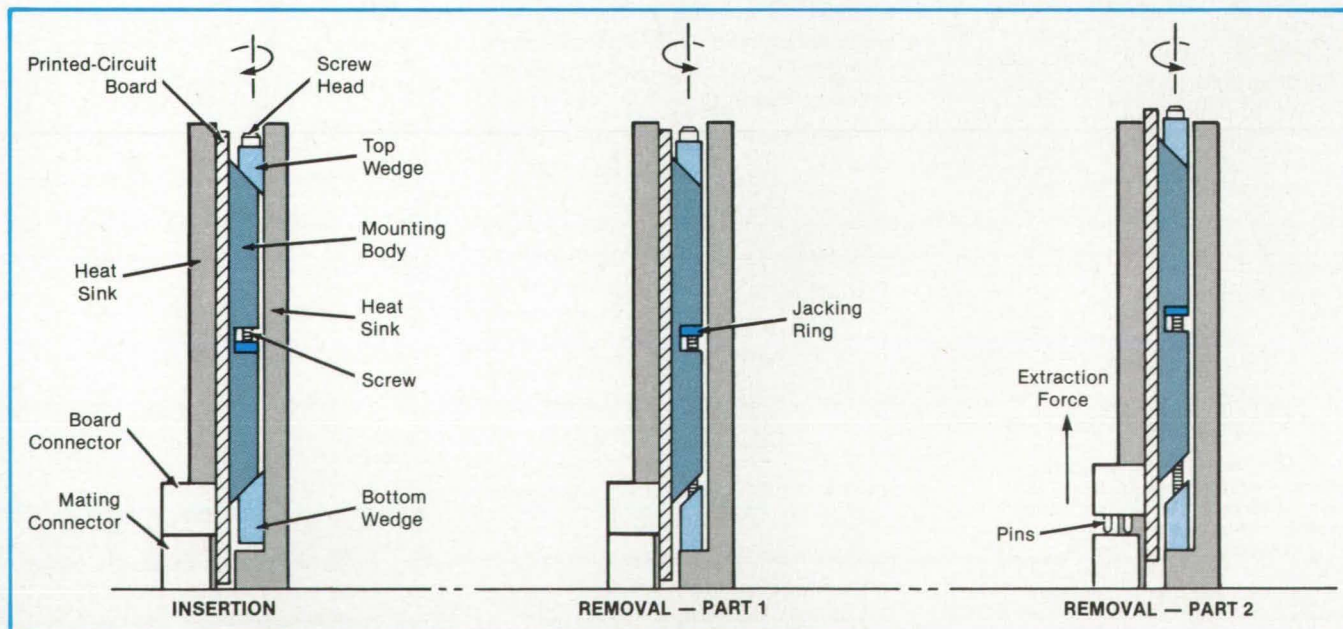
Lyndon B. Johnson Space Center, Houston, Texas

A mechanism attached to a printed-circuit board partially ejects the board from an electronics assembly so that an

operator can remove it for repair or replacement. A pulling tool, which could damage circuit patterns and compo-

nents, is unnecessary.

A screw in the mechanism is turned to produce a jacking force that disengages



Clockwise Rotation of the Screw Tightens the Wedges against the mounting body and the right heat sink. Counterclockwise rotation of the screw drives the bottom wedge downward and the jacking ring upward, pulling the pins away from the mating connector.

the board from its mating connector. The force is parallel to the connector pins so that they do not become bent or broken. When disengaged, the board protrudes from the assembly and can readily be grasped by the operator.

The retainer/extractor screw, along with top and bottom wedges, is inserted in a mounting body, which is crimped onto the circuit board (see figure). To fasten the circuit board in a board frame, the operator inserts the board in the frame between two heat sinks, then turns the

screw clockwise. The screw motion forces the wedges toward each other and against the wedging surfaces on the mounting body. This pushes the board against the left heat sink, and the wedges against the right heat sink, thereby locking the board in place and assuring thermal contact between the board and the heat sinks.

To remove the board from the frame, the operator turns the screw counterclockwise. This action drives the wedges away from the mounting body. Continued

turning of the screw thrusts the bottom wedge against the frame and pushes the jacking ring upward against the mounting body. The ring thus raises the circuit board away from the frame and disengages it from the connector.

This work was done by Takeshi L. Houff and Douglas Shinno of Hughes Aircraft Co. for Johnson Space Center. For further information, Circle 70 on the TSP Request Card.

MSC-20763

Broadband Ultrasonic Transducers

A new geometry spreads out the resonance region of a piezoelectric crystal.

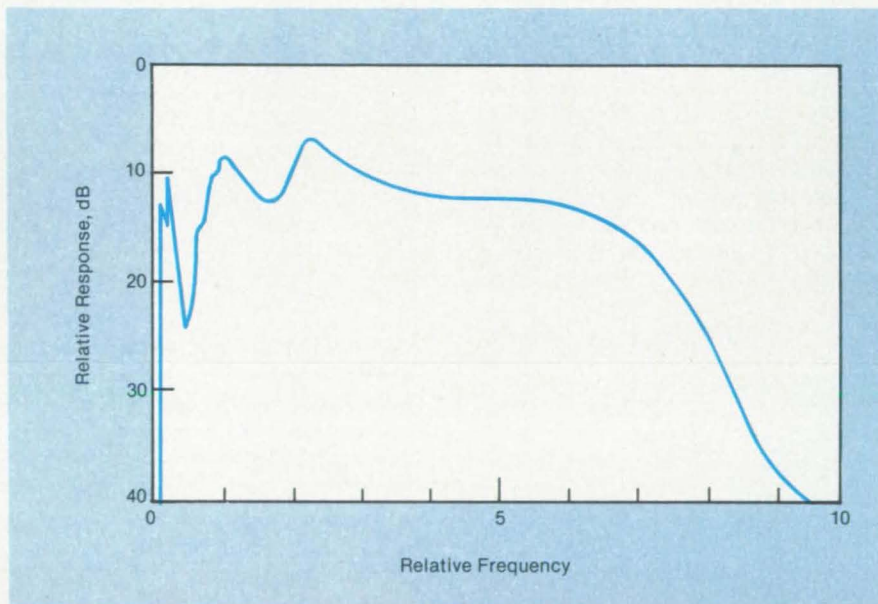
NASA's Jet Propulsion Laboratory, Pasadena, California

The bandwidth of a piezoelectric transducer can be greatly increased by fabricating the transducer with a nonuniform thickness. The greater bandwidth improves the accuracy of sonar and ultrasonic imaging equipment.

A conventional piezoelectric transducer consists of a crystal disk with metal films on its two flat, parallel surfaces. Applying an alternating electrical potential to the films expands and contracts the crystal rapidly so that it launches compressional elastic waves into the material around it. With its parallel faces, the crystal resonates at a narrow range of frequencies, and the ultrasonic waves it sets up in the surrounding medium have essentially the same narrow range.

In the new transducer, the crystal surfaces are made nonparallel. One surface may be planar; and the other, concave, for example. The geometry can be designed to produce a nearly uniform response over a predetermined band of frequencies and to attenuate strongly the frequencies outside the band (see figure).

The new transducer may make it unnecessary to use signal-processing circuits to compensate for the transducer frequency response or to use auxiliary



The **Frequency Response of a Plano-Concave Transducer** covers a broad range. The steep sides of the response curve show that the transducer cuts off extraneous frequencies cleanly.

circuits to modify the frequency spectrum of the voltage applied to the crystal. Such circuits would add to the cost of the transducer system.

This work was done by Richard C.

Heyser of Caltech for NASA's Jet Propulsion Laboratory. For further information, Circle 50 on the TSP Request Card.

NPO-16590

Correcting for Nonlinearity in a Photodetector

A simple positive-feedback circuit would vary the bias voltage as necessary.

NASA's Jet Propulsion Laboratory, Pasadena, California

Positive feedback is proposed for compensating for the internal series resistance of a photoconductive detector. The feedback would ensure that the detector-

circuit output current varies linearly with the photon flux. The principle can be applied

to linearizing mercury cadmium telluride infrared detectors in Fourier-transform spectrometers and other spectral and imaging instruments.

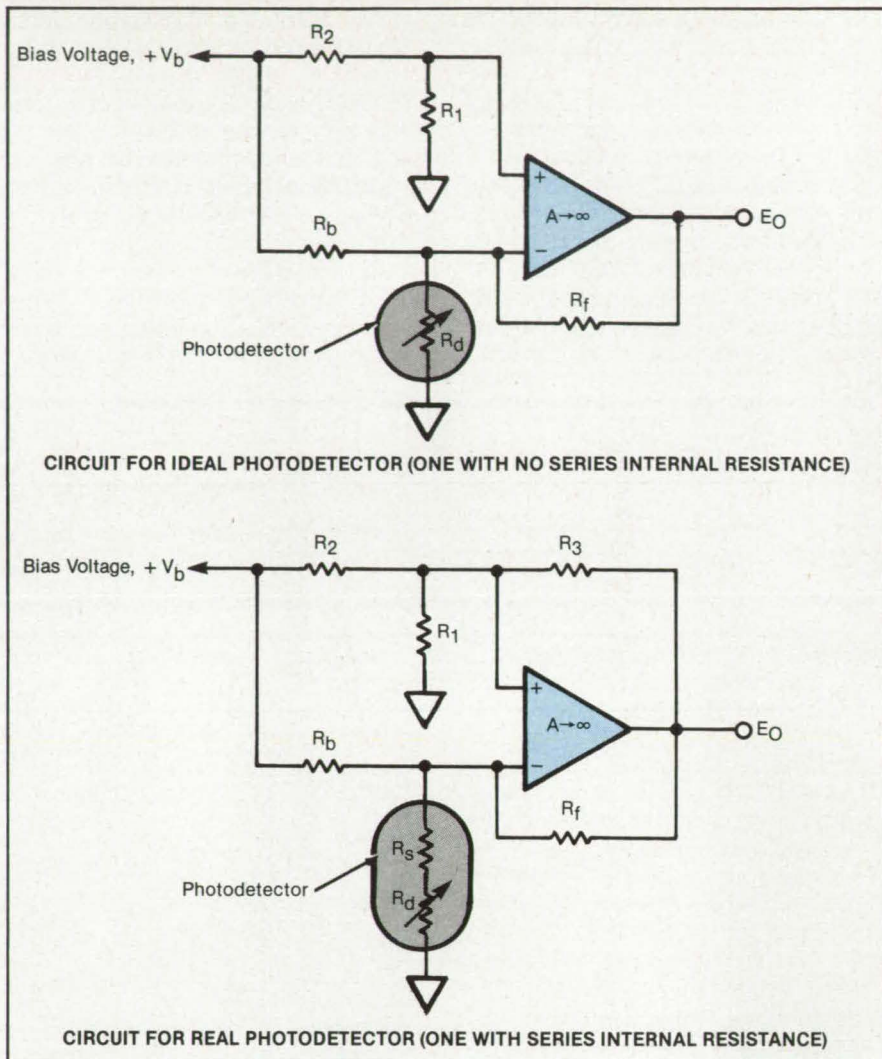
In an ideal photoconductive detector with no internal series resistance, the conductivity is proportional to the incident photon flux. If this ideal detector is biased with a constant voltage, the detector current is proportional to the photon flux plus a constant offset. Such a detector could be connected between an inverting input and ground (see top of figure), and feedback from an operational amplifier through feedback resistor R_f would make the voltage at the inverting input equal to that at the noninverting input. The bias voltage would thus be held constant.

A real photoconductive detector, however, contains an internal series resistance R_s so that the detector conductance no longer varies linearly with the photon flux. Adding a resistor R_3 to the circuit, as shown in the lower half of the figure, allows positive feedback to biasing resistors R_1 and R_2 . This feedback increases the detector bias voltage as the flux increases and opposes the effect of R_s . The value of R_3 can be selected so that the positive feedback is just enough to balance out the nonlinear effect of R_s , thereby making the output voltage E_o vary linearly with the photon flux. This value is given by

$$R_3 =$$

$$\frac{R_f R_1 R_2}{R_s R_b}$$

$$\frac{R_s + R_b}{R_1 + R_2}$$



For an **Ideal Photoconductor**, a simple negative-feedback resistor R_f provides a nearly constant bias voltage on the device. For a **Real Photoconductor**, an additional resistor R_3 provides positive feedback for linearity.

This work was done by Rudolf A. Schindler of Caltech for NASA's Jet Propulsion Laboratory. For further informa-

tion, Circle 52 on the TSP Request Card. NPO-16055

Improved High/Low Junction Silicon Solar Cell

The air-mass-zero open-circuit voltage is increased to 650 mV.

Lewis Research Center, Cleveland, Ohio

A method has been developed to raise the value of the open-circuit voltage in silicon solar cells by incorporating a high/low junction in the cell emitter.

The power-conversion efficiency of the low-resistivity silicon solar cell is considerably less than the maximum theoretical value mainly because the open-circuit voltage is smaller than simple p/n junction theory predicts. With this method, the air-mass-zero open-circuit voltage has been increased from the 600 mV level to approximately 650 mV.

The figure gives a cross-sectional schematic view of the proposed cell. Shown is the p-type substrate and the n-type emitter comprising a low region and a high-electron-accumulation region.

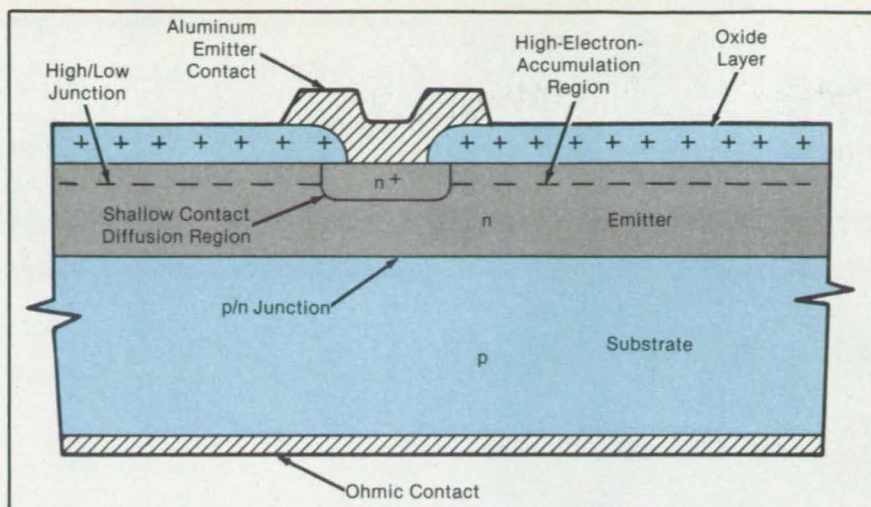
An oxide layer on the illuminated surface contains a high positive charge. Shallow n^+ contact diffusion regions underlie each of the one or more aluminum emitter contacts, and an ohmic contact underlies the p region.

A p/n junction exists between the emitter region and the substrate. A high/low junction has been formed between the

high-electron-accumulation region and the low emitter region. An aluminum metal contact is in ohmic contact with the emitter, and a shallow n^+ diffusion contact is made under this metalized portion of the top surface area. The aluminum emitter contact covers no more than 5 to 10 percent of the surface area.

Provided in the proposed solar cell is a suppression of dark emitter current and an increase of short-circuit current. The emitter is less heavily doped — preferably in the $\sim 10^{18}$ to 10^{19} cm^{-3} range — compared to emitters of conventional cells, which are typically doped to about 10^{20} cm^{-3} . A heavily doped emitter region has the disadvantage that the dark emitter recombination is so large that it limits the maximum open-circuit voltage to about 600 mV. The high/low emitter suppresses the dark emitter recombination current, resulting in power-conversion efficiencies significantly higher than were previously achieved.

This work was done by Arnost Neugroschel, Shing-Chong Pao, Fred A.



In an **Oxide-Charge-Induced High/Low Emitter Solar Cell**, electron accumulation layer is induced by a positive charge.

Lindholm, and Jerry G. Fossum of the University of Florida for **Lewis Research Center**. For further information, Circle 102 on the TSP Request Card. Inquiries concerning rights for the

commercial use of this invention should be addressed to the Patent Counsel, Lewis Research Center [see page 29]. Refer to LEW-13618.

A 25-kW Series-Resonant Power Converter

A prototype exhibited an efficiency of 93.9 percent.

Lewis Research Center, Cleveland, Ohio

The feasibility of processing 25 kW of power with a single, transistorized, series-resonant converter stage has been demonstrated by the successful design, development, fabrication, and testing of such a device. This technology was built on the strong technical base of multi-kilowatt series-resonant converters that have been developed in recent years. This technical base includes advanced switching components, magnetic components, filter components, mathematical circuit models, control philosophies, and switch-drive strategies.

Much of the recent effort had been centered around the application of high-power transistors in resonant converters. Transistor switches display marked advantages over the more commonly applied thyristors. Among these advantages are higher frequency operation, lower switch losses, positive commutation, lower-peak tank currents, and inherent current limiting in the switch. It is anticipated that the eventual application of this technology base to multikilowatt space-power systems will result in both reduced specific mass due to the higher conversion frequencies and in reduced thermal control due to more efficient operation.

To date, the highest-known power level of a resonant power converted designed

for space operation was 2.5 kW. However, studies had shown that a module size of 25 kW was appropriate for a multi-hundred-kilowatt space-power system. As a first step, a 10-kW transistorized dc/dc resonant power converter was designed and tested. As a result of this program, the development of series-resonant converters to the 25-kW power level for spaceborne and airborne applications was successfully accomplished.

A 25-kW resonant dc/dc power converter was designed, developed, fabricated, and tested, using Westinghouse D7ST transistors as the high-power switches. The D7ST transistor was characterized for use as a switch in series-resonant converters, and a refined base-drive circuit was developed.

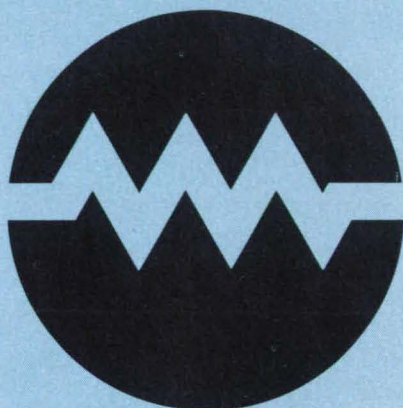
The converter developed employs four D7ST transistors in a full bridge configuration, operates from a 250- to 350-Vdc input bus, and provides an output power of 25 kW (1,000 V or ± 500 V at 25 Adc). It has a resonant frequency of 20.6 kHz, an output ripple of 3 percent peak-to-peak, regulation of better than 0.1 percent, a response time of less than 2 ms, and its output can be either constant voltage or constant current with automatic cross-over. The full-power, 250-V-input electrical

efficiency measured was 94.8 percent for the power stage alone, 94.4 percent with housekeeping power included, and 93.9 percent with the losses of the solid-state input circuit breaker and output transient-current limiters included. There are no inherent problems that would prevent this 25-kW design from being upgraded to a space-qualified status.

The developed converter technology provides an efficient, lightweight, high-power converter that can be used by itself or as a module for a higher power (multi-100-kW) system. This technology can also be used as the basis for a high-power, high-frequency (20-kHz), ac power distribution system. In either case, power-system benefits such as lower losses when used for high-voltage distribution, and reduced magnetics and filter mass will be realized.

This work was done by Robert J. Frye of **Lewis Research Center** and Ronald R. Robson of **Hughes Research Laboratories**. Further information may be found in NASA CR-168273 [N84-17481/NSP], "25 kW Resonant dc/dc Power Converter" [\$14.50]. A copy may be purchased [prepayment required] from the National Technical Information Service, Springfield, Virginia 22161. LEW-14197

Electronic Systems



Hardware, Techniques, and Processes

- 50 Digital Signal Combining for Conference Calling
- 52 Fast Initialization of Bubble-Memory Systems
- 55 Blending Gyro Signals To Improve Control Stability
- 56 Synchronization of Data Recorded on Different Recorders
- 58 Wind-Tunnel-Model Leak-Checking System
- 59 Laser Ranging System
- 59 Switched-Multibeam Antenna System
- 62 TV Video-Level Controller

Books & Reports

- 63 Simulation of PCM Data

Digital Signal Combining for Conference Calling

Signals are combined with minimal noise by use of sums in read-only memories.

John F. Kennedy Space Center, Florida

A digital signal-combining system reduces the number of signal-processing steps by use of read-only memories (ROM's) instead of linear arithmetic operations on the signal amplitudes. Like other digital signal adders, it degrades the signal-to-noise ratio less than do analog adders when a large number of signals is combined. The system is intended especially for combining a number of separate audio signals into one signal for retransmission, as in telephone conference calling.

Figure 1 depicts the operating mode for the simultaneous transmission of telephone signals from subscribers A and B to subscriber C. The audio outputs of

the microphones at A and B are processed through analog-to-digital converters, the outputs of which are parallel 8-bit, floating-point numbers representing the instantaneous sampled amplitudes. The parallel bits are converted to serial bit streams for transmission over a long distance to the signal-combining station.

At the combining station the serial bit streams are converted back to parallel. Each 8-bit parallel number provides half of a 16-bit address for a ROM. The ROM is preprogrammed to contain all of the 2^{16} possible sums of the digitized A and B signals. Thus, the ROM acts as an electronic lookup addition table, and its output is a parallel 8-bit floating-point number

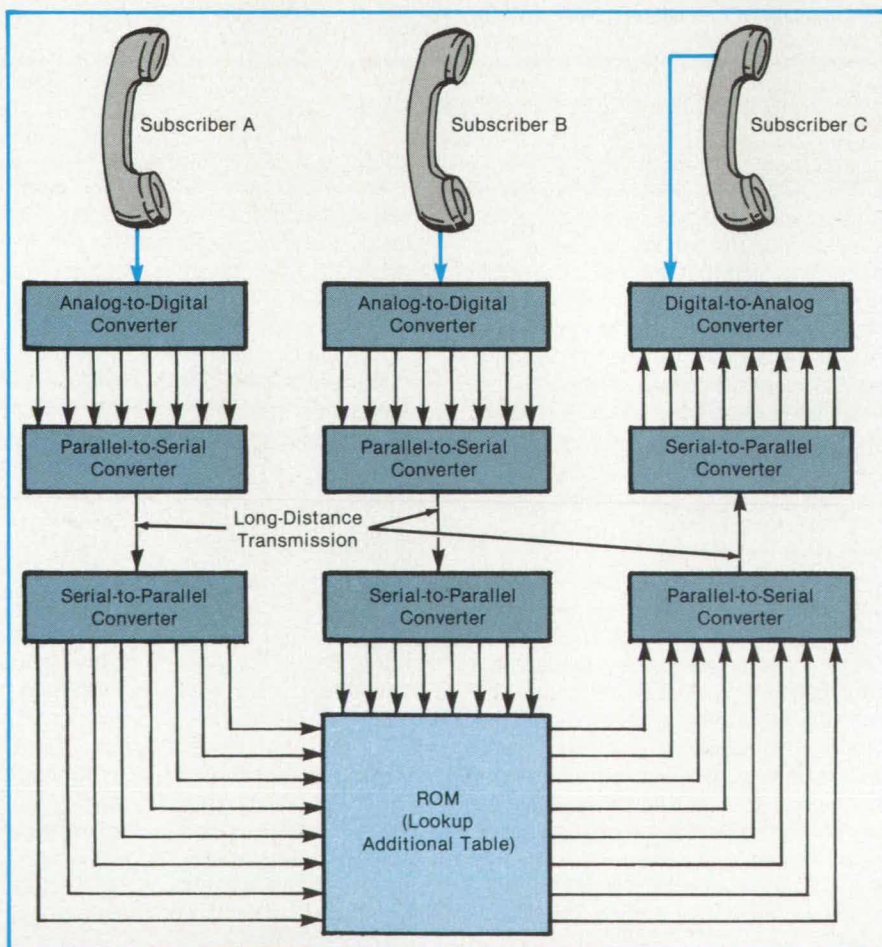
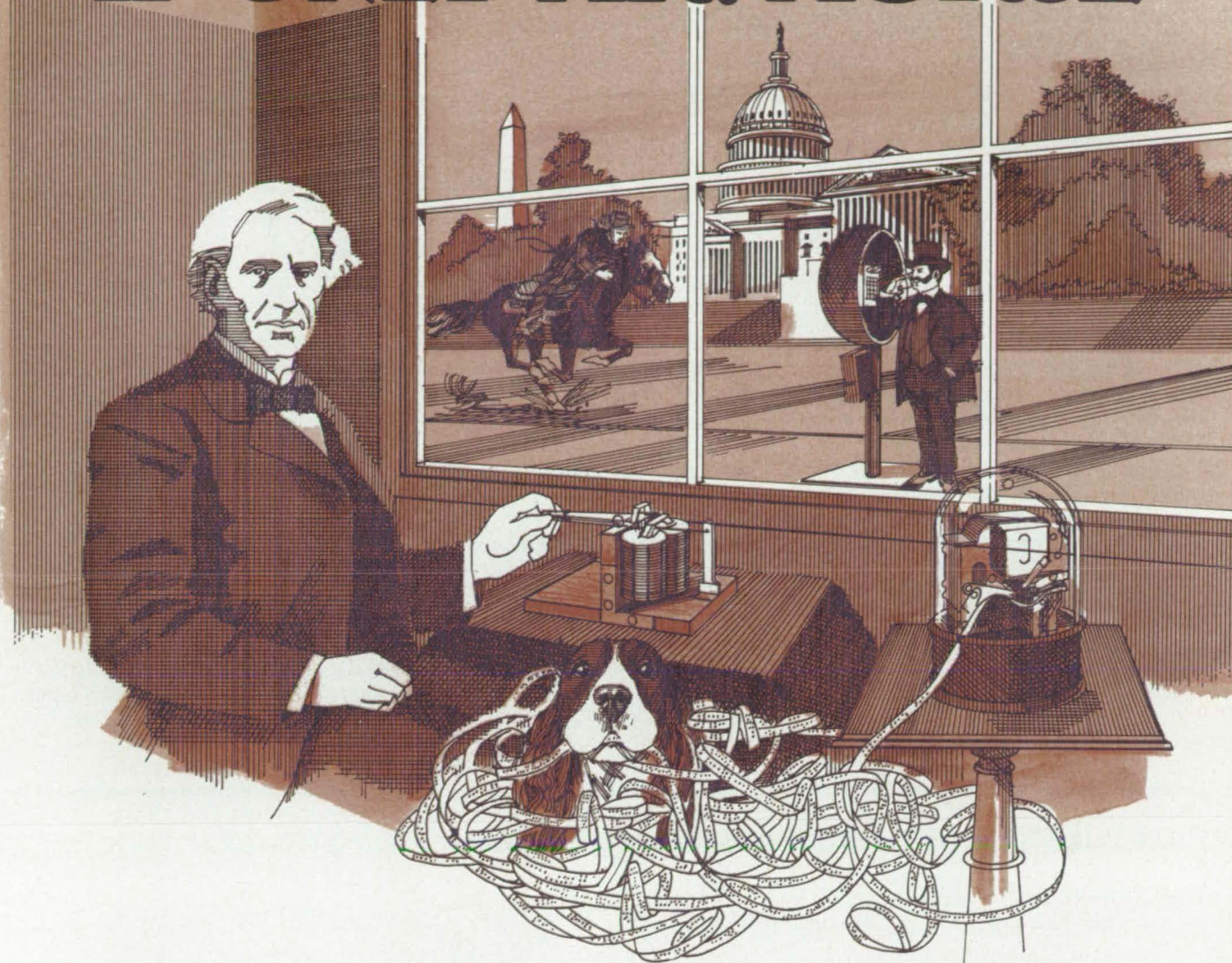


Figure 1. The Signals From Subscribers A and B are digitized, transmitted, and combined by addressing a ROM. The combining operation is the electronic equivalent of looking up the value of a function of two variables in a mathematical table. The combined digitized signal is transmitted, converted to analog form, and delivered to subscriber C.

IF ONLY MR. MORSE



... had gone through design analysis of his telegraph with the AOS/MAGNETIC™ Analysis Program. He could have learned its optimum electrical efficiency and cost effectiveness without making costly physical prototypes.

Imagine how the AOS/MAGNETIC Analysis Program would have helped Mr. Morse design a working telegraph sooner and with a lot less cost.

It may be too late for Mr. Morse but not for you see how you may improve your

designs by using the AOS/MAGNETIC Analysis Program. Just call us and we'll show you how we can help you look great and save you money.

CALL US AT

1-800-MAG-6442
IN WISCONSIN 414-357-2706



A.O. SMITH
DATA SYSTEMS, INC.

A SUBSIDIARY OF A. O. SMITH CORPORATION
8901 N. Kildeer Ct., • Milwaukee, WI 53209

While you're chatting, ask our representative to deliver a poster of Morse at work suitable for hanging in your office. Samuel F.B. Morse introduced his "relay" on September 4, 1837. The first telegram ("What hath God wrought") was tapped out on May 24, 1844 between Washington and Baltimore.

representing the instantaneous sum of the A and B signals.

The ROM output is converted to serial form for long-distance transmission. At the destination, the serial bits are converted to parallel, then to analog form and fed to the receiving headphone of subscriber C.

To increase the number of signals that can be combined, it is necessary to introduce multiple lookup steps or else to make the ROM address wider. Because the number of possible amplitude sums increases exponentially with the address width, an electronic "shortcut" is taken to decrease the size of the required memory: This shortcut is accomplished by elimination of the redundancy in positive and negative sums and differences of the same magnitude.

In the two-subscriber case of Figure 1, the ROM is replaced by the system of Figure 2. Inputs A and B are fed to a sign ROM, a sum ROM, and a difference ROM. The sign ROM determines the output-sign bit and whether the remaining seven output bits represent a sum or a difference. The sign ROM then enables the sum or the difference ROM, whichever is appropriate. The output-sign bit is combined with the seven output bits of the sum or difference ROM into the parallel 8-bit ROM output signal.

To compensate for volume differences

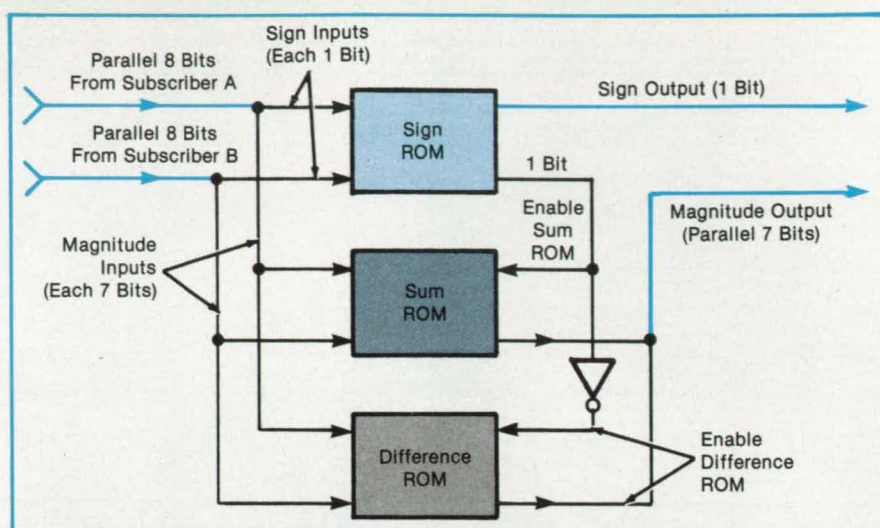


Figure 2. **Sign, Sum, and Difference ROM's** reduce the memory requirement of the ROM of Figure 1 by eliminating redundancy in the "lookup table".

among transmitting subscribers, the combining-ROM subsystem can be preceded by a multiplying-ROM subsystem in each subscriber line. In an operation similar to that of the combiner, the multiplier inputs are the seven magnitude bits of the audio signal (the sign bit is not changed) and the six bits of the volume-adjusting multiplication factor. Together, these two inputs provide 13 address bits for the multiplier lookup table, and the multiplier-ROM output comprises the 7

bits of the adjusted signal magnitude.

This work was done by Frank Byrne of Kennedy Space Center. For further information, Circle 2 on the TSP Request Card.

This invention is owned by NASA, and a patent application has been filed. Inquiries concerning nonexclusive or exclusive license for its commercial development should be addressed to the Patent Counsel, Kennedy Space Center [see page 29]. Refer to KSC-11285.

Fast Initialization of Bubble-Memory Systems

The improved scheme is several orders of magnitude faster than the normal initialization scheme.

Langley Research Center, Hampton, Virginia

Bubble-memory systems are quickly becoming preferred in environments where nonvolatile storage mediums are required. The implementation of large bubble-memory systems in spacecraft applications requires that the memory modules be power-strobed for the conservation of the available energy resources. Each time a module is turned on for use, it must be initialized to code the redundant loop information of the selected bubble devices into the bubble controller. Present structures of bubble systems dictate that a faster initialization procedure is needed to capitalize on the advantages offered by a bubble-memory system.

EPROM (electrically-programable read-only memory) was chosen as the simplest method to demonstrate the viability of this fast initialization technique.

A state-of-the-art commercial bubble-memory device was used. A hardware interface was designed to connect the controlling microprocessor to the bubble-memory circuitry. System software was written to exercise the various functions of the bubble-memory system. A comparison was made between the normal and fast techniques. Future implementations of this approach will utilize the E²PROM (electrically-erasable programmable read-only memory) to provide greater system flexibility.

The figure shows the flow charts for the normal and fast initialization procedures. Both initialization procedures require a system reset (ABORT) before the command is sent to the controller. When the system is initialized normally, the bubble-memory controller (BMC) reads the entire bootloop, decodes it,

transfers it to the bootloop register in the format/sense amplifier (FSA), and places the bubble at page zero. This process could take up to 160 ms since there could be two rotations of the minor loops to find and read the bootloop code.

Alternatively, the fast initialization procedure uses system software to load the bootloop information from an external memory into the bootloop register of the FSA. The first different step in the fast initialization process is to issue the PURGE command to clear the controller registers. Next, the parametric register data must be loaded with the same data as those required for the normal initialization. Upon the completion of this, the bootloop register must be loaded from the external memory to the bootloop register in the FSA, accomplished by using the WRITE BOOTLOOP REGISTER

Performance that transcends



Racal-Dana's broad spectrum of universal counters exceeds your performance expectations.

Each 1990 Series model gives you these standard features:

- 1 nanosecond time interval measurement
- Auto-trigger
- 9-digit resolution in one second
- Peak amplitude
- Phase

All for just \$1150.

For more sophisticated applications, choose the additional capabilities your system needs: high speed GPIB or MATE* programming, pulse characterization, statistical analysis, and much, much more.

Only Racal-Dana transcends tradition to give you performance, choice and value.

Call today for a fact-filled product and applications presentation. Racal-Dana, the enlightened choice in universal counters.

RACAL-DANA

Highlighting universal counters

United States: (714) 859-8999

United Kingdom: (07535) 68101

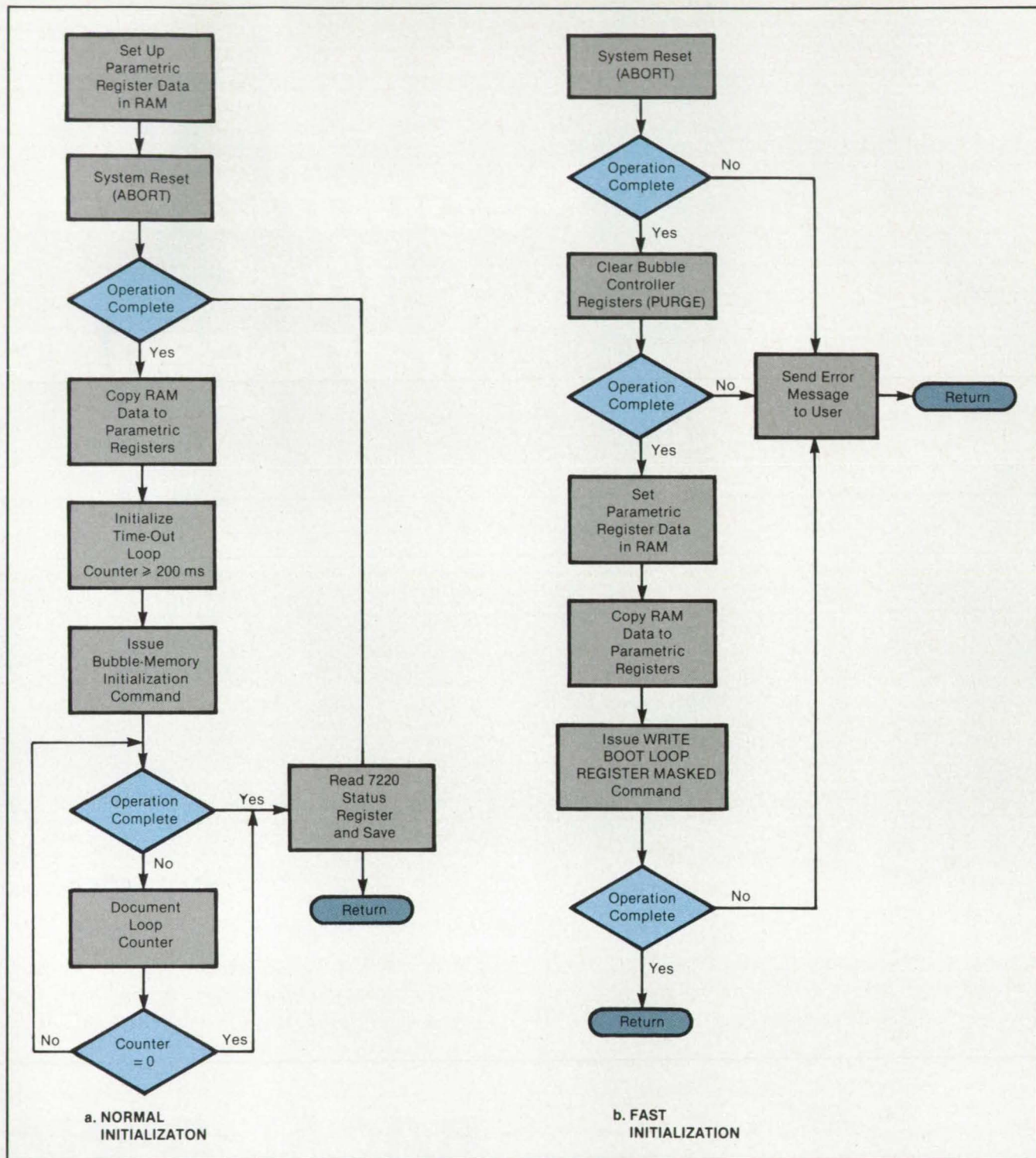
France: (3) 955-8888

Federal Republic of Germany: (06102) 2861/2

Italy: (02) 5062767

RACAL

*U.S. Air Force acronym for Modular Automated Test Equipment.
© Copyright 1986, Racal-Dana Instruments, Inc.



The **Normal and Fast Initialization Techniques** are represented by these flow charts. The fast technique uses a small amount of external storage to load the controller registers at high speed.

MASKED command.

A calculation of the normal initialization time was made from the time the command was issued to the BMC to the time that an "operation complete" status was received in the status register. This time was 117.84 ms. A calculation of the fast initialization time began with the issuance of the PURGE command and ended with the receipt of an "operation complete" in the BMC status register after the completion of the WRITE

BOOTLOOP REGISTER MASKED command. This time was only 641 μ s. The results of this experiment show that the fast-initialization concept provides several-orders-of-magnitude improvement over the normal initialization scheme. The fast-initialization technique is conceptually applicable to all bubble-memory devices and to systems having higher densities than that of the one used in this investigation.

This work was done by Karen T.

Looney, Charles D. Nichols, and Paul J. Hayes of Langley Research Center. Further information may be found in NASA TM-85832 [N84-27977/NSP], "Investigation of Fast Initialization of Spacecraft Bubble Memory Systems" [\$10]. A copy may be purchased [prepayment required] from the National Technical Information Service, Springfield, Virginia 22161. LAR-13357

Blending Gyro Signals To Improve Control Stability

Interference by structural vibrations is reduced by adding the signals from spatially separated gyros.

Lyndon B. Johnson Space Center, Houston, Texas

A signal-processing concept can suppress vibration-induced noise in attitude-control systems. The proposed technique involves blending signals from rate gyroscopes located at different parts of the structure to obtain a composite signal that more nearly represents the rotation of the entire structure. The most likely applications of the concept would be flight-control systems for aircraft.

To apply the technique, it is necessary to have prior knowledge of the vibrational modes of the structure — particularly the dominant modes that contribute to instability in the feedback-control system. As an example, a system that senses the pitch of an airplane must contend with structural vibrations of the fuselage (see figure). The local rate of change of bending slope contributes to the rotation sensed by a rate gyro.

To eliminate the vibrational component from the composite rate-gyro signal, the two pitch-rate gyros are placed forward and aft of the antinode of the dominant vibrational mode, in positions of opposite bending slope for that mode. The forward and aft gyro signals are proportional to

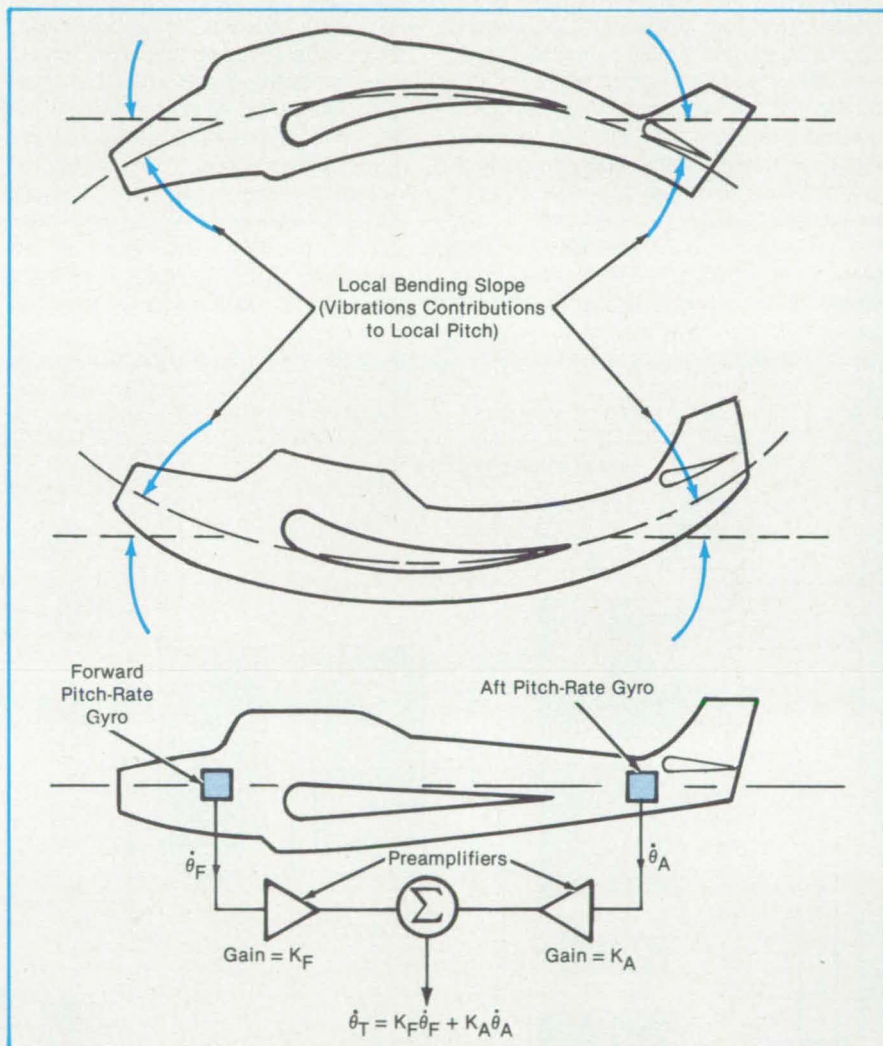
$$\dot{\theta}_F = \dot{\theta}_R + \sum_{i=1}^n \sigma_{iF} \dot{\eta}_i$$

and

$$\dot{\theta}_A = \dot{\theta}_R + \sum_{i=1}^n \sigma_{iA} \dot{\eta}_i$$

respectively, where $\dot{\theta}_F$ and $\dot{\theta}_A$ are the pitch rates sensed by the forward and aft gyros, respectively; $\dot{\theta}_R$ is the rigid-body pitch rate (the pitch rate that would be sensed if there were no vibrations); σ_{iF} and σ_{iA} are bending-slope coefficients for the i th mode; η_i is a generalized amplitude coordinate for the i th mode such that the bending slope at the forward and aft rate-gyro locations is given by $\sigma_{iF}\eta_i$ and $\sigma_{iA}\eta_i$, respectively; and n is the number of bending (vibrational) modes.

As shown schematically at the bottom of the figure, the two gyro signals are summed in such a way that the rigid-body-rotation signal $\dot{\theta}_R$ is not affected while the dominant vibrational-mode signal is suppressed. In principle,



Aircraft Vibrations Perpendicular to the Pitch Axis contribute to the rotations sensed by the pitch-rate gyros. Proper blending of the signals from the gyros can suppress the contribution of the dominant vibrational mode.

ple, the dominant-mode contribution is entirely eliminated by choosing the gains of the summing preamplifiers according to

$$K_F = \frac{-\sigma_{dA}}{\sigma_{dF} - \sigma_{dA}} \text{ and } K_A = \frac{\sigma_{dF}}{\sigma_{dF} - \sigma_{dA}}$$

where the subscript d refers to the dominant mode. With this choice, composite signal $\dot{\theta}_T$ contains only $\dot{\theta}_R$ plus small contributions from minor vibrational modes. This blending technique is

superior to band-rejection filtering of the dominant mode in that it has no adverse effect on the processing of rigid-body signal components in the rejection band.

This work was done by John F. L. Lee of Honeywell, Inc., for **Johnson Space Center**. For further information, Circle 64 on the TSP Request Card. MSC-20370

Synchronization of Data Recorded on Different Recorders

Electrical and mechanical timing errors would be corrected.

NASA's Jet Propulsion Laboratory, Pasadena, California

A conceptual electronic timing system would enable the time correlation of analog and digital signals recorded on different magnetic tapes or on different tracks of the same tape. The concept was proposed to improve the analysis of Space Shuttle flight-data tapes containing signals with frequency components up to 50 Hz, but can be used for higher frequencies, possibly in the kilohertz region. It may be useful in other applications requiring the synchronization of data on different data tracks.

The figure shows a simplified block diagram of the concept. The concept involves the recording of timing signals on the data tracks. Four types of timing signal are used (though not all at the same time on the same track):

- A sinusoidal speed reference is recorded

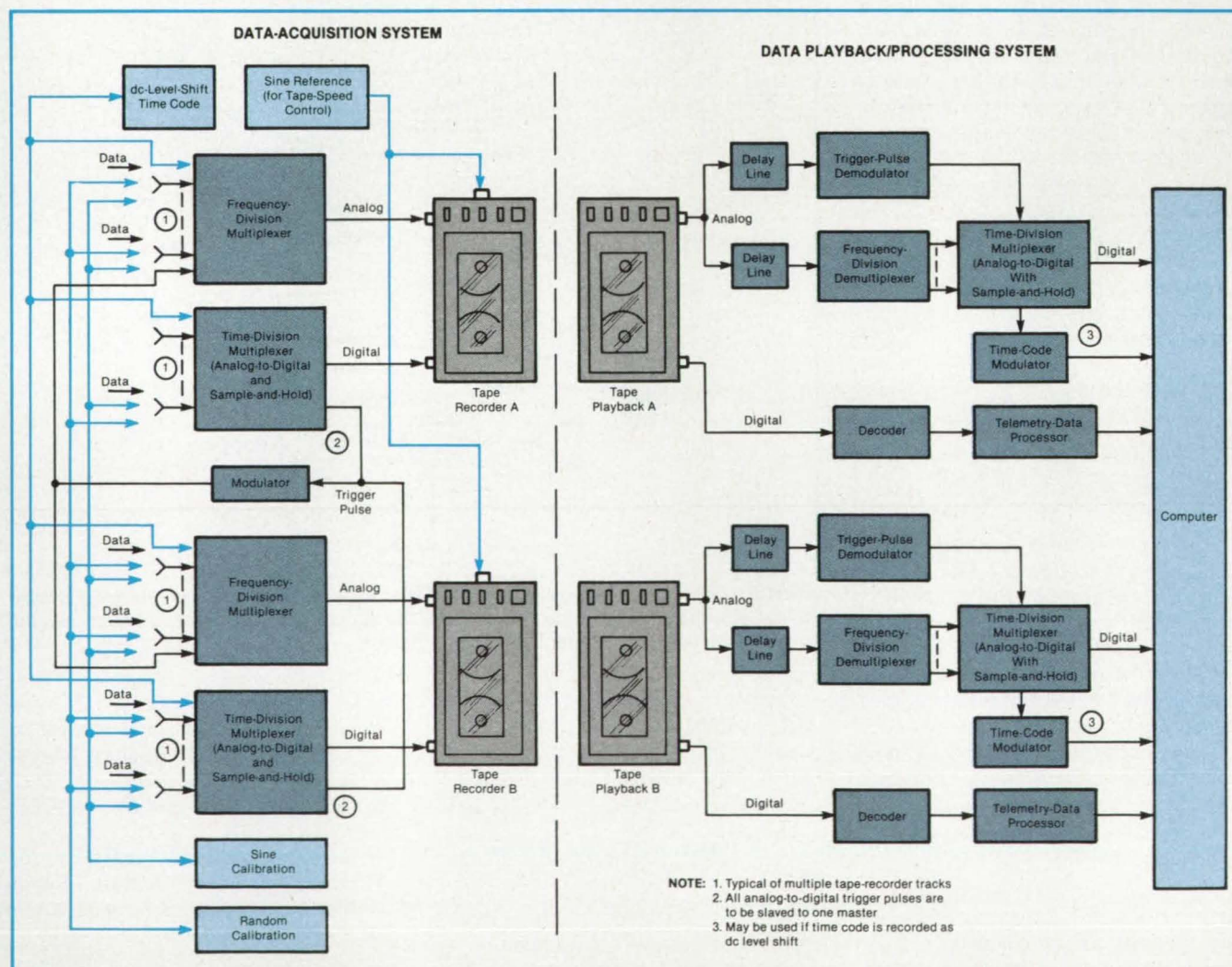
on each tape simultaneously with the data and operates through a servo-control system to maintain the same tape speed during playback as during recording;

- The first few minutes of each data channel is occupied by calibration signals consisting of some 50-Hz sinusoid plus some white-noise signal that resolves the integral-cycle phase ambiguity of the sinusoid;
- A train of master trigger pulses is placed simultaneously on all analog data tracks to control the timing of the analog-to-digital converter of each track during playback and laboratory analysis; and
- A dc-level-shift time code is recorded on each analog data track to update the counting of pulses and periods of the

reference sinusoid.

The system would correct both electrical and mechanical timing errors and frequency-dependent phase errors. All phase and time errors would be measured in the laboratory when the data tapes are played back. The calibration data would be used to correct the frequency-response and phase errors during the digitization process. Analog phase errors that are independent of frequency could be corrected by delay lines in the playback system or by the signal-analyzing computer after digitization.

This work was done by James H. Wise and James W. McGregor of Caltech for NASA's Jet Propulsion Laboratory. For further information, Circle 59 on the TSP Request Card.
NPO-16555



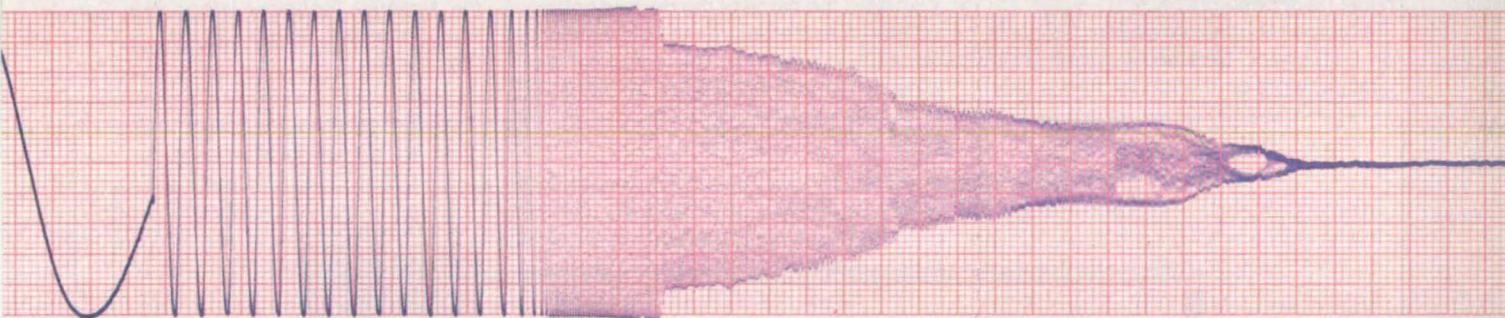
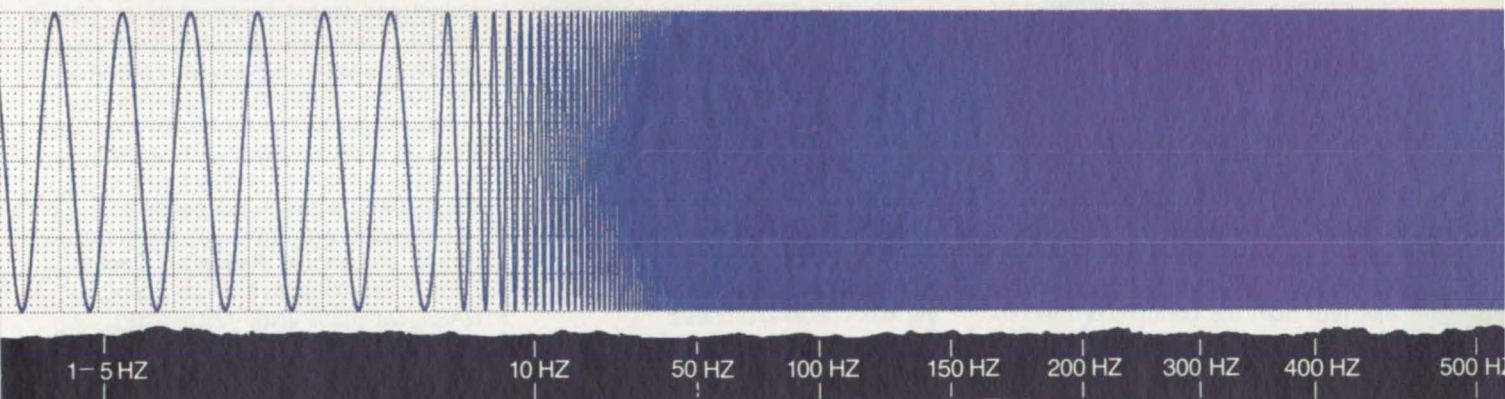
Timing Signals Are Recorded Simultaneously on different magnetic-tape tracks along with data signals to enable the subsequent time correlation of the data.

Multiple Pages Intentionally Left
Blank

ASTRO-MED RE-INVENTS THE 8 CHANNEL OSCILLOGRAPH

NOW RECORD DC TO 500 HZ FULL SCALE...FLAT ON LOW COST THERMAL PAPER

Astro-Med MT-8500



Conventional Stylus Recorder

Unretouched charts recorded at 25 mm per second

Stylus recorders with their moving mechanical components cannot maintain full scale amplitude above 75 Hz. The new 8 channel MT-8500 with no moving parts neatly solves the problem. It produces superb, permanent tracings to 500 Hz full scale, flat. And, since it prints its own chart on the fly, chart drift is a thing of the past.

Recording is thermal... no costly light sensitive papers. No messy inks or toners. The 8500 records 8 channels, introduces a unique new feature called "Wave Form Expansion", and records X-Y plots as well as X-T. Plus,

transient waveform capture to 5 KHz, and a full range of interchangeable plug-in signal conditioners.

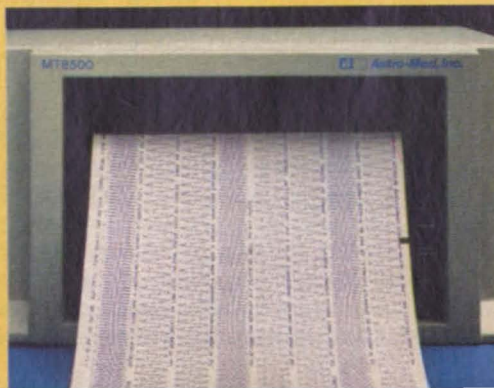
The 8500 can be controlled locally or through the host computer, which we offer as an option: an IBM PC... with complete operations manual on a disk.

For complete details on the new 8 channel MT-8500, phone for a free brochure.
Toll Free 800-343-4039.



Astro-Med, Inc.

Astro-Med Industrial Park, West Warwick,
Rhode Island 02893 ☐ (401) 828-4000
Telex Number 710-382-6409



Circle Reader Action No. 424

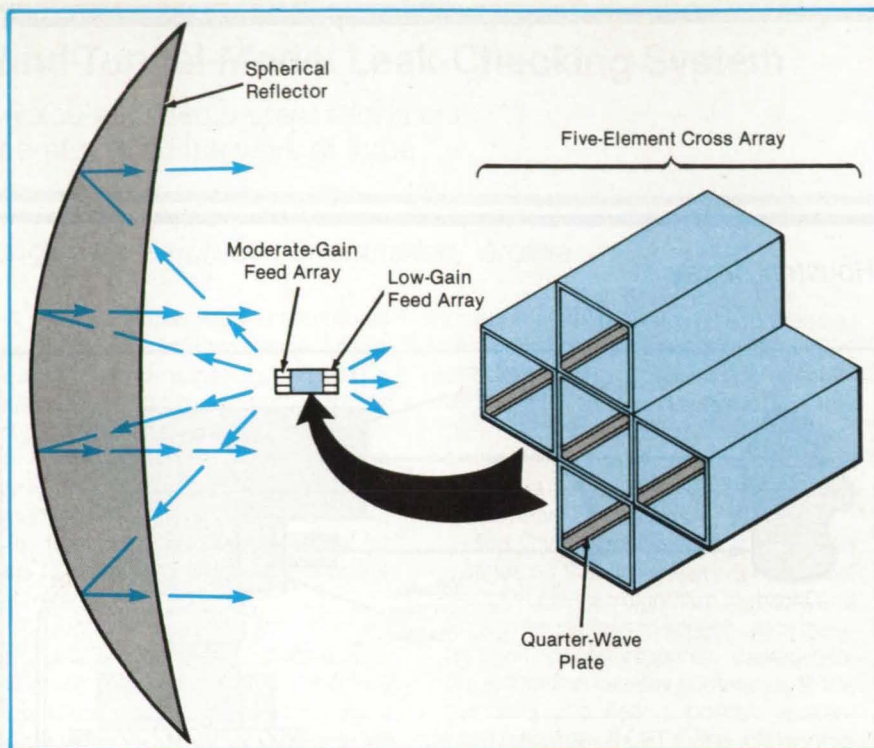


Figure 1. A Moderate-Gain, Five-Element, Cross-Array Feed Horn feeds a spherical reflector. A low-gain feed horn faces outwardly.

which the phase varies with frequency.)

Figure 2 shows a distribution and delay-switching network for both transmitted and received signals. If the transmitter beam is also switched at an IF, then up-conversion to the radio frequency is readily done immediately prior to the power-amplification stage.

The antenna feeds are essentially square waveguides with diagonal quarter-wave dielectric plates to generate circular polarizations. Since the transmitter input and the receiver output are orthogonal, there is inherent isolation between them. If additional isolation is desired, the transmitted signal can be attenuated by an abrupt transition to a narrower receiving waveguide having a cutoff frequency above the transmitting frequency.

This work was done by Richard S. Iwasaki of Axiomatix for Johnson Space Center. For further information, Circle 67 on the TSP Request Card.

Inquiries concerning rights for the commercial use of this invention should be addressed to the Patent Counsel, Johnson Space Center [see page 29]. Refer to MSC-20873.

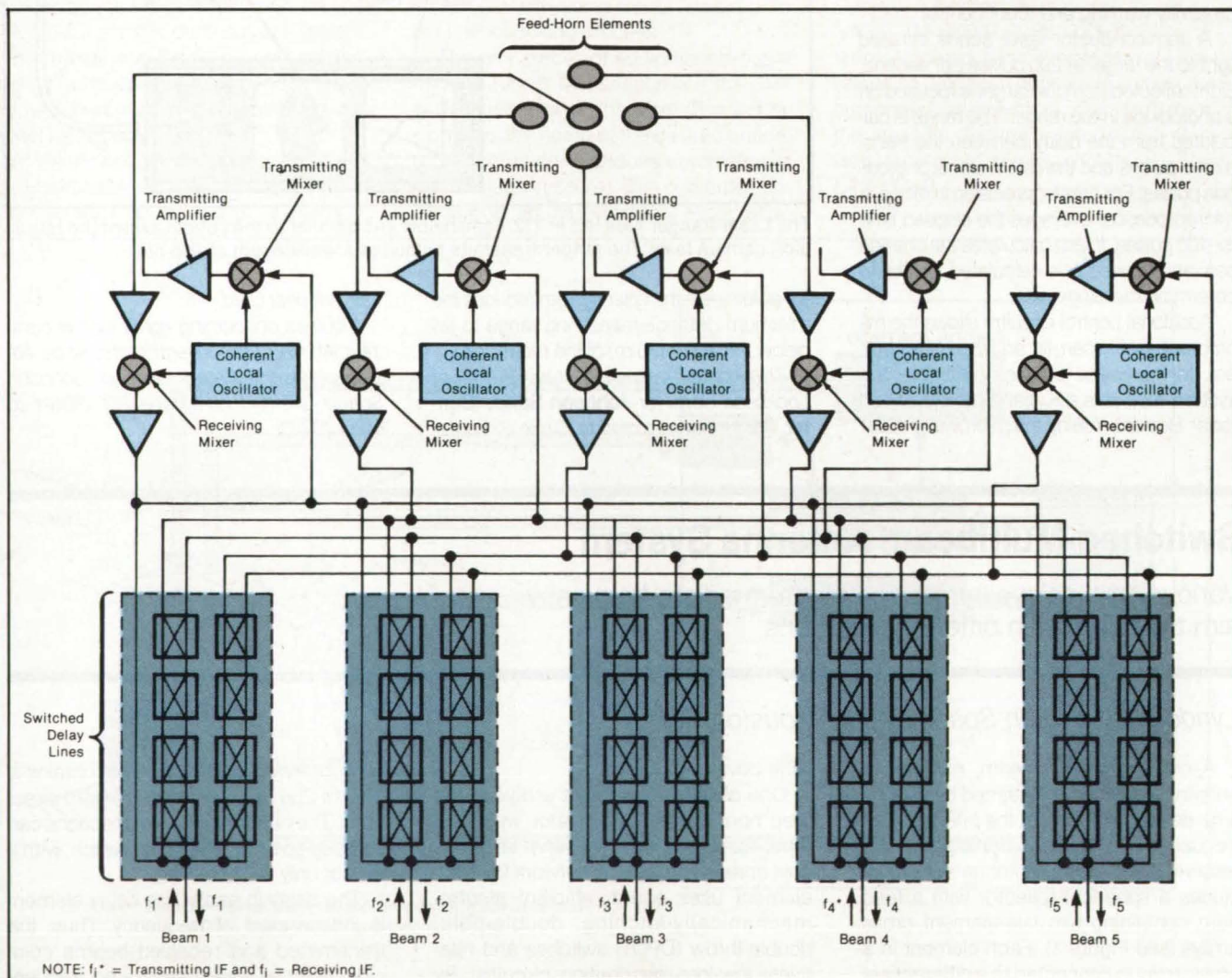


Figure 2. This Delay-Line Switching Network aims the antenna by variation of the delay in the feed to each element of the cross-array feed horn of Figure 1.



Buck never had it so good.

Motorola reliable power converters. Customized for spacecraft.

Motorola's technologically advanced power converters are customized for each spacecraft. Supported by special test equipment and software, these fully-redundant, radiation-hardened, EMP/EMI protected power converters provide

the reliability, efficiency, regulation, isolation and packaging needed for near and deep space missions. It's easy to have it much better than Buck. Call 602/897-4621 or write Box 2606, Scottsdale, AZ 85252.



MOTOROLA INC.

Government Electronics Group

Circle Reader Action No. 375

TV Video-Level Controller

Constant output is maintained, though luminance varies by 5 million to 1.

Lyndon B. Johnson Space Center, Houston, Texas

With the aid of automatic light control and gain control, a television camera accommodates a maximum light level 5 million times greater than the lowest light level, while outputting a constant 3-V peak signal to processing circuitry. The light-control loop maintains the highlight camera-output current at 330 nA by adjusting the iris opening and the tube voltage. The iris control allows a 50,625-to-1 change of input luminance, and the voltage control allows an additional factor of 20 to 1. Automatic gain control provides an additional 5-to-1 reduction for a net reduction slightly more than 5×10^6 to 1.

The camera output, after fixed-gain preamplification, is fed to a variable-gain amplifier (see figure), which establishes a dc reference for a clamp and dark-current circuit. The clamped video signal is fed to the automatic-light-control (ALC) loop and, simultaneously, to the auto-

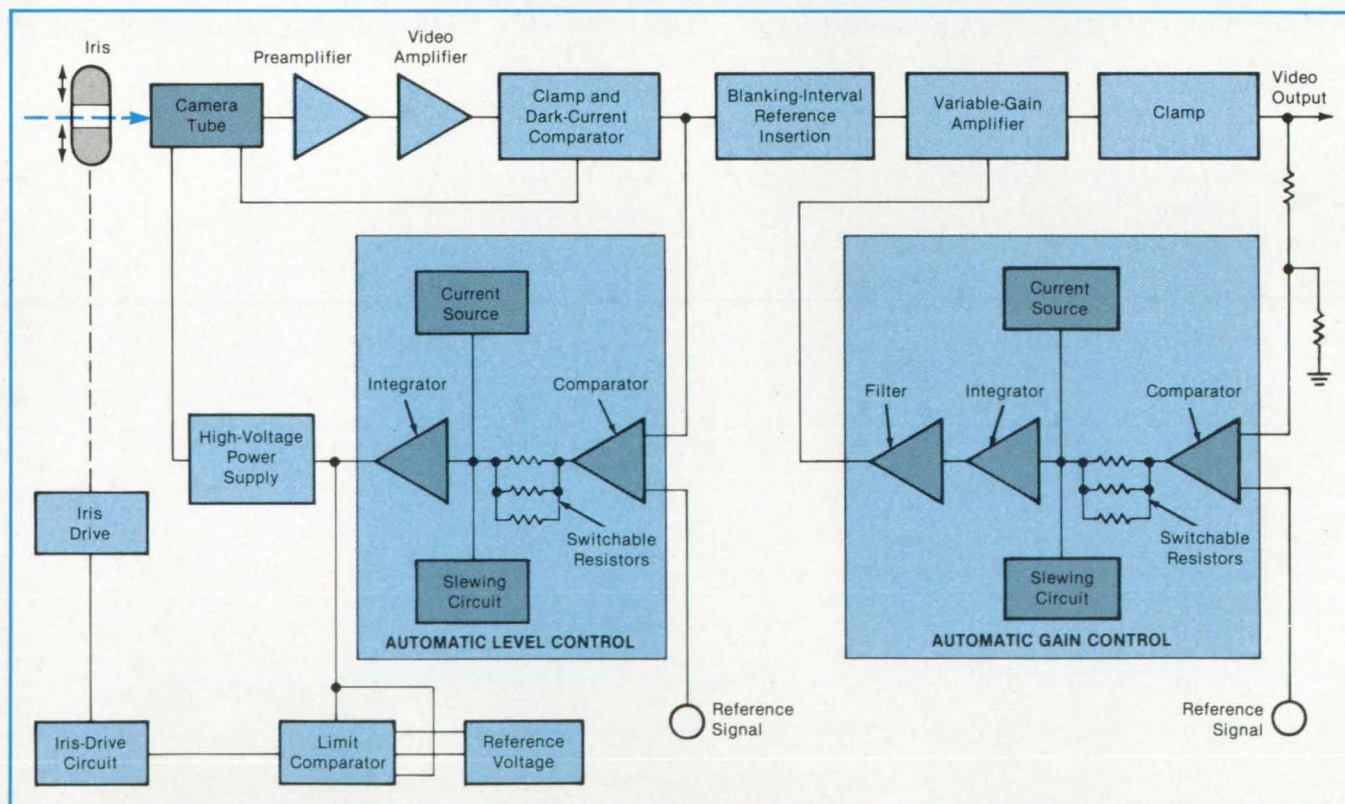
matic-gain-control (AGC) circuit.

In the ALC loop the clamped video is compared with a reference signal, and the comparator output is integrated. The integrator output controls the high-voltage power supply for the tube, which adjusts the camera gain. By switching in the different resistors in the integrator, one selects the fraction (0.005, 0.03, or 0.25) of the scene that exceeds the peak white level and is clipped to peak white in the output.

The integrator output is also fed to a comparator in the iris control loop, which compares the ALC output with a reference level. The comparator output is fed to an iris-drive circuit. Depending on the relationship of the ALC output to the reference, the iris-drive circuit activates a mechanism that increases or decreases the lens opening, thereby increasing or decreasing the amount of light entering the camera.

The AGC loop operates in a manner similar to that of the ALC loop. The video output is compared with a reference signal. The comparator output is fed to an integrator and a filter. As in the ALC circuit, the switchable resistors select the fraction of the scene that is allowed to exceed peak white. The filter output acts to control the gain of a variable-gain amplifier, and hence the video output. Sluing amplifiers in both the ALC and AGC allow rapid response to abrupt changes in light level.

The video-level controller may also be operated manually. In this mode, the lens iris is stationary. An operator manually adjusts the high-voltage power supply. The AGC operates as in the automatic mode. Manual adjustment accommodates a 2,000-to-1 range of light intensity. The high-voltage control allows for a 300-to-1 variation, while the AGC allows for a



Three Means of Normalizing Video Output are utilized in this video-level controller: iris adjustment, tube voltage adjustment, and automatic gain control.

6 $\frac{2}{3}$ -to-1 variation.

This work was done by Marvin Kravitz, Larry A. Freedman, Elmer H. Fredd, and Dan E. Deneff of RCA Corp. for **Johnson Space Center**. For fur-

ther information, Circle 60 on the TSP Request Card.

This invention is owned by NASA, and a patent application has been filed. Inquiries concerning nonexclusive or

exclusive license for its commercial development should be addressed to the Patent Counsel, Johnson Space Center [see page 29]. Refer to MSC-18578.

Books and Reports

These reports, studies, and handbooks are available from NASA as Technical Support Packages (TSP's) when a Request Card number is cited; otherwise they are available from the National Technical Information Service.

Simulation of PCM Data

A program for a communications and control computer simulates pulse-code-modulated data.

Software for simulating pulse-code-modulated (PCM) data from the Space Shuttle during launch preparations was developed for use with the checkout, control, and monitor subsystem (CCMS). The software facilitates testing of the CCMS with the data expected from the main engines, external fuel tanks, operational instrumentation, general-purpose computer, backup flight system, and payload. An understanding of the approach used in this NASA application could benefit designers of other PCM systems.

The table-driven simulator is loaded from disk into a front-end processor of the CCMS, and a menu is written onto the screen of the terminal. Subsequent interaction is through a series of responses to prompts occurring in a logical progression to facilitate easy building, saving, restoration, or execution of the desired simulation. The user's responses govern storage and retrieval of simulation tables, and the disk archives permit rapid format specification without resorting to a lengthy rebuilding process for each use. Simulations on disk are referenced by a six-character alphanumeric label assigned at the time of save-to-disk.

The simulator alternately processes two buffer areas: Data to be transmitted are built in one buffer (by reading through the tables), while the transceiver is transmitting the data from the other buffer.

Visibility into the "health" of the simulator during execution is provided by ob-

serving the contents of two memory locations. One location, the health counter, is incremented for each minor frame buffer filled, denoting cycling of the software. The other location, an error counter, increments once for each time the transceiver begins transmitting a buffer before software has completed filling the buffer. It indicates an overrun condition — software unable to keep pace with the transceiver.

The PCM simulator design stresses the

ease of use coupled with flexibility. It encompasses all PCM formats necessary for the validation of CCMS software and for hardware/software integration. The simulator program executes in standard CCMS hardware, so no new hardware is required.

This work was done by G.G. Bernstrom of IBM Corp. for **Kennedy Space Center**. For further information, Circle 45 on the TSP Request Card.
KSC-11239

**Widest choice,
best
performance,
most
flexible
options**



Specify ITT Image Intensifier Tubes

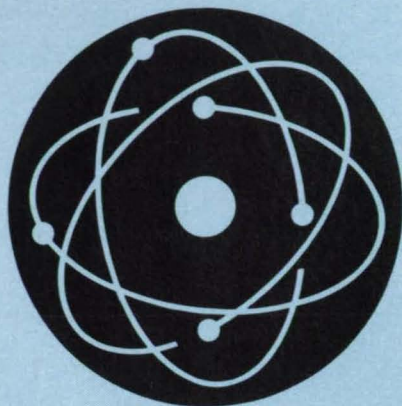
No other company offers you as broad a line of proximity focused channel intensifier tubes as ITT Electro-Optical Products Division. These advanced devices are used to display extremely fast, dimly lit phenomena for energy analysis, astronomy, biophysics, and industrial inspection.

Select from 18, 25, 40 and 75mm active diameters. Choose input and output window materials; one, two or more microchannel plates; photocathode responses and phosphor screens to meet your specific needs. No matter what your choice, these tubes gate as rapidly as a few nanoseconds.

A standard line of products is also available. For more information, contact: ITT Electro-Optical Products Division, P.O. Box 3700, Fort Wayne, IN 46801, (219) 423-4341, TWX: 810-332-1413, Telex: 232-429.

ELECTRO-OPTICAL PRODUCTS DIVISION

ITT



Hardware, Techniques, and Processes

- 64 Heat-Pipe Array for Large-Area Cooling
- 66 High-Flux Atomic-Oxygen Source
- 68 Partial-Transmission Scintillation Detector for Ions
- 68 Solid-Sorbent Air Sampler
- 70 Mapping the Structure of Heterogeneous Materials
- 72 Electro-optical Tuning of Fabry-Perot Interferometers
- 74 Recording Interferograms Holographically
- 75 Comparative Thermal-Conductivity Test Technique

Books & Reports

- 76 Three-Dimensional Radiative-Transfer Equation

Heat-Pipe Array for Large-Area Cooling

High rates of heat transfer are anticipated.

Lyndon B. Johnson Space Center, Houston, Texas

A prototype evaporative cold plate would gather waste heat from equipment mounted on it. The plate is made by welding together the flanges of several sections of heat pipe (see figure). The heat pipe is a slightly modified version of a type used in heat-rejecting radiator elements.

The heat pipe contains a vapor channel, a liquid channel, and a porous nickel felt wick connecting the channels. The walls of the vapor channel contain 160 circumferential grooves per inch (63 grooves per centimeter). As the heat-transfer liquid evaporates from the grooves, more liquid is drawn up from the liquid channel through the wick.

As the liquid depletes, an ultrasonic sensor detects its absence. The sensor signals a solenoid valve to open to fill the liquid channel from a pressurized supply. When the liquid channel is replenished, the sensor signals the valve to close.

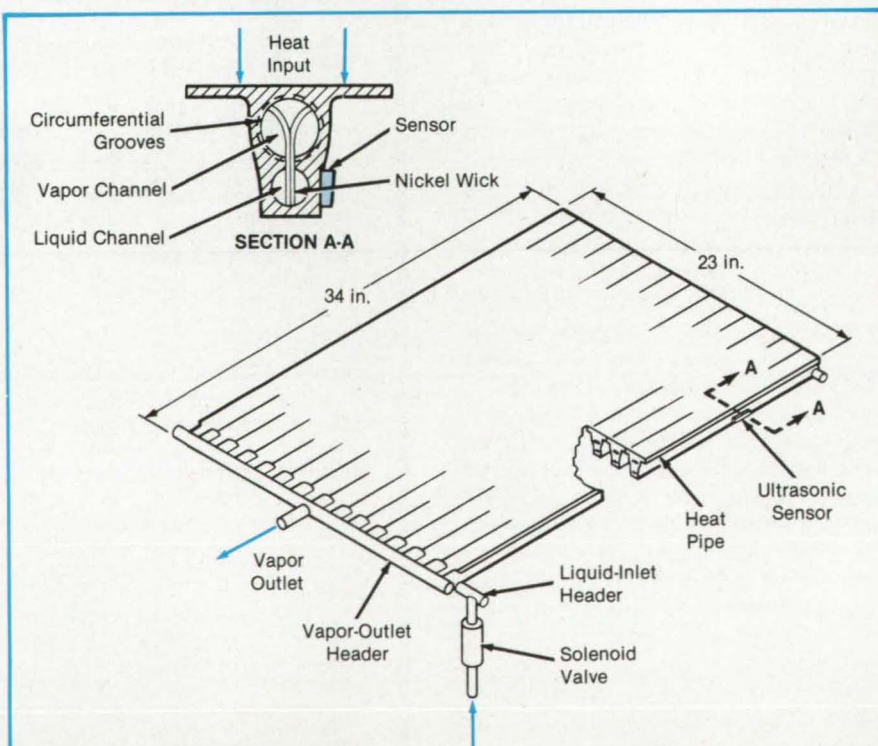
Evaporation occurs continuously while the valve cycles on and off. Vapor from the vapor channels in the separate heat pipes is combined into a single outlet header, which directs it to a condenser. The vapor header contains a liquid trap to catch any

liquid that is carried into the vapor space. Two liquid headers on each end of the plate assure proper filling and liquid flow to the more-heavily-loaded plate sections.

The plate is expected to transfer heat at high rates by surface evaporation from the many sites in the grooved channels. Heat fluxes in zero gravitation are expected to be 2 W/cm² for refrigerant 11 (CCl₃F) and substantially higher for ammonia. Since the plate separates the liquid and vapor phases at the inlet and outlet ports, it eliminates the complexities and uncertainties of two-phase flow in zero gravity. On Earth, the inlet valve enables the plate to operate at relatively-large height differences with other plates in the same system.

This work was done by Fred Edelstein and Richard F. Brown of Grumman Aerospace Corp. for Johnson Space Center. No further documentation is available.

Inquiries concerning rights for the commercial use of this invention should be addressed to the Patent Counsel, Johnson Space Center [see page 29]. Refer to MSC-20946.



The **Cold Plate** consists of sections of heat pipe welded together side-by-side at the flanges.

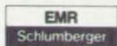
EMR photomultipliers and accessories perform accurately and dependably under even the most demanding conditions.

EMR photomultiplier tubes have met the exacting demands of dozens of space missions, from Mariner to Galileo/Jupiter and beyond. Today, the same ultraviolet- and visual-sensitive, radiation-hard PMTs and accessories that have proven themselves in outer space are available for critical applications here on earth, from the vacuum UV to the near IR.

The rugged structural elements of these individually calibrated tubes are designed for extreme resistance to shock and vibration. For example, each beryllium-copper Venetian blind dynode assembly is welded in place, and each defines a distinct compartment within the tube, isolating individual stages from feedback

effects while providing excellent interstage electrical isolation. Similarly rugged power supply and amplifier/discriminator accessories also operate with unsurpassed reliability — from sea level to deep space over a wide range of temperatures.

Whenever — and wherever — the data is critical, write or call: EMR Photoelectric, P.O. Box 44, Princeton, NJ 08542. Tel: 609-799-1000.



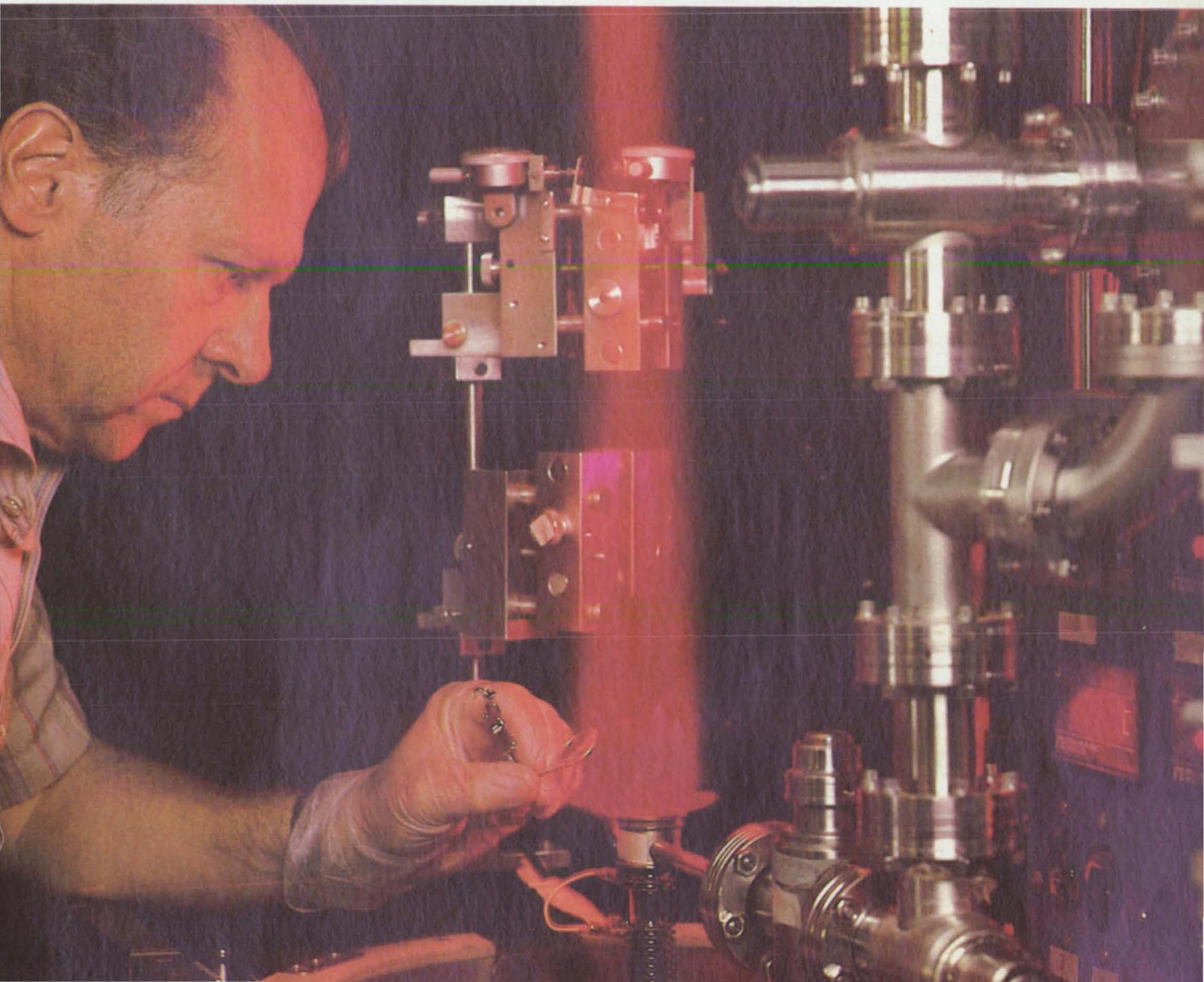
EMR PHOTOELECTRIC



EMR: When the data is critical.

Production of gallium arsenide infrared-sensitive image dissector. Use of an activated single-crystal gallium arsenide cathode provides improved response in the visible and near-IR spectrum.

Circle Reader Action No. 356



High-Flux Atomic-Oxygen Source

Beams of pure ground-state oxygen atoms would be produced.

NASA's Jet Propulsion Laboratory, Pasadena, California

A proposed apparatus can generate high fluxes (about 10^{15} atoms/cm²-s) of ground-state (3P) oxygen atoms. The kinetic energy would be variable in the range of 3 to 10 eV, and the beam would be free of contaminants, such as ions, metastable 1S or 1D oxygen atoms, or other neutral species. Designed specifically to study the degradation of materials and spacecraft glow phenomena in low Earth orbits, this oxygen-atom beam source could be used to study gas-phase collision phenomena involving energetic oxygen atoms.

In the proposed source (see figure), electrons are generated at a heated filament of LaB₆ or W. Bias voltages V_1 and V_2 accelerate the electrons to the proper energy (6.5 eV) to maximize the dissociative attachment of a beam of O₂ gas (that is, the separation of O₂ molecules into O⁻ ions). A solenoidal magnetic field provided by superconducting coils contains the electrons e and the ions O⁻ produced in the

dissociative-attachment process.

The ions are accelerated to the desired final energy eV_2 and pass through a cavity containing a laser beam where the electrons are photodetached. The laser is tuned to 2.5 eV, which is the photon energy at which the detached neutral atoms are entirely in the ground 3P state. The detachment efficiency is increased by the multiple reflection of the laser beam between two mirrors: Typically 50 to 100 passes are made.

After the detachment, the O(3P) atoms travel toward the surface of the target to be tested. The sample should be placed as closely as possible to the detachment region — to minimize the loss of O(3P) by divergence after detachment. Electrons and undetached O⁻ ions are deflected by electric-field plates (giving a trochoidal deflection by $\mathbf{E} \times \mathbf{B}$) into a collecting Faraday cup.

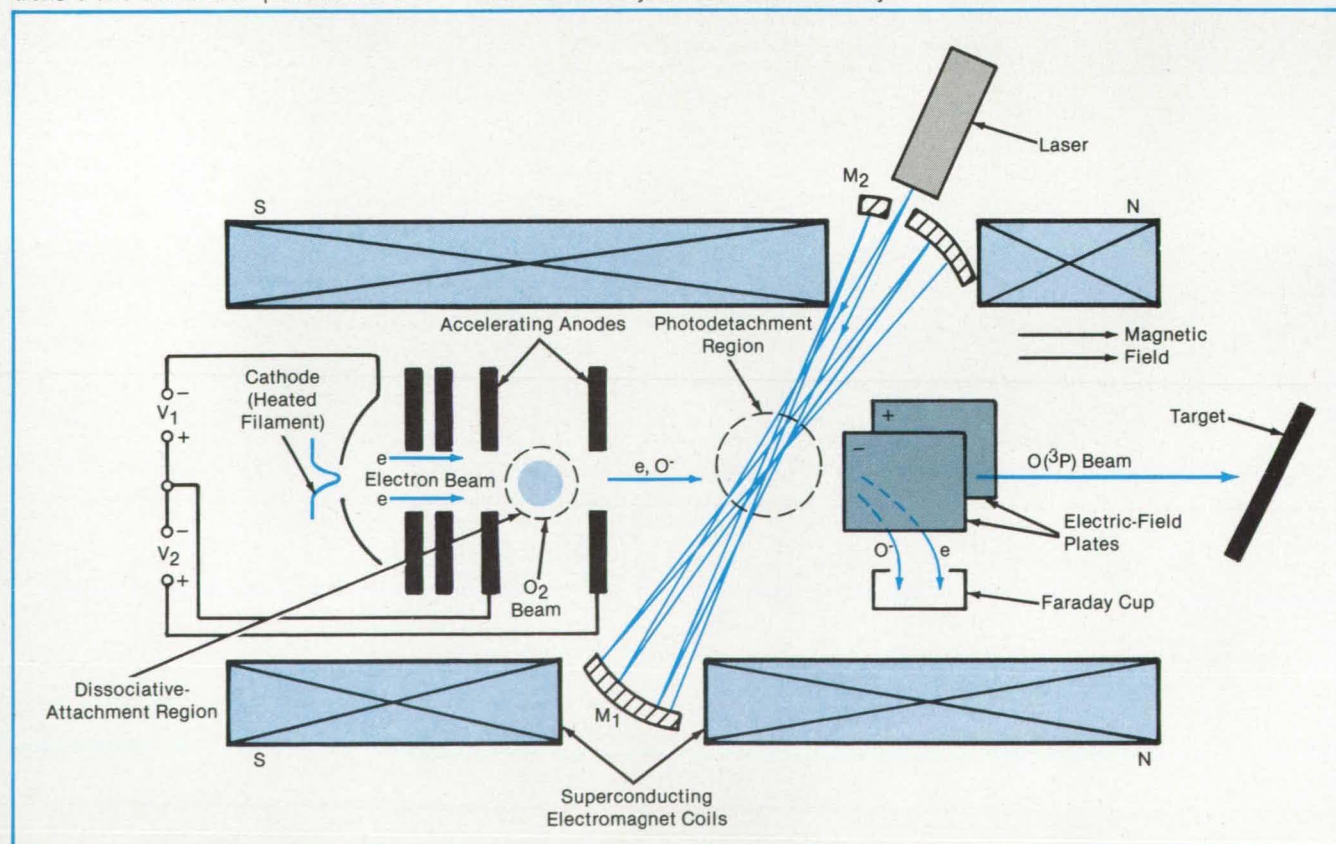
It should be possible to increase the source intensity to about 10^{17} /cm² by

scaling of the sizes of the beams from the currently proposed 1 cm diameter to 5 cm diameter. If lower atomic fluxes are desired (up to 10^{13} /cm²-s), then a lower confining magnetic field is required, and nonsuperconducting windings may be used in the magnet. In this case, the extraction of the O⁻ ions is possible in the dissociative-attachment region in a direction perpendicular to the magnetic axis.

It should also be possible to use the same scheme to prepare atomic-oxygen beams from a variety of oxygen-containing gases (for example CO, NO, N₂O, and CO₂). The particular gas used determines the energy spread and divergence angle in the O(3P) beam.

This work was done by Ara Chutjian and Otto Orient of Caltech for NASA's Jet Propulsion Laboratory. For further information, Circle 30 on the TSP Request Card.

NPO-16640



Accelerated Electrons Strike a Beam of O₂ Gas in the dissociative-attachment region, producing O⁻ ions. The O⁻ ions are accelerated to the desired final energy and pass through the photodetachment region to form O(3P) atoms. These pass between electric field plates to remove O⁻ and e and then strike the target.



Your technology needs can't wait this long

At Allied we've cut nature's timetable from centuries to days. We advance the state-of-the-art for single crystal garnet material every day. We have to.

To meet increasingly demanding needs for rods and slabs as solid state laser hosts.

To raise the standard and definition of both quality and size in Czochralski crystal growth and liquid phase epitaxy.



To maintain our leadership in meeting customer needs for Alexandrite, Nd:YAG, GSGG, LiNbO_3 , GGG, and LPE garnet films.

Let our resources help you take your technology into the 21st Century. Contact Allied Corporation, Synthetic Crystal Products, P.O. Box 31428, Charlotte, NC, 28231, 704/588-2340, Telex 572 573.

We can't wait either.



Partial-Transmission Scintillation Detector for Ions

Only the outer portion of the ion beam is sampled to prevent unnecessary energy losses.

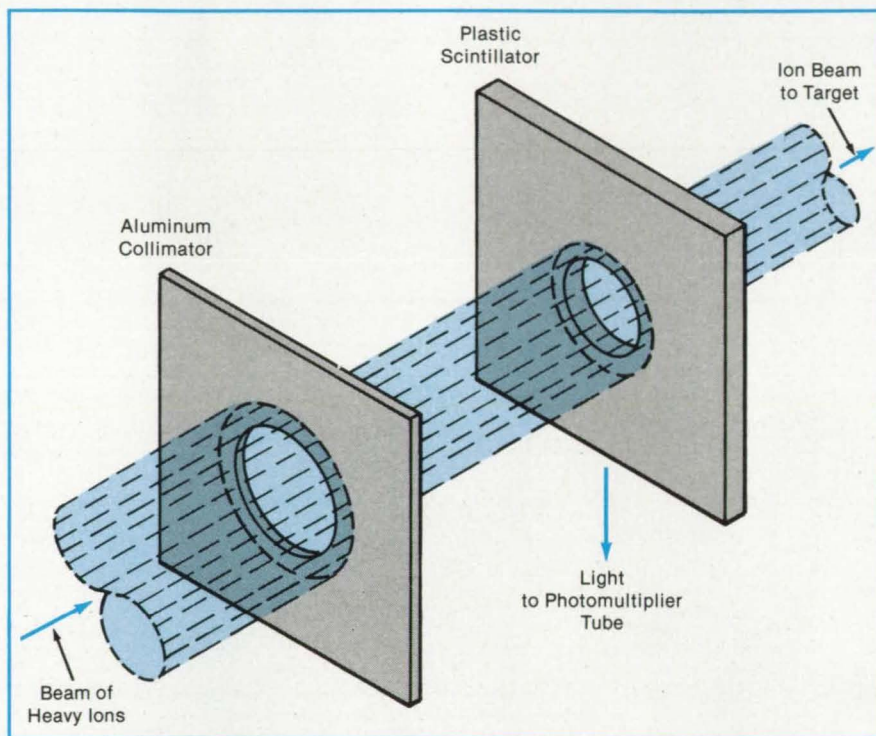
NASA's Jet Propulsion Laboratory, Pasadena, California

The flux of heavy ions in a beam can now be measured without significantly reducing the energies of the ions in the central part of the beam. Previously, the ion flux was measured by passing the beam through a scintillation foil coupled to a photomultiplier tube. The ions lost kinetic energy as they traversed the foil. The use of thin foils (0.5 micrometer or less in thickness) to reduce the energy loss was difficult, however, because the foils were fragile and often could not withstand the handling and vibration.

A new measurement device allows only the periphery of the beam to pass through a scintillation material. The total flux in a uniform beam can be inferred from the peripheral flux. The device thus provides readings without reducing the energy of the ions in the middle of the beam.

The ion beam is collimated by a hole in an aluminum plate (see figure). The beam then passes through a hole in a plastic scintillation plate. This second hole is coaxial with the first one and slightly smaller in diameter. This hole thus intercepts the edge of the beam. The ions impinging on the plastic cause it to scintillate, and the scintillation is measured by a photomultiplier tube.

This work was done by Carl J. Malone and John A. Zoutendyk of Caltech for NASA's Jet Propulsion Laboratory. For



A Plastic Scintillation Screen measures heavy-ion flux with minimal effect on the middle of the ion beam. The measurement device was developed for ion beams used in studies of how fast, heavy ions affect integrated-circuit chips.

*further information, Circle 12 on the TSP Request Card.
NPO-16501*

Solid-Sorbent Air Sampler

Portable unit takes eight 24-hour samples.

Lyndon B. Johnson Space Center, Houston, Texas

Volatile organic compounds in air are collected for analysis by a portable, self-contained sampling apparatus. The sampled air is drawn through the sorbent material, a commercial porous polymer of 2,3-diphenyl-p-phenylene oxide. High-boiling-point organic compounds are adsorbed onto the polymer, while low-boiling-point organics, O_2 , N_2 , Ar, CO_2 ,

CO , and H_2O , pass through and are returned to the atmosphere.

The sampling apparatus (see figure) includes eight glass-lined stainless-steel sample tubes filled with the sorbent. The tubes are normally isolated from each other (to prevent cross-contamination) and from the atmosphere by a manually-operated 18-port switching valve.

As shown schematically at the bottom of the figure, the valve is turned to connect the desired sample tube to the atmosphere, and air is drawn through the tube by a pump. At the end of the sampling period (normally, 24 hours), the operator turns the valve handle to the next position, thereby exposing a new sample while isolating and protecting the

**DRAWING A LINE ON THE
HIGH COST OF GHz ACOUSTO-OPTICS**

\$5995

GHz GAP BRAGG CELL
(limited time offer)

- **GaP BRAGG CELL**
- **GHz FREQUENCY**
- **EFFICIENCY 30%**
- **30 DAY DELIVERY**



brimrose

brimrose corporation of america • 7720 belair road • baltimore, maryland 21236
301/668-5800 • telex: 910-997-6817

Various custom devices available.

UNITED KINGDOM

Walmore Electronics Limited
Registered Office
Laser House
132/140 Goswell Road
London EC1V 7LE
Tel: 01-251 5115
Telex: LONDON 28752
Fax: 01-250 4143

WEST GERMANY

Hiltrion GMBH
Lochhauser Str. 4
8039 Puchheim b. Munchen
Tel: (089) 806616
806633
Telex: 5-28 139 hilt d

ISRAEL

Applied Technologic Services
51 Haoranim Street
P.O. Box 9031
Ramat Efal. 52 190
Tel: 03-716855
Telex: 341787 ATS 1L

N.Calif., Oregon, Washington

Allis Associates
P.O. Box 1256
Cupertino, CA 95014
Tel: (408) 252-2883
Telex: 383810

previous sample(s).

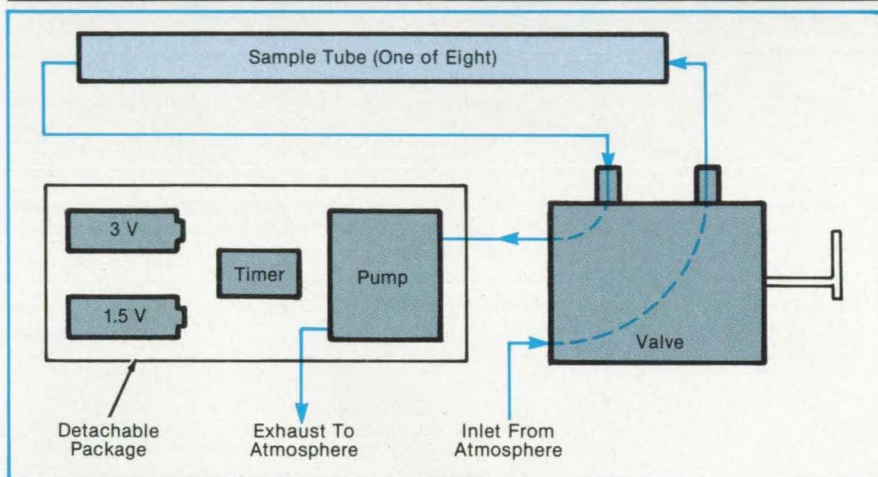
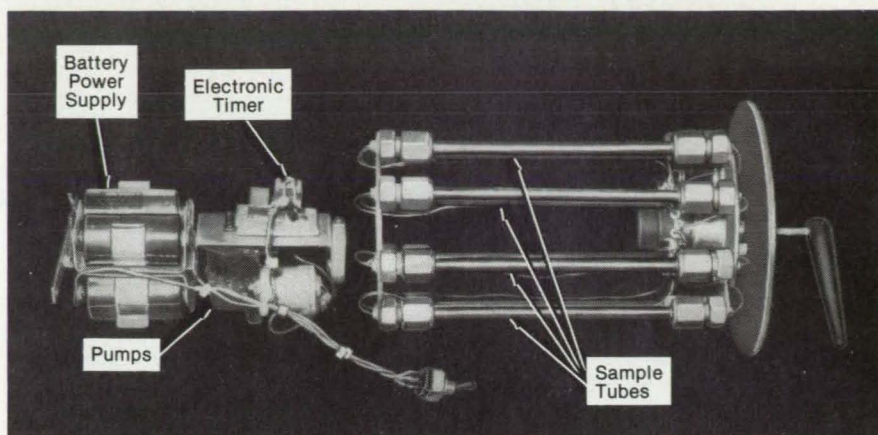
Electrical power for the 1.5-V pump motor is controlled by a 3-V timing circuit, the output of which is adjustable from one pulse every 7 seconds to continuous: This enables the sampling airflow rate to be preset at a value between 0.1 and 0.5 cm³/min. The motor and timer are both powered by alkaline C-cells, which operate continuously for up to 21 days.

For analysis, the sample tubes remain in place and are connected through the valve to a standard gas-chromatographic/mass-spectrometric system. Since the tubes do not have to be handled or exposed to the atmosphere during analysis, the risk of sample contamination is further reduced.

Although designed for checking air in spacecraft, the sampler is readily adaptable to such other applications as leak detection, gas-mixture analysis, and ambient-air monitoring. The unit is lightweight and compact [3.3 lb (1.5 kg), 4.5 in. (11.4 cm) in outside diameter, and 8 in. (20.3 cm) long]. Operation is simple: Power must be turned on and off, and the valve handle must be turned manually; but no other operator intervention is required.

This work was done by Theodore J. Galen of Northrop Services, Inc., for Johnson Space Center. For further information, Circle 40 on the TSP Request Card.

This invention is owned by NASA, and a patent application has been filed. Inquiries concerning nonexclusive or ex-



The **Solid-Sorbent Air Sampler** includes eight sample tubes filled with a polymeric sorbent. Organic compounds in the atmosphere are adsorbed when air is pumped through the sorbent.

clusive license for its commercial development should be addressed to the

Patent Counsel, Johnson Space Center [see page 29]. Refer to MSC-20653.

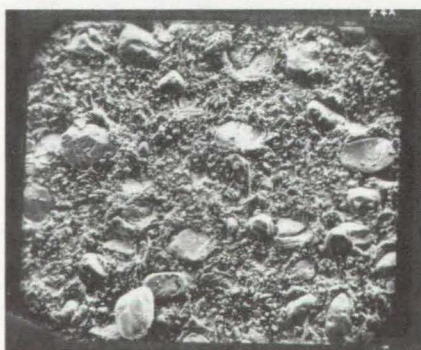
Mapping the Structure of Heterogeneous Materials

An image-processing microdensitometer/Fourier analyzer yields statistics of subcomponent distribution.

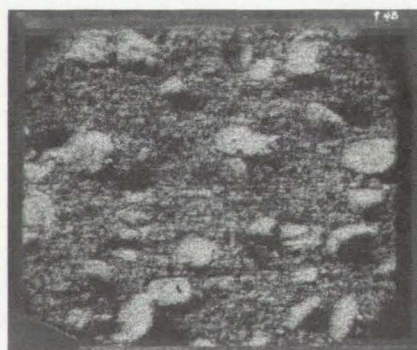
NASA's Jet Propulsion Laboratory, Pasadena, California

A nondestructive method for studying the structure of heterogeneous materials uses energy-dispersive X-ray analysis in a scanning electron microscope. A scanning microdensitometer/Fourier analyzer (SMFA) is applied to the SEM images to obtain statistics about the sample structure.

The method was originally developed for studying the effect on combustion of the fine structure of composite solid propellants. The propellant studied includes ammonium perchlorate as an oxidizer and hydroxyl-terminated polybutadiene as a binder. Three samples were prepared for analysis; one with coarse oxidizer particles (mass mean particle size approximately 200 μ m), one with fine particles (10 μ m),



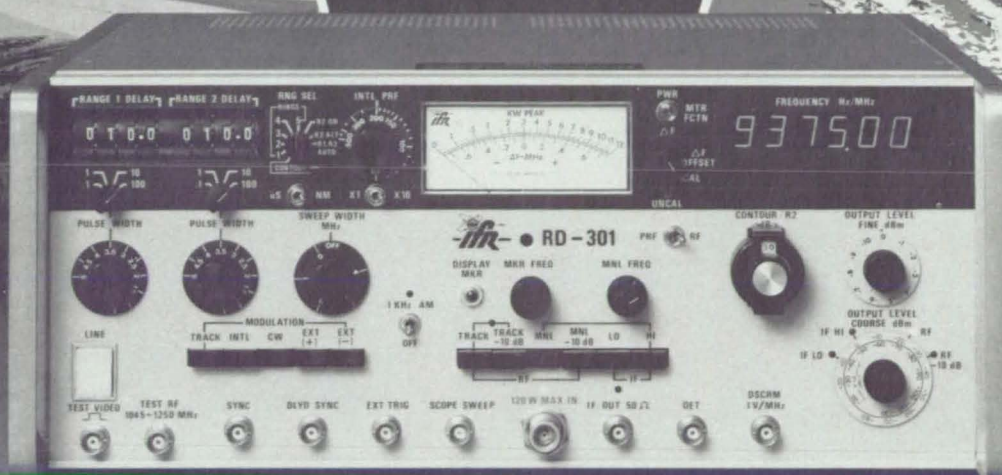
SCANNING-ELECTRON-MICROSCOPE PHOTOGRAPH OF A PROPELLANT



ENERGY-DISPERSIVE X-RAY ANALYSIS CHLORINE MAP OF THE PROPELLANT SHOWN AT THE LEFT

Figure 1. Aspects of the Oxidizer Chlorine Distribution in a propellant are shown by simple scanning-electron microscopy with energy-dispersive X-ray analysis.

The RD-300's First No-Compromise Competitor



The RD-301

with improved performance plus surveillance and marine radar testing capabilities.

Improving on the RD-300 —

Superior Airborne Weather Radar Testing:

- Improved tracking accuracy for new generation, low power systems
- Wide/Narrow interlace capabilities for dual EFIS displays and turbulence
- Calibrated contour boost for color radar
- Greater stability

And Introducing —

Surveillance Radar Testing:

- Two fully independent range replies. Reply delays respond to wide and narrow pulse widths. Contour Mode provides additional 0 to 20 dB amplitude boost above the selected output level.

Marine Radar Testing for 360° narrow pulse:

- Accurate tracking of narrow pulses to 50 ns

Features — All standard with the RD-301

- Built-in IF sweep generator from 20 to 70 MHz and marker generator for IF and AFC testing
- Radar UUT sensitivity testing
- Detector, discriminator and spectrum analyzer outputs
- Transmitter peak pulse power measurements
- Respond to radar transmitter pulse widths of 50 ns to 30 μ s
- Two-year limited warranty

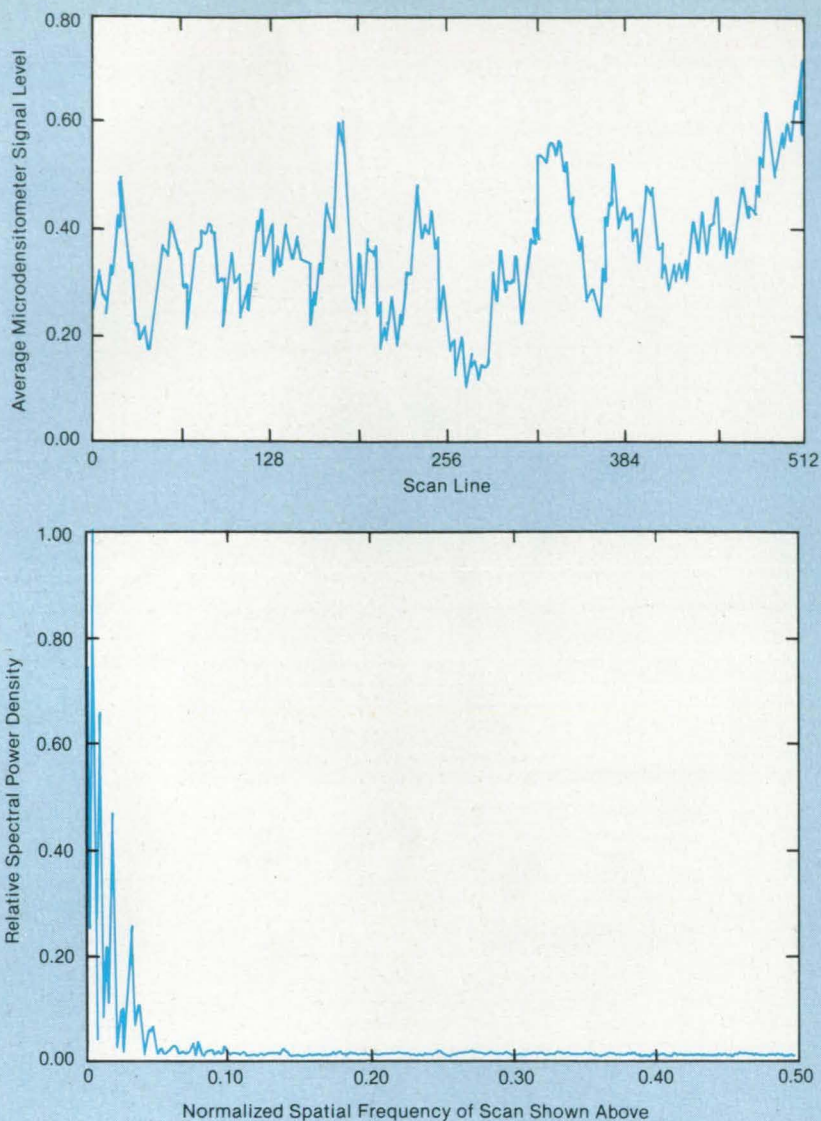
Call your IFR distributor today for a demonstration. Or contact IFR SYSTEMS, INC., 10200 West York Street / Wichita, Kansas 67215 U.S.A. 316/522-4981 / TWX 910-741-6952

Precision
Simulators
from



Remember IFR. The only no-compromise radar test equipment.

Circle Reader Action No. 317



and one containing both size groups. The results for a representative bimodal sample are shown in the figures.

Since there is chlorine in the oxidizer, but not in the binder, its presence maps the oxidizer distribution. The SEM images are analyzed with the SMFA, first to obtain the projection of the chlorine concentration along the axis, and then to obtain the spatial-frequency distribution of the fluctuations in that distribution. Finally, by taking the reciprocals of the frequencies of peaks in the spatial frequency distribution, characteristic dimensions related to the sample are obtained.

From tabulations of the characteristic dimensions for a number of samples, it appears that the characteristic dimensions correspond approximately to the range of particle sizes in the samples. The characteristic dimensions for the coarse samples ranged from 45 to 398 μm ; those for the fine samples, from 8 to 381 μm .

This work was done by Leon D. Strand, Norman S. Cohen, and Miguel A. Hernan of Caltech for NASA's Jet Propulsion Laboratory. For further information, Circle 17 on the TSP Request Card.
NPO-16487

Figure 2. **Analyses of Scanning-Microdensitometer Measurements** of the chlorine map in Figure 1 yield data that help to characterize the oxidizer-density distribution.

Electro-optical Tuning of Fabry-Perot Interferometers

A compact unit can operate much faster than conventional piezoelectric scanners.

Goddard Space Flight Center, Greenbelt, Maryland

A proposed electro-optical method of tuning or scanning the passband of a Fabry-Perot interferometer can be much faster than previous methods and employ more compact equipment. In a Fabry-Perot interferometer, two parallel glass plates, separated by a few centimeters, are partly silvered on their inner surfaces so that an incoming light beam is repeatedly reflected between them before it is transmitted to instrumentation. Until now, this type of interferometer has been

tuned by the adjustment of separation between the plates. This separation could be changed either by a voltage applied to a piezoelectric transducer on one of the mirrors or by a change in pressure of a gas between the mirrors.

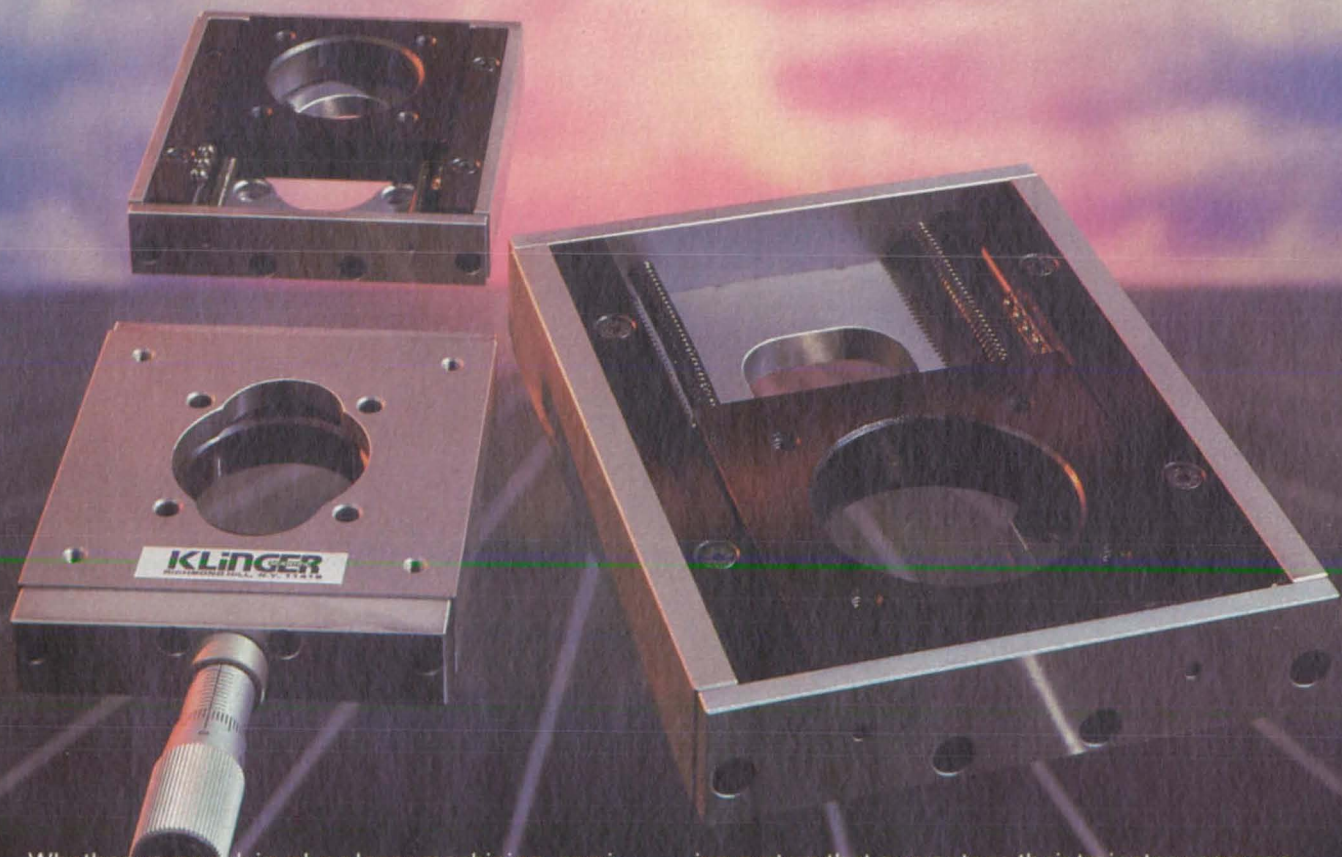
Piezoelectric scanners, however, are limited in their tuning speeds. For visible light, a piezoelectric scanner takes about 10 milliseconds per interferometer order, and scanning time is longer for light of longer wavelengths. Moreover, piezoe-

lectric scanners add to the interferometer size and become bulkier when greater scanning range is needed. Pressure scanners are even slower than the piezoelectric models and require gas-handling equipment.

In one version of the proposed scanner, a Pockels cell crystal is placed between the mirrors of the Fabry-Perot interferometer (see figure). Such a cell, usually made of a birefringent material like potassium dihydrogen phosphate, changes its

THE KLINGER ARGUMENT AGAINST COMPROMISE:

**ONLY WE LET YOU SELECT FROM OVER
200 DIFFERENT STAINLESS STEEL LINEAR STAGES THAT
GUARANTEE POSITIONING TO 1 MICRON OR BETTER.**



Whether your work involves laser machining, semiconductor probing, inspection, optical systems, or any other positioning application, Klinger's high accuracy MR/MRT stages provide cost-effective solutions to the most demanding design problems.

From the smallest manually operated stage made to one capable of carrying 150 pounds, these linear positioners offer a choice of drive methods which include precision micrometers, fine pitch screws, or digital micrometers.

Our MRS linear stages are provided without any drive mechanism allowing you to devise your own method of actuation.

All of our linear stages use a precision-ground bear-

ing system that guarantees their trajectory accuracy, and they can be assembled for XY or XYZ applications. Options include preparation for vacuum and clean room environments.

Don't compromise. The best is always a bargain. Klinger standards of engineering and manufacturing, as exemplified by our manually operated linear stages, have made us the world leader in micropositioning systems. Get our free 212-page micropositioning handbook for complete specifications on these and thousands of other components.

Write or call Klinger Scientific Corporation,
110-20 Jamaica Avenue, Richmond Hill, NY 11418
(718) 846-3700.

KLINGER

SCIENTIFIC

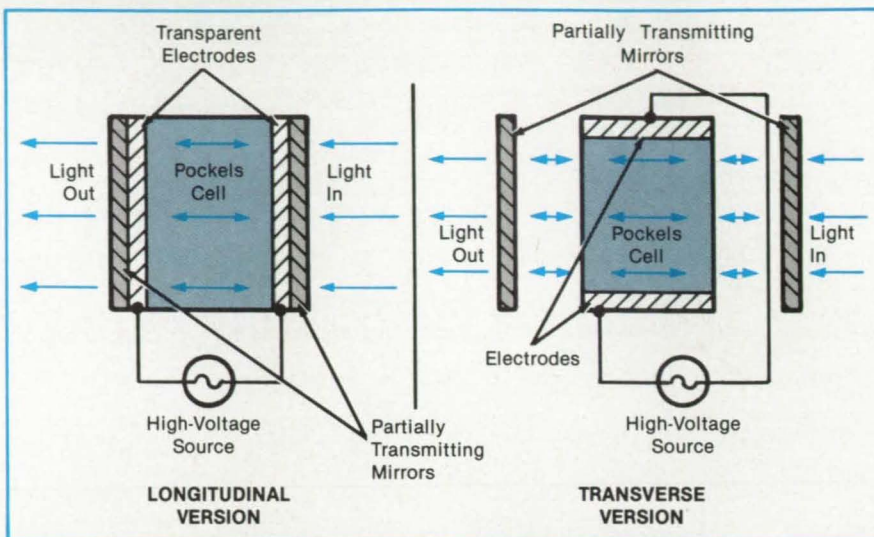


Worldwide Network to Meet Your Needs • France: Micro Controle, Evry, (tel.) 6-077-82-83 • West Germany: Spindler & Hoyer, Gottingen, (tel.) 49/551/620/16
Canada: Optikon Corp. Ltd., Waterloo, Ontario, (tel.) 519/885/2551 • England: Unimatic Engineers Ltd., London, (tel.) 44/1/455.00.12
Netherlands: Elmekanik N.V., Hilversum, (tel.) 31/35/43.070 • Sweden: Martinsson & Co. Hagersten, (tel.) 09/744/03/00
Switzerland: G.M.P.S.A., Lausanne, (tel.) 41/21/33/33/28 • Italy: Leitz Italiana, Milano, (tel.) 39/2/27/55/46 • Japan: Hakuto Co. Ltd., Tokyo, (tel.) 03/341/2611.

refractive index under an applied electric field. The Pockels crystal is oriented so that one of its electrically induced axes is parallel to the plane of polarization of the incident light beam. A voltage applied across the crystal surfaces changes the optical path length between the mirrors without changing the gap between them. The interferometer therefore can be scanned by changes in voltage on the Pockels cell.

The voltage is applied through electrodes on opposite faces of the cell. The mirrors may be affixed directly to the cell faces. If a longitudinal electric field is used and the electrodes are not only conductive but also transparent to the incident light, these electrodes can be deposited as films over the entire end faces of the crystal. (Indium tin oxide, for example, is conductive and is transparent at visible wavelengths.) The electrodes would then create a highly-uniform electric field within the crystal, and the Pockels cell could be made very thin. Reflective film could be deposited directly on the electrodes, and the entire interferometer would be compact.

The new electro-optic scanner would scan a given range in one-millionth the



A High Voltage creates an electric field in a Pockels cell, changing its refractive properties. The cell therefore changes the optical path length between the mirrors without mechanically moving anything in the gap. The high voltage can be varied rapidly to scan the interferometer. The voltage is applied longitudinally or transversely, depending on the type of Pockels cell.

time of a piezoelectric scanner — tens to hundreds of nanoseconds per interferometer order. At the same time, its small size would reduce the size of an interferometer.

This work was done by Geary K. Schwemmer of Goddard Space Flight Center. For further information, Circle 73 on the TSP Request Card. GSC-12971

Recording Interferograms Holographically

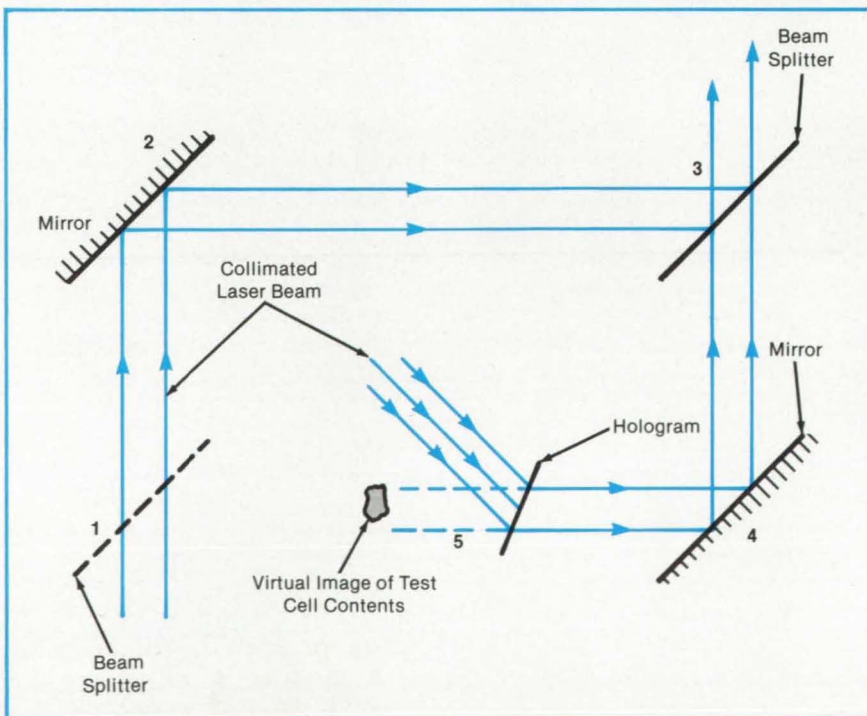
Images of experiments are stored for later analysis.

*Marshall Space Flight Center,
Alabama*

A holographic system reconstructs interferometer images recorded during experiments for later, more detailed analysis. The system was developed for experiments on crystal growth during space flights. With it, images are recorded rapidly under the constraints of the experiments and are later examined on the ground.

The holographic images are reconstructed in a modified Mach-Zehnder interferometer, an instrument often used to measure the spatial variation of the index of refraction of a gas. In its classical form, the Mach-Zehnder interferometer consists of two beam splitters (semitransparent mirrors) and two wholly reflecting mirrors at alternate corners of a rectangle. Halves of an incoming light beam travel along opposite faces of the rectangle. The halves combine at a semitransparent mirror to form an interference pattern.

The classical interferometer was modified for holography by removing the en-



In a **Classical Mach-Zehnder Interferometer**, path 1-2-3 is the reference leg, and path 1-4-3 is the object leg. In the interferometer modified for holography, the beam splitter at 1 is removed, as indicated by the dotted line, and path 1-2-3 is still the reference leg, but path 5-4-3 is now the object leg.

trance semireflecting mirror and inserting the holographic recording in one of the legs (see figure). A collimated laser beam is projected through the hologram and directed to the remaining semitransparent mirror. There it combines with a refer-

ence beam from the same laser to form a virtual image of the original experiment.

This work was done by Ellis R. Comeens and Robert L. Kurtz of TAI Corp. for Marshall Space Flight Center. No further documentation is available.

Inquiries concerning rights for the commercial use of this invention should be addressed to the Patent Counsel, Marshall Space Flight Center [see page 29]. Refer to MFS-26024.

Comparative Thermal-Conductivity Test Technique

Approximate thermal conductivities are determined rapidly.

*Lyndon B. Johnson Space Center,
Houston, Texas*

The thermal conductivity of a material can be estimated conveniently in a test procedure that compares it to a material of known conductivity. This procedure can be used to rate quickly the candidate materials for applications in which thermal conductivity is a prime consideration. Once the selection has been reduced to one or two candidates, formal thermal-conductivity test methods can be used to verify the results of the inexpensive comparative technique.

An exploded view of the test arrangement is shown in the figure. The two 1- by 6-in. (2.5- by 15-cm) test specimens, one of known thermal conductivity, are well separated by insulation and then wrapped in insulation. This assembly is then partially inserted into a tube furnace so that one end of each specimen is exposed to the furnace temperature, and the other end is open to the atmosphere. Thermocouples are attached to both ends and to the middle of each sample. The thermocouple readings are monitored for 15 to 30 min.

The steady-state conduction equations for each specimen are ratioed and solved for the conductivity ratio (candidate sample to known sample). The heat-flow ratio — needed for this calculation — is determined using the temperatures of the heated ends of the specimens to calculate the convective and radiant interchanges between the specimens and the furnace. The data-reduction procedure can be programmed into a hand-held calculator. Originally applied to advanced carbon/carbon composite materials at temperatures above 3,000° F (1,600° C), this procedure should be applicable to a wide variety of materials and a wide range of temperatures.

This work was done by Charles N. Webster and James K. Willis of LTV Aerospace Corp. for Johnson Space Center. No further documentation is available.

NASA Tech Briefs, March/April 1986

WITH EG&G'S NEW FIBER OPTICS RECEIVERS YOU DON'T HAVE TO CHOOSE BETWEEN SPEED AND SIZE

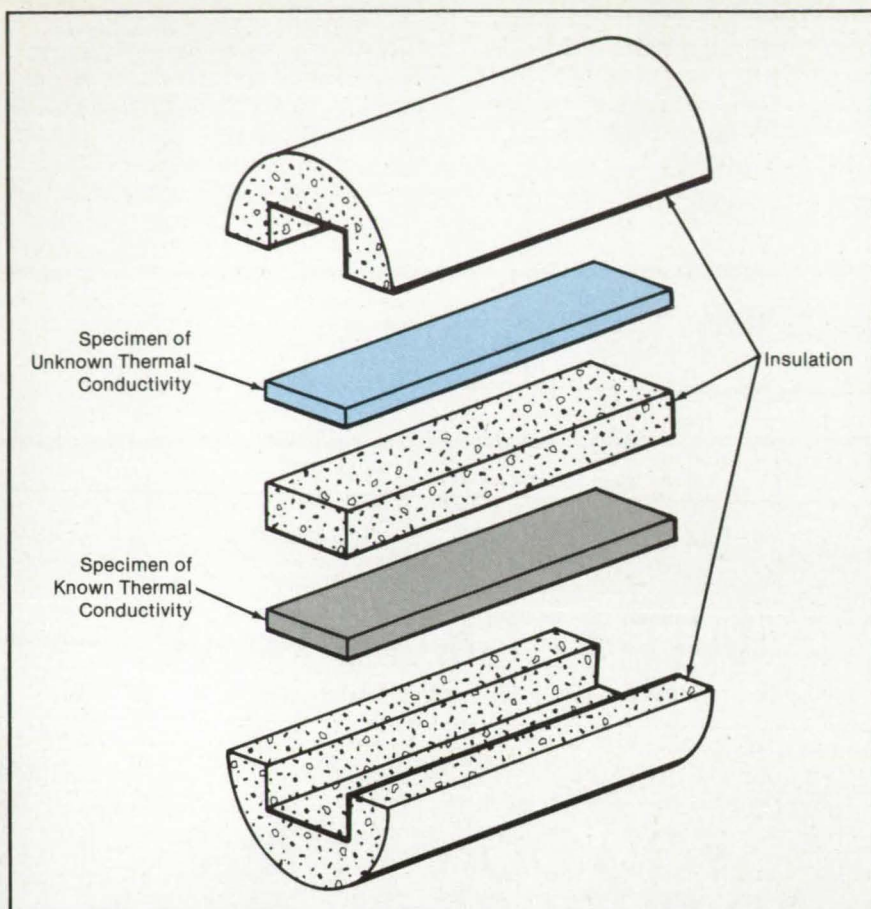
- Responsivity @ 904nm = $> 0.60\text{A/W}$
- Active Area = 5.1mm^2
- Rise Time = $< 1\text{ nanosecond}$



EG&G ELECTRO-OPTICS

For further information, contact EG&G Electro-Optics
35 Congress Street, Salem, MA 01970. (617) 745-3200.
No. California (408) 735-1450. So. California (818) 344-3696.
Central States (312) 253-0335. Mid-Atlantic States (609) 452-7772.
Southeastern States (904) 383-0758.

Inquiries concerning rights for the commercial use of this invention should be addressed to the Patent Counsel, Johnson Space Center [see page 29]. Refer to MSC-20980.



The Two Specimens, the conductivities of which are to be compared, are placed in an assembly with insulation. One end of the assembly is then placed in a furnace. The temperature of the furnace, of each end, and of the center of each specimen are then recorded.

SPACE

...on board NASA Tech Briefs' next launch

"NASA Tech Briefs WORKS for advertisers."

That's according to Bill Waskey, Director of Business Development for Fairchild Industries' Control Systems Division, and other executives now advertising in NASA Tech Briefs. Companies like Rockwell, Amoco, Data General, and DuPont have already received more than 7500 top-quality responses to their ads in just one issue of NASA Tech Briefs. If your company is on the leading edge of technology, shouldn't you be marketing in the #1 magazine on the leading edge of technology?

Confirm Your Space on Board.

To find out how you can be on board the next launch of NASA's official magazine, call Robin DuCharme, Dick Soule or Wayne Pierce in New York at (212) 490-3999; Irene Froehlich in Chicago at (312) 848-8144; or Bob Bruder in Los Angeles at (213) 477-5866.

NASATechBriefs
is published by
Associated Business Publications
41 East 42nd Street, Suite 921
New York, NY 10017

Books and Reports

These reports, studies, and handbooks are available from NASA as Technical Support Packages (TSP's) when a Request Card number is cited; otherwise they are available from the National Technical Information Service.

Three-Dimensional Radiative-Transfer Equation

Progress is made toward the interpretation of radiometric observations.

A theoretical paper discusses the equation of radiative transfer in a three-dimensional, inhomogeneous, scattering medium illuminated from above and bounded below by a laterally-inhomogeneous, reflective plane. A representation of the radiation field with full three-dimensional variability is derived by use of a spatial Fourier transform and matrix-operator techniques developed previously for the

one-dimensional version of the problem. The equations should be useful for radiometric measurements from aircraft and spacecraft.

Initially, the problem is stated generally in terms of spatial integrals expressing the radiation incident upon, generated within, reflected from, and passing through, a horizontal planar layer. The horizontal spatial dependence of all quantities is approximated as periodic for discretization of the Fourier wave-number spectrum. In practical problems, such an approximation does not give rise to errors as long as an appropriate buffering zone is constructed within the primary pattern to prevent contamination by the adjacent repetitions of the pattern. The periodicity assumption makes it convenient to take the two-dimensional Fourier transform of the radiative-transfer equation in the horizontal plane.

Explicit expressions for the reflectivity and transmissivity operators and emission functions for an infinitesimally thin layer bounded by the z and $z + \Delta z$ planes are obtained by expansion of the Fourier-transformed radiation equations about the vertical coordinate z . By use of these operators and functions in the context of the interaction principle, expressions are obtained for the mathematical synthesis of a vertically inhomogeneous, arbitrarily thick medium. A doubling theorem makes it possible to obtain the operators and functions for an arbitrarily thick, homogeneous layer from a similar layer of infinitesimal thickness. Because a thick, inhomogeneous layer can be conveniently simulated by a vertical sequence of homogeneous layers, each in sequence having slightly different properties, the radiation-transfer functions for the entire thick, inhomogeneous layer can be built up by the combination of adding and doubling techniques.

Following the derivation described above, the basic equations are restated, and all equations are rederived in matrix form. The scattering medium is vertically stratified into a number of different layers, each of which is internally homogeneous. As before, the adding and doubling relations are derived and used to model thick layers. Although the derivations and the resulting equations are complicated, the use of the Fourier-transform, matrix-operator approach to solve practical problems is expected to be simpler than direct solution of the complete three-dimensional, linear wave equations.

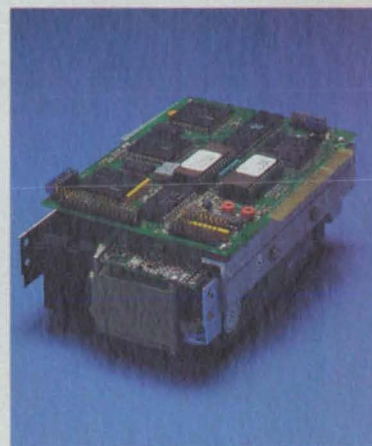
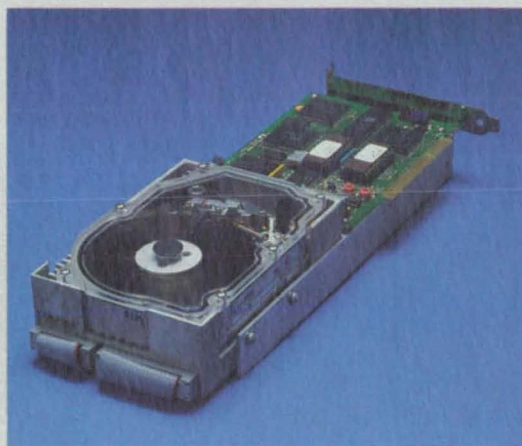
This work was done by John V. Martonchik and David J. Diner of Caltech for NASA's Jet Propulsion Laboratory. To obtain a copy of the report, "Three-Dimensional Radiative Transfer Using a Fourier Transform Matrix Operator Method," Circle 107 on the TSP Request Card.

NPO-16563

Circle Reader Action No. 346 ►

Announcing the 20 Megabyte Express Hard Disk Card™ for only \$595

Comes complete with everything you need, installs in minutes, and has a 1 to 1 interleave factor. For an extra \$95 you can add it to an existing hard disk and have both disks act as one volume.



Easy Installation

If you're someone who hates reading installation manuals, doesn't understand directions, or who gets intimidated installing internal disk drives, then the Express Hard Disk Card™ is for you. Simply insert it inside your IBM® PC, PC XT, or compatible, like any other add-on card.

High Performance

The Hard Disk Card gives you 20 megabytes—and something more. The Controller comes with a 1 to 1 interleave factor, which means that you retrieve data 6 times faster than the PC XT's 6-to-1 interleave controller.

Express Systems, Express Hard Disk Card and Coalesce are Trade Marks of Express Systems, Inc. Coalesce requires DOS 3.1

One File Across Two Hard Disks

With Express Systems' new Coalesce™ Software, you can add our 20 megabyte Hard Disk Card™ to your existing hard disk. They will both work together as though they were one disk—*regardless of their size*. Coalesce not only merges the two hard disks together, it bypasses the DOS barrier of 32 megabytes. That means that if you're using a 32 megabyte hard disk, you can add our Hard Disk Card and have a total of 52 megabytes as a single file!

For the best buy in a convenient, easy to install 20 megabytes of hard disk storage, call Express Systems.

1-800-341-7549

In Illinois, call 1-312-882-7733



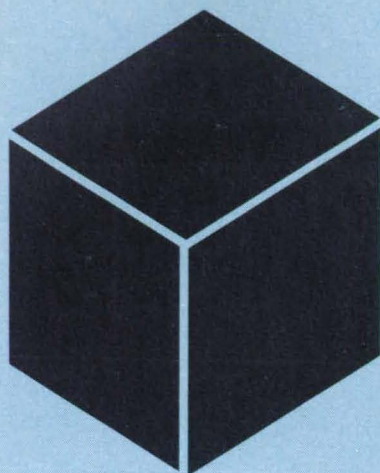
EXPRESS SYSTEMS

Call Toll Free 1-800-341-7549 Ext. 2800
In Illinois call (312) 882-7733 Ext. 2800

Express Systems, Inc. 1254 Remington, Schaumburg, IL 60195

IBM® is a registered trademark of the International Business Machines Corporation.

Materials



Hardware, Techniques, and Processes

- 78 Ball-and-Socket Mount for Instruments
- 80 Si_3N_4 -Based Ceramic With Greater Hot Strength
- 80 Compression-Failure Mechanisms in Composite Laminates
- 82 Detoxification of Halon Fire-Extinguishant Products
- 83 Phosphazene Polymers Containing Carborane
- 84 Room-Temperature Deposition of NbN Superconducting Films
- 85 Increasing the Cryogenic Toughness of Steels
- 86 Impact-Resistant Ceramic Coating
- 86 Carbon Shields for Intercalated Fiber Conductors
- 87 Producing Large-Particle Monodisperse Latexes
- 88 Process Produces Low-Secondary-Electron-Emission Surfaces
- 90 Antisoiling Coatings for Solar Energy Devices
- 92 Heat- and Radiation-Resistant Lubricants for Metals

Books & Reports

- 93 Fundamentals of Alloy Solidification
- 93 Composite Refractory Felt/Ceramic Material

Computer Programs

- 94 Intraply Hybrid Composite Design

Ball-and-Socket Mount for Instruments

Jaws engage an instrument precisely but release it readily.

Marshall Space Flight Center, Alabama

A mounting mechanism holds a scientific instrument securely, allows the instrument to be oriented, and minimizes conduction of heat to and from the instrument. The mechanism also allows quick replacement of the instrument.

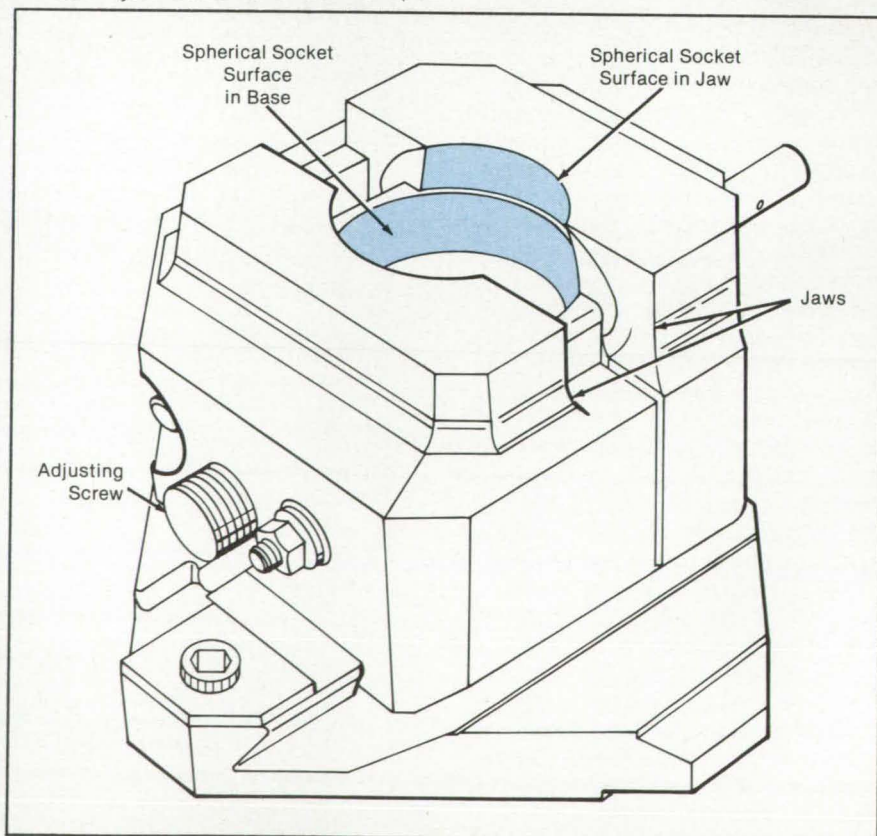
The mechanism includes a stationary base containing part of the spherical-socket surface, two jaws that contain the rest of the socket surface, and an adjusting screw. A ball on the instrument sits in the spherical socket formed by the opposing jaws and base (see figure). The adjusting screw is threaded into one of the jaws and rotates in a collar in the opposite jaw. Rotating the screw counterclockwise opens the mechanism by sliding the jaws outward on a dovetail track on the base. The instrument ball can then be removed from the opened socket. Turning the screw clockwise draws the jaws together until the socket captures the ball.

Each jaw contains three T-shaped

parts that maintain the alignments of the jaw parts and serve as internal stops. These parts have cylindrical arms that seat in cylindrical holes in the base as the jaws draw together. When the tees are seated, the adjusting screw is further turned to a torque of 35 lb-ft (47 N-m) to preload the mechanism and prevent the tees from separating from the base. When thus assembled, the mechanism maintains a diametral clearance of 80 to 240 μm (2 to 6 μm) between the socket and the ball.

This work was done by Everett Kaelber of Perkin-Elmer Corp. for Marshall Space Flight Center. For further information, Circle 110 on the TSP Request Card.

Inquires concerning rights for the commercial use of this invention should be addressed to the Patent Counsel, Marshall Space Flight Center [see page 29]. Refer to MFS-28064.



Opposing Jaws Sliding on a Base form a socket that holds the mounting ball of a scientific instrument.

SCHOTT ... Precision Optical Glass Made in America and More!!!



Schott Glass Technologies is geared to work with the largest production quantities or the smallest prototype development right here in the USA. Our 300,000 square feet of manufacturing facilities, backed by our scientific knowledge and technical skills, are ready to work for you at every stage of your program.

Our in-house research and development is among the most modern of its kind

anywhere. And we have the marketing and sales know-how to assure you that products made from Schott materials or components get to your customers on time and to specification.

And, above all, Schott Glass Technologies has the widest range of precision optical glass and components available in the Western Hemisphere today.

OPTICAL DIVISION

- OVER 250 TYPES OF OPTICAL GLASSES
- FIBER OPTICS RODS
- HIGH HOMOGENEITY GLASS BLANKS FOR MASSIVE OPTICS
- ZERODUR® — LOW EXPANSION MATERIAL
- PHOSPHATE AND SILICATE LASER GLASSES
- CERENKOV COUNTERS

COMPONENTS DIVISION

- CRT FACEPLATES
- SCIENTIFIC FILTER GLASS
- INTERFERENCE FILTERS
- CRT CONTRAST ENHANCEMENT FILTERS
- FIBER OPTICS SPECIALTIES
- B-270/CLEAR SHEET GLASS
- X-RAY LEAD GLASS
- RADIATION SHIELDING GLASS AND WINDOWS

OPHTHALMIC DIVISION

- CROWN GLASS — CLEAR AND TINTS
- 1.60 LIGHTWEIGHT CROWN GLASS
- HIGH-LITE® — HIGH INDEX LOW DENSITY GLASS
- SUN MAGIC® PHOTOCROMICS — FOR SUNWEAR
- PHOTOCROMICS — FOR PRESCRIPTION
- INDUSTRIAL SAFETY GLASS
- UV FILTERING CROWN
- SPECIALTY GLASS

TECHNICAL SERVICES

- CONTRACT RESEARCH AND DEVELOPMENT
- CUSTOM MELTING
- ANALYTICAL/PHYSICAL/OPTICAL MEASUREMENTS

— and the list goes on . . .

Our commitment . . .

**Research & Development, Manufacturing, Sales, Service — Total Capability
... your advantage.**



400 York Ave., Duryea, Pennsylvania 18642
(717) 457-7485 TWX 510-671-4535
Telefax (717) 457-6960

Circle Reader Action No. 383

Si₃N₄-Based Ceramic With Greater Hot Strength

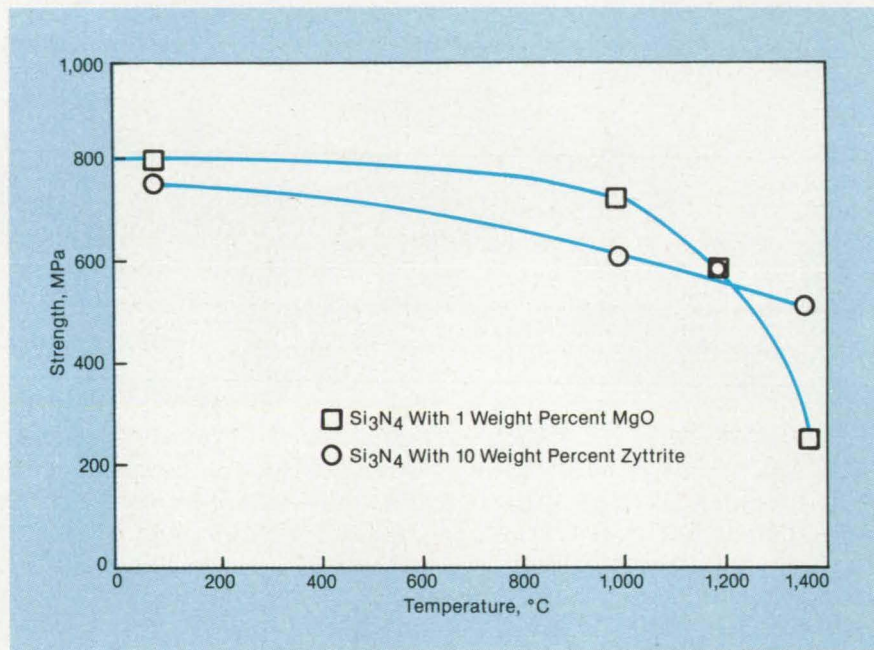
Zyttrite-doped material outperforms
MgO-doped material above 1,200° C

Lewis Research Center, Cleveland, Ohio

A new ceramic material has been produced by the addition of 10 weight percent zyttrite (yttria-stabilized zirconia) to Si₃N₄ (silicon nitride) that offers significantly-improved high-temperature properties (nearly double those of MgO-doped Si₃N₄ ceramic, as shown in the figure). The work also showed that by using controlled Si₃N₄ powder with 10 weight percent zyttrite, a significant improvement in room-temperature strength can be achieved.

Advanced ceramic materials that are of great interest for a variety of high-temperature structural applications are silicon nitride (Si₃N₄) and silicon carbide (SiC). Si₃N₄ and SiC ceramics have potential for use in aircraft and automobile engines and in electric-power generating systems. These ceramics combine high thermal conductivity and low coefficients of thermal expansion and consequently have high thermal-shock resistance. Because of their high refractory nature, these ceramics are capable of operating at temperatures in the range of 2,500° to 3,000° F (1,370° to 1,650° C). However, for sintering to full density, sintering aids are required that often form a glassy phase at the grain boundaries. In Si₃N₄, a glassy phase is responsible for strength loss at high temperatures.

With the new ceramic material, time-dependent flexure tests showed very little strength degradation at 1,400° C (2,552° F).



The **Four-Point-Bending Strengths** of two Si₃N₄-based ceramics are compared at different temperatures.

The creep resistance at 1,350° C (2,462° F) was one to two orders of magnitude better than Si₃N₄ materials containing MgO and Y₂O₃ as sintering aids. Further, the Weibull modulus "m" (for 30 test bars) was estimated to be 17, which is relatively high for Si₃N₄ materials, and the oxidation resistance at 1,370° C (2,500° F) in air compared favorably to the oxidation

resistance of silicon carbide material. These improved properties strongly suggest that the 10-weight percent zyttrite/Si₃N₄ material has a strong potential for high-temperature applications.

This work was done by Sunil Dutta and Bruno Buzek of **Lewis Research Center**. For further information, Circle 93 on the TSP Request Card. LEW-14193

Compression-Failure Mechanisms in Composite Laminates

Failure mechanisms are observed using transparent fiberglass/epoxy birefringent materials.

Langley Research Center, Hampton, Virginia

The efficient use of composites in aircraft structural components requires a thorough understanding of the failure mechanisms of these materials. The opaqueness of graphite/epoxy laminates prevents direct observation of the mechanisms involved in the initiation and prop-

agation of damage. Although destructive failure-assessment methods are available, the sequence of failure within the laminate is difficult to determine using these methods.

An in situ nondestructive technique was developed to observe failure as it de-

velops and as it propagates within the laminate. This technique is based on the use of a transparent fiberglass/epoxy birefringent material. The transparency allows visual observation of the location of initial laminate failure and of the subsequent failure propagation; the birefringence

allows the laminate stress distribution to be observed during the test and also after the test if permanent residual stresses occur.

Two $(+45_2/-45_2)_s$ fiberglass/epoxy specimens, each with a single, centrally-located circular hole, were tested. The specimens were fabricated from commercially-available glass cloth preimpregnated with epoxy resin. Specimens were nominally 6.0 by 3.0 by 0.11 in. (15.2 by 7.6 by 0.28 cm), and the hole diameters were 0.19 and 0.50 in. (0.48 and 1.27 cm).

The specimens were tested by slowly applying a compressive end load to simulate a static loading condition. The ends were machined flat and parallel to permit uniform compressive loading. Loaded edges were clamped by fixtures during testing while unloaded edges were supported by knife-edge restraints to prevent the specimen from buckling as a wide column. The polarizer and analyzer were oriented at $+45^\circ$ and -45° , respectively, to the load axis.

Experimental results shown in Figures 1 and 2 illustrate the value of the birefringent material for observing the failure of composite specimens. The specimens in Figure 1 were loaded and then unloaded. When these unloaded specimens were illuminated with polarized light, the isochromatic fringe patterns indicated that plastic deformation had occurred.

The pattern on specimen A indicates that high stresses exist in bands oriented at $\pm 45^\circ$ to the load axis. For this uniaxially loaded laminate, the in-plane shear stress is a maximum on elements oriented 45° to the applied load, resulting in high stresses in the epoxy matrix between fibers. The high stresses in the bands in specimen A are caused by in-plane fiber/matrix shearing in these regions and are identified as matrix-shearing bands in the figure. While the specimen was being loaded, these bands initiated at the hole boundary and grew toward the specimen edges.

Specimen B was loaded further into the plastic range than was specimen A. This specimen also has matrix-shearing bands, but the isochromatic fringes are not observed in the region of these bands. While the specimen was being loaded, severe internal damage occurred within the bands, disrupting the light path and destroying the birefringence. The damage was caused by local delamination and in-plane shearing failure mechanisms.

When this specimen is illuminated with white light (Figure 2), the damage in the matrix-shearing bands is indicated by the $\pm 45^\circ$ dark bands. The damage is most severe at the two locations where the hole boundary intersects the horizontal centerline of the specimen: the locations

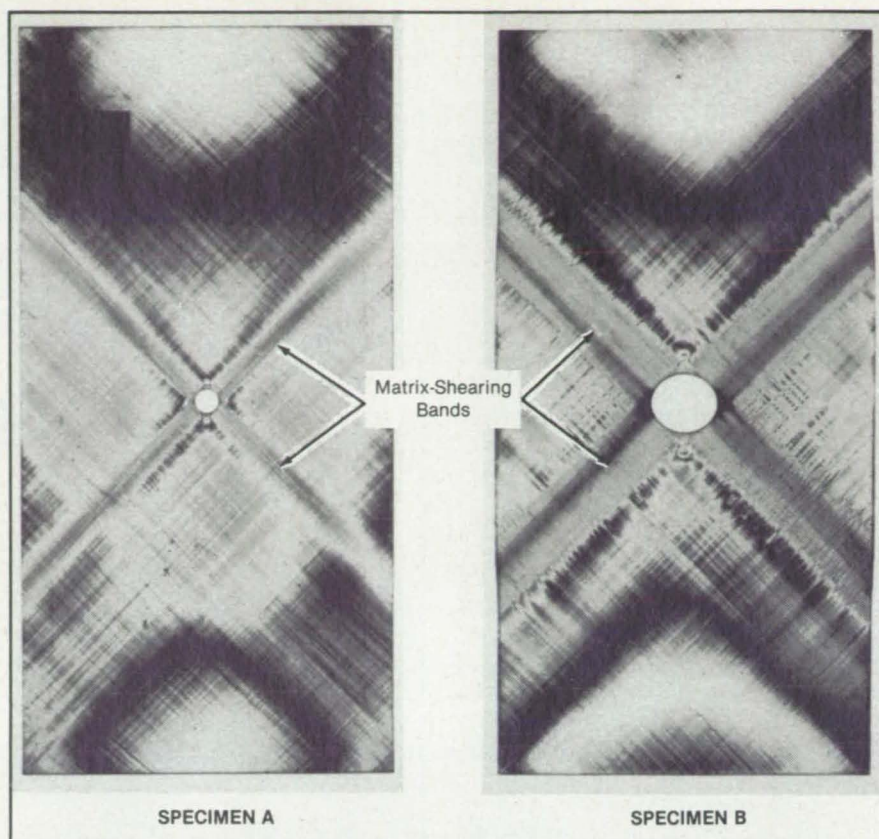


Figure 1. Polarized Light Reveals matrix-shearing bands in damaged regions of the specimen.

Super durable Kapton®

performs reliably year after year

Components made with KAPTON polyimide film provide enduring performance in hostile environments and harsh chemicals. They handle temperatures from -269°C to 240°C . They survive millions of flexes. Dielectric strength and tensile strength are excellent.

If your components need to perform reliably year after year, consider durable KAPTON, made only by Du Pont. For facts and a free sample, write Du Pont Co., KAPTON Rm. X40804, Wilmington, DE 19898.



where damage initiated.

Closer inspection of the damaged regions reveals a fiber-kinking mechanism. The kinking results from a $+45^\circ$ layer partially restraining the in-plane shearing occurring in an adjacent -45° layer, or vice versa. The fiber kinking occurs without fiber breakage due to the flexibility in the matrix provided by extensive shear failures.

The transparency and birefringence properties of the fiberglass/epoxy material enable regions of high stress to be located and the mechanisms of local failure and of failure propagation to be identified within the laminate. This fiberglass/epoxy material may also be useful for studying stress fields and for identifying failure initiation and propagation mechanisms in a wide variety of composite structures.

This work was done by Mark J. Stuart, Jerry G. Williams, and Paul A. Cooper of Langley Research Center. Further information may be found in:

NASA CR-165709 [N81-26183/NSP], "Development of Orthotropic Birefringent Materials for Photoelastic Stress Analysis" [\$10], and

NASA TM-86306 [N84-20259/NSP], "Investigating Compression Failure Mechanisms in Composite Laminates with a Transparent Fiberglass-Epoxy Birefringent Material" [\$7].

Copies of these reports may be pur-

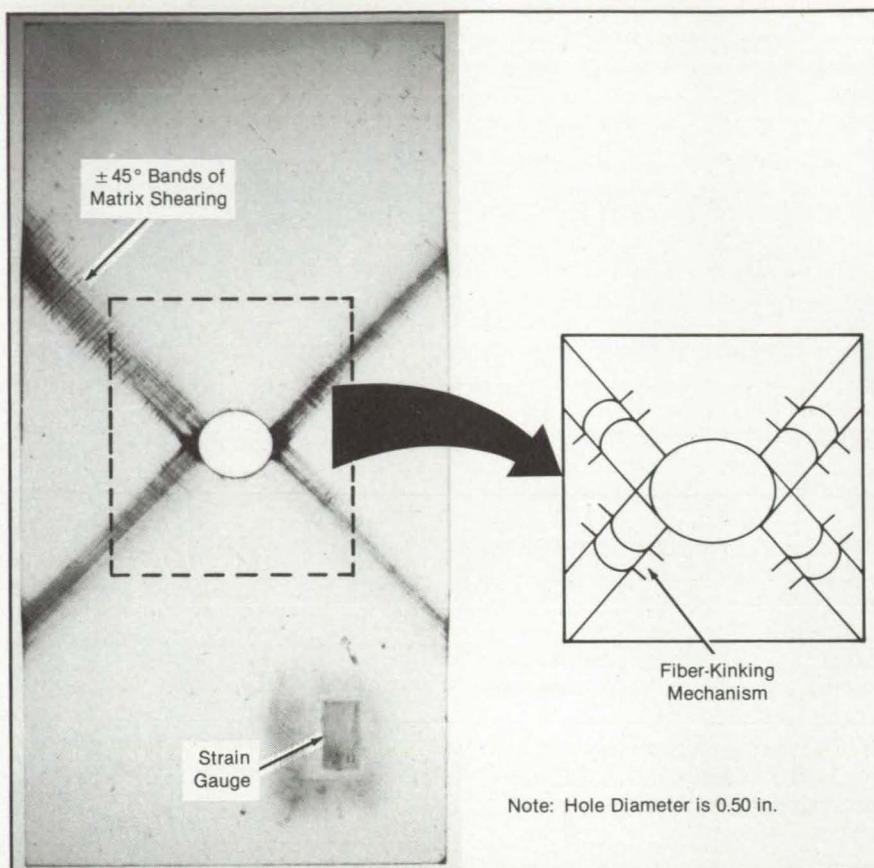


Figure 2. White Light Reveals matrix-shearing bands plus a fiber-kinking mechanism.

chased [prepayment required] from the National Technical Information Ser-

vice, Springfield, Virginia 22161. LAR-13345

Detoxification of Halon Fire-Extinguishant Products

Ammonia compounds absorb toxic hydrogen halides as they are produced.

Lyndon B. Johnson Space Center, Houston, Texas

Toxic acid vapors resulting from the use of Halon (or equivalent) fire extinguishers are immediately changed into nontoxic ammonium compounds when the extinguishers contain some ammonia or ammonium carbonate. If ammonium carbonate is used, the particle size of the resulting neutral compounds can be controlled to eliminate virtually any absorption into the lungs.

When used to extinguish a fire, a Halon (halogenated hydrocarbon) is partially decomposed to form hydrogen fluoride, chloride, or bromide, which are toxic, irritating, and corrosive vapors. In some instances lethal concentrations of these gases are formed.

However, when the Halon fire extinguishers contain powdered ammonium

carbonate, aqueous ammonia, or ammonia gas, the ammonia compound is discharged with the Halon and reacts with the toxic vapors to produce solid, nontoxic, nonirritating, and much less corrosive ammonium halides. These are stable at all pressures and temperatures up to 300°C . (When ammonium carbonate is used, water and carbon dioxide are also produced as byproducts.)

The quantities of ammonia or ammonium carbonate placed in the extinguishers are about three times the stoichiometric amounts required to neutralize the quantities of acid gases formed by the extinguishing process, as determined in previous tests. Ammonium carbonate is a dry powder and aqueous ammonia is a liquid; neither is significantly soluble in any

Halon extinguishing agent. Theoretical considerations and actual test results have demonstrated that the presence of ammonium carbonate or aqueous ammonia in the extinguishing agent impairs neither its capacity nor its rapidity of extinguishment.

In a White Sands Test Facility application, in which a diesel fuel fire within a 600-ft^3 (17-m^3) armored personnel carrier was extinguished, 250 g of ammonium carbonate, or 250 ml of aqueous ammonia were added to the Halon extinguishing compound. The estimated amount of Halon 1301 required to extinguish a fire in this volume is 4.4 kg. Therefore, the weight of the ammonium carbonate (250 g) added to the extinguisher is only 5.6 percent of the weight of the Halon 1301 —

amounting to a negligible increase in extinguisher weight.

This work was done by Eric L. Miller of Lockheed Engineering & Management

Services, Inc., for Johnson Space Center. No further documentation is available.

Inquires concerning rights for the com-

mercial use of this invention should be addressed to the Patent Counsel, Johnson Space Center [see page 29]. Refer to MSC-20962.

Phosphazene Polymers Containing Carborane

The addition of carborane may increase thermal stability.

Ames Research Center, Moffett Field, California

Polymer	Nitrogen Atmosphere			Air Atmosphere		
	Polymer Decomposition Temperature, °C	Temperature of Maximum Rate of Weight Loss, °C	Percent Char Yield at 800° C	Polymer Decomposition Temperature, °C	Temperature of Maximum Rate of Weight Loss, °C	Percent Char Yield at 800° C
Poly(phenylcarboranyltrifluoroethoxy)phosphazene	110	395	61	110	380	57
Same as Above but Dried at 75° C for 16 h	120	465	59	120	495	65
Poly(2,2,2-trifluoroethoxy)phosphazene	370	410	0	180	412	0

Char Yields and Decomposition Temperatures of two phosphazene polymers are compared.

Carborane-substituted polyphosphazenes have been prepared by the thermal polymerization of phenylcarbonyl-pentachlorocyclotriphosphaene followed by reaction with sodium trifluoroethoxide to replace the remaining chlorine atoms with trifluoroethoxy groups. These improved polymers offer high char yields and resistance to hydrolysis.

Organophosphazene polymers offer a valuable combination of properties: They are resistant to some alkalis and acids, water- and oil-repellent, fire-resistant, and flexible at temperatures as low as -80° C. The alternating phosphorus and nitrogen atoms in the backbone of the polymers give them torsional mobility and a low glass-transition temperature and make them transparent to ultraviolet radiation.

Polydichlorophosphazenes are susceptible to hydrolysis, but are made immune by replacing the chlorine atoms with aryl, alkyl, amino, alkoxy, and aryloxy groups. The resulting hexachlorocyclotriphosphaene trimer is then hydrolyzed to oxophosphazene. Unfortunately, this product, while resistant to hydrolysis, is thermally unstable. The polymer can be stabilized, however, if carborane is added before replacing the chlorine.

The synthesis of the improved polymer requires the prior synthesis of a number of reactants, including phenyl-lithiocarborane, hexachlorotriphosphazene (I) trimer, and sodium trifluoroethoxide. The carborane is introduced by the reaction of the phenyl-lithiocarborane with the hexachlorotriphosphazene (I) trimer. The purified product of this reaction is thermally polymerized by heating to 250° C.

The resulting polymer is reacted with the sodium trifluoroethoxide.

In one of the thermal-stability tests of the carborane-containing material, an aluminized mirror coated with a film of the polymer was subjected to successive

vacuum pyrolyses. After each episode of pyrolysis, the polymeric residue was examined for structural changes by infrared spectroscopy. The following changes were observed:

- Up to 200° C, the material first lost

Boeing 747s now use Kapton®

#1 in wire insulation for aerospace

The 707, 727, 737, 757, 767 and now the 747. Boeing relies on KAPTON polyimide film to meet their high-temperature wire insulation requirements. The reasons: KAPTON saves weight and space. It won't melt, drip or propagate flame. And even in a current overload condition, it emits practically no smoke.

Learn why Boeing and other leading aerospace manufacturers rely on KAPTON, made only by Du Pont. For a new booklet on why nearly all high-performance aircraft use KAPTON, write Du Pont Company, KAPTON, Room X40804, Wilmington, DE 19898.



weight by giving off low-molecular-weight compounds and products resulting from the pickup of atmospheric moisture;

- At 300° C, the polymer lost borane and trifluoroethoxy groups; the loss of trifluoroethoxy groups resulted in cross-linking between the phosphazene chains and a more thermally stable residue;
- At 400° C, the polymer lost most of the

remaining carborane; and

- Pyrolysis above 400° C resulted in no further changes discernable by infrared spectroscopy.

Thermogravimetric analysis was performed in dry nitrogen and in air. Although the polymer decomposition temperatures were lower than those of a phosphazene polymer without carborane, the char yields were much higher, as shown in the table.

This work was done by L. L. Fewell and J. A. Parker of **Ames Research Center** and R. J. Basi of San Jose State University. For further information, Circle 4 on the TSP Request Card.

Inquiries concerning rights for the commercial use of this invention should be addressed to the Patent Counsel, Ames Research Center [see page 29]. Refer to ARC-11487.

Room-Temperature Deposition of NbN Superconducting Films

Films with high superconducting transition temperatures are deposited by reactive magnetron sputtering.

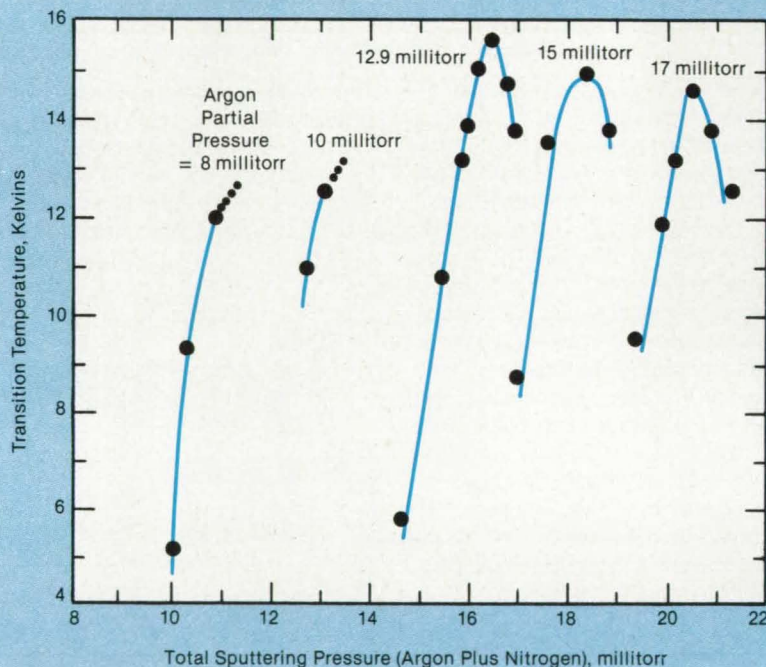
NASA's Jet Propulsion Laboratory, Pasadena, California

Thin films of refractory niobium nitride with superconducting transition temperatures (T_c) as high as 15.7 K have been deposited on glass, fused quartz, and sapphire substrates by dc reactive magnetron sputtering in a mixture of Ar and N_2 gases. Although substrate temperature increased gradually during the sputter deposition process, it never rose above $\sim 90^\circ$ C. Since this deposition process does not involve significantly high substrate temperatures, it can be employed to deposit a counter electrode in a superconductor/insulator/superconductor junction without causing any thermal or mechanical degradation of the underlying delicate tunneling barrier. Furthermore, substrates for the room-temperature deposition of NbN could be polymeric or coated with photoresist, making the films accessible to conventional lithographic patterning techniques.

A planar magnetron sputtering source with a 2-in. (5.08-cm) diameter, 0.125-in. (0.318-cm) thick niobium target (99.91 percent pure) was used to deposit the NbN films onto the precleaned substrates fixed on a substrate holder located about 2.75 in. (6.98 cm) from the target. An oil-free ultra-high-vacuum system was evacuated to a background pressure of around 8×10^{-8} torr (1×10^{-5} N/m²) by a 300-l/s ion pump, further supported by a titanium cryosublimation pump. The sputtering was carried out in a reactive gas mixture of 99.999-percent pure argon and nitrogen, the flow rates of which were controlled by independent flowmeters. The pressure in the chamber was monitored by a capacitance manometer. A Chromel/Alumel thermocouple was mounted on a control substrate to monitor the substrate temperature during sputter deposition.

In each run, the voltage was adjusted

The Temperature (T_c) of the Superconducting Transition in the deposited NbN film depends on the argon and nitrogen pressures in the sputtering chamber.



to a value between 320 and 350 volts to obtain a constant discharge current of about 1 ampere. The flow rates varied in the ranges of 2 to 4 standard cubic centimeters per minute for Ar and 0.3 to 1 standard cubic centimeters per minute for N_2 . Both the flow rates and the chamber pressure were closely monitored. Sets of NbN films were deposited under various partial pressures of argon, ranging from about 5 to about 17 millitorr (0.7 to 2.3 N/m²), mixed in each case with different partial pressures of nitrogen in the range of 2 to 6 millitorr (0.3 to 0.8 N/m²).

The films with relatively high T_c have

face-centered-cubic crystal structure (like that of NaCl) as revealed by their X-ray diffraction patterns. An initial increase in the injection pressure of N_2 for a constant argon pressure results in a remarkable increase in the (111) diffraction line intensity due to a strong orientation of the film with the (111) direction perpendicular to the substrate plane. This increase correlates distinctly with an increase in the T_c (see figure). However, beyond a threshold, a further increase in the N_2 injection pressure causes a distortion of the crystal structure towards the lower-stoichiometry (NbN_x , $x < 1$) tetragonal

phase, accompanied with a reduction in the T_c .

The films with the high transition temperature ($T_c = 15.7\text{K}$) had a superconducting transition width of about 0.2K. This could be attributed to slight gradients in the stoichiometry and/or microstructure of the films along their thickness. Further refinements in the deposition technique may yield films with smaller transition widths, the T_c of which might approach the predicted value of 18 K.

This work was done by Sarita Thakoor,

James L. Lamb, Anilkumar P. Thakoor, and Satish K. Khanna of Caltech for NASA's Jet Propulsion Laboratory. For further information, Circle 31 on the TSP Request Card. NPO-16681

Increasing the Cryogenic Toughness of Steels

Grain-refining heat treatments increase toughness without substantial strength loss.

Langley Research Center, Hampton, Virginia

High-strength, high-toughness steels are often required in applications involving the safety and reliability of components exposed to cryogenic temperatures. Fuel tanks and pressure vessels on aircraft and spacecraft are good examples. Unfortunately, strength must often be traded off against fracture toughness: the higher the yield strength, the lower the fracture toughness. The so-called "technological limit" represents the highest attainable toughness for a given strength level, considering all available alloys.

NASA has developed two high-Reynolds-number cryogenic wind tunnels that can subject aircraft-component models to high windloads at very low temperatures. These conditions require that the models be constructed from steels with strength and toughness values above the current technological limit. One way to increase toughness without trading too much strength in a given alloy is to refine its grain size. In the iron/nickel/cobalt steels of interest, grain refinement can be achieved by cycling the material across the austenite/austenite-plus-ferrite phase-transformation boundary. Therefore, a program was initiated to investigate the improvement of the fracture toughness of several iron/nickel/cobalt alloys by grain refinement through heat treatment.

Five alloys were selected for study, all of them at or near the technological limit. Production plates of these alloys were the baseline materials against which all improvements in properties were measured. Standard Charpy V-notch specimens were machined from plates that had been given various grain-refining heat treatments. These treatments involved several cycles of heating the material above the austenite or austenite-plus-ferrite transformation temperature, holding for various intervals, and quenching in water. After heat treatment, Charpy V-notch tests and tensile tests were per-

formed at 77 K (-321°F), followed by optical and scanning electron microscopy.

The results showed clearly that the grain sizes of these alloys could be refined by such heat treatments and that the grain refinement could indeed result in a large improvement in toughness without a substantial loss in strength. The best improvements were seen in HP-9-4-20 Steel, at the low-strength end of the technological limit, and in Maraging 200, at the high-strength end. These alloys, in the grain-refined condition, are being consid-

ered for model applications in the high-Reynolds-number cryogenic wind tunnels.

This work was done by Homer F. Rush of Langley Research Center. Further information may be found in NASA TM-85816 [N84-30014/NSP], "Grain-Refining Heat Treatments To Improve Cryogenic Toughness of High-Strength Steels" [\$8.50]. A copy may be purchased [prepayment required] from the National Technical Information Service, Springfield, Virginia 22161.

LAR-13376

Heat resistant Kapton[®]

#1 in wire insulation for aerospace.

DuPont KAPTON polyimide film.

A high-performance wire and cable insulation rated for 200°C continuously and up to 400°C for short periods. Won't melt, drip or propagate flame. Practically no smoke in a fire.

Send for more information and a list of wire manufacturers. Write DuPont Co., Room X40804, Wilmington, DE 19898.



Impact-Resistant Ceramic Coating

Refractory fibers more than double the strength of the coating.

Lyndon B. Johnson Space Center, Houston, Texas

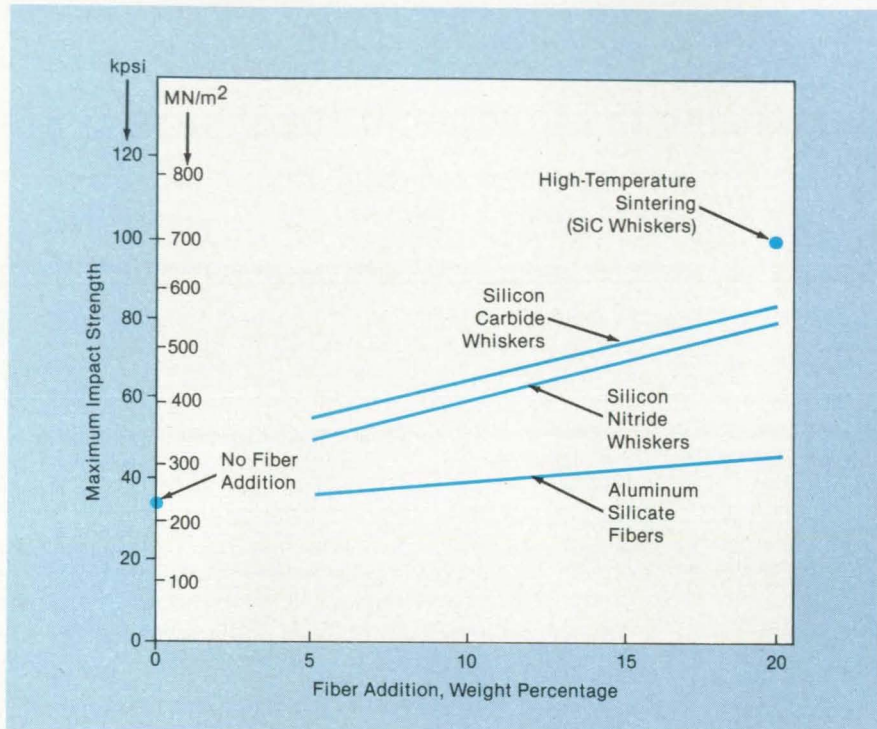
A coating for ceramic insulating tiles has increased impact strength as well as high thermal emittance. The addition of whiskerlike ceramic fibers in controlled amounts to the standard coating for Space Shuttle insulating tiles increases the impact strength to about 2½ times that of the standard coating alone. The new coating can also be used to improve the thermal and mechanical properties of electromagnetic components, mirrors, furnace linings, and ceramic parts for advanced internal-combustion engines.

The whiskers may be aluminum silicate, silicon carbide, or silicon nitride. They should have a high fiber aspect ratio (the ratio of length to diameter) for greatest effectiveness.

In comparative tests, each of the three types of whiskers was blended into a slurry of the standard coating material in proportions of 5, 10, 15, and 20 percent by weight. The mixtures were applied to tiles and baked at 2,250° F (1,232° C) for 90 minutes. The impact strengths of the coated tiles were then measured in an impact-testing apparatus in which the fractures of the coatings were detected acoustically.

For all whisker materials, the impact strength increased with the amount of the additive (see figure). Silicon carbide whiskers produced the greatest increase in impact strength. The strength of the silicon carbide coating was increased even further by sintering at 2,400° F (1,300° C) for 60 minutes.

The formation of cristobalite, which causes microcracking of the coating, was not a problem, even after long exposures to high temperatures. X-ray diffraction tests of the coatings after 15 hours at



The Impact Strengths of Ceramic Coatings increase with increasing whisker content. Silicon carbide whiskers clearly produce the largest increase, and the improvement grows even more with high-temperature sintering.

2,300° F (1,260° C) showed that the concentration of cristobalite was within acceptable levels.

The whisker-reinforced coating can be applied and processed by methods that are compatible with existing production equipment. The reinforcement concept is adaptable to other refractory coating and can lend them improved impact resistance without detracting from other properties.

This work was done by William H.

Wheeler, John F. Creedon, and Yamato D. Izu of Lockheed Missiles & Space Co., Inc. for Johnson Space Center. For further information, Circle 57 on the TSP Request Card.

Inquiries concerning rights for the commercial use of this invention should be addressed to the Patent Counsel, Johnson Space Center [see page 29]. Refer to MSC-20829.

Carbon Shields for Intercalated Fiber Conductors

Stability in air is increased by depositing amorphous carbon.

Lewis Research Center, Cleveland, Ohio

Intercalated graphite-fiber conductors are more or less air-stable at room temperature. However, the uncoated intercalated fibers can react with oxygen, moisture, and other chemicals surrounding the conductor, causing it to lose desirable properties. Their stability in air and moisture at ambient and elevated temperatures is greatly enhanced by the use

of a protective shield. The protective shield coats the fiber after intercalation, preventing reactive gases or liquids from interacting with the intercalation compound and the intercalant from leaving the fiber.

Initially the graphite fibers are intercalated (insertion of atoms or molecules between the graphite layers), which

changes (lowers) the electrical resistivity and makes the fibers metalliclike. The intercalant species used should be of those found to form intercalation compounds that lower the electrical resistivity. Copper chloride, bromine, and arsenic pentafluoride are examples of materials that have worked well in the past.

As the next step, the conductor is

coated with a diamondlike amorphous carbon. This coating is applied in the same chamber as the intercalation reaction, or an alternate deposition chamber can be used. The deposition of carbon can be accomplished by any number of techniques. Ion-beam sputter-deposition and RF plasma techniques have been used, but dc plasma and others will work also.

In addition to a pure carbon coating, other combinations will work. The best example is amorphous silicon/carbon in varying ratios of the two elements. A coating of several hundred to a few thousand angstroms in thickness is in the desired range. Thickness, however, is not a critical factor in performance as long as complete coverage of the surface is obtained. Potential uses include conductive epoxy composites, tether conductors, signal wire, and power cables.

This work was done by Bruce A. Banks of Lewis Research Center and John A. Woollam of the University of Nebraska. Further information may be found in NASA TM-81721 [N81-21129/NSP], "Ion Beam Applications Research — a 1981 Summary of Lewis Research Center Programs" [\$10]. A copy may be purchased [prepayment required] from the National Technical Information Service, Springfield, Virginia 22161.

Inquiries concerning rights for the

commercial use of this invention should be addressed to the Patent Counsel, Lewis Research Center [see page 29]. Refer to LEW-14063.

Producing Large-Particle Monodisperse Latexes

A process using seed particles offers a large-size, uniform product.

*Marshall Space Flight Center,
Alabama*

A chemical process produces latex particles of relatively large, uniform size for use as size standards for instrument calibration. The process, based on seeding of a mixture by very small latex particles, yields particles measuring 2 to 30 μm or more in average size. It produces monodisperse latexes —

those in which the deviation from the average size is less than 2 percent. The particles can therefore be used directly, without the tedious separation procedures for removing the off-size particles.

The process is efficient: The quantity of coagulum byproducts is low. Previous processes have been hampered by poor uniformity, inadequate particle size, and inefficient use of materials.

In the microgravity environment of space, the process creates monodisperse latexes of even larger size. Particles of 100 μm or more are possible. In these cases, it is estimated that particle yields can reach as much as 50 percent by weight of the reaction mixtures.

The starting mixture for the process consists of the following:

- 2 to 30 parts (by weight) of a monodisperse seed latex (particle size about 2 μm);
- 10 to 50 parts of a polymerizable, monofunctional (noncross-linking) monomer;
- Up to 0.1 parts of a polyfunctional (cross-linking) monomer;
- 0.01 to 0.2 parts of an initiator that is soluble in the monomer and less soluble in water;
- 0.001 to 0.1 parts of an inhibitor that is soluble at least in water;
- Up to 2 parts of a mixture of poly-

**ELECTROMAGNETIC INTERFERENCE
ELECTRONIC CORES**

**POWDER METALLURGY
INJECTION MOLDING**



carbonyl iron powders

"The Right Stuff"

GAF is the sole domestic manufacturer of Carbonyl Iron Powders. For more detailed information, contact GAF Corporation, Chemical Division, 1361 Alps Road, Wayne, NJ 07470, (201) 628-3000.

meric, comonomeric, and anionic emulsifiers; and

- Enough water to make 100 parts by weight.

The formulation is mixed to form an emulsion and agitated mildly for 8 to 24 hours at a temperature below the decomposition temperature of the initiator. This step swells the seed particles. The inhibitor prevents the radicals from forming in the water phase of the emulsion during this part of the process. The

mixture is then polymerized by heating it above the decomposition temperature of the initiator — typically at 60° to 90° C — for 10 to 30 hours under continued mild agitation.

The procedure can be repeated to create larger particles; that is, the monodisperse product of polymerization can be used as seed particles. Several generations of increasingly larger monodisperse particles can be produced.

This work was done by John W. Vanderhoff of Lehigh University for Marshall Space Flight Center. For further information, Circle 109 on the TSP Request Card.

Inquiries concerning rights for the commercial use of this invention should be addressed to the Patent Counsel, Marshall Space Flight Center [see page 29]. Refer to MFS-26026.

Process Produces Low-Secondary-Electron-Emission Surfaces

A textured carbon layer is applied to copper by sputtering.

Lewis Research Center, Cleveland, Ohio

A process has been developed for applying a very thin layer of highly textured carbon to a copper surface by a sputtering technique. The carbon surface is characterized by a dense, random array of needle-like spires or peaks that extend perpendicularly from the local copper surface. The spires are approximately 7 micrometers in height and are spaced approximately 3 micrometers apart, on the average.

An electron microscope photomicrograph of a typical surface is presented in Figure 1. The copper substrate is essentially completely covered by the carbon layer, which is tenacious and not damaged by vibration loadings representative of multistage depressed collector (MDC) applications.

The process was developed primarily to provide an extremely low-secondary-electron-emission surface for copper for use as high-efficiency electrodes in MDC's for microwave amplifier traveling-wave tubes (TWT's). These tubes are widely used in space communications, aircraft, and terrestrial applications.

One of the significant factors in maximizing MDC efficiency is the use of electrode materials having low-secondary-electron-emission characteristics. Specifically, to recover the maximum kinetic energy from the spent electron beam after it has passed through the TWT's interaction (signal-amplifying) section and entered the MDC, the electrodes must have low-secondary-electron-emission characteristics so that the impinging electrons are not excessively reflected or reemitted from the surfaces. In an untreated condition, copper surfaces have relatively very high-secondary-electron-emission levels.

The carbon surface is applied by means of a triode sputtering process, in which a carbon target and copper substrate are simultaneously exposed to an

argon plasma in a low-pressure environment. Other than the removal of oxide or oil or dirt from the copper by simple abrasion of the surface, no special pretexturing treatment of the copper is required. The carbon target and copper substrate are held at the same potential relative to the plasma during the texturing process.

In a typical case, where the substrate is circular in shape, the carbon target closely surrounds the substrate and is shaped so that its surface slopes radially upward and outward at an angle of approximately 45°. Further, the target is positioned approximately one-half the diameter of the substrate above the surface of the substrate to promote uniform application of the textured carbon layer.

Most of the electrons in a primary elec-

tron beam that impinges the textured carbon layer strike the conical sloping walls of the spires or the base of the spires. Secondary electrons that are then emitted from these regions are repeatedly intercepted (with consequent repeated partial retention) by nearby adjacent spire walls, thereby greatly reducing net emission from the normal projected surface area. The highly textured surface, therefore, is the principal factor in producing the extremely low-secondary-electron-emission characteristics exhibited by this material.

The true secondary-electron-emission ratio; i.e., the ratio of low-energy-emitted electrons to impinging electrons is shown in Figure 2(a), and the reflected primary electron yield, indexed to that of a carbon-

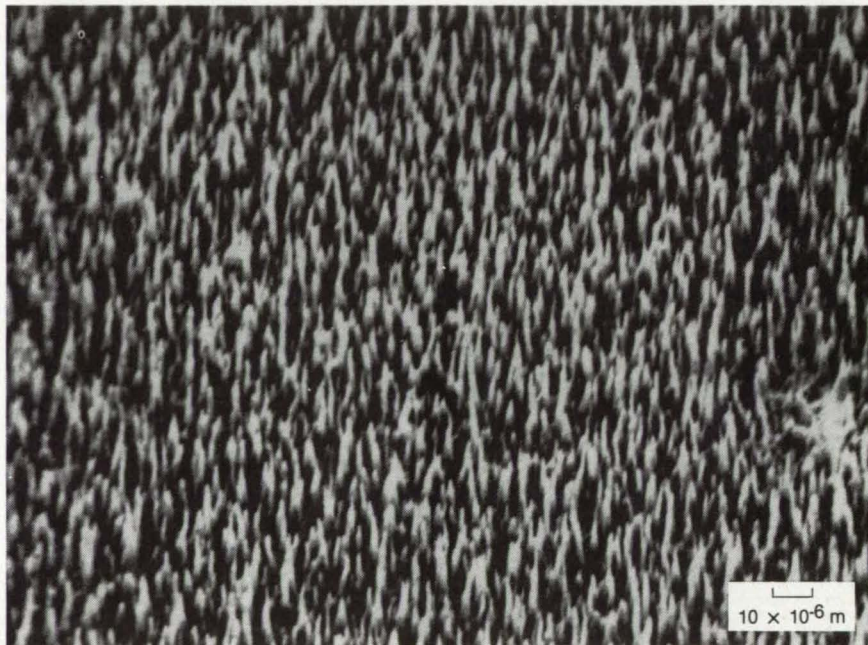


Figure 1. **Textured-Carbon Surfaces** on a copper substrate are shown here on an electron microscope photograph. The angle with the surfaces is 30°.



Wyle at work.

Helping explore the new commercial frontier.

Our nation's growth was possible because of the individual's opportunity to excel. The first frontier was broken when our country's founders moved westward. Frontiers have fallen rapidly ever since.

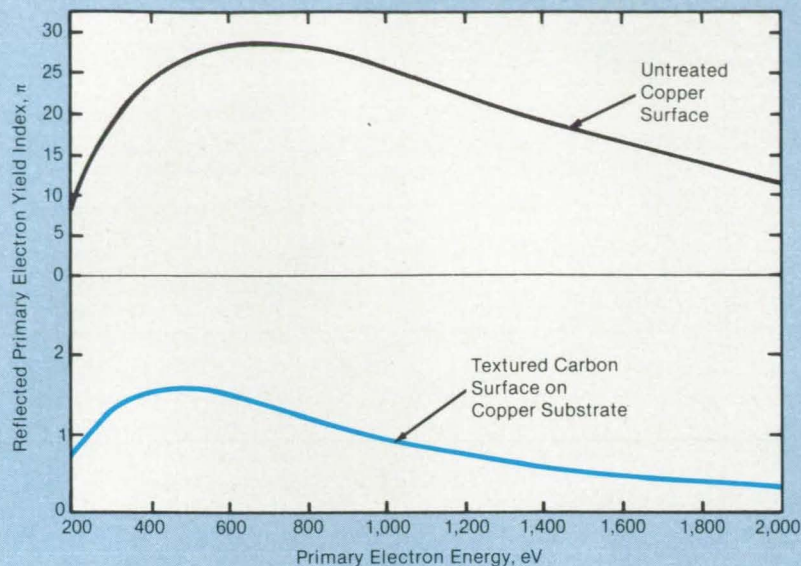
Today we are seeing the development of one of the most exciting commercial frontiers yet. Space itself. Wyle is playing a vital part in that development. We've had an active role in all of our nation's space programs, including the Space Shuttle. We're already at work on the Space Station. We're identifying commercial opportunities in space, including materials processing in microgravity environments. And we're starting in on projects that as yet are still unnamed.

Wyle Laboratories has excelled in aerospace testing since 1949. We're the nation's leading independent testing laboratory. We have the testing facilities, experience, and scientific specialists to conduct any kind of developmental or test program. Our standards of performance are unsurpassed.

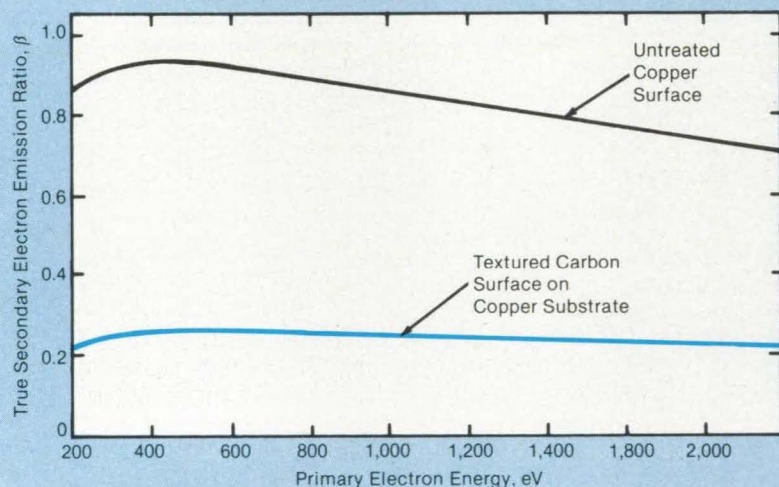
For more information on Wyle's testing programs, call collect: Drexel Smith in Norco, California, (714) 737-0871, Don McAvin in Huntsville, Alabama, (205) 837-4411, John Wood in Hampton, Virginia, (804) 865-0000, or Paul Turkheimer in El Segundo, California, (213) 322-1763.

WYLE SCIENTIFIC SERVICES
LABORATORIES & SYSTEMS
GROUP

Huntsville, AL Arlington, VA Norco, CA
Lanham, MD El Segundo, CA Hampton, VA



(a)



(b)

coated control surface at 1,000 eV primary beam energy, is shown in Figure 2(b). For comparison, characteristic curves for untreated copper are also shown. The sharply lower emission levels for the carbon-coated surface relative to those of untreated copper are clearly evident.

While developed primarily for the MDC electrode application, the process should have many other potential uses in other electron devices and components where low-secondary-electron emission is desirable. These uses might include power tube grids, output waveguide transformers, waveguides, and other related applications.

This work was done by Arthur N. Curren, Kenneth A. Jensen, and Robert F. Roman of **Lewis Research Center**. For further information, Circle 41 on the TSP Request Card.

Inquiries concerning rights for the commercial use of this invention should be addressed to the Patent Counsel, Lewis Research Center [see page 29]. Refer to LEW-14130.

Figure 2. The **Reflected Primary Electron Yield Index** is plotted in (a) as a function of electron energy. In (b), the true secondary electron emission ratio is plotted against primary electron energy.

Antisoiling Coatings for Solar-Energy Devices

Fluorocarbons resist the formation of adherent deposits.

NASA's Jet Propulsion Laboratory, Pasadena, California

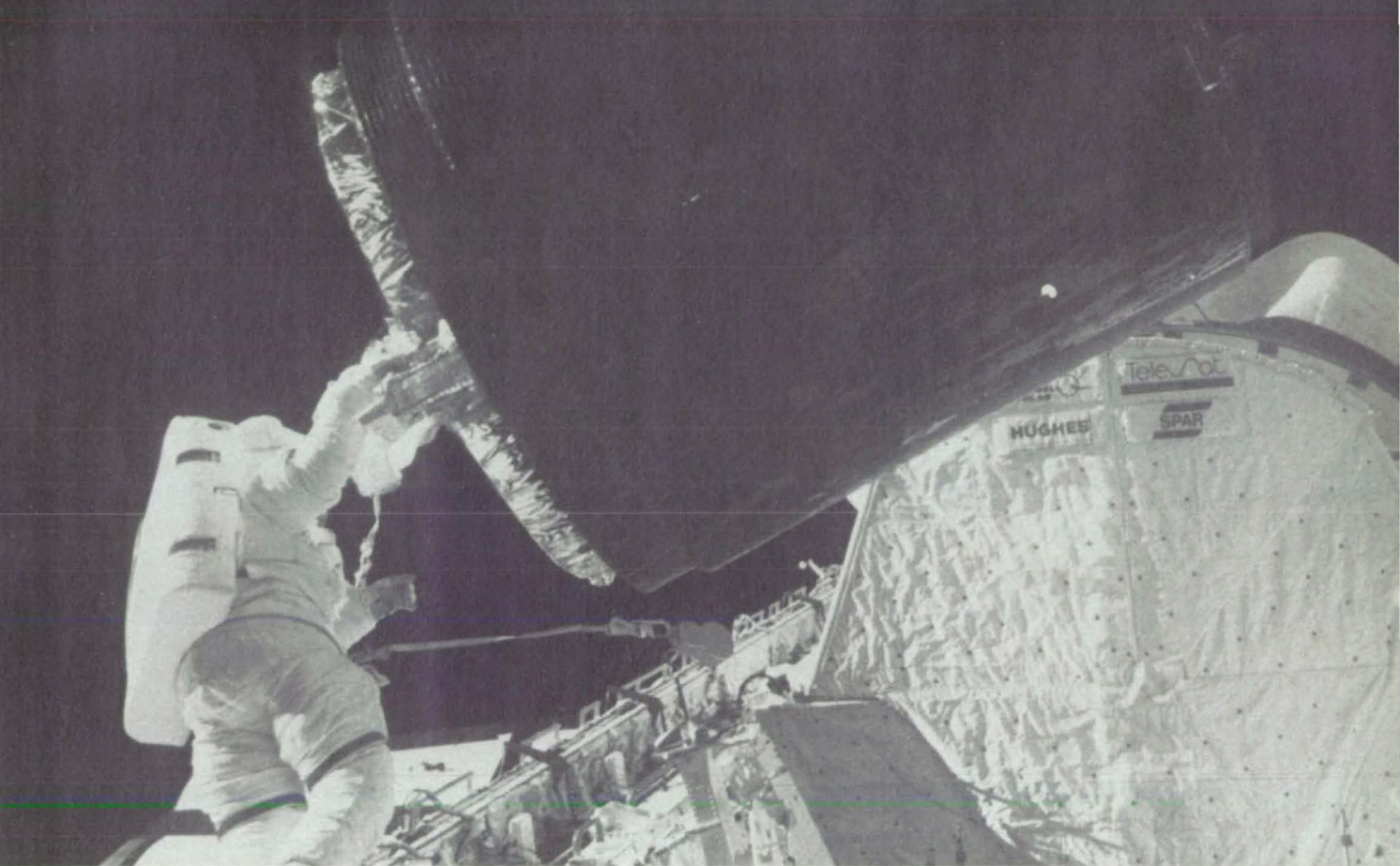
An experimental program has identified promising coating materials that can reduce the soiling of solar photovoltaic modules and possibly solar thermal collectors. Contaminating layers of various degrees of adherence (see figure) form

on the surfaces of these devices, partially blocking the incident solar energy, which reduces the output power. Loose soil deposits during dry periods but is washed off by rain. The new coatings help to prevent the formation of the more-adherent,

chemically and physically bonded layers that rain alone cannot wash away.

Prior research had shown that a soil-resistant surface must be hard, smooth, hydrophobic, low in surface energy, and chemically clean of sticky materials,

ANDUS. . .



PERFORMANCE TO MATCH YOUR DEMANDS

The aerospace industry is among the most demanding of customers. That's why they rely on us. ANDUS. Our thin film coatings combine the optical and mechanical properties required in a variety of applications including thermal blankets for satellites.

In fact, ANDUS film products are used by quality conscious customers across a broad spectrum of industries for a wide variety of specialized applications. Applications calling for custom coatings on a wide array of standard and exotic substrates are ANDUS's speciality.

Using magnetron sputtering, ANDUS produces the highest quality coatings available. What's more, our continuous roll-to-roll manufacturing techniques result in coatings which offer excellent adhesion and outstanding electrical and optical properties. All of this adds up to superior materials and lower costs for you.

Only ANDUS has the advanced techniques and modern facilities, coupled with years of experience, to provide custom coatings that allow you to manufacture products that satisfy...or exceed...the most stringent application requirements.

ANDUS...Performance to match your demands. Our customers continually depend on us to meet the rapidly evolving demands of thin film coatings for the aerospace industry.

ANDUS. ADDED VALUE WITHOUT ADDED COST.



ANDUS CORPORATION/21019 Osborne Street/Canoga Park, CA 91304/Phone (818) 882-5744 Telex 182374

Circle Reader Action No. 436

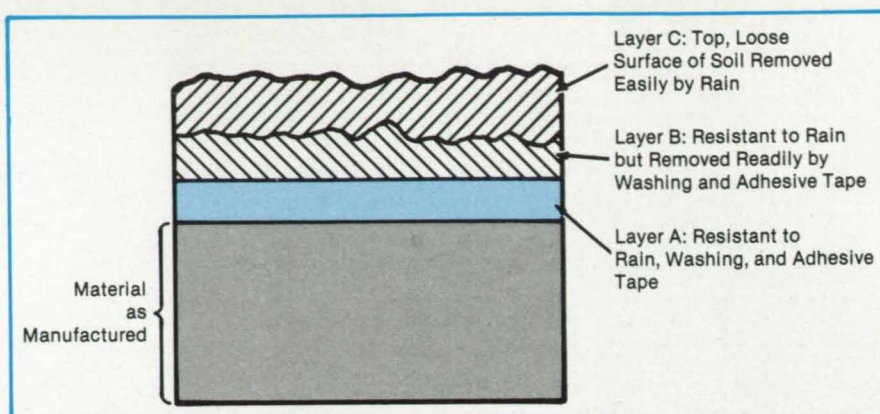
water-soluble salts, and first-period elements, both on and below the surface. It must also be resistant to ultraviolet photo-oxidation, hydrolysis, or both. The base-material/coating combinations most likely to satisfy these requirements are a hard, smooth fluorocarbon and a fluorocarbon coating a few microns thick on a hard, smooth backing such as glass.

Candidate materials for the outer coverings of photovoltaic modules include low-iron glass, Tedlar (or equivalent) polyvinyl fluoride (PVF), and Acrylar (or equivalent) biaxially-oriented acrylic film. These materials are all hard, smooth, and free of water-soluble residues.

Two candidate fluorocarbon coating materials were selected. One is L-1668 (or equivalent), an experimental silane used to impart water- and oil-repellency to glass. The other is E-3820 (or equivalent), an experimental compound obtained by reacting perfluorodecanoic acid with Z-6020 (or equivalent), a commercial silane. Both compounds bond chemically to glass surfaces and both are supplied in solvent solutions.

The coatings were applied by brushing, followed by curing and drying in air for 24 hours. The samples were then tested for adherence of the coatings by observing the degree of hydrophobicity after immersion in water.

Without special surface preparation, both coatings adhered to glass; the E-3820 adhered to the PVF; and the



Soil Deposits on a Weathering Surface in three layers, as shown in this simplified cross section. The antisoiling coatings described in the text help to prevent the formation of tenacious layers A and B.

L-1668, to the acrylic. When the PVF and acrylic surfaces were activated by exposure to ozone, the L-1668 then adhered to the PVF, and the E-3820 adhered to the acrylic.

Uncoated and coated glass and plastic samples were mounted in outdoor racks. A record of rainfall was kept to correlate soiling effects with precipitation. The degree of soiling was monitored by measuring the decrease in short-circuit current output of a standard silicon solar cell covered by a sample.

Of the uncoated samples, glass had the least tendency to retain soil, followed by PVF and acrylic. With the fluorocarbon coatings, however, the soiling behavior of

all three materials was essentially the same. The best substrate/coating combinations were glass with E-3820, PVF with E-3820, and ozone-treated acrylic with E-3820. The time-averaged optical losses of the coated substrates compared to those of the same substrates uncoated were 1.55/2.65, 1.70/5.38, and 2.59/7.20 percent for glass, PVF, and acrylic, respectively.

This work was done by Edward F. Cuddihy of Caltech and Paul Willis of Springborn Laboratories for NASA's Jet Propulsion Laboratory. For further information, Circle 51 on the TSP Request Card. NPO-16552

Heat- and Radiation-Resistant Lubricants for Metals

Protective and lubricating coatings are formed in situ.

NASA's Jet Propulsion Laboratory, Pasadena, California

A class of high-performance lubricants is under investigation at NASA's Jet Propulsion Laboratory. These lubricants are useful as additives to oils and greases in gears, transmissions, motors, and other machines where rubbing loads between metal parts may be severe. Because of their low volatility and lack of requirement for air or moisture, these lubricants should also be useful in vacuums.

One type of additive includes orthophthalonitrile and its derivatives. The additive would ordinarily be dissolved or suspended in a base fluid. Under high mechanical loads that cause lubricating fluid films to become thin, metal parts rub together. The orthophthalonitrile reacts with metal-surface asperities at high frictional temperatures to form lubricating films of metal phthalocyanine. These compounds are also formed with the hot metal frag-

ments torn from the asperities. Bearing surfaces are thereby better protected from scoring, and fragments are rendered less harmful to the base fluids.

On heating to 250 to 260 °C, the additive also forms metal-free phthalocyanine, which is extremely thermally stable and an efficient lubricant. The phthalocyanine molecular structure is planar like that of graphite. However, it is even more effective than graphite as a lubricant because metal-free phthalocyanine can form extremely stable bonds to metal. At high temperatures in air, it does not form corrosive compounds as does molybdenum disulfide.

Without modification, orthophthalonitrile is not a suitable additive to conventional motor oils because of its low solubility in aliphatic compounds. One way of making soluble additives is to synthesize orthodinitriles substituted with aliphatic

groups. Other potential substituents are cyclohexanes, linear polyethers, and fluoro-compounds.

Very little of the precursor compounds to the formed solid phthalocyanine lubricant is needed. Moreover, since the additives can probably be synthesized from inexpensive materials, their low cost and high performance should make them suitable for commercial use.

Other chelating/lubricating additives are under consideration. Molecules can be tailored to confer solubility on the additives. Candidate molecular groups includes pyridino, sulfhydro, pyrrole, phenoyl, cyano, indolino, amino, keto, diketo, nitroso, hydroxylamino, thiophene, and carboxyl.

This work was done by Emil A. Lawton of Caltech for NASA's Jet Propulsion Laboratory. For further information, Circle 108 on the TSP Request Card. NPO-16341

Books and Reports

These reports, studies, and handbooks are available from NASA as Technical Support Packages (TSP's) when a Request Card number is cited; otherwise they are available from the National Technical Information Service.

Fundamentals of Alloy Solidification

The potential benefits of microgravity processing are discussed.

A symposium was held at the Lewis Research Center in September of 1984. It dealt with the subject of microgravity and some basic metallurgical factors involved in the production of metals. General metallurgical areas of interest were metal solidification and processing. The five specific areas covered included (1) the undercooling of liquids, (2) porosity, (3) mi-

crostructure, (4) solidification, and (5) segregation.

Metallurgy today is characterized by processes that have evolved over the years in the unit gravity of Earth. Future processing will not be confined to Earth and may take place in a low or microgravity environment such as might be found on satellites, Space Shuttle-type vehicles, or a future space station. Because of this new access to a space environment, renewed interest is being generated in the role of gravity on basic metallurgical phenomena.

Fourteen individual papers were presented at this symposium entitled "Fundamentals of Alloy Solidification Applied to Industrial Processes." The authors represented material experts in government, academia, and industry. The underlying theme of this symposium was the possible benefits of microgravity processing and its beneficial effects on industry processing. Information contained in the conference publication is of such a nature that it would readily lend itself to inclusion in educational programs at the college level.

This work was done by F. Harf of Lewis Research Center. Further information may be found in NASA CP-2337 [N84-34589/NSP], "Fundamentals of Alloy Solidification Applied to Industrial Processes," [\$17.50]. A copy may be purchased [prepayment required] from the National Technical Information Service, Springfield, Virginia 22161. LEW-14229

Composite Refractory Felt/Ceramic Material

Ceramic protective coatings on combustor liners should adhere better.

Advanced commercial and military gas-turbine engines may operate at combustor-outlet temperatures in excess of 3,000° F (1,920 K). At these temperatures, combustor liners experience extreme convective and radiative heat fluxes. The ability of a plasma-sprayed ceramic coating to reduce liner-metal temperatures has been recognized. However, the brittleness of the ceramic

layer and the difference in thermal expansion with the metal substrate have caused cracking, spalling, and some separation of the ceramic coating. Research originally directed at turbine-tip seals (or shrouds) has shown the advantage of applying the ceramic to a compliant metal pad such as FELTMETAL® (or equivalent).

A report discloses the results of recent combustor-liner research where thick yttria-stabilized zirconia ceramic was plasma-sprayed on BRUNSBOND® substrates and exposed to nearly stoichiometric combustion. The compliant layer is a Hoskins Alloy 875 BRUNSBOND® (or equivalent) pad, 0.100 in. (0.25 cm) thick and 35 percent dense, brazed to an Inconel Alloy 718 (or equivalent) sheet 0.030 in. (0.08 cm) thick, using a high-temperature nickel-base braze compatible with both the felt and the backing. After brazing, all specimens were alumina-grit blasted immediately prior to application of a bond coat. All specimens were plasma-sprayed with a Ni_{16.2}/Cr_{5.5}/Al_{0.6}/Y bond coat 0.003 to 0.005 in. (0.008 to 0.013 cm) thick. Specimens were then plasma-sprayed with an yttria-stabilized zirconia ceramic 0.008 or 0.013 in. (0.19 or 0.33 mm) thick.

Combustor screening tests exposed 30 test specimens to nearly-stoichiometric flame temperatures of 3,450° F (2,170 K) for 4 cycles. After completion of the screening tests, all 30 specimens showed no visible evidence of discoloration or failure. There were no mudflat cracks, felt/ceramic, or backing/felt separations on any of the panels.

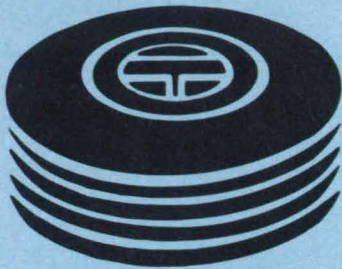
Two panels were then chosen for endurance testing. These two specimens were exposed to the same conditions listed above but for 30 cycles. This repeated thermal cycling produced nonlinking, noncatastrophic mudflat cracks in the ceramic coating of one test specimen and caused partial ceramic separation from the felt pad in the other specimen.

This work was done by David B. Ercegovic, Curtis L. Walker, and Carl T. Norgren of Lewis Research Center. Further information may be found in NASA TM-83490 [N84-14145/NSP], "Ceramic Composite Liner Material for Gas Turbine Combustors." [\$7]. A copy may be purchased [prepayment required] from the National Technical Information Service, Springfield, Virginia 22161. LEW-14238

Are you reading someone else's copy of NASA Tech Briefs?

Qualified engineers and other new product development personnel can receive their own personal copies of NASA Tech Briefs by checking the subscription box and filling in one of the bound-in cards.

Computer Programs



- 94 Intraply Hybrid Composite Design
- 98 Analyzing Static Loading of Complex Structures
- 98 Shadowed Space Heating of Sparse Structures
- 98 Rendezvous BET Program
- 100 Variable-Conductance Heat Pipes
- 100 Programming Structural Synthesis System
- 100 Vibration-Response Analysis
- 102 Fatigue-Crack-Growth Structural Analysis
- 102 Aircraft Takeoff and Landing Analysis
- 102 Nonconical Relaxation for Supersonic Potential Flow
- 104 Analysis of Lubricant Jet Flow
- 104 Aerodynamic Characteristics of NACA 16-Series Airfoils
- 104 Wall Interference in Two-Dimensional Wind Tunnels
- 106 Predicting Vortex Shedding in Supersonic Flow
- 106 Predicting Wall Modifications for Adaptive Wind Tunnels
- 106 Two Programs for Supersonic Wing Design and Analysis
- 107 Second-Order-Potential Analysis and Optimization
- 107 Shaded-Color Picture Generation of Computer-Defined Arbitrary Shapes

COSMIC: Transferring NASA Software

COSMIC, NASA's Computer Software Management and Information Center, is the one central office established to distribute software that is developed with NASA funding. COSMIC's role as part of NASA's Technology Utilization Network is to ensure that NASA's advanced software technology is made available to industry, other government agencies, and academic institutions.

Because NASA's software development efforts are dynamic and ongoing, new programs and updates to programs are added to COSMIC's inventory on a regular basis. Tech Briefs will continue to report information on new programs. In addition, the 1986 edition of the COSMIC Software Catalog is available with descriptions and ordering information for available software. Several new programs for control systems/robotics, expert systems, thermal analysis, turbomachinery design, structural analysis, and computer graphics are offered.

For additional information on any programs described in this issue of Tech Briefs, circle the appropriate number on the TSP card at the back of the publication. If you don't find a program in this issue that meets your needs, you can call COSMIC directly at (404) 542-3265 and request a review of programs in your area of interest. There is no charge for this information review.

Part of COSMIC's service involves maintaining and supporting the NASA Structural Analysis System, NASTRAN®. Each year new features are added to extend the system's capabilities. In May, the annual NASTRAN User's Colloquium will include 11 training seminars and 20 contributed papers reviewing NASA, DoD, and industrial applications of NASTRAN. Registration is open to all engineers and programmers who are involved with NASTRAN. Contact COSMIC for details.

COSMIC

Computer Services Annex, University of Georgia, Athens, GA 30602; Phone (404) 542-3265

John A. Gibson, Director

NASTRAN is a registered trademark of the National Aeronautics and Space Administration.

Computer Programs

These programs may be obtained at a very reasonable cost from COSMIC, a facility sponsored by NASA to make raw programs available to the public. For information on program price, size, and availability, circle the reference number on the TSP and COSMIC Request Card in this issue.



Materials

Intraply Hybrid Composite Design

Several theoretical approaches are combined in this program.

Intraply hybrid composites have been investigated theoretically and experimentally at Lewis Research Center over the past several years. Theories developed during these investigations and corroborated by attendant experiments were used to develop a computer program identified as INHYD (Intraply Hybrid Composite Design). INHYD includes several composites micromechanics theories, intraply hybrid composite theories, and an integrated hygrothermomechanical theory. Equations from these theories are used by the pro-

gram as appropriate for the user's specific applications.

The theories embedded in INHYD are summarized in a recent NASA publication (NASA TM 82593). Instructions for using the program are outlined in a recently-completed User's Manual. The User's Manual provides step-by-step instructions for using INHYD, in both the interactive and the batch modes. INHYD has considerable flexibility and capability that the user can exercise through the several options described in the User's Manual.

Initially the manual presents test cases for the interactive mode, first for a dry, room temperature case and then for a case with moisture present. Then an interactive case is presented wherein the data are preentered, as they would be for a batch case. Next several cases for using INHYD in the batch mode are described. After following through the test cases presented, a user should be able to use INHYD either in the interactive or batch mode and with or without temperature and moisture effects to predict properties for uniaxial intraply hybrid composites.

The User's Manual also includes Appendices with: (1) a list of elements and subroutines in INHYD, (2) a list of symbols used in the program, and (3) a copy of the NASA TM 82593 where the theory in INHYD is summarized. It is planned to make INHYD available for public release through COSMIC.

This program was written by C. C. Chamis and J. H. Sinclair of Lewis Research Center. For further information, Circle 28 on the TSP Request Card. LEW-14079


Ada[®]

Understood!

We at General Systems understand what the needs are, and will be for the Ada community. For example, why spend 50 or 100 thousand dollars for some Ada System when our P.C. based GS/ICC compiler can be had for as little as **\$1,195** and compile just as fast! Unlike most of our so called "vapor ware" competition out there who say they will "soon have" or are "working on" a comparable compiler to ours why not buy the real thing? — Now! Our GS/ICC P.C. based Ada compiler is presently operating with 8086/88 or 80286 backends and does not need any hardware except your own IBM PC, XT, AT or compatible machine!

Interested?

Call or write:

 **GENERAL
SYSTEMS[®]**
1-800-ADA-PROS

General Systems Corporation
1184 Chapel Street New Haven, CT 06510

*Ada is a registered trademark of the U.S.
Government Ada Joint Program Office (AJPO)

IBM is a registered trademark of the International
Business Machines Corporation.

Circle Reader Action No. 306

The first forward pass was



Run on first down. Run on second.
Run again on third. Then punt.

For years, that's the way the game of football plodded up and down the field.

But on a brisk autumn afternoon around the turn of the century, a young college quarterback and his coach made a careful and calculated game-breaking decision.

To go beyond the tried and true. To take a giant step forward. To throw the ball.

And the game would never be played the same again.

Today, a company called Symbolics™ is offering business the opportunity to

take a similar giant step forward.

Not with a computer that's just faster or more powerful, but with a computer that lets you tackle and solve more complex problems than ever before.

The Symbolics 3600™ series provides a more flexible and productive programming environment than numeric computing systems. So it dramatically expands both the amount and kinds of work you can perform with a computer.

That's why symbolic processing is the most widely accepted basis for the development of many AI programs. And is impacting a broad range of traditional

a management decision too.



The Ohio State University Photo Archives

computing applications as well.

The people at Symbolics have pioneered this advanced technology every step of the way. From initial development in the laboratory to practical application in the field. And we're ready to put it in your hands today.

But the next step is yours. To see symbolic processing in action, contact Symbolics, Inc., 11 Cambridge Center, Cambridge, MA 02142.

symbolics[™]
Your next step in computing.[™]

Circle Reader Action No. 446





Analyzing Static Loading of Complex Structures

Critical loading conditions are determined from the analysis of each structural element.

The Automated Thrust Structures Loads and Stresses (ATLAS) system is a series of programs developed to analyze the elements of a complex structure under static-loading conditions. ATLAS calculates internal loads, beam-bending loads, column- and web-buckling loads, beam and panel stresses, and beam-corner stresses.

ATLAS determines the most critical loading conditions from the analysis of each element. This eliminates the traditional approach of preselecting a limited number of conditions that are arbitrarily designated as critical before analysis. Although written for investigation of the Space Shuttle orbiter fuselage assembly, ATLAS could be adapted for such other complex structures as tall buildings, offshore oil rigs, and aircraft.

There are four main programs: (1) CONDENSE reformats and condenses input data obtained from the Monte Carlo flight tapes containing data on engine thrust, pitch, yaw, and other flight measurements; (2) FILTER significantly reduces the number of conditions to be processed, yet retains the critical load cases that meet selected criteria; (3) GLOBAL calculates the loads on the actuator and gimbal bearings due to engine thrust; and (4) ATLAS sums the loads due to thrust, pitch, yaw, and inertia.

The five extreme positive and negative values are listed for the following: (a) shear panel loads (trim3 and quam4 components), (b) beam-corner stresses, (c) beam-element webbing loads, and (d) axial strut loads. The margins of safety for beam-element webbings and struts are also calculated.

These programs are written in FORTRAN IV and Assembler for batch execution and have been implemented on an IBM 370-series computer with a central-memory requirement of approximately 2,200K of 8-bit bytes for the maximum number of elements (150 trim3, 75 quam4, 450 corners, 150 webs, and 100 struts). Fewer elements require less core. ATLAS was developed in 1983.

The programs were written by Darrell C. Gallear of Rockwell International Corp.

for **Johnson Space Center**. For further information, Circle 29 on the TSP Request Card.
MSC-20896

Shadowed Space Heating of Sparse Structures

Complete heat-flux and temperature maps can be computed.

A computer program SSQ has been developed to address and quantify the complex, solar-shadowing conditions inherent in sparse, lattice-type space structures. The analysis procedure is one of assessing partial shadowing of structural elements by multiple, similar slender members. The program yields schedules of incident-solar, Earth-thermal, and Earth-albedo radiation throughout a complete orbit for elemental locations on selected structural members. Thermal response can be computed in an optional routine. Complete heat-flux and temperature mapping can be obtained by repeated computations for selected elements of interest.

Thermal analysis of relatively sparse structures in the space environment has customarily omitted the consideration of shadowing by up-Sun structural members. This convention has been frequently questioned in the case of lattice-type structures supporting very large, near-planar, Earth-facing surfaces (e.g., antennas). For these, significant shadowing can occur whenever the solar vector is nearly tangent to the orbital path. It thus becomes advisable to quantify the shadowing effect, but sparse structures present an exceptional element of complexity.

Space-heating analysis procedures usually assume either total shadowing or total solar irradiation of individual elemental areas of mapped surfaces. While the latter convention is reasonably sound for structural assemblies of which most or all geometric dimensions are of the same order of magnitude, it is less realistic for sparse structures composed of slender members having extremely-high length-to-diameter (L/d) ratios. In such cases, multiple up-Sun (i.e., shadowing) members may yield only partial shadowing of an elemental area of interest, with the degree and duration of shadowing being a strong function of the size and density of the structural assembly. No prior analysis procedure addressing this problem is known to have been developed.

The SSQ program permits the definition of numbered structural-node locations in the spacecraft coordinate system, followed by the definition of line segments (structural members) in terms of bounding-node numbers. Slender structural members are assumed to be cylindrical and are

assigned values of diameter, thermal mass per unit of length, solar absorptance, emittance, and view factor to space. Partially or totally opaque bodies are also defined in terms of bounding-line segments, and the latter surfaces are assigned transmissivities that may vary as functions of solar angle of incidence.

The SSQ program heat-flux output can easily be formatted as required for input to other thermal-analysis programs. Temperature output can also be formatted to accommodate the input requirements of structural-analysis programs.

This program was written by R. F. O'Neill and J. L. Zich of General Dynamics Corp. for **Lewis Research Center**. For further information, Circle 117 on the TSP Request Card.
LEW-13977

Rendezvous BET Program

It computes the relative positions of two vehicles in concentric orbits.

The LRBET3 program is a best-estimate-of-trajectory (BET) calculation for postflight trajectory analysis of Shuttle orbital rendezvous maneuvers. LRBET3 produces estimated measurements for reconstructing relative positions of two vehicles in approximately concentric orbits based on tracking data from one or both vehicles. A Kalman filter and a smoothing filter are applied to the relative measurement input data to estimate the state vector, reduce noise, and produce the BET output. The BET calculation minimizes the variances of all the trajectory estimation errors.

LRBET3 incorporates a Kalman filter to process all rendezvous measurement data prior to a given time. This output is then used by a backward-smoothing filter to make a state vector based on relative tracking data before and after the given time. The normal LRBET3 output is the state vector from the smoothing filter. Abbreviated runs can be performed to check data quality using only the forward Kalman filter. The state vector is propagated every fourth time episode, with the nominal time interval being 0.96 second.

LRBET3 is written in FORTRAN IV for batch execution and has been implemented on a CDC CYBER 170-series computer with a central-memory requirement of approximately 76K (octal) of 60-bit words. The program was written in 1982.

This program was written by William Murphey Lear of TRW, Inc., for **Johnson Space Center**. For further information, Circle 14 on the TSP Request Card.
MSC-20785



DATA GENERAL ASKS: ARE YOU PLAYING RUSSIAN ROULETTE WITH YESTERDAY'S TECHNOLOGY?

FOR ADVANCED COMPUTER SYSTEMS, TALK TO US. IT'S WHY SO MANY GOVERNMENT DEPARTMENTS HAVE CHOSEN DATA GENERAL.

Government business is too critical to be taken for granted. Too much depends on it.

No wonder nineteen of the top twenty U.S. defense contractors have bought a Data General system. As have all the Armed Services and most major departments of the federal government.

And to date, nearly thirty U.S. Senate offices and committees have chosen Data General.

TODAY'S BEST VALUE

Why such unanimity? Because Data General offers a complete range of computer solutions for government programs, with one of the best price/performance ratios in the industry.

From our powerful superminis to the DATA GENERAL/One™ portable.

From unsurpassed software to our CEO® office automation system. Plus complete systems for Ada® and Multi Level Secure Operating Systems, and a strong commitment to TEMPEST.


All Data General systems have full upward compatibility. And because they adhere to international standards, our systems protect your existing equipment investment. We give you the most cost-effective compatibility with IBM outside of IBM—and the easiest to set up and use.

SOLID SUPPORT FOR THE FUTURE

We back our systems with complete service and support. As well as an investment in research and development well above the industry norm.

So instead of chancing yesterday's technology, take a closer look at the computer company that keeps you a generation ahead. Write: Data General, Federal Systems Division, C-228, 4400 Computer Drive, Westboro, MA 01580. Or call 1-800-DATAGEN.



 **Data General**
a Generation ahead.

© 1985 Data General Corp., Westboro, MA. Ada is a registered trademark of the Department of Defense (OUSDRE-AIPO). DATA GENERAL/One is a trademark and CEO is a registered trademark of Data General Corporation.

Variable-Conductance Heat Pipes

It calculates the length of the gas-blocked region and the vapor temperature in the active portion.

In response to a need to accurately and efficiently predict the performance of variable-conductance heat pipes (VCHP's) incorporated in spacecraft thermal-control systems, a computer code VCHPDA has been developed to interact with thermal analyzer programs such as SINDA (Systems Improved Numerical Differencing Analyzer). Given the axial temperature distribution and design specifications of the VCHP, the code is used to calculate the length of the gas-blocked region and the vapor temperature in the active portion of the heat pipe from the simultaneous solution of nonlinear, coupled integro-differential equations governing conservation of non-condensable gas species and thermal energy based on the "flat gas-front" theory.

Historically, the code originated in efforts carried out under the Advanced Thermal Control Experiment program, during which a method to analytically simulate a gas-loaded, variable-conductance heat pipe was developed. A computer subroutine VCHP2 was implemented to numerically solve the analytical model. The VCHP2 code, which interfaced with general thermal models involving heat pipes, was used successfully in steady-state thermal simulation of systems such as the transmitter experiment package (TEP) variable conductance heat pipe system (VCHPS) on the Canadian Communications Technology Satellite (CTS) *Hermes*. Subsequent attempts, however, to utilize VCHP2 for transient thermal analyses yielded unsuccessful results due to numerical instabilities arising during the gas/vapor front-location/vapor-temperature calculations.

As part of efforts to investigate several thermal anomalies that occurred during operation of the CTS spacecraft, the solution scheme in VCHP2 was analyzed in order to uncover the source of the numerical problems. The analysis revealed that the iterative approach used in the subroutine to obtain a convergent solution (starting from an initial, guessed gas length and vapor temperature) was inadequate in view of the nonlinear nature of the model. A new analytical method was formulated which, under most physically realizable operating modes, unconditionally circumvents numerical instabilities.

In addition, two new features were introduced into the VCHP model that permit simulation of the effects of an ice-plug formation and open-artery capacity on the

performance of a VCHP system. The appropriate logic for solution of the analytical model was incorporated into the revised version of the VCHP2 subroutine, now called VCHPDA.

The advantages of the VCHPDA code over prior programs are the improved accuracy, unconditional stability, and increased efficiency of the solution resulting from the novel approach and the use of the state-of-the-art numerical techniques for solving the VCHP mathematical model.

The code is a valuable tool in the design and evaluation of advanced thermal-control systems using variable-conductance heat pipes. It is written in FORTRAN IV for use on CDC 600 computers.

This program was written by David Antoniuk of TRW, Inc. for Lewis Research Center. For further information, Circle 7 on the TSP Request Card.
LEW-14075

Programing Structural Synthesis System

This program aids research in analysis and optimization.

The Programing Structural Synthesis System (PROSS2) was developed to provide a structural-synthesis capability by combining access to SPAR with the CONMIN program and a set of interface procedures. SPAR is a large general-purpose finite-element structural-analysis program, and CONMIN is a large general-purpose optimization program.

The implementation of the PROSS2 analysis/optimization process results in a minimized objective function, typically the mass defined in terms of a set of such design variables as the cross-sectional dimensions of a structural member. Also, the member is subject to a set of constraints; for example, the stress must be less than some allowable value.

PROSS2 is intended to be used in the following three basic ways: (1) as a research tool for the development of optimization techniques that will interface with an efficient analysis program, (2) as a research tool for testing new analysis techniques that will interface with an efficient optimization program, and (3) as an application tool that can be adapted to a wide range of different problems.

With PROSS2, the analysis and optimization programs are executed repeatedly in a looping manner until the process is stopped by a user-defined termination criteria. This part of the system is referred to as the repeatable part of PROSS2. However, some of the analysis, such as model definition, need be done only once and can be saved for future use. These parts are performed outside the loop and

are referred to as the nonrepeatable part of PROSS2. Three options are provided for organizing optimization procedures by combining nonlinear or piecewise-linear programming methods with analytic or finite-difference gradients.

In this newest release, PROSS2 is controlled by SPAR run streams instead of by the control language of the computer. This is accomplished by integration of the entire PROSS2 program as new processors within the SPAR program. The user supplies PROSS2 with problem-dependent routines that express the relationships between the structural parameters of interest in SPAR and the design variables used in CONMIN.

PROSS2 is written in FORTRAN IV for batch execution and has been implemented on a CDC CYBER-series computer. However, the code is machine-independent and can be run with any computer on which SPAR has been implemented. The implementation of PROSS2 on the CDC requires approximately 51K (octal) of 60-bit words. The PROSS2 user must have access to the SPAR program. PROSS2 was developed in 1984.

This program was written by James L. Rogers, Jr., of Langley Research Center. For further information, Circle 72 on the TSP Request Card.
LAR-13408

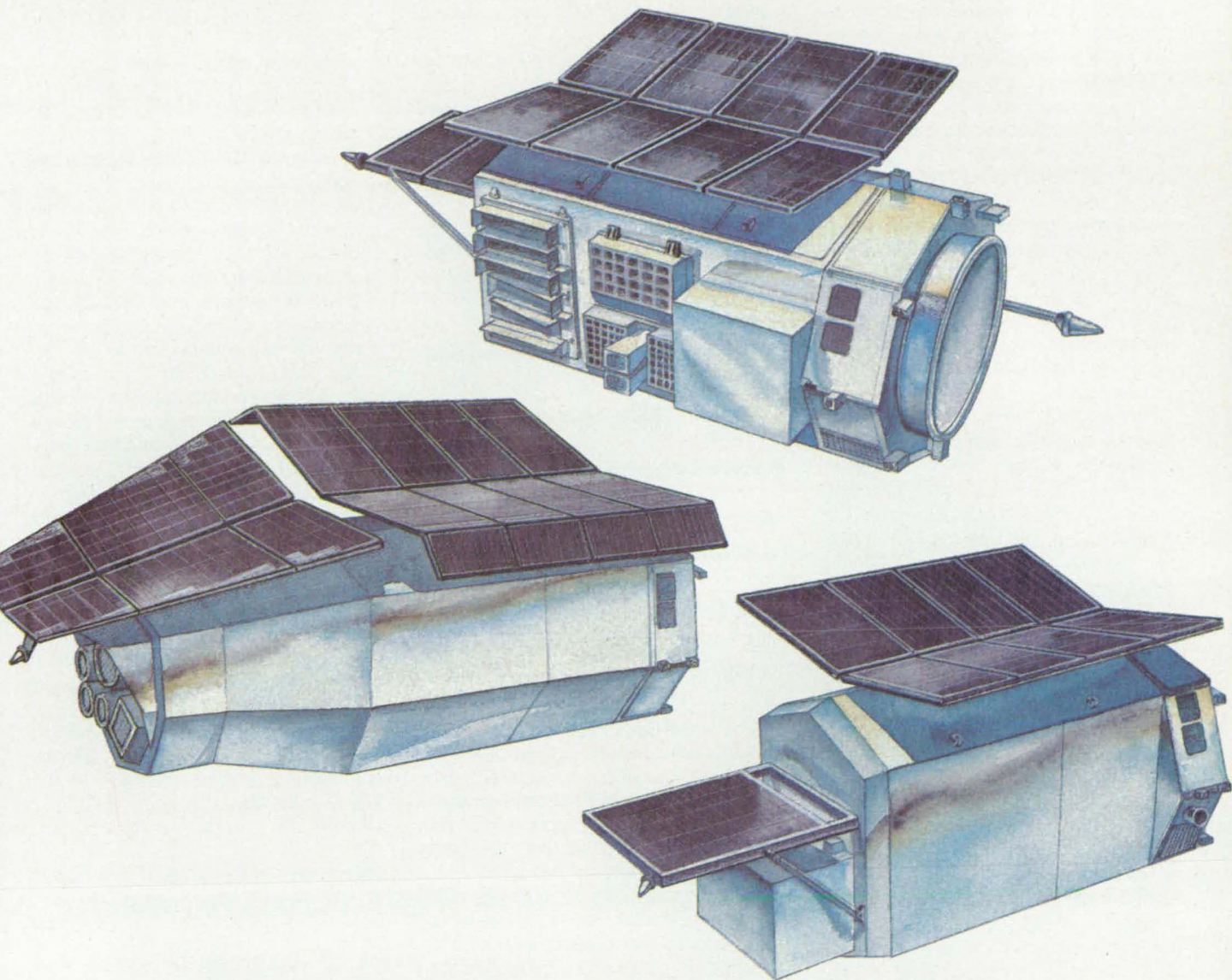
Vibration-Response Analysis

The dynamic behaviors of structures are analyzed interactively.

An interactive steady-state vibration-response program, VIBRA, has been developed. Frequency-response analyses are commonly used in evaluating the dynamic behaviors of structures subjected to cyclic external forces. VIBRA calculates the frequency response using a modal-superposition approach. This method is applicable to single or multiple forces applied to a linear, proportionally damped structure in which the damping may be viscous or structural.

VIBRA computes the forced-acceleration response at any selected point on the structure for a given vibratory loading. VIBRA provides tabular output with optional plots of response versus frequency. The interactive capability enables rapid evaluation of the structural response.

VIBRA requires the input of modal data from only the selected response and applied-vibratory-load points. These data may be obtained either from ground vibration measurements or from a natural vibration analysis. VIBRA can use results from any vibration analysis that has out-



THE RIGHT ATTITUDE

It was NASA's goal to measure, with a pointing accuracy of 1 arc minute, X-ray sources in outer space. So Control Data's 469R² micro-miniature computer was selected for the High Energy Astronomical Observatory (HEAO) satellites to keep critical instruments right on target.

The 469R², with large-scale integrated circuits, is specially designed to operate in the rigorous environment of space; the 'R²', in fact, stands for rugged and reliable—so reliable that this computer's meantime-to-failure is calculated to exceed 200,000 hours.

Other applications to which 469R² computers have been delivered include the Teal Ruby experiment, an infrared sensor satellite which will be launched from the space shuttle.

Find out how Control Data's spaceborne technology and capabilities can help meet your needs. Get more information, along with a print of the spacecraft above, by calling 612/853-5000. Or write Government Systems Resource Center, Control Data Corporation, P.O. Box 609, Minneapolis, MN 55440.

CD CONTROL DATA

put in the form of generalized masses, eigenvalues, and eigenvectors. Thus, VIBRA can be used as a postprocessor for such finite-element codes as NASTRAN.

The user specifies a starting frequency, ending frequency, and frequency step for the VIBRA response analysis. VIBRA output can be plotted on the screen as real acceleration versus forcing frequency, imaginary acceleration versus forcing frequency, acceleration amplitude versus forcing frequency, and phase angle versus forcing frequency. The interactive graphics user has a zoom facility available for detailed examination of the plots. Optionally, the response data are stored for later use.

VIBRA is written in FORTRAN 77 for interactive execution and has been implemented on a CDC CYBER 170-series computer with a central-memory requirement of 120K (octal) of 60-bit words. The graphic output requires the Plot-10 plotting package. The VIBRA program was developed in 1984.

This program was written by Lynn M. Bowman of the U.S. Army Aviation Systems Command for Langley Research Center. For further information, Circle 74 on the TSP Request Card.
LAR-13291

Fatigue-Crack-Growth Structural Analysis

Elastic and plastic deformations are calculated under a variety of loading conditions.

The prediction of fatigue-crack-growth lives can be made with the Fatigue-Crack-Growth Structural Analysis (FASTRAN) computer program. As cyclic loads are applied to an initial crack configuration, FASTRAN predicts crack length and other parameters until a complete break occurs. The loads may be tensile or compressive and of variable or constant amplitude. FASTRAN incorporates linear-elastic fracture mechanics with modifications for load-interaction effects caused by crack closure. FASTRAN is considered a research tool, because of lengthy calculation times.

Surface cracks, surface cracks at holes, and corner cracks at holes in a three-dimensional body can be modeled. The representation is based on the Dugdale model, with alterations to allow plastically deformed material along crack surfaces as the crack advances. Plane stress and plane strain conditions are simulated in FASTRAN by using a constraint factor on tensile yielding to account for three-dimensional effects. FASTRAN has suc-

cessfully predicted crack growth in metallic-alloy sheet materials under aircraft-spectrum loading.

FASTRAN is written in FORTRAN IV for batch execution and has been implemented on a CDC CYBER 170-series computer under NOS 1.4 with a central-memory requirement of approximately 200K (octal) of 60-bit words. The program was developed in 1981.

This program was written by J. C. Newman, Jr., of Langley Research Center. For further information, Circle 101 on the TSP Request Card.
LAR-13412



Machinery

Aircraft Takeoff and Landing Analysis

The behavior of a flexible or rigid aircraft is simulated under a variety of conditions.

The Active Gear, Flexible Aircraft Takeoff and Landing Analysis program, AGFATL, completely simulates aircraft takeoff and landing dynamics. AGFATL represents an airplane either as a rigid body with six degrees of freedom or as a flexible body with multiple degrees of freedom.

The airframe flexibility is represented by the superposition of up to 20 free vibration modes on the rigid-body motions. The analysis includes maneuver logic and autopilots programed to control the aircraft during the glide slope, flare, landing, and takeoff. The program is modular so that the performance of the aircraft in flight and during landing and ground maneuvers can be studied separately or in combination. A program-restart capability is included in AGFATL.

Eleven effects simulated in the program include the following:

1. Flexible aircraft control and performance during glide slope, flare, landing roll, and takeoff roll under conditions of changing winds, engine failures, brake failures, control-system failures, strut failures, restrictions due to runway length, and control-variable limits and timelags;
2. Landing-gear loads and dynamics for up to five gears;
3. Single and multiple engines (maximum of four), including selective engine reversing and failure;
4. Drag-chute and spoiler effects;
5. Wheel braking (including skid control) and selective brake failure;
6. Aerodynamic ground effects;

7. Aircraft-carrier operations;
8. Inclined runways and runway perturbations;
9. Flexible or rigid airframes;
10. Rudder and nose-gear steering; and
11. Actively-controlled landing-gear shock struts.

The input to AGFATL includes data that describe runway roughness; vehicle geometry, flexibility and aerodynamic characteristics; landing gear(s); propulsion; and such initial conditions as attitude, attitude-change rates, and velocities. AGFATL performs a time integration of the equations of motion and produces comprehensive information on the airframe, state-of-maneuver logic, autopilots, control response, and aircraft loads from impact, runway rollout, and ground operations. Flexible-body and total (elastic plus rigid-body) displacements, velocities, and accelerations are also produced in the flexible-body option for up to 20 points on the aircraft.

AGFATL is written in FORTRAN IV for batch execution and has been implemented on a CDC CYBER 170-series computer with an overlaid central-memory requirement of approximately 141K (octal) of 60-bit words. The program was last updated in 1984.

This program was written by John R. McGehee of Langley Research Center. For further information, Circle 80 on the TSP Request Card.
LAR-13390

Nonconical Relaxation for Supersonic Potential Flow

Nonlinear, three-dimensional effects are computed from the full potential-flow equation.

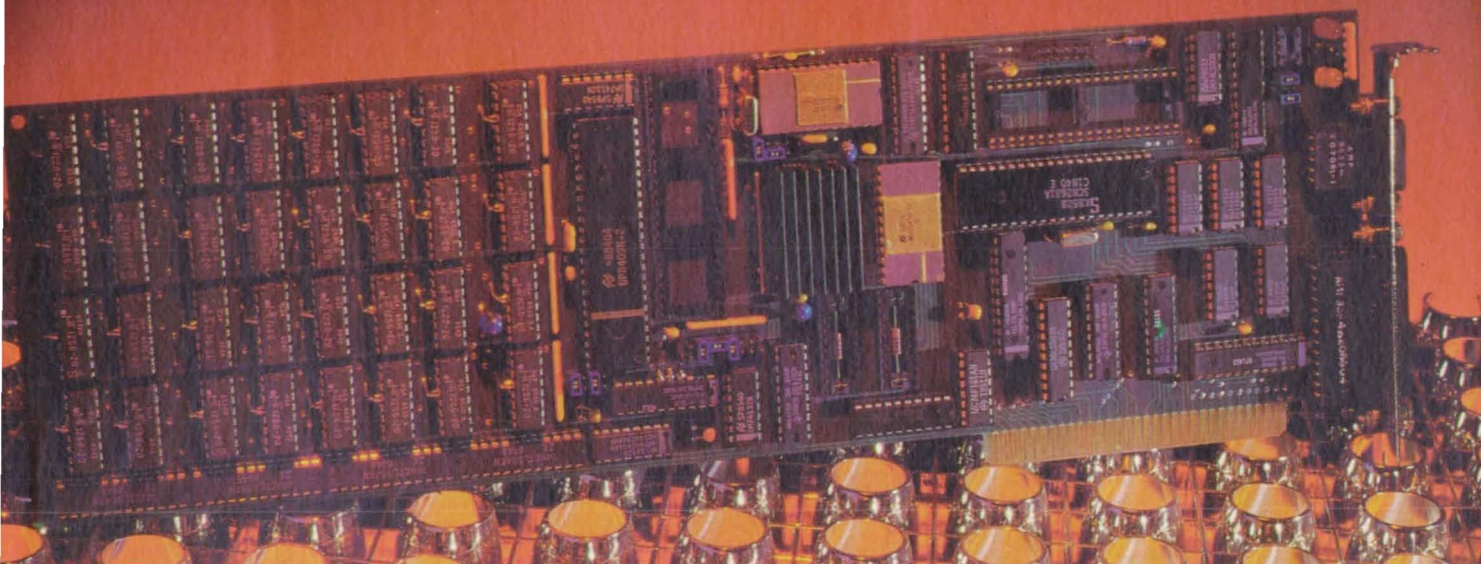
The Nonconical Relaxation program, NCOREL, employs a new computational technique for the prediction of inviscid, nonlinear supersonic aerodynamics. Unlike conventional linear potential equations, NCOREL utilizes the full potential-flow equation to predict the formation of supercritical crossflow regions, embedded shocks, and bow shocks.

The embedded shocks are of great importance to design engineers because these features can significantly alter wing characteristics at low-to-moderate supersonic speeds. Nonlinear effects are also important on wings that have supersonic leading edges or bodies that have slopes greater than the mach angle.

NCOREL has been applied successfully to a wide variety of body and wing configurations in the mach-number range from 1.5 to 3. With NCOREL, the aerodynamicist can reliably predict the detailed

CONVERT

NOW YOUR PC CAN RUN 35 TIMES FASTER



Turn Your PC Into A Powerful 32-BIT Super-Mini

DSI-32 Ever wish your PC could have more power and speed than a VAX? The **DSI-32** Co-Processor Board is a totally self-contained 32-bit computer on a single PC board. It runs at super-mini speeds (10MHz and no wait states) using its own large 32-bit memory space and floating point processor. It's fully compatible with your standard PC MS/DOS system, no re-training or file conversions is needed. Total installation is accomplished in just a few minutes.

It enables you to port scientific or commercial applications without the grueling task of recoding or restructuring your software to accommodate Intel's architecture. **DSI-32** gives you freedom of choice, either MS/DOS or Unix, without having to commit your entire system to one or the other.

Plug it in and let **DSI-32** expand your horizons.

- Uses just one slot.
- Comes with National Semiconductor's 32032 processor running at 10MHz—a full 32-bit data path.
- 1MB to 8MB available on board. (Greater memory options available soon.)
- Choice of two Operating Systems: — MS/DOS Standard or Unix V Option.
- Operates in any IBM/PC, AT or look-alike.
- Has its own Floating Point Processor.
- Supports a variety of native high level, optimizing languages: C, Pascal, Fortran, and soon ADA. Supplied with Assembler, Linker, Loader and Debugger.
- Turns your PC into a powerful concurrent processor Mini. The host 8088 or 80286 handles all I.O. functions while the 32032 runs uninterrupted.
- Transport a large variety of Mini and Mainframe programs in minutes to run on your micro.
- Now you can run large time consuming applications on a PC at warp speeds.
- Get the power and performance of computers costing tens of thousands more for less than many micros.
- Try our board now at no risk. 30 Day Money Back Evaluation Period

Sieve Benchmark

N*	IBM XT	IBM AT	VAX 750	VAX 780	DSI-32
20,000	35.30	8.13	6.11	3.04	4.52
40,000	351.50	99.71	13.13	6.38	9.07

Float Benchmark

40,000	11.46	17.71	.83	.50	.80
--------	-------	-------	-----	-----	-----

Unix Benchmarks

	DSI-32	VAX 780	VAX 750
O.S. Overhead	3.88	4.4	7.0
C Compiler Test	.55	1.0	1.7
Sieve of Eratosthenes	1.93	1.7	2.4

ECOTECH[®]
COMPUTER SYSTEMS

3711 35th Street, N.W.
Washington, D.C. 20016.

800 826-2189

202 244-3858

spanwise behavior of realistic three-dimensional supersonic wings and bodies in high-lift maneuvers.

The approach used by NCOREL consists of solving the nonconservative finite-difference analog of the full potential equation in a spherical coordinate system. Conformal mappings are used to generate a grid in the spherical crossflow plane capable of resolving large gradients in the vicinity of the leading edge.

NCOREL computes a conical flow at the apex of the coordinate system and uses an implicit marching technique to obtain three-dimensional crossflow solutions. Relaxation techniques for supersonic and subsonic regimes form the basis for the crossflow-plane solutions. The numerical technique allows for the capture of both embedded crossflow and bow-type shocks. In addition, the bow shock can be fitted and used as the crossflow-plane outer boundary.

There are several input geometry options built into NCOREL, including the Harris wave-drag input format. Isolated-wing or isolated-body cross sections are usually considered, but wing/body cross sections can be input if the necessary mesh resolution is available. NCOREL calculates moments, areas, forces, lift and drag coefficients, and coordinates of shocks and crossflows.

NCOREL is written in FORTRAN IV for batch execution and has been implemented on a CDC CYBER 170-series computer with a central-memory requirement of 310K (octal) of 60-bit words. This program was developed in 1983.

This program was written by Michael J. Siclari of Grumman Aerospace Corp. for Langley Research Center. For further information, Circle 76 on the TSP Request Card.

LAR-13346

Analysis of Lubricant Jet Flow

A computer program helps assure adequate pinion lubrication.

A computer program, IMPOUT 2, has been developed using newly-established "limit formulas" to prevent lubricant non-impingement on the pinion. The standard nozzle orientation usually found in gearsets where the offset is zero and the inclination angle is zero will often cause the pinion to be deprived of preliminary impingement. This can be an important cause of incipient scoring failure in high-speed drives. This work is an extension of a previous study that was limited to standard centers and tooth proportions only. This work includes long and short adden-

da and modified center distances.

The analysis developed the equations for the limit values of variables necessary to remove prior severe limitations or constraints necessary to facilitate the computer analysis. Results of an analysis determined that (a) the industrial standard nozzle orientation with an offset $S = 0$ and inclination angle $B = 0$ will often cause the pinion to be deprived of primary impingement, which can be an important cause of incipient gearing failure in high-speed drives; (b) for ratios larger than 1:1, the oil jet will impinge on the gear teeth only, unless a minimum calculated jet velocity is provided to lubricate the pinion teeth; (c) when a minimum jet velocity is provided, the oil-jet offset must be equal to or greater than a minimum calculated offset to assure impingement on the pinion; and (d) as the oil-jet velocity is increased above this calculated minimum value, the impingement depth will increase but at a decreasing rate. The maximum impingement depth will generally not exceed 10 percent of the tooth profile depth.

The IMPOUT 2 program is written in ANSI FORTRAN IV for use on a CDC 750. The computer program can be used to analyze impingement depth on the gear teeth for an oil jet located at the out-of-mesh position with arbitrary offset and inclination angles and with arbitrary addendum and center-distance modification.

This work was done by Dennis P. Townsend of Lewis Research Center and Lee S. Akin of California State University at Long Beach. Further information may be found in NASA TM-83723 [N84-29224/NSP], "Lubricant Jet Flow Phenomena in Spur and Helical Gears with Modified Center Distances and/or Addendums — for Out-of-Mesh Conditions" [\$8.50]. A copy may be purchased [prepayment required] from the National Technical Information Service, Springfield, Virginia 22161.

LEW-14242

Aerodynamic Characteristics of NACA 16-Series Airfoils

Standard data from the literature are incorporated into the program.

A comprehensive and easily-accessible data bank of the aerodynamic characteristics of NACA 16-series airfoils is incorporated into the AIRFOIL program for use in propeller performance research. The low-drag, high-critical-speed airfoils could be effective in advanced turbo-prop designs currently under investigation.

Until AIRFOIL, aerodynamic charac-

teristics were available for only a small range of cambers, thicknesses, angles-of-attack, and mach numbers. AIRFOIL incorporates digitized data from standard curves in the literature and interpolates between thickness ratios and design-lift coefficients. Linear extrapolation is used to obtain data from each set of mach numbers, angles-of-attack, and lift coefficients beyond those previously available. Additional calculations are included to account for the nonlinear behavior of lift and drag coefficients beyond the stall angle.

The AIRFOIL performance mode requires an angle-of-attack, a mach number, and a geometry as input, while the design mode requires a design-lift coefficient, a mach number, and a geometry. Both modes compute the drag coefficient and lift-to-drag ratio. AIRFOIL can be used for sections with lift coefficients up to 0.8, thickness ratios from 4 to 21 percent, mach numbers from 0.3 to 1.6, and angles-of-attack from -4° to 8° . AIRFOIL gives reasonable results when compared to wind-tunnel data.

AIRFOIL is written in FORTRAN IV for batch execution and has been implemented on a CDC CYBER 170-series computer with a central-memory requirement of approximately 137K (octal) of 60-bit words. The program was developed in 1983.

This program was written by Catherine M. Maksymiuk of Langley Research Center and Sally A. Watson Viken of the University of Kansas Center for Research, Inc. For further information, Circle 77 on the TSP Request Card.

LAR-13355

Wall Interference in Two-Dimensional Wind Tunnels

Viscosity and tunnel-wall constraints are introduced via boundary conditions.

The TWINTN4 computer program was developed to implement a method of posttest assessment of wall interference in two-dimensional wind tunnels. Classical methods for evaluating wind-tunnel wall interference are generally unsatisfactory for use with wind tunnels for two major reasons: (1) It has not been possible to define the boundary conditions for slotted or perforated walls with the required generality and accuracy, and (2) the principle of linear superposition on which the classical approach is based becomes invalid at transonic speeds. The method used by TWINTN4 involves the successive solution of the transonic small-disturbance potential equation to

When the Air Force demanded Total Performance, Zenith delivered.

Total performance. It's the only option for the U.S. Air Force. To measure up is to outperform the merely superior.

After extensive evaluation, the Air Force selected one official stand-alone microcomputer. The Zenith Z-120 desktop.



Zenith Z-150 PC

Now, from the same tradition as the Zenith Z-120, come the "total performance" business computers: the Zenith Z-100 PC's. They're IBM PC-compatible, but are designed with enhanced features that go beyond IBM PC compatibility. Including greater internal expandability. Storage that can expand up to 11 megabytes. A detached keyboard with an improved key layout. And the ability to run virtually all IBM PC software. We also offer Z-150 PC's that are "Tempest Accredited." (Zenith-modified listed

on Preferred Products List under Inteq, Inc.)

For your free Zenith PC Information Kit and the name of your nearest Zenith Data Systems dealer, please call **1-800-842-9000, Ext. 1**



calculate the wind-tunnel flow, the perturbation attributable to the model, and the equivalent free airflow around the model.

The total procedure employed by TWINTN4 can be considered as a nonlinear counterpart of classical wall-interference theory, with the effects of both viscosity and tunnel-wall constraints being introduced through experimentally-measured boundary conditions. These boundary conditions are developed from pressure-distribution measurements made on the model and the tunnel walls.

The wall-induced perturbation field is taken as the difference between the model perturbation and the total perturbation in the tunnel flow solution. A correction for the angle-of-attack and the corrected far-field mach number are determined during the equivalent free-air solution. The influence of nonuniformities in the wall-induced velocity field is determined by comparing the equivalent free-air pressure distribution with the experimental distribution adjusted to the new reference mach number.

TWINTN4 offers two methods for combining sidewall boundary-layer effects with upper and lower wall interference. In the sequential procedure, the Sewall method is used to define a flow free of sidewall effects, which is then assessed for upper and lower wall effects. In the unified procedure, the wind-tunnel flow equations are altered to incorporate effects from all four walls at once.

The TWINTN4 program is written in FORTRAN IV for batch execution and has been implemented on a CDC CYBER 175 computer with a central-memory requirement of approximately 47K (octal) of 60-bit words. This program was developed in 1977 with refinements added in 1984.

This program was written by William B. Kemp, Jr., of Virginia Associated Research Campus for Langley Research Center. For further information, Circle 81 on the TSP Request Card.
LAR-13394

Predicting Vortex Shedding in Supersonic Flow

Nonlinear aerodynamic characteristics of missile bodies are computed.

The program NOZVTX calculates the nonlinear aerodynamic characteristics and flow fields of missile bodies at various angles-of-attack and roll in supersonic flow. At high angles-of-attack, boundary-layer fluids leave the body surface from separation points on both sides of the body and roll up into a symmetrical vortex pair on the lee side. The vortex-shedding

characteristics are directly influenced by the body shape.

The vortex wake is modeled by tracking discrete vortexes in crossflow planes. NOZVTX reduces the three-dimensional steady flow around the body to a two-dimensional, unsteady, separated-flow system. The predicted vortex distributions and velocity components are in reasonable agreement with the actual measurements of flow characteristics about slender bodies of circular or non-circular cross section, for large angles-of-attack and moderate mach numbers.

NOZVTX models the airborne body by using a supersonic panel method for non-circular cross sections or an axisymmetric line source and doublets for circular cross sections. The vortex cloud in NOZVTX consists of many point vortexes, each represented by a viscous core. Pressure and vortex-trajectory calculations are carried out by the conformal mapping of any noncircular cross sections to a circle and using a full Bernoulli equation.

The surface pressure distribution on the body is used to calculate the forces on the body and the separation points. The user can specify vortex separation as either laminar or turbulent. The NOZVTX output includes (a) the geometry, centroids, and surface pressure of the source panels and (b) the positions, strengths, and velocity components of the shed vortexes.

NOZVTX is written in FORTRAN IV for batch execution and has been implemented on a CDC CYBER 170-series computer with a central-memory requirement of approximately 231K of 60-bit words. This program was developed in 1983.

This program was written by M. R. Mendenhall and S. C. Perkins, Jr., of Nielsen Engineering and Research, Inc., for Langley Research Center. For further information, Circle 79 on the TSP Request Card.
LAR-13375

Predicting Wall Modifications for Adaptive Wind Tunnels

The wall shape is changed iteratively until it matches the streamlines.

FLEXWAL predicts the upper and lower wall modifications necessary to remove wall-interference effects in adaptive-wall wind tunnels. FLEXWAL aids in the elimination of wall-interference effects on objects being tested in a typical two-dimensional wind tunnel with rigid sidewalls and flexible, solid floor and

ceiling boundaries. The iterative procedure is valid for subsonic and transonic test conditions, and the convergence of the method has been verified both analytically and experimentally.

The flow field around a test article in a wind tunnel is constrained by the walls of the tunnel. FLEXWAL uses the Cauchy integral formula to extend the real internal flow field around the test article to infinite distance by solving for an imaginary flow outside the wind tunnel. These two flows are coupled at the wall boundary where modifications of the real internal flow are made until the external and internal flows match. Continuity occurs when the measured wall data match the calculated data.

The wall-shape correction is applied iteratively until the contour of the flexible wall matches the streamline of the flow about the model being tested. The required input includes the mach number, temperature, pressure, and wall-relaxation factors. The output contains the wall-position corrections required to match the flow-field contour.

FLEXWAL is written in FORTRAN IV for batch execution and has been implemented on a CDC CYBER 170-series computer with a central-memory requirement of approximately 52K (octal) of 60-bit words. This program was developed in 1981.

This program was written by Joel L. Everhart of Langley Research Center. For further information, Circle 75 on the TSP Request Card.
LAR-13301

Two Programs for Supersonic Wing Design and Analysis

Many useful parameters are calculated for design, analysis, and optimization.

COREL and W12SC3 are useful in the aerodynamic design and analysis of wings for supersonic speeds. Both programs were used in developing the Super Critical Conical Camber (SC3) concept, in which high supersonic lift coefficients are obtained efficiently by controlling cross-flow development. The COREL (Conical Relaxation) program solves the nonlinear full potential equation for a spanwise section of a wing in the crossflow plane, and an option exists to correct the result for nonconical geometry. W12SC3 applies linear-theory panel methods to compute solutions for a wing/body configuration. The programs are restricted to supersonic flows and are useful for many design, analysis, and optimization applications.

NASA Tech Briefs, March/April 1986

COREL computes full potential solutions, including the nonlinear mixed subsonic/supersonic crossflow that develops on supersonic wings with high lift coefficients. The solution is obtained for a non-conservative form of the governing equations, and the bow and crossflow shocks are captured as part of the solution. An initial aerodynamic solution is obtained on a crude grid to estimate the bow-shock position; then a finer mesh is mapped, keeping the computed bow-shock location within the problem boundaries. The input geometry can be specifically defined or calculated in COREL using Craighero bicubic-spline patches.

W12SC3 combines source and vortex-panel-singularity distributions for calculating the linear-theory estimate of the configuration aerodynamics. The user can specify Woodward II calculations for arbitrary body models or Woodward I calculations for an interference shell that approximates the actual body shape. Carlson's nonlinear correction to the supersonic linear-theory wing pressures can be applied. If desired, COREL will produce conical-panel pressure data for further processing by W12SC3. W12SC3 can perform the following five aerodynamic functions: (1) full analysis, (2) full design, (3) full optimization, (4) mixed design/analysis, and (5) mixed design/optimization. Results from W12SC3 include the wing camber distribution, surface velocities, pressure coefficients, integrated forces and moments.

COREL and W12SC3 are written in FORTRAN IV for batch execution and have been implemented on a CDC CYBER 170-series computer with a central-memory requirement of 252K (octal) of 60-bit words. These programs were developed in 1983.

This program was written by William H. Mason, Bruce S. Rosen and Bernard Grossman of Grumman Aerospace Corp. for Langley Research Center. For further information, Circle 71 on the TSP Request Card.
LAR13239

Second-Order-Potential Analysis and Optimization

An optimum camber is designed for supersonic and hypersonic vehicles.

The Second Order Potential Analysis and Optimization (SOPA) package is a set of computer programs used to predict aerodynamic characteristics and to design optimum camber for both supersonic and hypersonic vehicles. The analysis program incorporates second-order-potential, small-disturbance theory for the analysis of wing/body configurations. The optimization program uses analysis results to generate optimum camber, twist, or flap deflections by minimizing zero suction drag.

Conventional aerodynamic linear panel methods have proved inexact, while finite-difference methods are computationally exorbitant. SOPA calculates a first-order linear solution, which is then used as input to a nonlinear Prandtl-Glauert approximation. The complete first-order solution is a linear combination of the crossflow solution, the camber solution, the lift due to thickness, and the lift due to the body. This second-order-potential approach accurately predicts airfoil- and cone-surface pressures.

Using SOPA, the user can perform first-order optimizations on configurations having up to 10 surfaces and 1 body. Second-order optimizations can be performed on planar configurations without a body. The input to SOPA consists of the body geometry, lifting-surface geometry, and various aerodynamic and numerical-control values. The geometry information may either be generated by the user or created by the APAS program [see "Aerodynamic Preliminary Analysis" on page 362 of *NASA Tech Briefs*, Vol. 5, No. 3, Fall 1980 (LAR-12404)]. SOPA output consists of pressure coefficients and aerodynamic coefficients.

SOPA is written in FORTRAN V for batch execution and has been implemented on a CDC CYBER 170-series computer under NOS 1.4 with a central-memory requirement of approximately 351K (octal) of 60-bit words. SOPA was developed in 1984.

This program was written by Willard C. Clever of Rockwell International Corp. for Langley Research Center. For further information, Circle 49 on the TSP Request Card.
LAR-13314

This program was written by James V. Cozzolongo of Ames Research Center and Dexter L. Hermstad and Daniel S. McCoy of Informatics General Corp. based on an original program written by James Clark of Silicon Graphics. For further information, Circle 115 on the TSP Request Card.
ARC-11496

Mathematics and Information Sciences

Shaded-Color Picture Generation of Computer-Defined Arbitrary Shapes

Objects are displayed as smooth, color-shaded surfaces.

Many engineering applications require the development of geometric models of

shapes for use in computational procedures. The best way for the engineer to verify a geometric model, and the numerical data it represents, is to look at a graphic display of the model. The graphic display must be as realistic as possible in order to provide the engineer with as much visual information as possible.

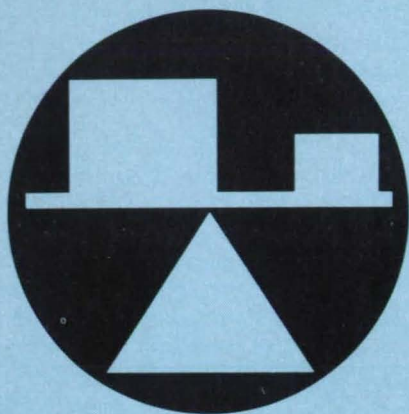
The SHADE computer program generates realistic color-shaded pictures from computer-defined arbitrary shapes. Objects that are defined for computer representation can be displayed as smooth, color-shaded surfaces, including varying degrees of transparency. SHADE-generated results can also be used for the presentation of computational results. By performing a color mapping, SHADE can color the model surface to display such analysis results as pressures, stresses, and temperatures. NASA has used SHADE extensively in the design and analysis of high-performance aircraft. Industry should find applications for SHADE in computer-aided design and computer-aided manufacturing.

Objects can be defined for SHADE in terms of polygons, PAN AIR networks, or parametric bicubic splined patches. The image data used to generate the picture consist of polygons. The parametric bicubic patch definition is subdivided to yield a polygonal definition for shaded display purposes. Defining polygons can have a different color associated with each corner point. SHADE offers numerous options including:

- Varying the resolution from 256 to 4,096 pixels,
- Displaying text with the graphics,
- Creating and editing a user view field,
- Controlling the shading techniques (i.e., transparency, highlights, and specular reflectivity, and
- Generating color bars for displayed results correlation.

SHADE is written in VAX FORTRAN and MACRO Assembler for either interactive or batch execution on a DEC VAX 11/780 operating under VMS. The memory requirements for the SHADE program are a function of the array sizes, which can be varied according to the user's needs. The program as currently configured requires 2.5 million bytes of memory. The program is written to generate graphics data files for the DICOMED D48 film plotter, but should be adaptable to any raster-scan graphics device. SHADE was developed in 1983.

This program was written by James V. Cozzolongo of Ames Research Center and Dexter L. Hermstad and Daniel S. McCoy of Informatics General Corp. based on an original program written by James Clark of Silicon Graphics. For further information, Circle 115 on the TSP Request Card.
ARC-11496



Hardware, Techniques, and Processes

- 108 Quick-Connect Heavy-Duty Fastener
- 109 Stable Ejection Seat
- 110 Finite-Element Fracture Analysis of Pins and Bolts
- 111 Three-Axis Load-Cell Assembly
- 112 Acoustic/Magnetic Stress Sensor
- 113 Matching Vibration Testing to "Real-World" Conditions
- 114 Stress Measurement by Geometrical Optics
- 114 Variable Control Port for Fluidic Control Device
- 115 Measuring Water-Layer Thickness
- 116 Dynamic Pressure Calibration Standard

Books & Reports

- 117 Mixer Analysis of Nacelle/Nozzle Flow

Computer Programs

- 98 Analyzing Static Loading of Complex Structures
- 98 Shadowed Space Heating of Sparse Structures
- 98 Rendezvous BET Program
- 100 Variable-Conductance Heat Pipes
- 100 Programing Structural Synthesis System
- 100 Vibration-Response Analysis
- 102 Fatigue-Crack-Growth Structural Analysis

Quick-Connect Heavy-Duty Fastener

An attaching device combines fast connection and disconnection with high strength.

NASA's Jet Propulsion Laboratory, Pasadena, California

A fastener combines the best features of quarter-turn fasteners and threaded fasteners. Like quarter-turn attaching devices, it can be connected and disconnected quickly. Like threaded devices, it can be adjusted to a desired preload, withstand high loads, and accommodate a wide range of grip lengths.

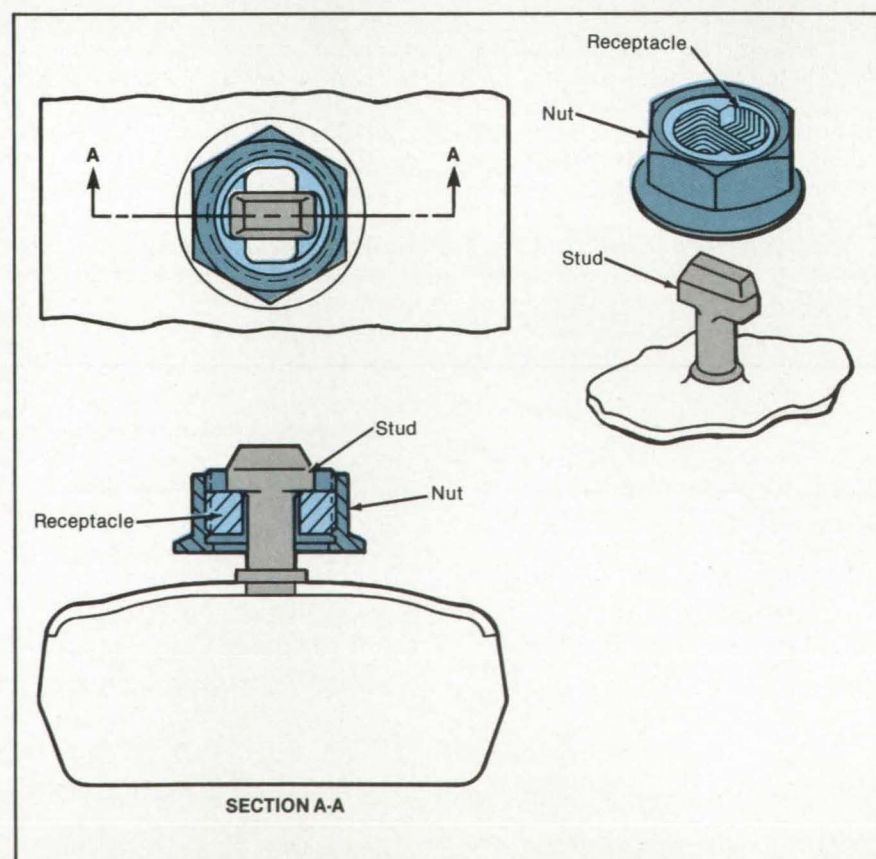
The fastener consists of two mating parts: a T-shaped stud and a receptacle with an external thread and nut (see figure). The receptacle is placed over the stud and rotated with the nut so that it engages the stud. After one-quarter turn, the nut continues to rotate while the receptacle remains still, so that the nut starts to rotate with respect to the receptacle. With continued rotation, the nut bears against the base of the stud. Finally, the nut is tightened with a torque wrench to the desired prestress.

The reverse procedure removes the fastener. The nut is backed off several turns with a wrench until a lip on the internal thread of the nut engages the bottom

of the quarter-turn receptacle: This engagement prevents further rotation of the nut with respect to the receptacle and the receptacle then turns with the nut. An additional quarter-turn disengages the receptacle from the stud.

The fastener was developed for attaching pads to the tracks of tracked vehicles. In this application, it prevents pad separation under tension loads and resists loosening under compression loads. It establishes the required prestress within fairly narrow bounds (± 25 percent) even though the grip length varies widely because of variations in the dimension of the pad plate (a stamping) and the track shoe (a forging). The fastener takes slightly longer to attach than a standard quarter-turn fastener but not as long as a standard threaded fastener.

This work was done by Donald M. Moore of Caltech for NASA's Jet Propulsion Laboratory. For further information, Circle 34 on the TSP Request Card. NPO-16370



The **T-Shaped Stud** engages a groove in the receptacle after one-quarter turn. Further turning tightens the nut on the receptacle.

Stable Ejection Seat

A square drogue with truss-like connections would prevent yaw and pitch of the ejected seat.

Lyndon B. Johnson Space Center, Houston, Texas

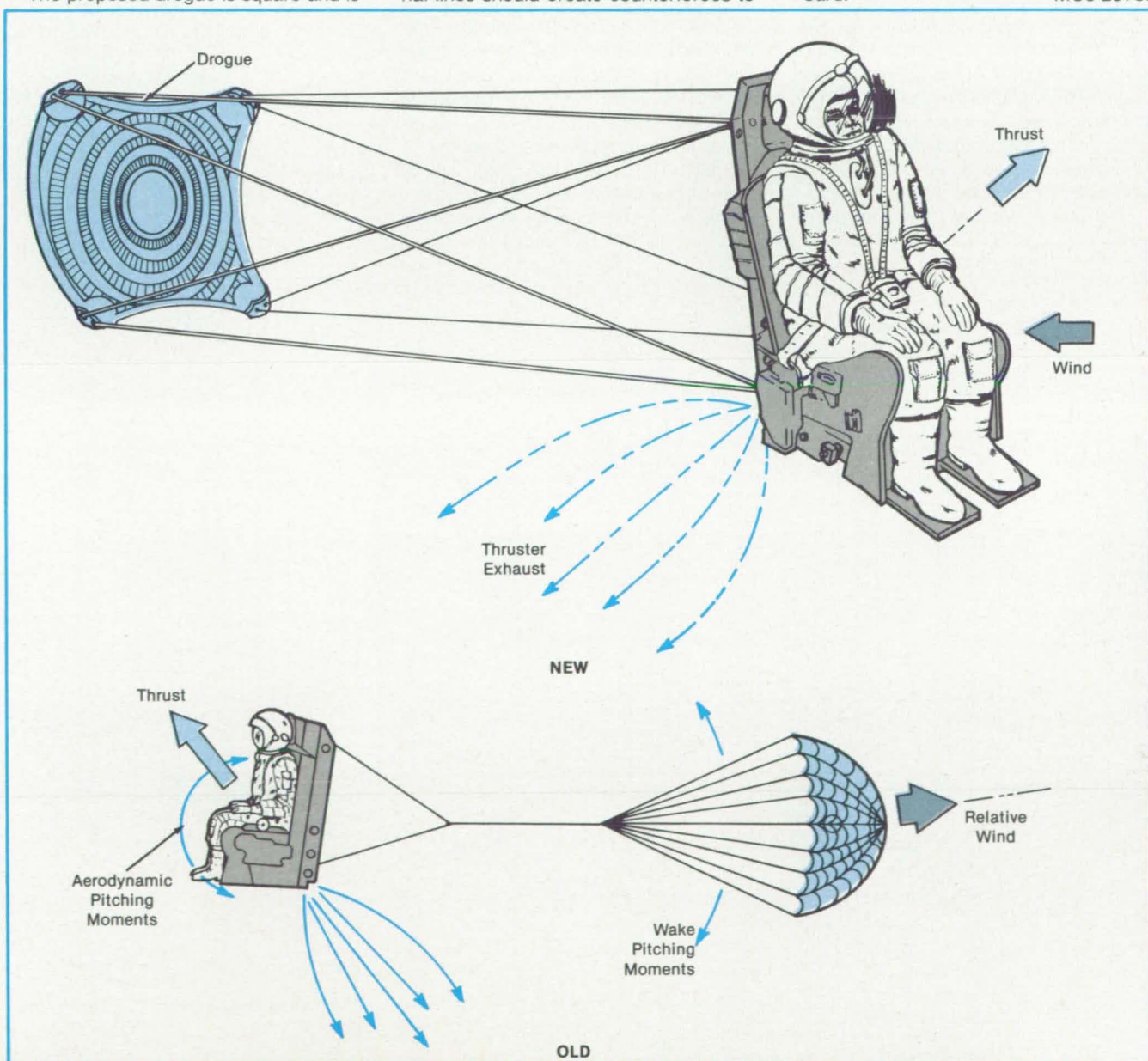
A proposed drogue chute for an ejection seat promises to slow down the seat in a more stable fashion than conventional parachutes and thus improve the chances for survival. The new parachute is expected to reduce dynamic forces on the ejected person and extend the maximum possible ejection altitude by 50 percent. It could be used at high or low speeds.

The proposed drogue is square and is

attached by a network of lines from its corners to the seat corners (see figure). A conventional ejection parachute, in contrast, is a circular drogue that is attached by a single line to lines extending to the seat corners. The single-point fulcrum attachment can allow pitch and yaw forces to turn the seat and wrap the cable and parachute around the seat. With the new parachute, however, the direct and diagonal lines should create counterforces to

the pitch and yaw forces. It should thus allow the seat and its passenger to decelerate and descend stably and safely. With it, gyro stabilization and seat-mounted aerodynamic balancing devices should be unnecessary.

This work was done by Robert S. Hirsch of Rockwell International Corp. for Johnson Space Center. For further information, Circle 54 on the TSP Request Card.
MSC-20780



The **Square Drogue** linked to the seat from its corners suppresses the tendency of the seat to rotate in pitch and yaw. The conventional drogue, however, allows the seat to pivot about the point at which the parachute line is joined to the seat lines.

Finite-Element Fracture Analysis of Pins and Bolts

Stress intensities are calculated in bending and tension.

Marshall Space Flight Center, Alabama

A finite-element stress-analysis method gives stress-intensity estimates for surface flaws on smooth and threaded round bars. Calculations were done for purely tensile and purely bending loads. The results, presented in dimensionless form, will be useful for determining the fatigue lives of bolts and pins.

The first step in the computation is to construct a mathematical model of the part to be analyzed (see Figure 1), using a standard three-dimensional finite element known as quadratic isoparametric. A computer program has been written to take a coarse-element model and refine it in the vicinity of the crack edge. Thus, a sufficient number of elements is provided to characterize the variation of stress intensity along the crack edge.

The mathematical model is considered

to be subjected to forces or enforced displacements across the crack edge. Nodal displacements of the elements along the crack are obtained: The forces and displacements are related by a stiffness matrix that has been evaluated for the particular finite-element model by previously developed methods.

The differential displacement at the crack affects the stiffness matrix only through the contributions of the elements adjacent to the crack. The stiffnesses of all other elements of the model remain unchanged. This leads to the observation that the strain-energy release rate due to the crack extension is completely determined by the displacements of only these elements. This rate is calculated from a sum of products of stiffness-matrix elements with displacements. In view of the

foregoing observation, only the displacements of the nodes defining the two elements containing the perturbed node (see Figure 2) are required to evaluate this rate.

The stress intensity K_I is calculated from

$$K_I = \left[E \frac{dS}{dA} \left(\frac{1}{1-\nu^2} + \frac{\nu}{1+\nu} \frac{\epsilon_y}{\epsilon_x + \epsilon_z} \right) \right]^{1/2}$$

and

$$\frac{dS}{dA} = \frac{dS}{dn} \frac{dn}{dA}$$

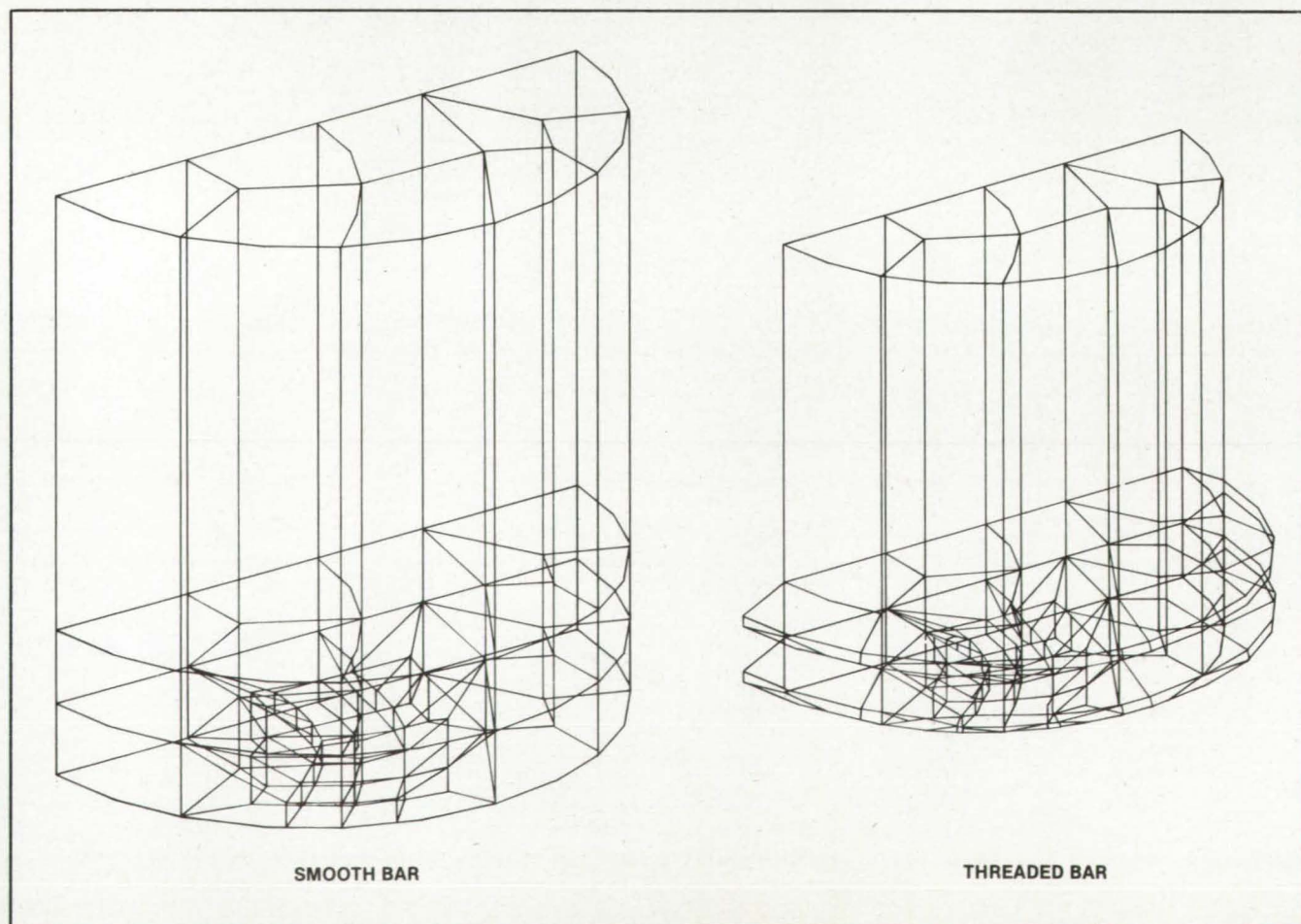


Figure 1. These are **Typical Finite-Element Models** for use in the stress analysis of pins (above) and bolts (below).

where S = strain energy, dn = the element of displacement in the direction of crack growth, A = the surface area of the crack, E = the modulus of elasticity, ν = Poisson's ratio, and ϵ_x , ϵ_y , and ϵ_z represent the strains in the perturbed elements, with ϵ_y along the crack edge. dA/dn is calculated as a function of the crack size and shape.

The method was verified satisfactorily with a center-cracked strip and an elliptical crack in an infinite medium. The method was then applied to surface flaws on smooth and threaded round bars. For each case, relative stress intensities were calculated and expressed as configuration-related correction factors for a range of crack sizes and aspect ratios. The results of these calculations are comparable to previously published results (where applicable) and are useful in practical problems involving pins and bolts.

This work was done by Kermit J. Nord of Teledyne Brown Engineering Corp. for Marshall Space Flight Center. For further information, Circle 39 on the TSP Request Card.
MFS-28061

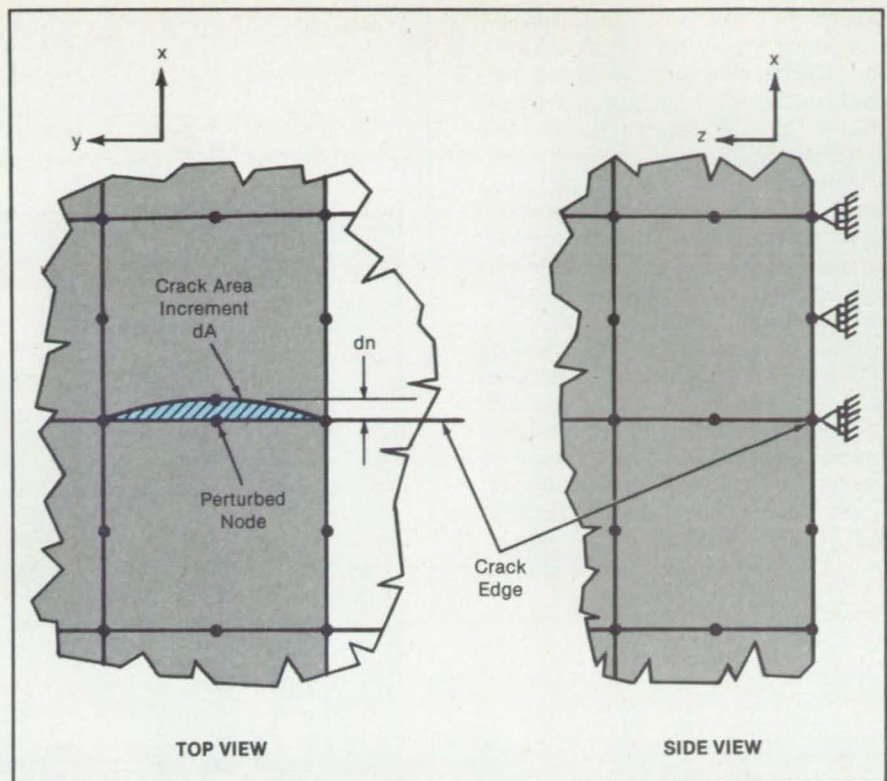


Figure 2. Finite Elements Adjacent to a Crack are used to calculate the stress intensity and related quantities involved in crack growth.

Three-Axis Load-Cell Assembly

A force-measuring device is both sensitive and rugged.

Lyndon B. Johnson Space Center, Houston, Texas

A load-cell assembly measures the forces applied to an object along each of three orthogonal axes. It was developed for use with a remote manipulator that bends cryogenic ducts. Usually, the required bending forces are low, but occasionally a substantial force must be applied. The device is therefore designed to be rugged and to function over a wide range, having potential applications in automatic testing equipment, industrial robots, and force-measuring equipment.

Previously, load cells were located in and under the remote manipulator. The repeatability and accuracy of measurement were poor, because the forces sensed by the cells also included those caused by the friction and inertia of the manipulator. The problem became worse when smaller ducts, with smaller deflection forces, were used.

The device is placed between the manipulator and the duct or other object to sense the applied loads directly (see Figure 1). Load cells are mounted on the x, y, and z axes (see Figure 2). Linear ball bushings and an intermediate ring assembly separate the forces acting on the axes. A force in the x

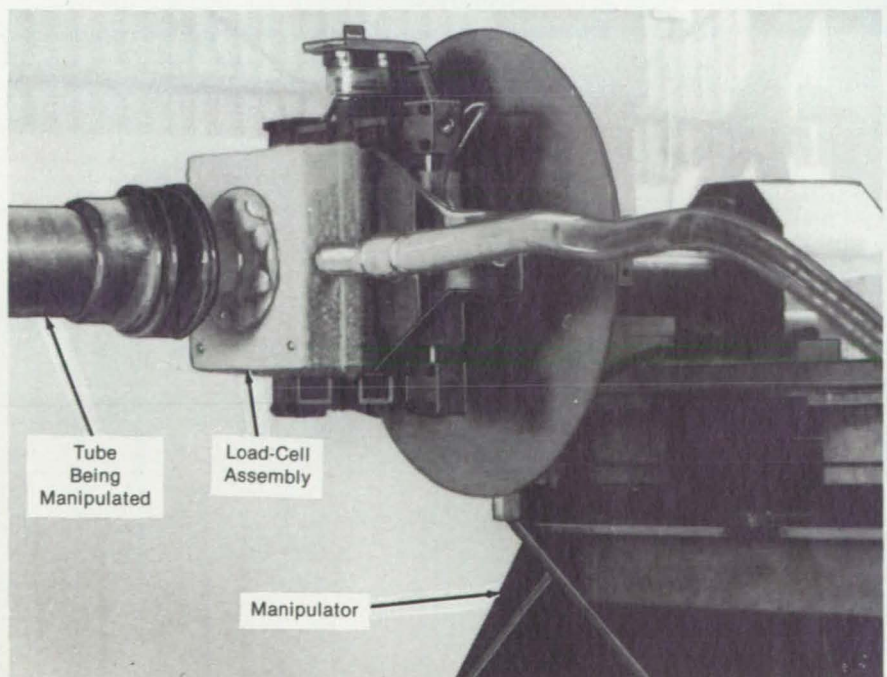


Figure 1. The Load-Cell Assembly is placed between a manipulator and the object being manipulated. The load cells thereby measure the forces on the object almost directly, without interference by intervening manipulator forces.

direction, for example, registers only on the x-axis load cell because its bushings, yoke, and intermediate ring assembly allow the cell to accept force only in that direction. Thus, the crosstalk between the three sensors is very low.

Although they are sensitive to low forces, the load cells can withstand much higher forces. Similarly, the ball bushings have low axial friction but can withstand high side loads without being damaged or introducing inaccuracy.

This work was done by Gene R. Rewerts of Ametek, Inc. for Johnson Space Center. No further documentation is available.

Inquiries concerning rights for the commercial use of this invention should be addressed to the Patent Counsel, Johnson Space Center [see page 29]. Refer to MSC-20875.

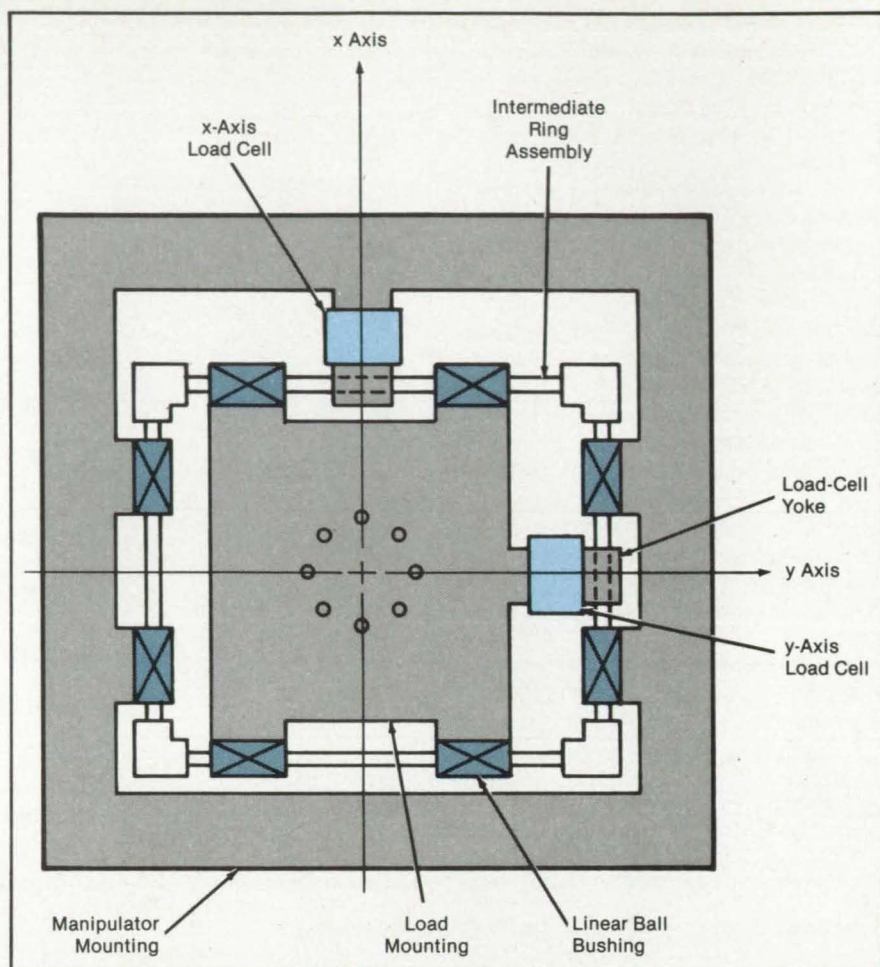


Figure 2. **Load Cells Are Mounted** on three mutually perpendicular axes. The x- and y-axis cells appear in this diagram; the z-axis cell extends out of the page. All cells are similarly equipped with linear ball bushings and intermediate ring assemblies, which isolate the axes from each other.

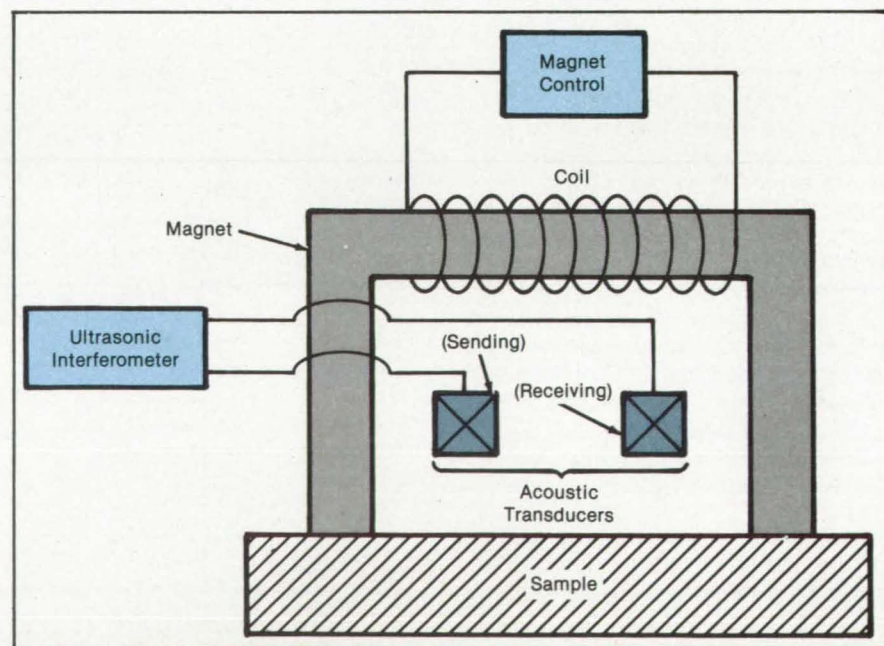
Acoustic/Magnetic Stress Sensor

This high-resolution sensor is fast, portable, and does not require permanent bonding to the structure.

*Langley Research Center,
Hampton, Virginia*

A high-resolution acoustic/magnetic stress sensor measures nondestructively the type (compressive or tensile) and magnitude of stresses and the stress gradients present in a class of materials. The sensor (see figure) includes a precise high-resolution acoustic interferometer, a sending acoustic transducer, a receiving acoustic transducer, an electromagnet coil and core, a power supply, and a magnetic-field-measuring device such as a Hall probe.

The device is portable, fast, nondestructive, and does not require permanent bonding to a structure. The technique requires small magnetic fields and thus fits many applications where magnetization is difficult. Because the sensor functions very well with magnetic steel



The **Acoustic/Magnetic Stress Sensor** measures stress in the sample via the interactions among the magnetic and stress fields and the speed of sound.

solids, it promises to be very useful for alloys.

The sensor uses low magnetic field effects that alter magnetic domains in a way that interrogates local stress fields. The measurement depends on the shift in acoustic velocity that accompanies the change in magnetization. Since stress also changes the magnetic-domain structure, the acoustic measurement senses

the presence of stress through the cycling of the magnetic field. Only low magnetic fields can sense the effect on magnetization without compromising effects from the domain-wall rotation that occurs at high fields.

This type of measurement is especially important for construction and applications where steel is widely used. The sensor may be useful especially for

the nondestructive evaluation of stress in steel members because of its portability, rapid testing, and nonpermanent installation.

This work was done by Joseph S. Heyman of Langley Research Center and Min Namkung of the College of William and Mary. For further information, Circle 96 on the TSP Request Card. Card. LAR-13320

Matching Vibration Testing to "Real-World" Conditions

Vibration spectrum of test machine is adjusted to that observed in operation.

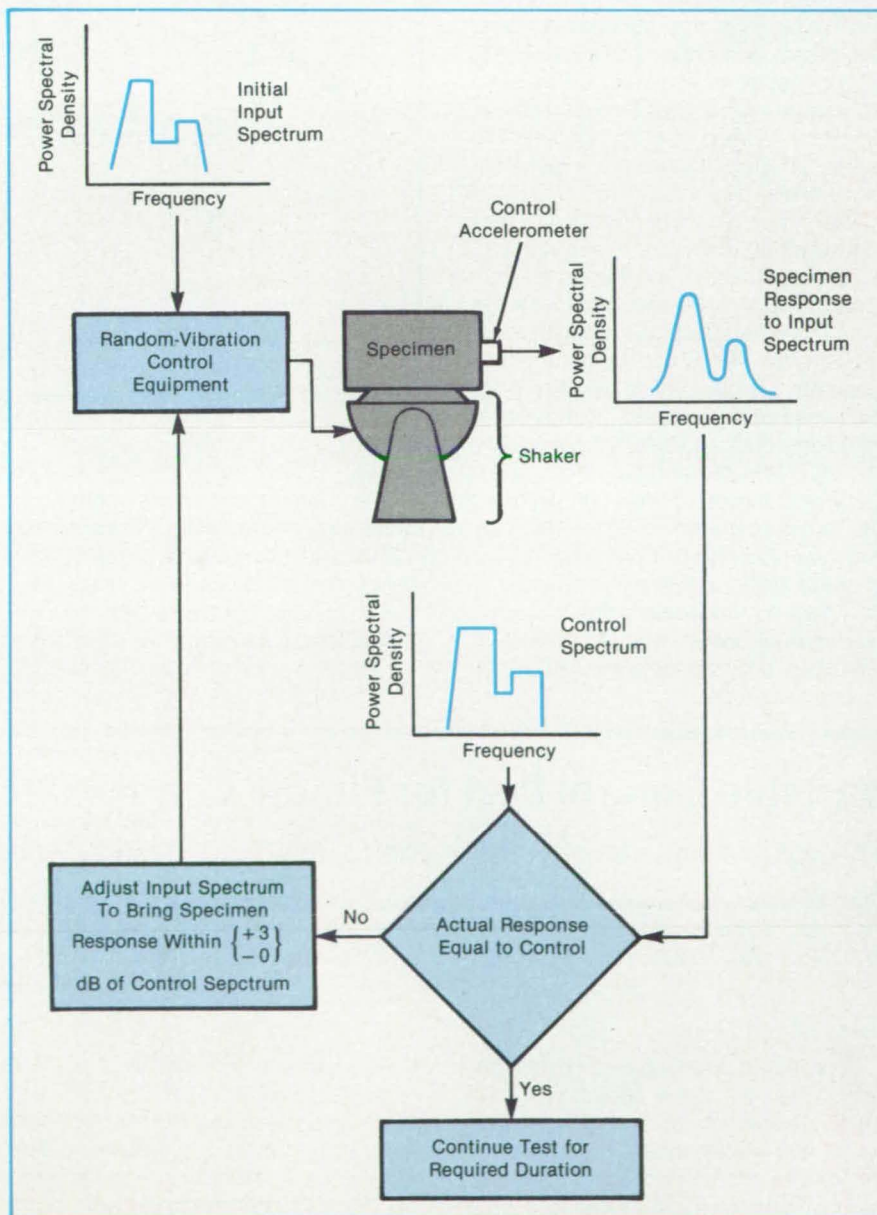
Lyndon B. Johnson Space Center, Houston, Texas

A method for vibration testing uses feedback to ensure that a test specimen is exposed to the same vibration spectrum that it would experience in service. In a conventional vibration test, the specimen and its mounting fixture are subjected to a preset excitation spectrum. This spectrum may not cause the correct vibrational response of the specimen because the support fixture may amplify, attenuate, or otherwise alter the vibrational response.

First, the vibrational response of the specimen to random excitation is measured in service. From the in-service spectral response, an arbitrary worst-case spectral response (maximum amplitude as a function of frequency) is constructed from these measurements and is called the "control" spectrum. An estimate is also made of the input spectral setting that ought to cause the shaker table to produce a specimen spectral response like that of the in-service tests.

A test specimen is placed in a test fixture and attached to a shaker (see figure). The shaker is initially operated at one-quarter the full level of the input spectrum to prevent overloading. A short vibration test is run, and the specimen response is compared to the control spectrum. The input spectrum is then adjusted until the response resembles the control spectrum.

This work was done by Albert D. Olsen, Jr., of Beech Aircraft Corp. and Albert V. Keblaitis of Rockwell International Corp. for Johnson Space Center. For further information, Circle 58 on the TSP Request Card. MSC-20665



In an Iterative Procedure, the vibrational response of a test specimen is matched to the previously-determined worst-case in-service response. An accelerometer on the test specimen provides feedback.

Stress Measurement by Geometrical Optics

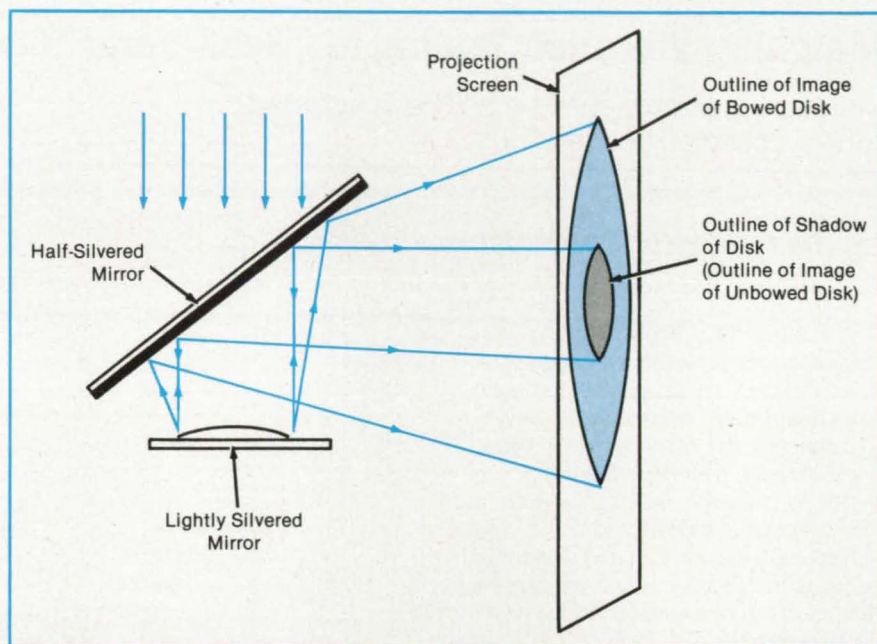
A fast, simple technique measures stresses in thin films.

Lewis Research Center, Cleveland, Ohio

A new, quick, and accurate method employing geometrical optics has been developed to measure stress in thin films. The stress in a thin film on a bulk substrate is an important factor relating to the film's adhesion and behavior under temperature variation. If the stress in the film becomes large enough, it will exceed the adhesion of the film/substrate interface, and the film will fail.

Present stress-measuring techniques, such as Newton rings, surface analyzers, and others, are rather complicated and time consuming, requiring up to 30 to 40 minutes for a typical measurement. The new method applying geometrical optics reduces it to a minute or less without sacrificing accuracy.

When a thin film is deposited on a very thin substrate, such as a common microscope cover slide, it will deform the substrate because of the stress buildup in the film. From the radius of the curvature of the film, the stress can be determined. Geometrical optics are applied to project the image of the stressed film by a laser light beam onto a screen (see figure). The measurement of the focal length of the "spherical mirror" closely approximates the radius of curvature of the thin film. Any magnification or contraction of the image of the film is indicative of the distortion of the substrate due to the film stress. Such magnification, whether greater or less than one, immediately determines the sign of stress.



The **Sample Disk Is Bowed** by stress into an approximately spherical shape. The reflected image of the disk is magnified by an amount related to the curvature and, therefore, to the stress.

The geometrical optics method for measuring stress in thin films is simple, quick, and accurate. The method requires a sample substrate, such as a cheap microscope cover slide, two mirrors, a laser light beam, and a screen.

This work was done by Raymond S. Robinson and Stephen M. Rossnagel of

Colorado State University for **Lewis Research Center**. Further information may be found in NASA CR-168172 [N84-18322/NSP], "Sputtering Phenomena in Ion Thrusters" [\$8.50]. A copy may be purchased [prepayment required] from the National Technical Information Service, Springfield, Virginia 22161. LEW-14169

Variable Control Port for Fluidic Control Device

The volume and velocity of the control flow can be independently adjustable.

NASA's Jet Propulsion Laboratory, Pasadena, California

A proposed throttling mechanism can adjust the size of the control port of a fluidic vortex flow-control device. This would allow independent adjustment of the volume and the velocity of the control flow — to match a wider range of supply and output requirements.

In a conventional fluidic vortex flow-control device (see top of figure), the con-

trol fluid strikes the supply fluid (the fluid to be controlled) at a right angle. The supply fluid enters the vortex chamber through the supply port. The control-fluid motion pushes the supply fluid into a vortex that circulates along the walls of the chamber. As the control flow is increased, the vortex is accelerated, delaying the exit of the combined fluids through the

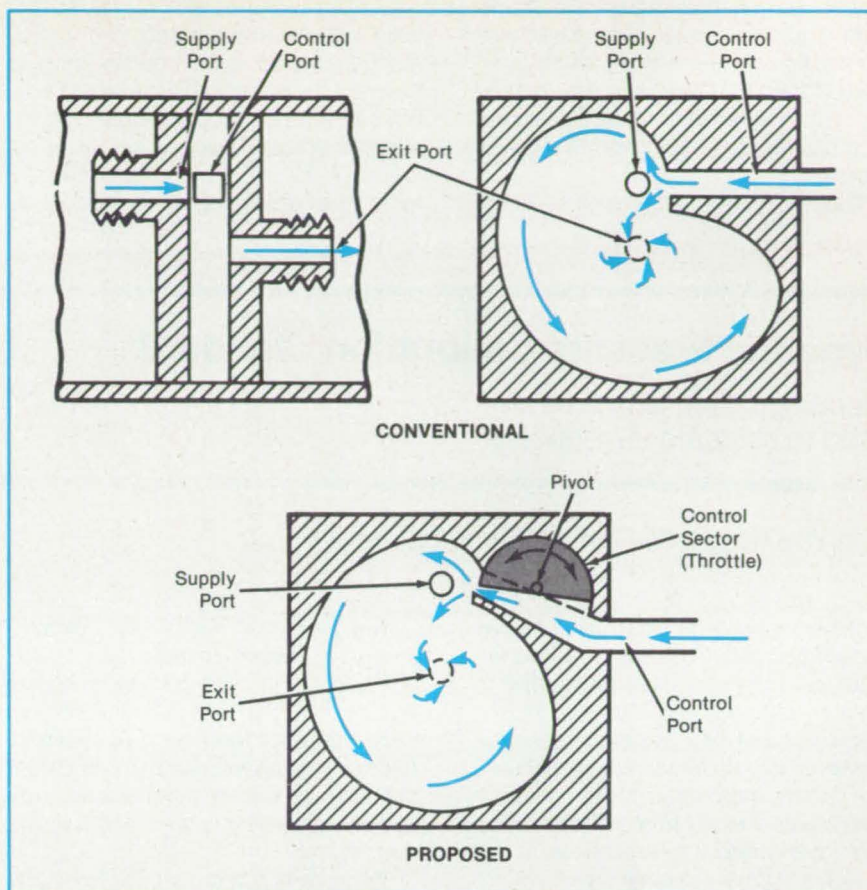
centrally-located exit port.

The volume and pressure of the control fluid entering the chamber are determined by the pumping pressure exerted against the control fluid and the hydraulic head losses of the control-flow tubing and the control port; the higher the control-fluid pressure, the greater the volume and velocity of the control-fluid jet striking

the supply-fluid stream. For a given control-fluid pressure, the head loss, and hence the control flow, depends on the cross-sectional area of the control port. In any one device, this area is fixed; if it does not fit a desired set of supply/output control conditions, the device must be replaced by another having a different ratio of supply- and control-port geometries. While in the laboratory, this device allows the output-flow rate to vary by up to a factor of 5; under field conditions, it is more common for this rate to vary by as little as a factor of 2.

In the proposed device (see bottom of figure), a rotatable D-shaped control sector could throttle down the control port or open it completely and could be set to any intermediate control-port cross-sectional area. Although this adjustment would affect the volume and control-port head loss, the volume and velocity could be controlled independently by also adjusting the fluid-supply pressure. This would allow adjustment to a wider range of control conditions and the ability to maximize control efficiency. Fluidic control theory suggests the possibility of improvement in the control ratio of at least 2:1 over conventional devices.

This work was done by Earl R. Collins, Jr., of Caltech for NASA's Jet Propulsion Laboratory. For further information, Circle 32 on the TSP Request Card. NPO-16603



A Fluidic Vortex Flow-Control Device of the conventional type (above) has a control port of fixed cross section. In the proposed device (below), the control port is equipped with a throttle to enable the independent adjustment of control-flow volume and velocity.

Measuring Water-Layer Thickness

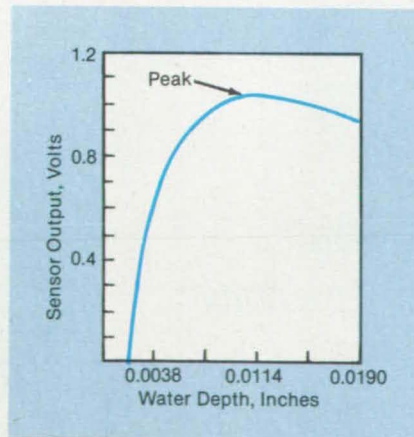
The technique uses an optical proximity detector.

Langley Research Center, Hampton, Virginia

The feasibility of determining the thickness of a water layer above a surface has been investigated by use of a commercially-available optical proximity detector. The detector is a noncontacting instrument, and it measures linear distance, displacement, or motion by means of light rays.

The detector consists of a sensing probe, a cartridge containing a photocell and light source, and an electronics package, housed in a metal carrying case. Light transmitted from the fiber-optic probe is reflected by the observed surface and transmitted back through the probe to a photoreceiver, the output of which is indicated on a digital voltmeter or other suitable instrument.

The sensor is specified to have high sensitivity [permitting measurements in millionths of an inch (several one-hundredths of a micrometer)], to have linear



The **Water-Depth Measurement** is limited to about 0.011 in. (0.28 mm), the region to the left of the peak, because of the equipment design.

ear output with distance over a significant operating range, and to possess a signifi-

cant frequency response. As the distance between the probe and the surface increases, there is a rapid increase in signal level until it reaches a peak. Beyond the peak, the output sensitivity changes sign, and the detector becomes less sensitive to changes in distance.

A test was performed to determine whether this sensor could be used in determining water-layer thickness. A 0.032-in. (0.81-mm) fiber-optic probe with random fiber configuration was sealed through the bottom of a plastic container. Water was added, and the output voltage versus water depth above the probe was plotted. It was found that reflection does occur, and the output voltage increases with the water level, reaches a peak, then begins to decrease.

Several problems arose. Zero water depth over the sensor was uncertain because of meniscus effects. It was also

found that output voltages increased with increasing light levels and with the presence of bubbles above the probe. Furthermore, the water-depth range (see figure) of about 0.011 in. (0.28 mm) was very limited.

Despite these shortcomings as an ac-

curate water-depth-measuring instrument, the sensor could possibly be used to detect the presence of bubbles or particles in a water stream or to trigger an alarm when condensing water becomes present in the bottom of a supposedly dry tank. Fiber-optic probes of sizes up to

0.285 in. (7.24 mm) with varying sensitivities and configurations are available for use with this system.

This work was done by Nettie Faulcon of Langley Research Center. For further information, Circle 99 on the TSP Request Card. LAR-13347

Dynamic Pressure Calibration Standard

Vibrating columns of fluid are used to calibrate transducers.

Langley Research Center, Hampton, Virginia

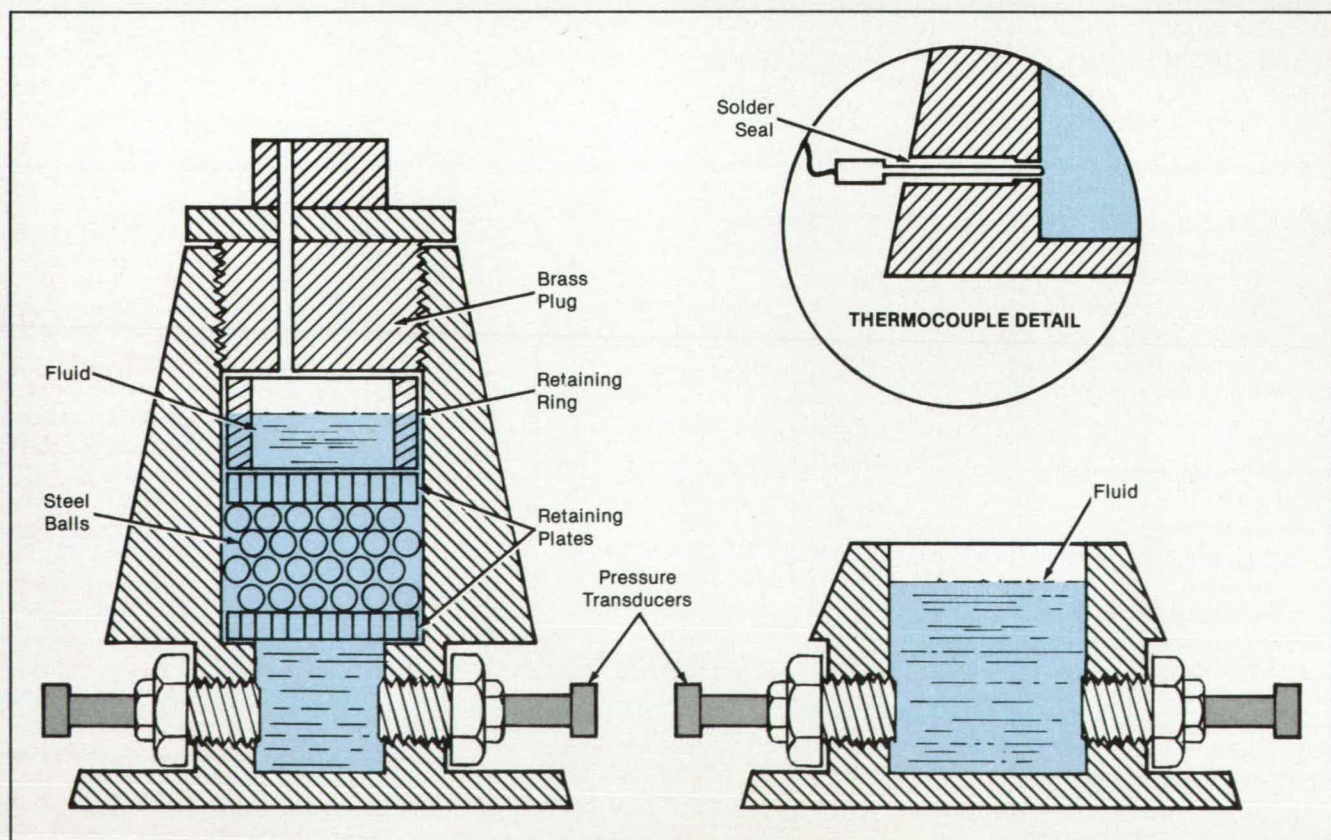
Advancements in wind-tunnel testing capabilities and needs for increased aircraft performance have given rise to greater accuracy requirements for the measurement of dynamic pressures. However, a recognized national standard for dynamically calibrating pressure transducers does not exist. In a step toward meeting this need, a dynamic pressure calibration standard has been developed for calibrating flush diaphragm-mounted pressure transducers. Pressures up to 20 kPa (3 psi) have been accurately generated over a frequency range of 50 to 1,800 Hz.

The system includes two conically shaped aluminum columns (see figure), one 5 cm (2 in.) high for low pressures and another 11 cm (4.3 in.) high for higher pressures, each filled with a viscous fluid. Each column is mounted on the armature of a vibration exciter, which imparts a sinusoidally varying acceleration to the fluid column.

Pressure transducers mounted at the bases of the columns sense the sinusoidally varying pressures. These pressures are determined from measurements of the density of the fluid, the height of the

fluid, and the accelerations of the columns. A section of the taller column is filled with steel balls to control the damping of the fluid to extend its useful frequency range. The short column has a sufficiently-high natural frequency so that no damping is required. The vibration armature and the standard are enclosed in a chamber that is thermally and acoustically insulated. The chamber is equipped with an air-conditioning unit for thermal control.

The data are recorded using two digital multimeters, a frequency counter, and a



Pressure Transducers are calibrated in this apparatus, which produces sinusoidally varying pressures at the bottoms of the fluid columns. Accurate calibrations are obtained up to 20 kPa.

desk-top computer. The computer records the data from the multimeters, displays the data in both graphic and tabular forms, and stores them on a disk. A bell-jar evacuation system is used to evacuate the fluid to remove entrapped gases, which cause cavitation and degradation in the viscosity and density of the fluid. Quartz piezoelectric pressure transducers are used because of their minimal diaphragm deflection due to pressure, their high natural frequency, and compatibility with the calibration fluid.

This standard has a total measurement uncertainty of ± 5.95 percent and an average repeatability of ± 2.5 percent

for pressures up to 5 kPa (0.75 psi) using the shorter column. From 5 kPa to 20 kPa (3 psi), the measurement error of the taller column increases to ± 10 percent and an average repeatability of ± 3.2 percent due to mechanical resonances and acceleration gradients within the column. The signal noise is low, and the waveform is highly dependent on the quality of the drive signal in the vibration exciter.

This work was done by Paul C. Schutte and Kenneth H. Cate of Langley Research Center and Steven D. Young of the West Virginia Institute of Technology. For further information, Circle 13 on the TSP Request Card.
LAR-13443

Books and Reports

These reports, studies, and handbooks are available from NASA as Technical Support Packages (TSP's) when a Request Card number is cited; otherwise they are available from the National Technical Information Service.

Mixer Analysis of Nacelle/Nozzle Flow

Flow over an idealized nozzle is computed.

The calculation of the flow field around an actual mixer nozzle is a formidable task. It is generally worthwhile to first consider an idealized version of such a problem before undertaking a calculation of the general case. A NASA/Contractor report describes an idealized analysis and computer program made for the mixer problem.

The analysis and computer program calculate the flow over an idealized mixer nozzle. The nozzle is idealized by unwrapping it so that the planform lies in the $z=0$ plane. Linearized compressible flow is used to calculate the flow and the mixer shape given the loading on the mixer.

The loading is chosen to satisfy the Kutta condition at the mixer trailing edge, and the loading in the vicinity of the trailing edge has a square-root-of- x behavior to give a smooth flow in this region.

A set of computer programs and sub-routines is given for calculating the flow field. The overall program is given the name PLANMIX, and sample calculations of the individual programs are given.

Work now remains on the interpretation of the results of the computer program. The end goal is to achieve the maximum amount of mixing downstream of the mixer while retaining a reasonable shape for the mixer. Because the analysis assumes linearized flow, calculation of the effects of deep lobe penetration cannot be made using this program.

This program was written by T.J. Barber and R. Amiet of United Technologies Corp. for Lewis Research Center. For further information, Circle 95 on the TSP Request Card.
LEW-14073

EMPLOYEES APPRECIATE THE PAYROLL SAVINGS PLAN. JUST ASK THE PEOPLE AT GEORGIA-PACIFIC.

"Besides being a good investment in my country, Bonds help me save for my two daughters."

—Craig Heimbigner

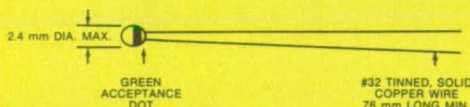


U.S. Savings Bonds now offer higher, variable interest rates and a guaranteed return. Your employees will appreciate that. They'll also appreciate your giving them the easiest, surest way to save.

For more information, write to: Steven R. Mead, Executive Director, U.S. Savings Bonds Division, Department of the Treasury, Washington, DC 20226.

U.S. SAVINGS BONDS
Paying Better Than Ever

A public service of this publication.



YSI Space-Qualified Thermistors

...with performance and traceability documentation

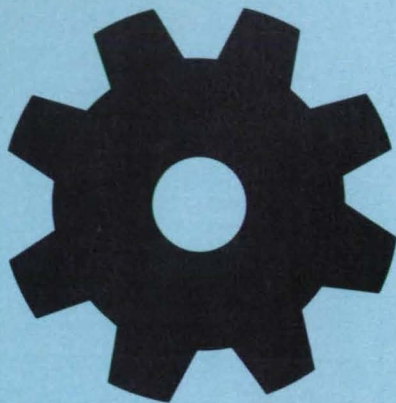
YSI 44900 Series Precision Thermistors, with interchangeability to $\pm 0.1^\circ\text{C}$, meet the requirements of GSFC S-311-P-18 for precise temperature compensation, measurement and control during extended space flight. NASA-monitored procedures for qualification testing and acceptance screening make YSI 44900 Series Thermistors ideal for a wide range of critical scientific and high-reliability industrial applications.

from Yellow Springs



Industrial Division
Yellow Springs Instrument Co., Inc.
Yellow Springs, Ohio 45387 USA • Phone 513 767-7241

Machinery



Hardware, Techniques, and Processes

- 118 Device for Extracting Flavors and Fragrances
- 119 Multipurpose Scribing and Drawing Tool
- 120 Variable-Force Eddy-Current Damper
- 127 Improved Seal for NTF Fan Shaft
- 128 Gentle End Effector for Robots
- 129 Automated Conduit Unloading
- 130 Oil-Free Compressor
- 131 Pressure-Letdown Machine for a Coal Reactor
- 132 Helicopter Tail-Boom Strakes
- 134 Air-Bearing Table for Machine Shops
- 134 Electromechanical Turboprop-Pitch-Control Mechanism

Books & Reports

- 137 Operating a Remote Manipulator in Simulated Low Gravity

Computer Programs

- 102 Aircraft Takeoff and Landing Analysis
- 102 Nonconical Relaxation for Supersonic Potential Flow
- 104 Analysis of Lubricant Jet Flow
- 104 Aerodynamic Characteristics of NACA 16-Series Airfoils
- 104 Wall Interference in Two-Dimensional Wind Tunnels
- 106 Predicting Vortex Shedding in Supersonic Flow
- 106 Predicting Wall Modifications for Adaptive Wind Tunnels
- 106 Two Programs for Supersonic Wing Design and Analysis
- 107 Second-Order-Potential Analysis and Optimization

Device for Extracting Flavors and Fragrances

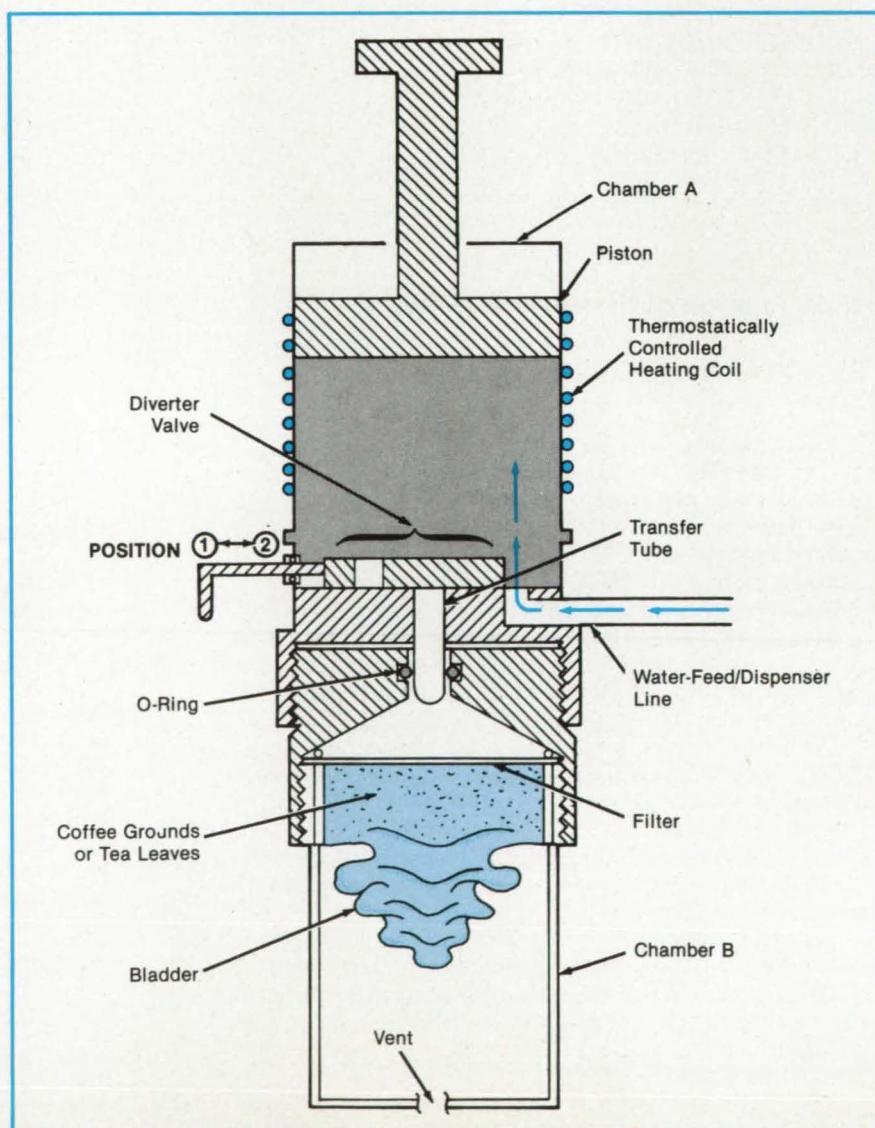
Pressurized extraction apparatus may have industrial uses.

Lyndon B. Johnson Space Center, Houston, Texas

A proposed machine for making coffee and tea in a weightless environment may prove even more valuable on Earth as a general extraction apparatus. The machine functions like a conventional coffeemaker during part of its operating cycle and includes additional features that enable operation not only in zero gravity but also extraction under pressure in the presence or absence of gravity.

Coffee- and teamaking is similar to other processes for extracting flavors

and fragrances from plants by means of cold or hot water, alcohol, or other solvents. Because the proposed system is enclosed, volatiles are contained: It is important to prevent the loss of volatile constituents since they are often important parts of flavors and fragrances. Also, because the system is enclosed, it can be pressurized for such processes as supercritical solvent extraction or pressurized fermentation. A bench-scale general pressurized-extraction apparatus would be useful in research and



The **Zero-Gravity Beverage Maker** uses a piston instead of gravity to move the hot water and beverage from one chamber to the other and to dispense the beverage.

development.

The figure shows the machine during the first part of the beverage-making cycle. The stages of the cycle are as follows:

1. With the diverter valve in position 1, water is fed into chamber A, forcing the piston up until it reaches the limit of its travel or until the desired amount of water has been fed in.
2. The thermostatically controlled heater is turned on, raising the temperature of the water to about 100° C.
3. The diverter valve is moved to position 2. The piston is pushed down, forcing the water through the transfer tube and the filter into the coffee grounds or tea leaves. The liquid/solid mixture is contained in a bladder in chamber B.
4. The piston is pulled up to suck the coffee or tea liquid into chamber A. The filter retains the grounds or leaves in chamber B.
5. Once the coffee or tea liquid is in chamber A, the diverter valve is returned to position 1. The water-feed/dispenser line is disconnected from

the water supply and connected to a cup or other beverage container. The beverage is dispensed by pushing on the piston.

6. The beverage is kept warm in chamber A by the thermostatic heater.

This work was done by Franklin R. Chang of **Johnson Space Center**. No further documentation is available.

Inquiries concerning rights for the commercial use of this invention should be addressed to the Patent Counsel, Johnson Space Center [see page 29]. Refer to MSC-20761.

Multipurpose Scribing and Drawing Tool

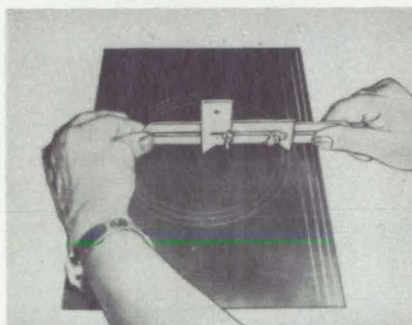
A two-part tool can be reconfigured for a variety of jobs.

Lyndon B. Johnson Space Center, Houston, Texas

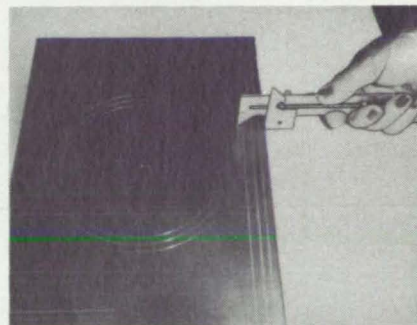
A multipurpose tool speeds up the laying out of patterns on sheet metal, wood, plastic, or paper. The tool can be carried in a pocket, then quickly assembled for service as a height gauge, pair of dividers, protractor, surface gauge, or square (see figure). For example, the tool can be used to scribe several parallel lines for rivet holes on a long sheet of metal, then reassembled as a pair of dividers to mark the other axes of the rivet holes. The tool can be used as a scribe or with a pencil, depending on the material to be marked.

The tool consists of two elongated, flat, slotted parts with winglike protuberances that serve as cutters, pencil holders, and supports. The parts are held together by a pair of screws and wingnuts in various configurations, depending on the function required of the tool. The user can thus easily and quickly change the configuration.

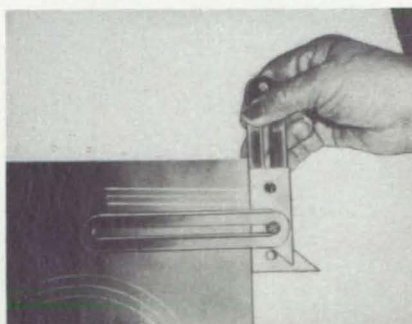
This work was done by James M. Ellis of **Johnson Space Center**. For further information, Circle 65 on the TSP Request Card. MSC-20913



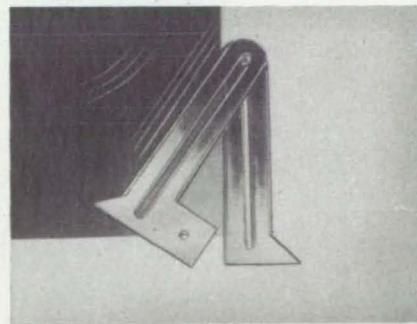
DIVIDERS



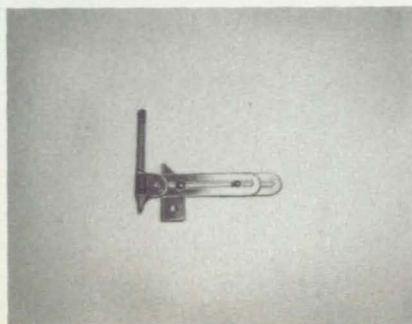
HEIGHT GAUGE



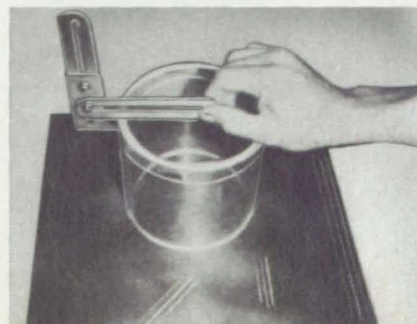
SQUARE



PROTRACTOR



WITH PENCIL



SURFACE GAUGE

This **Tool Performs Several Functions** useful in layout. Lines, curves, and angles are made visible as either bright scribe marks or as dark pencil (or ink) marks.

Variable-Force Eddy-Current Damper

Variable damping is achieved without the problems of containing viscous fluids.

Lewis Research Center, Cleveland, Ohio

An eddy-current damper has been conceived and tested that provides the capability of varying, either manually or automatically, the stiffness and damping characteristics of a rotor or shaft-support system without having to bring the rotor to rest. This variable damping force and stiffness can also be provided without the need for viscous fluids. Fluid-film dampers, which employ a viscous fluid film between relatively moving parts, are used in a number of contemporary turbomachines. Examples would be turbojet aircraft engines, radial and axial compressors, and oxygen expanders (high-speed gas liquefiers), to name just a few. Vibrational energy induced in the rotor and transmitted to the bearing supports is dissipated as heat in shearing the viscous fluid.

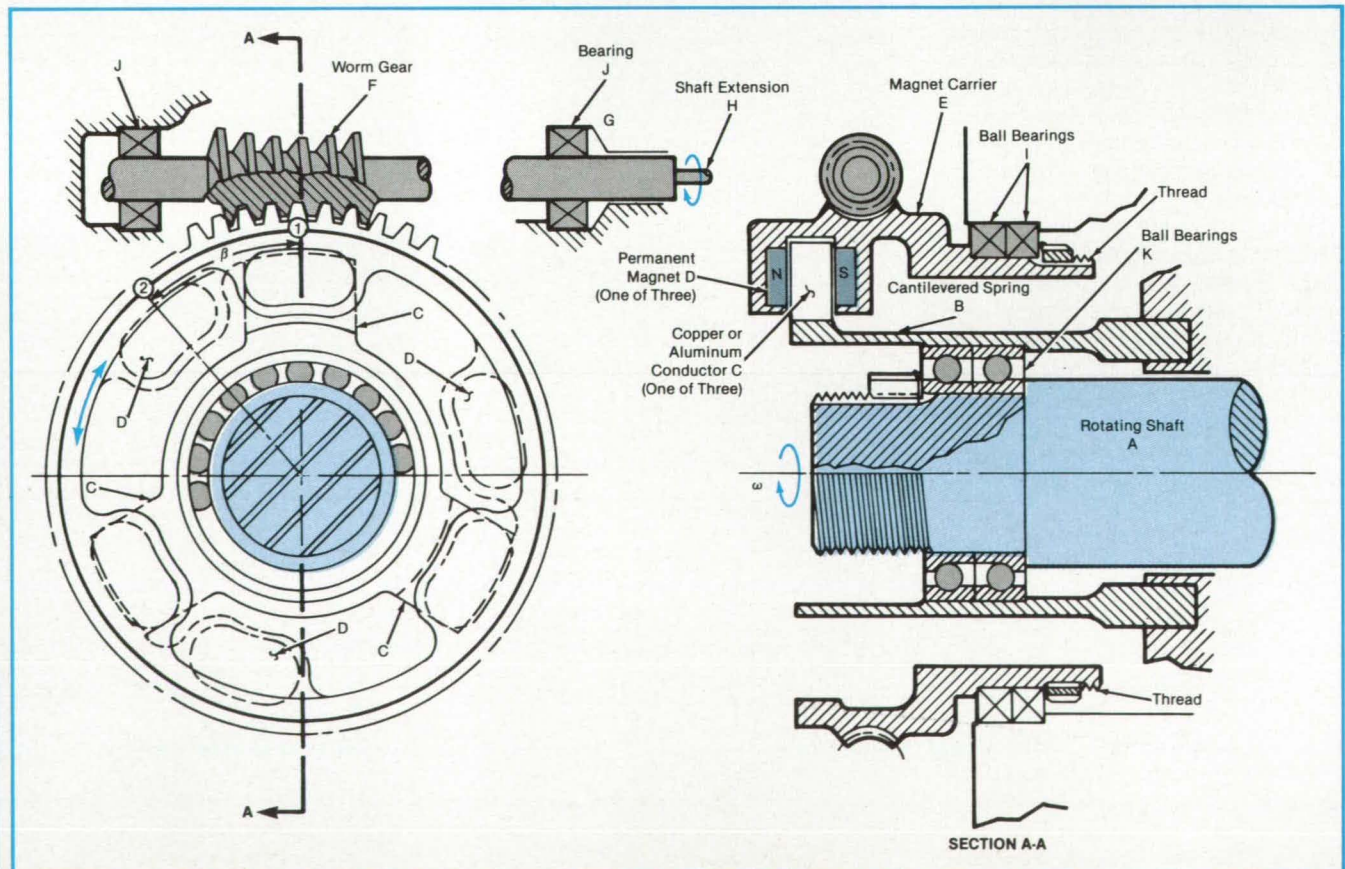
The so-called "squeeze-film" damper

dissipates the energy by pumping a viscous fluid in and out of a narrow annulus. In these types of dampers, the amount of damping and stiffness is determined by the original design and calculated amplitudes of vibration that are expected to be encountered. Should actual operating conditions differ from those anticipated, there is normally no method provided for altering the damper characteristics, once the damper has been installed. Also, for this damper to be effective, it must be supplied with relatively large quantities of a viscous fluid. This means, in most cases, that these dampers are required to be located very close to a bearing where lubricating oils are available in large quantities.

An eddy-current damper, not requiring lubricating oils, is free to be positioned at other locations in the machine. In fluid

viscous-shear dampers, the magnitudes of damping and stiffness are functions of fluid viscosity, clearances between relatively moving surfaces, and temperature. Without a means of external adjustments or control, too much stiffness and damping for any given set of vibrational frequency and amplitude can result.

The variable-force eddy-current damper operates as depicted in the figure. One end of a rotating shaft, A, turns in ball bearings K. The outer races of the ball bearings are fixed from rotating in a cantilevered type of spring, B, which is fixed in the machine frame. When shaft A is caused to vibrate with a measurable amplitude, as is produced by rotating unbalance forces, it causes the cantilever spring mount to precess in an orbital motion, and predominantly in a plane perpendicular to the rotor axis. An electrically



Eddy-Current Damping is obtained by moving copper or aluminum conductors through magnetic fields. The position of the magnet carrier determines the amount of field engagement and, therefore, the amount of damping.

Multiple Pages Intentionally Left
Blank

conducting material, such as copper or aluminum C, is firmly attached to spring B, at three equally spaced positions around the shaft A. These are more clearly seen in the side elevation.

The conductors are so located axially that they fit into the opening or gap of the U-shaped magnet carrier E. Permanent magnets D are attached to the carrier E at the three positions coinciding with the conductors C. These permanent magnets could just as well be electromagnets. The magnetic flux field in the gap between the two facing magnets (north and south poles) is repeatedly interrupted, or cut, by the vibrating conductors. In so doing, an electromotive force is induced, some of which opposes the motion that produced it.

This damping coefficient varies with the volume of conductor material that is moving more or less perpendicularly to the magnetic lines of force in the gap between the magnets. The magnet carrier E

is provided with gear teeth around its periphery, and these teeth mesh with the teeth of a worm gear, F. A shaft extension, H, connected to the worm gear F, can be made to rotate in bearing J, either manually, by servomotor, or stepping motor, all of which can be located remotely from the damper. Turning shaft H will cause the magnet carrier E to rotate through an angle from position 1 to position 2. The magnet E is located in ball bearings I.

At position 1, all of the conductor material C lies within the magnetic flux field emanating from magnet D, and therefore a maximum amount of damping and stiffness is realized. At position 2, none of the conductor material is within the magnetic field; and in this case, the stiffness and damping available will be zero. The amount of damping and stiffness then is continuously variable from positions 1 through 2.

The three advantages of this concept are as follows: (1) Magnitudes of stiffness

and damping can be continuously varied from a maximum to zero without bringing the rotor or shaft to a stop; (2) a damper of this type can be used in rotating machines not having viscous fluids available, such as lubricating oils; and (3) a damper of this type can produce sizable damping forces in machines that pump liquid hydrogen at -246°C and liquid oxygen at -183°C and can be compact in size.

This work was done by Robert E. Cunningham of **Lewis Research Center**. Further information may be found in "Preliminary Results on Passive Eddy Current Damper Technology for SSME Turbomachinery." To obtain a copy, Circle 82 on the TSP Request Card.

Inquiries concerning rights for the commercial use of this invention should be addressed to the Patent Council, Lewis Research Center [see page 29]. Refer to LEW-13717.

Improved Seal for NTF Fan Shaft

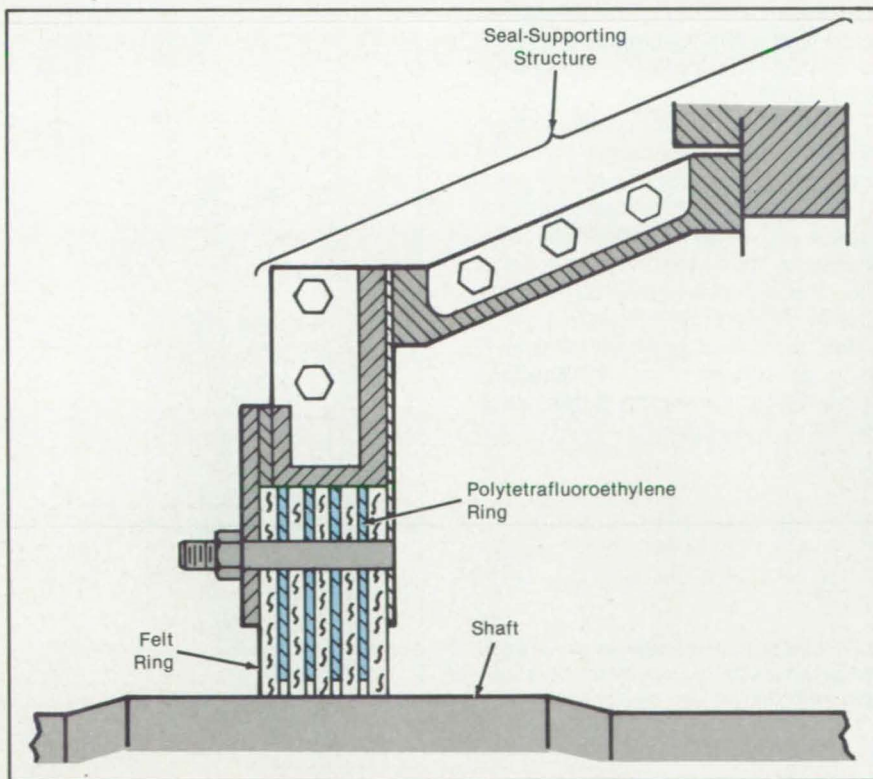
The new seal is more effective and lasts longer.

Langley Research Center, Hampton, Virginia

The National Transonic Facility (NTF) main-drive fan hub and part of the drive shaft are housed in the upstream nacelle, which provides both structural support and an aerodynamic fairing for the assembly. Inside the nacelle, nitrogen-gas flow is restricted by a seal around the fan shaft at the upstream nacelle bulkhead. Operational temperatures from $+150^{\circ}$ to -320°F ($+66^{\circ}$ to -196°C), absolute pressures from 8 psi to 130 psi (55 kN/m^2 to 900 kN/m^2), and a pressure differential of 2 psi (14 kN/m^2) combined with severe bulkhead thermal distortions result in a very serious design problem. The problem is compounded by the 600-r/min shaft speed. A conventionally designed seal using glass fibers and polytetrafluoroethylene proved to have an operating life of only a few hours.

An analysis of the seal failure revealed two causes. The first, bulkhead thermal distortion, was alleviated by relocating the seal to another part of the shaft. The second cause was shaft surface speed; the 48.5-in. (123.2-cm)-diameter shaft turning at 600 r/min has a surface speed of 7,600 ft/min (38.7 m/s), which is much too high for most materials.

To improve the seal efficiency, a high-density wool felt treated with a fire retardant was incorporated into the final design.



The **Seal** consists of five felt rings interspersed with four polytetrafluoroethylene rings having an inner diameter slightly larger than that of the shaft. The spaces between the polytetrafluoroethylene rings and the shaft produce a labyrinth effect, which increases the degree of sealing.

The commercially purchased felt sheets 1/4 in. (6 mm) thick were cut into 90° segments, four segments to a ring. Polytetrafluoroethylene spacers were cut in a similar manner from sheets 1/8 in. (3 mm) thick. The seal (see figure) is made up of five felt rings, separated by four polytetrafluoroethylene rings held in place by an

aluminum structure. The seal runs on a 9-percent-Ni steel shaft treated with a MoS₂ surface-bonded lubricant. Since the polytetrafluoroethylene rings are slightly larger than the shaft, a small cavity is formed on either side of the felt rings, providing the labyrinth effect, which improves the seal efficiency.

This work was done by E. A. Crossley, Jr., Jeffrey A. Jones, Roger Messier, and G. Warren Johnson of Langley Research Center and Keith Felton of North Carolina State University. To obtain a set of nine construction drawings, Circle 97 on the TSP Request Card. LAR-13218

Gentle End Effector for Robots

A gripper handles electronic components without damaging them.

*Marshall Space Flight Center,
Alabama*

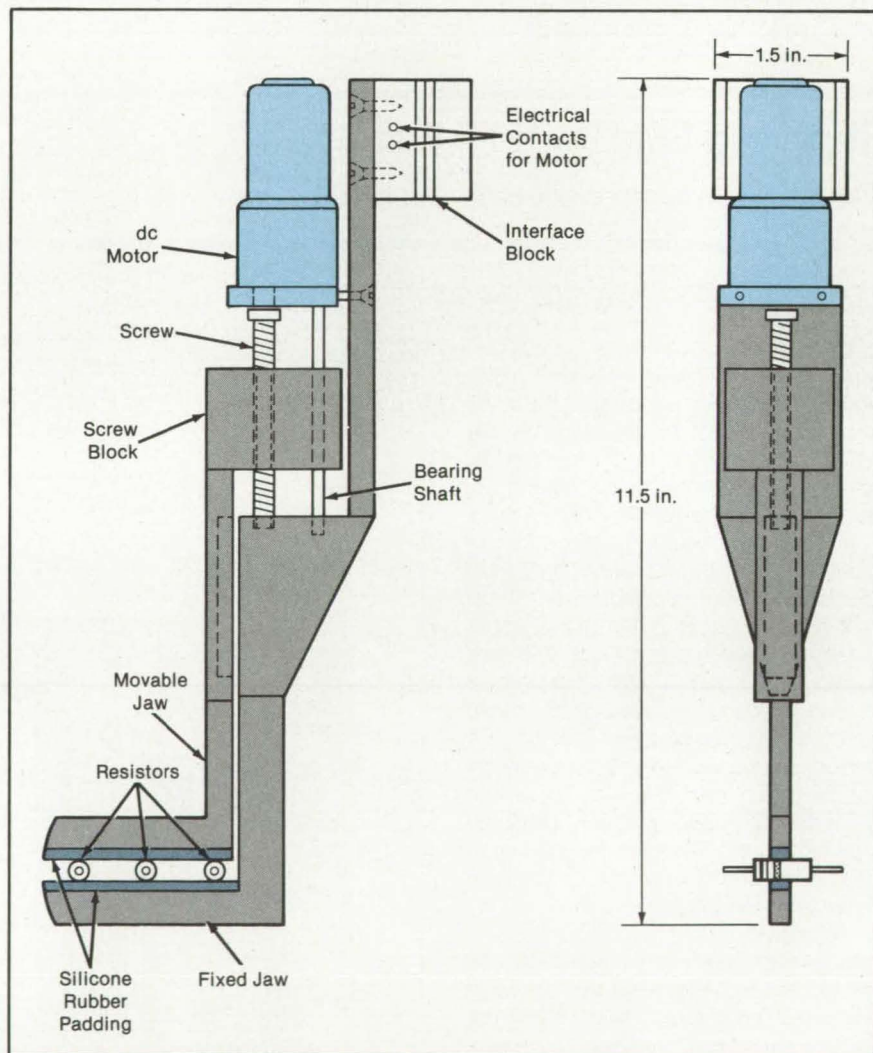
An end effector for a robot handles delicate small parts firmly but gently. It grips such electronic components as resistors, capacitors, and transistors without damaging them and holds them during soldering or other processing.

Designed for use with a Puma (or equivalent) robot arm, the end effector is driven by a dc motor instead of the usual pneumatic drive. The motor is mounted on the fixed jaw of the effector and drives the movable jaw through a screw block (see figure).

The end effector grips components between the fixed and movable jaws. The jaws are made of steel, and their gripping surfaces are lined with silicone rubber to cushion and therefore further reduce the chance of damaging the components. The jaws withstand soldering temperatures in excess of 500°F (260°C).

This work was done by Winston S. Webb of Honeywell Inc., for Marshall Space Flight Center. No further documentation is available. MFS-28119

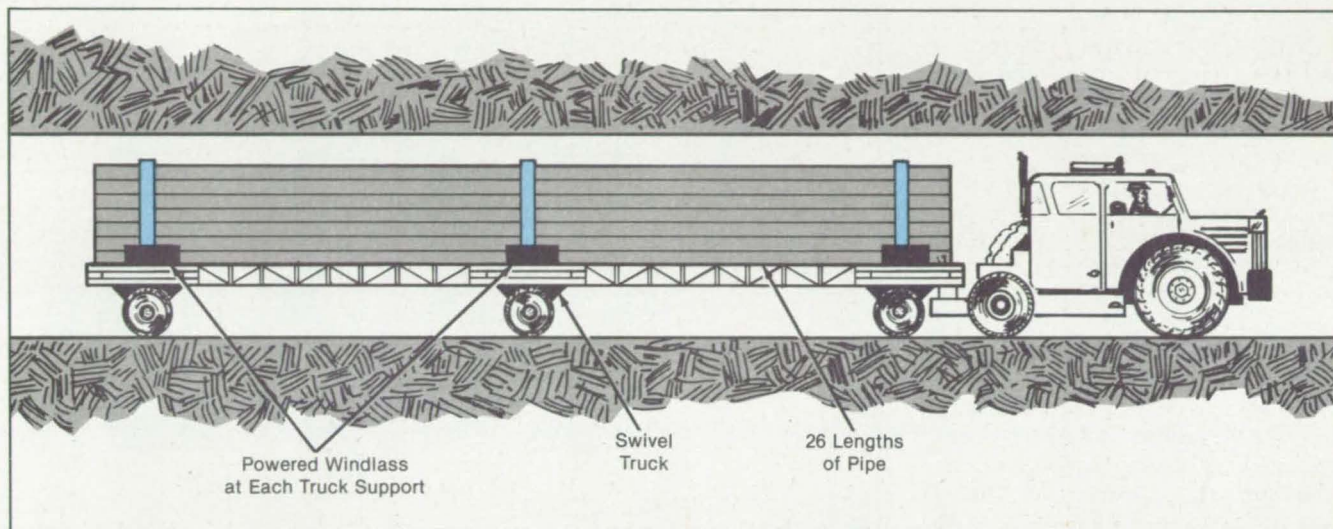
Driven by a dc motor, a **Movable Jaw** gently clamps an electronic component—in this case resistors, viewed along the axis.



Automated Conduit Unloading

Large, cumbersome pipes would be removed from a trailer by one operator.

NASA's Jet Propulsion Laboratory, Pasadena, California



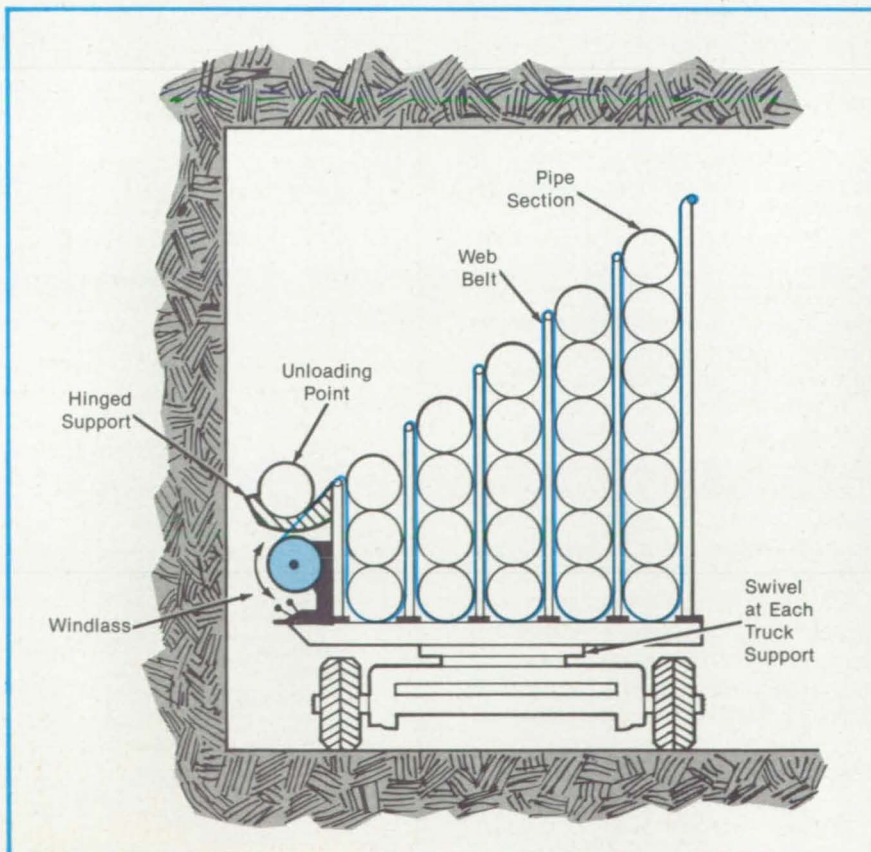
A proposed transporting and unloading apparatus would make it possible for one worker to position and connect pipe and duct sections for the hydrojet-jaw coal-mining system [see "Automated Coal-Mining System (NPO-16177) on page 128 of *NASA Tech Briefs* Vol. 9, No. 2.] The apparatus consists of a flatbed trailer equipped with vertical storage bins and three powered windlasses connected to web-belt hoists. The trailer (see figure) would carry 26 lengths of pipe or duct, each 20 feet (6.1 meters) long.

Pipe 1 moves by gravity to the unloading position, where it is held by the hinged support until it is removed for use. Thereafter, the web belt elevates pipes 2 through 26, one after the other, to a point at which they can fall by gravity into the support and fork. The movement of the pipe sections is thus achieved by continued tensioning of the belt. A clamp at the top of the partition at the left of each bin prevents the tension from acting on a pile of sections until the preceding bin has been emptied.

The same windlass and web-belt system can be used for loading the trailer. Simple adjustments in the bin-partition and web-belt positions are all that is needed to adapt the system to different conduit cross sections.

This work was done by Edward V. Lewis of Caltech for NASA's Jet Propulsion Laboratory. For further information, Circle 83 on the TSP Request Card. NPO-16187

This **Swivel-Truck Trailer** carries conduit and unloads it. Vertical bins are interconnected by web belts that elevate conduit sections for delivery by gravity to the unloading point. The trailer here is loaded with slurry-pipe sections 6 inches (15.2 centimeters) in diameter, but the bin width can readily be changed to hold other sizes.



Oil-Free Compressor

Compressor pistons moved by an eccentric shaft need no lubricants.

Lyndon B. Johnson Space Center, Houston, Texas

Originally proposed for use in space, a new compressor for refrigerators or freezers does not depend on a pool of oil for lubricating its pistons. It can thus be operated in any orientation.

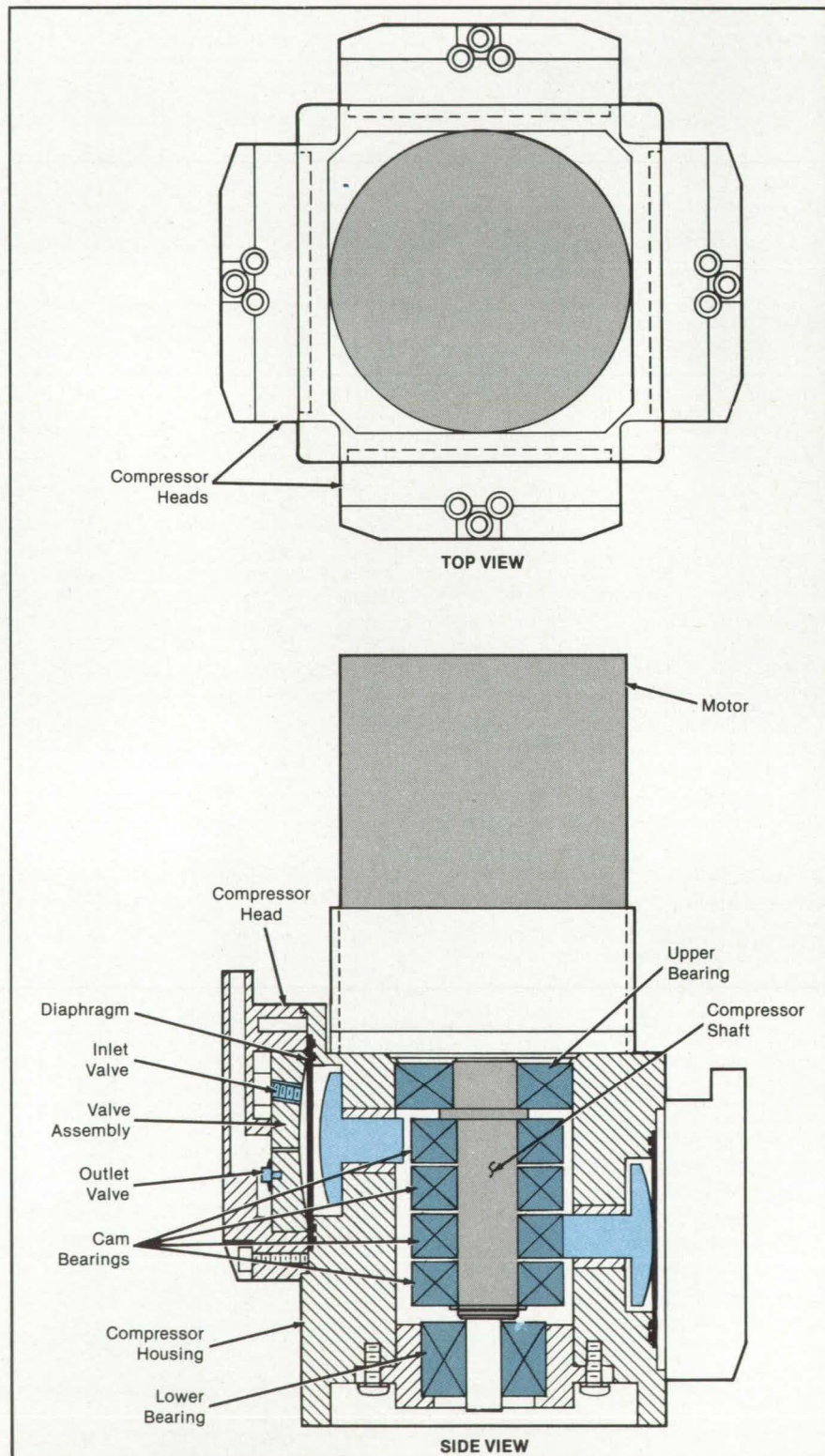
The compressor has a shaft, the middle section of which is eccentric in relation to the end sections (see figure). Driven by a brushless dc motor, the shaft turns the inner races of a set of four cam bearings. The outer cam-bearing races in turn actuate four pistons spaced equally apart, around and along the shaft. Each outer bearing race is held in position by the pressure exerted on it by the piston. Because there is no frictional motion between the piston and the outer bearing race, lubricant between them is unnecessary. The cam bearings themselves contain a potted internal lubricant.

The movement of the outer races of the cam bearings moves the pistons radially in and out. When the piston moves out, its domed head pushes a diaphragm into a dome-shaped chamber, thereby compressing the refrigerant in the chamber. Further rotation of the eccentric shaft removes the outward force on the piston. The pressure of the refrigerant on the diaphragm then pushes the piston radially back to its starting position.

Each dome-shaped compression chamber contains a one-way inlet valve and a one-way outlet valve. The inlet valve opens to admit refrigerant to the chamber as the piston moves away from the diaphragm and closes as compression begins. The outlet valve opens to release the compressed refrigerant and closes at the end of the compression stroke. Commercially available cylinder heads house the four valve assemblies; the four pistons are also commercial items.

The diaphragms are flat, round elastomer sheets. The elastomer is selected for chemical compatibility with the refrigerant. The compressor housing is machined from a solid piece of aluminum. It can be designed for two, three, or more than the four pistons illustrated, depending on the required system cooling capacity.

This work was done by D. G. Fitzjerrrell, T. L. Belver, and H. E. Moore of Management and Technical Services Co. (a subsidiary of General Electric Co.) for Johnson Space Center.



Four Pistons Are Actuated in sequence by the eccentric compressor shaft. Two of the pistons are shown in the cross section.

Pressure-Letdown Machine for a Coal Reactor

Pumps operating in reverse can generate power.

NASA's Jet Propulsion Laboratory, Pasadena, California

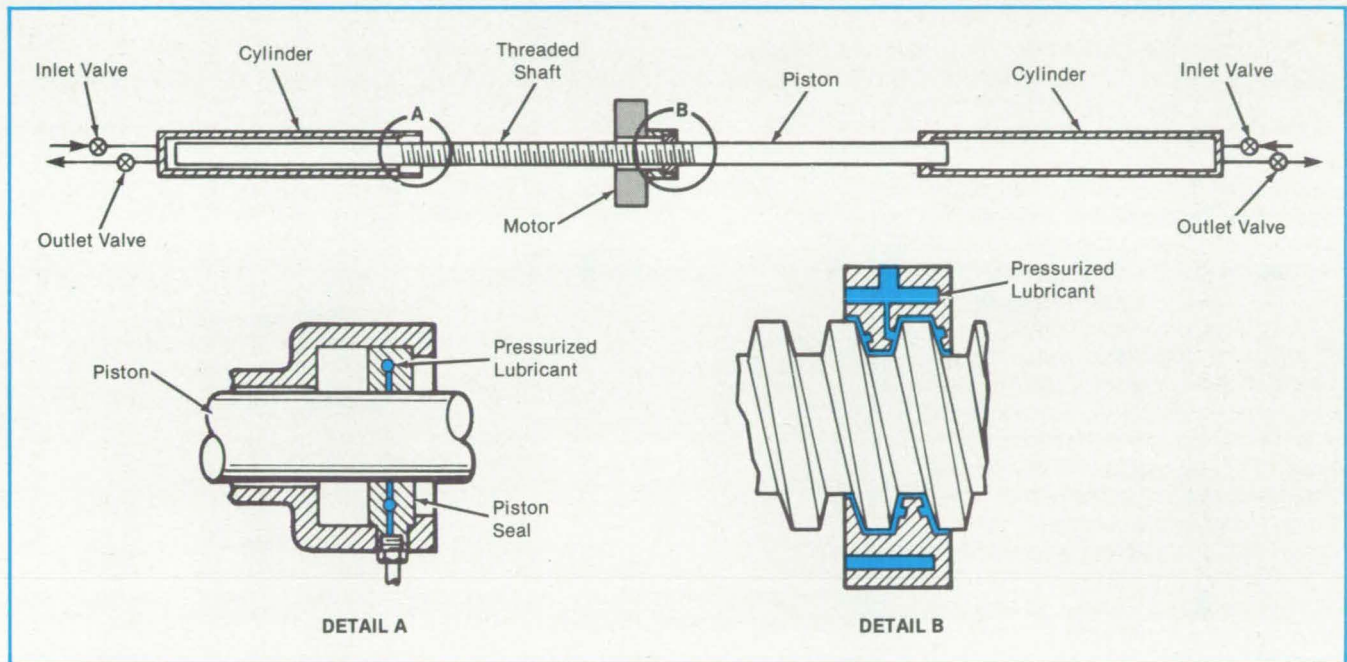


Figure 1. A **Mud Pump** resists abrasion by use of a pressurized lubricant to keep critical mating parts clean. The pump would be operated in reverse, using the expansion of the pressurized coal-liquefaction product to generate power.

A conceptual pressure-letdown machine for a coal-liquefaction system can extract energy from the expansion of the product fluid. Mud pumps, originally intended for use in oil drilling, would be operated in reverse so that their motors would act as generators. Several pumps could be operated in alternating phase to obtain multiple stages of letdown from the inlet pressure [typically 2,000 psi (14 MPa)] to the outlet pressure [typically 100 psi (0.7 MPa)]. About 75 percent of the work that generates the inlet pressure should be recoverable as electrical energy.

The mud pump (see Figure 1) includes two opposed cylinders with pistons on a slowly-reciprocating common shaft. A nut rides on the threaded middle portion of the shaft to couple the motor to the shaft, converting the rotational motor power to axial shaft power, or vice versa.

The piston seals and the threaded nut/shaft interface are lubricated by cleaned pressurized product fluid. As the fluid seeps out, it washes the pistons and

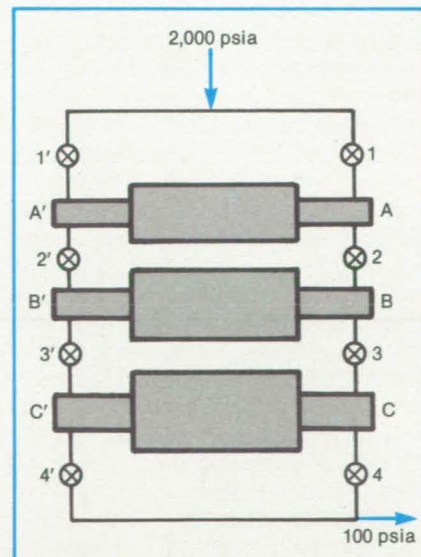


Figure 2. A **Triple-Expansion, Pressure-Letdown System** uses mud pumps and synchronized control valves. Each stage is larger than the preceding one to allow for expansion.

the threaded surfaces. This washing action makes the pump resistant to abrasion by oil-drilling mud and is expected to help it withstand abrasion by the coal-liquefaction product.

Figure 2 illustrates a triple-expansion scheme that uses three pumps, the motions of which are synchronized through valve controls. Valves 1 and 1' are connected to the high-pressure inlet. Valves 1 and 1' are controlled so that one is open while the other is closed, or vice versa, except during part of the expansion phase of each cycle. Valve sets 2 and 2' and 3 and 3' are similarly controlled. All valve openings and closings are made when the pressure differentials across the affected valves are near zero, and product expansion across the valves is minimized.

If the piston in cylinder A is at the right end, valves 2 and 1' are closed, while valves 1 and 2' are open. Pressurized fluid enters cylinder A, driving its piston toward the left. The piston in cylinder A'

pushes the fluid out of that cylinder, through valve 2, and into cylinder B'. When the piston has moved a prescribed distance, valve 1 closes, and the piston continues to move as gas is released from the high-pressure fluid.

When the piston reaches the left end of its stroke, valve 2' closes, and valves 1' and 2 open. Pressurized fluid then flows

through valve 1' into cylinder A', the shaft moves to the right, and piston A forces its fluid out through valve 2 into cylinder B.

The subsequent stages operate similarly, driven by the expanded fluid from the preceding stages. To accommodate the expansion, the cylinders of each stage are larger than those of the previous stage. The last stage is connected

through valves 4 and 4' to a single outlet pipe, so that the pipe is always receiving fluid at the third-stage pressure from one side or the other.

This work is done by Gerald S. Perkins and William B. Mabe of Caltech for **NASA's Jet Propulsion Laboratory**. For further information, Circle 84 on the TSP Request Card. NPO-15083

Helicopter Tail-Boom Strakes

Yaw control and overall efficiency are increased at hover and low speeds.

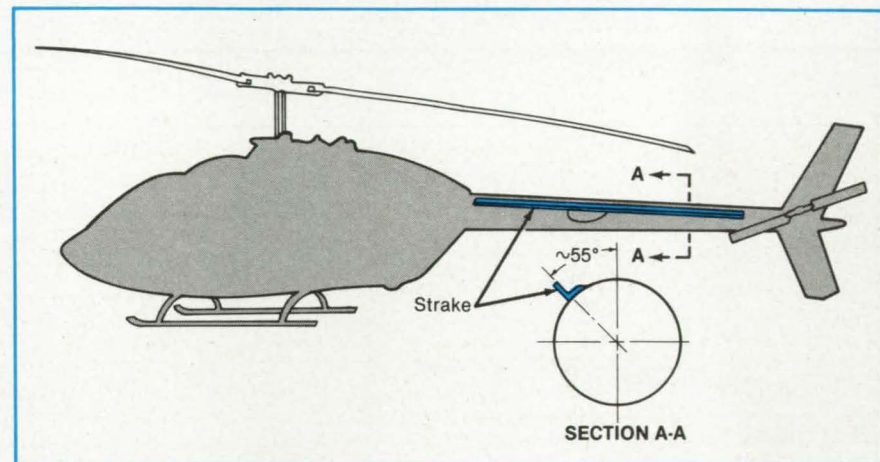
Langley Research Center, Hampton, Virginia

Wind-tunnel tests in the Langley Research Center 4- by 7-Meter Tunnel indicated that flow over the tail boom induced by the main rotor wake and by sideward and yawing flight can result in high side loads on helicopter tail booms. Also, the tunnel investigation showed that a strake located on the left side of the tail boom has the potential to reduce the high adverse side loads on a tail boom in hover and in sideward flight. A reduction in the adverse side loading on the boom, in turn, would result in a reduction in the tail-rotor thrust required for trim. Also, recent preliminary flight results obtained by the U.S. Navy Flight Test Center indicated that a strake located on the left side of the boom of a medium-size helicopter substantially increased the right sideward speeds obtainable.

The current work investigated the potential effectiveness of simple strakes on the tail boom of a lightweight Army helicopter in increasing the yaw-control pedal-position margin in right sideward flight and in reducing the effects of the tail-rotor vortex-ring state during left sideward flight. Several strake designs were evaluated in flight to determine the most effective design and to define potential benefits and problems. It was recognized that the effects of tail-boom forces and moments were likely to be only a part of the directional-control problem of the test helicopter.

The flight investigation was conducted at the Applied Technology Laboratory, Fort Eustis, Virginia. The figure shows the helicopter used in these tests with a strake installed. Onboard instrumentation measured the pedal position and angular yawing velocity, both of which were recorded on a tape recorder. A ground pace vehicle equipped with a calibrated fifth wheel provided an accurate measure of ground speed.

The aircraft speed was maintained through the use of a pace vehicle for



The Test Helicopter was equipped with a strake. Of the many straked installations tested, this one was the most effective.

speeds of 0 to 35 kn (0 to 18 m/s) in increments of 5 kn (2.6 m/s). Several azimuth angles were investigated with emphasis on left and right sideward flight. Aircraft and meteorological parameters were monitored closely to ensure data quality.

Test results demonstrated that the addition of a single long strake to the left side of the tail boom was the most effective configuration for reducing left pedal requirements in right sideward flight [5 to 6 percent of the total pedal range at 33 kn (17 m/s)]. Much larger reductions in pedal are expected on more heavily loaded helicopters and helicopters with tail-boom cross-sectional shapes that would yield larger side forces. Strakes on the boom did little to reduce the unsteady effects in the tail-rotor vortex-ring state and usually resulted in a minor shift in the velocity range over which it occurred [12 to 25 kn (6 to 13 m/s) left]. With strakes on or off, rapid and large changes in the static-directional stability (stable to unstable) in the vortex-ring state [left sideward flight 15 to 20 kn (8 to 10 m/s)] can occur and contribute to the control problems experienced in this flight regime.

Since a strake placed on one side of

the tail boom will also give rise to new forces for other flight conditions and will act as a lifting surface producing additional effects, the strake may be designed to be retractable when not in use to avoid any undesirable effects. Flight-test data obtained at Fort Eustis verified the trends observed in the Langley wind-tunnel tests.

For U.S.-built helicopters, the strakes would be mounted on the upper left side of the boom. For helicopters with rotors turning in the opposite direction, the strakes would be placed on the upper right side of the boom.

This work was done by Henry L. Kelley, Arthur E. Phelps III, and John C. Wilson of the U.S. Army Aerostructures Directorate located at the **Langley Research Center**. For further information, Circle 3 on the TSP Request Card.

This invention is owned by NASA, and a patent application has been filed. Inquiries concerning nonexclusive or exclusive license for its commercial development should be addressed to the Patent Counsel, Langley Research Center [see page 29]. Refer to LAR-13233.

This is not an ad for the world's finest helicopter. It is an opportunity for the world's finest engineers.

At Bell, our engineers have proven that a challenging and advanced work environment encourages the most creative engineering thinking.

It's that kind of thinking which has involved Bell in projects like the V-22 Osprey program (the soft mock-up of this tilt-rotor craft is shown here), the advancement in redundant 'fly-by-light' and 'fly-by-wire' technology and many other progressive R&D programs. Bell currently employs engineers in 75 distinct disciplines, and we have many openings for experienced engineering professionals now.

Your chance to enhance your career potential begins today with a call to Bell Helicopter.

Help us make tomorrow unlike anything today.

Here's what we'd like: if you have appropriate degrees and three or more years experience in your specialty, our engineers are eager to meet you and detail the positions open in these areas now at Bell:

RADAR CROSS SECTION ANALYSIS

PRELIMINARY DESIGN OPERATIONS ANALYSIS

AIRFRAME LOADS

STRUCTURAL ANALYSIS

STRUCTURAL DYNAMICS

FLUTTER ANALYSIS

SHOCK & VIBRATION ANALYSIS

ICING PROTECTION

COMPOSITE MATERIALS TECHNOLOGY

HEAT TRANSFER/ PROPULSION

Here's what you'll like: the competitive salary ranges, superior benefit package, liberal vacation programs and sunny Texas location. But most of all, the hands-on responsibility and the opportunity to be involved with people who challenge themselves to the fullest: the best, creating the best. To learn more, call David McDavid at (817) 280-2377 today, or send your resume to him at Bell Helicopter, P. O. Box 482, Dept. NTB-1, Fort Worth, TX 76101.

U.S. Citizenship Required.

Bell Helicopter **TEXTRON**

A Subsidiary of Textron Inc.

Air-Bearing Table for Machine Shops

Frequent workpiece repositioning is made easier.

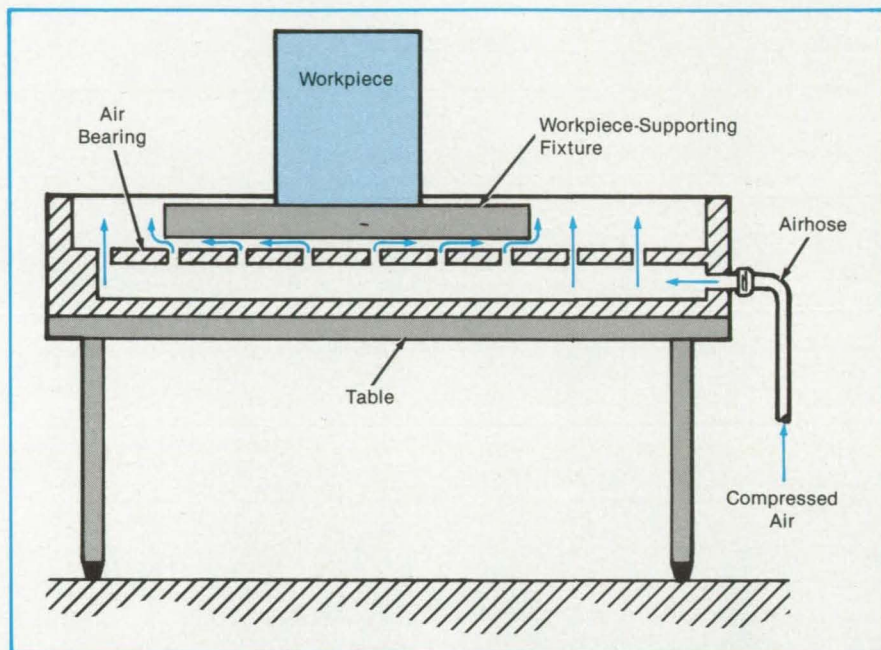
Marshall Space Flight Center, Alabama

An air-bearing table facilitates the movement of a heavy workpiece during machining or between repeated operations at different positions. The table assembly consists of a workpiece-supporting fixture riding on an air bearing. The table is especially useful for inertia welding, in which the ease of mobility is important.

As shown in the figure, compressed air is fed to a plenum, from which it escapes through small holes in the table surface. A low-friction air cushion is thus formed under the workpiece-supporting fixture: This enables the fixture to slide easily over the table, even when bearing a heavy workpiece.

This work was done by Don Ambrisco of Rockwell International Corp. for Marshall Space Flight Center. No further documentation is available.

MFS-29035



The **Air-Bearing Table** supports the workpiece so that it can be moved easily.

Electromechanical Turboprop-Pitch-Control Mechanism

The propeller-control system is autonomous and tolerant of failure.

Lewis Research Center, Cleveland, Ohio

An advanced autonomous electromechanical turboprop-pitch-control mechanism has been designed that meets the demanding requirements of a high-power advanced turboprop. Although propeller-driven aircraft have flown successfully for over 70 years, the exceptionally-large blade torques and synchrophasing requirements of future turboprop aircraft, with blade diameters up to 13 ft (4 m) necessitate the use of advanced propeller-pitch-control mechanisms (PCM's).

The electromechanical PCM pitch-control mechanism described here (see figure) represents a significant improvement in the accuracy, reliability, and maintainability of state-of-the-art, hydraulically-controlled propeller systems. This system takes maximum advantage of recent advances in electric-motor, fiber-optic, mechanical-drive-

system, and digital-control technologies. Mounting the electrical-power module and conditioning/control systems inboard the rotating propeller hub eliminates failure-prone slipping devices and creates an autonomous, failure-tolerant propeller-control system. Modular component design facilitates on-the-wing maintenance. The system is highly adaptive to various sizes and gearbox configurations.

The features and capabilities described are unmatched by any comparable PCM now in existence. These capabilities will be needed by large, fuel-efficient, commuter turboprop aircraft now being developed by the aircraft industry.

The all-electromechanical PCM system accurately controls the propeller-blade angle of large (10,000-kW) turboprop-aircraft propellers over a wide spectrum of flight operating conditions.

The PCM is housed within the propeller hub, as illustrated in the figure. The system is appropriate for 150-passenger, advanced turboprop commuter aircraft that cruise at mach numbers between 0.7 and 0.8. An autonomous, solid-state digital-control module, located in the nose of the spinner for ease of maintenance, commands blade-angle position based on digital control-signal information passed from the cockpit. These control-signal data are optically encoded and passed across the rotating interface through a fiber-optic data link (rotary coupling) having superior noise rejection and data bandwidth characteristics.

The autonomous electronic-control module onboard the spinner contains sufficient internal logic to maintain normal, constant propeller-speed operation in the event of a failure of the fiber-optic data



WHY THERE'S NOTHING STOCK ABOUT OUR STOCK AND TRADE.

At Inland Motor we make very special motion control products — unique motors and controls for unique applications. As we've added these one-of-a-kind designs, our product base has evolved into an exceptional line of motion control products. "Standard" models...that deliver extraordinary solutions.

Specifically, at Inland Motor we offer products with a proven record of reliable, state-of-the-art performance in aerospace, robotics, defense, machine tool, process control and medical applications.

Our current product base includes the following:

FRAMELESS DIRECT-DRIVE DC MOTORS

These motors are especially well suited for applications where the aim is to maximize velocity and position accuracies. These near-infinite resolution motors are coupled precisely where the torque is required. (Direct drive means no gearing and no backlash.) Available in peak torques from 1 oz-in to 1,000,000 oz-in (5200 lb-ft).

FRAMELESS DC TACHOMETERS

Frameless DC tachometers are used where the requirement is quality angular velocity feedback. These devices are coupled directly where the velocity is to be measured. Available with ripple voltages down to 0.1% (average to peak), these tachometers will enhance the performance of your servo system.

BRUSHLESS DC MOTORS

These motors are especially well-suited to explosive, dry, liquid or low pressure environments, as well as ultra high speed or high power applications. Available in peak torques from 1 oz-in to 300,000 oz-in (1560 lb-ft).

LIMITED ANGLE MOTORS

Limited angle motors, which are also brushless, are suitable when torque is required over just a portion of a revolution, such as with scanners, throttle controls, and vibration test equipment. Available with excursion angles of up to $\pm 75^\circ$.

If we don't already have the model you're looking for, we'll customize our motors to your exact requirements or design a new one — whether you need 10,000 or just 1. We can put them in a housing, and we can provide drive electronics.

If you'd like to know more about our stock and trade, or if you'd like help with a specific application, give us a call today at (703) 639-9045.

You can bet you won't get a stock answer.

Where imagination combines with technology.

INLAND MOTOR

KOLLMORGEN CORPORATION

SPECIALTY PRODUCTS GROUP

Radford, VA 24141 TWX 710-875-3740



link. A high-power-density, high-speed (20,000-rpm), electronically-commutated, permanent-magnet (PM) synchronous motor located within the rotating spinner provides the mechanical power to change blade angle. Electrical power for this motor is generated onboard the rotating spinner by a similarly-constructed PM synchronous alternator colocated with the motor on the centerline of the propeller hub. Mechanical power to drive this alternator is shipped across the rotating interface from a power takeoff shaft extending from the main propeller gearbox. This arrangement eliminates the need for high-maintenance, rotating power-transfer devices, such as electrical-power sliprings or hydraulic-fluid-transfer seals (in the case of hydraulic actuators).

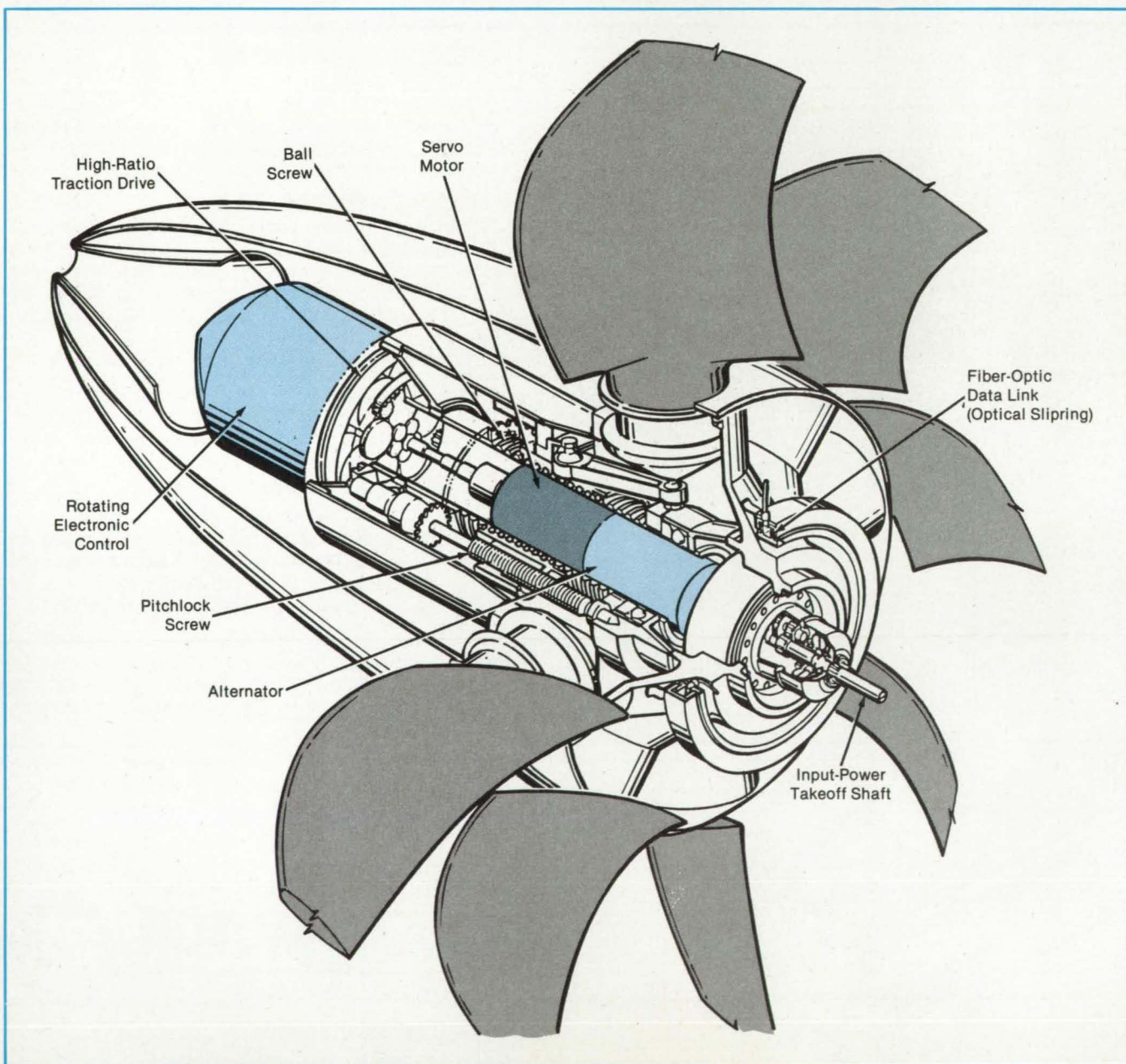
The servocontrol motor is mechanical-

ly coupled to the blades through an 8,000-to-1 reduction drive train, effecting a maximum blade slew rate of 15°/s for emergency feather and reverse-thrust operation. Since cruise occupies the bulk of the mission, the drive mechanism normally is functioning in a low-speed, hunting mode (blade slew rates from 0° to 1°) to achieve synchrophasing. (Synchrophasing may be defined as the synchronization of multiple engine-blade positions to minimize the annoying "beating" noise.) The drive mechanism consists of a torsionally-stiff, low-loss hybrid traction drive, which couples the motor to a ball screw. The ball screw, in turn, articulates the individual blades through stiff links, connected at one end to an eccentric pin at the blade root and at the other end to the translating ball-screw nut. Blade-angle settings typically range from about

- 7° at maximum reverse pitch to + 85° at flight feather.

In the event of any mechanical or electrical component failure, the system is also equipped with an independently-driven, emergency pitch-lock screw mechanism, which tracks the current position of the ball-screw nut and will lock the blades within approximately 1° of their last position. This required safety feature eliminates any danger of propeller overspeeding and allows engine operation in the "fixed-prop" mode.

Blade-position accuracies are within 3 arc-minutes of a degree for the system described. The three primary factors that contribute to this precision are the digital electronic feedback control system, the programable servocontrol motor, and the torsionally-stiff, low-hysteresis mechanical drive mechanisms.



The **Autonomous Electromechanical Pitch-Change Mechanism** accurately controls propeller-blade angles on large (10,000-kW) aircraft engines. Modular component design facilitates maintenance.

In comparison with current hydraulic-control systems, the electromechanical PCM described here will reduce estimated maintenance costs by 9 percent, reduce weight by 5 percent, and increase mean time between all maintenance actions from the current 2,700 hours to 3,250 hours. Other identifiable benefits with the proposed electromechanical PCM include the following:

- The elimination of high-maintenance,

high-pressure hydraulic pumps and motors;

- Inherent compatibility between the brushless PCM servomotor and electronic digital controls; and
- The elimination of the PCM oil-lubrication system with greased, packed motor/generator bearings, linkage joints, ball screw, and traction roller-drive module.

This work was done by B. M. Steinetz

and S. Lowenthal of **Lewis Research Center**, D. F. Sargisson of General Electric Co., and G. White of Transmission Research, Inc. Further information may be found in NASA TM-83709 [N84-25605/NSP], "An Advanced Pitch Change Mechanism Incorporating a Hybrid Traction Drive" [\$7]. A copy may be purchased [prepayment required] from the National Technical Information Service, Springfield, Virginia 22161. LEW-14234

Books and Reports

These reports, studies, and handbooks are available from NASA as Technical Support Packages (TSP's) when a Request Card number is cited; otherwise they are available from the National Technical Information Service.

Operating a Remote Manipulator in Simulated Low Gravity

A microgravity simulator shows that control is adversely affected, but compensation is possible.

Efforts to control remote manipulators in simulated microgravity are described in a report. The experiments were conducted to determine the effects of weightlessness on the performance of an operator controlling a remote manipulator, or slave arm, by a master arm at a control station.

A six-dimensional force-reflecting hand controller was used as the master arm. With this controller, the operator's hand and arm movements are translated into movements of the remote manipulator. Through the hand controller, the manipulator feeds back to the operator sensory information about the forces acting on it.

A gravity-compensation support for the operator's upper arm and hand simulated the nearly zero gravity that would prevail in a space station in Earth orbit. The support provided a constant force at the center of mass of each limb segment. The force was equal and opposite to the gravitational force acting on the segment. The forces were furnished by low-inertia, constant-tension springs that are adjustable to the body characteristics of the individual operator.

An operator's performance using the hand controller with the support was compared with the same operator's performance with the support. In general, operators were less accurate with the support—that is, in simulated microgravity—than in normal gravity.

The report concludes that microgravity disturbs neuro-motor control of the human arm. It also suggests that the disturbance can be compensated for by adjustments in the controller.

This work was done by Antal K. Bejczy and Kevin M. Corker of Caltech for NASA's Jet Propulsion Laboratory. To obtain a copy of the report, "Experiments in Simulated Microgravity of Manual Control of Teleoperators," Circle 16 on the TSP Request Card. NPO-16477

New! Metal Spring/PTFE Seals With Unique Dual-Lip Design For Double Leak Protection



Greene, Tweed MSE™ Series F are the only metal spring/PTFE seals with two lips to offer double leak protection and trap lubricant for longer life. These low-friction, self-lubricating seals for rod, piston and face sealing applications—



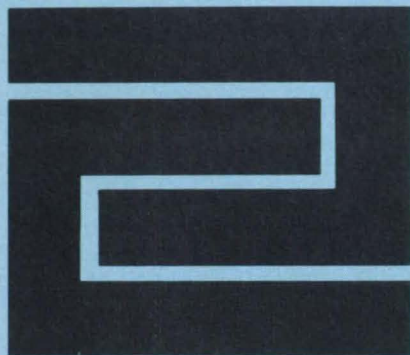
- Provide excellent static and dynamic sealing at pressures to 10,000 psi.
- Operate at temperatures from cryogenic to 500F+.
- Fit MIL-G-5514F glands.
- Are compatible with aggressive aerospace fluids, and are non-contaminating.

MSE seals are available in a variety of PTFE's and spring energizers; they are ideal for applications in fuel systems, emergency blow down systems, electronic cooling systems, etc.

Call or write for details.

GREENE, TWEED & CO

North Wales, PA 19454 • USA • (215) 256-9521



Hardware, Techniques, and Processes

- 138 Ion-Deposited Polished Coatings
- 139 Heating Bonding of Irradiated Ethylene Vinyl Acetate
- 140 Thermoplastic Composites for Research-Model Components
- 141 Controlling Arc Length in Plasma Welding
- 142 Optical Monitoring of Weld Penetration
- 142 Crystal-Growing Crucible To Suppress Convection
- 143 Void-Free Lid for Food Packaging
- 144 Metalizing Solar Cells by Selective Electroplating
- 144 Transfer Casting From Ion-Beam-Textured Surfaces

Books & Reports

- 145 Making Latex Microspheres in Space

Ion-Deposited Polished Coatings

Polished, dense, adherent coatings are relatively free of imperfections.

Lewis Research Center, Cleveland, Ohio

A process has been developed to provide a highly-polished and adherent dense coating to a substrate that is free of voids, contaminants, and inclusions. A broad-beam ion source is used to sputter-polish while a vapor or sputter deposition is occurring simultaneously on the substrate surface. Prior techniques removed material from the surface, exposing sub-surface voids and contaminants. No simultaneous fill of voids occurred and therefore the surface was not free of defects since these were removal processes.

The new process consists of using a broad-beam ion source in an evacuated chamber to ion-clean a rotating surface that allows the grazing incidence of the ion beam. This sputter cleans off absorbed gases, organic contaminants, and oxides of the mirror surface. In addition to the cleaning, surface protrusions will be sputter-etched away.

Once the surface has been ion-cleaned, a variety of vacuum-deposition techniques can be used to deposit adherent coatings on the cleaned mirror surface. Figure 1 depicts grazing-incidence ion polishing with simultaneous, normally incident vapor or sputter deposition. The simultaneous sputter polishing and vacuum deposition must be done in a manner so that the sputter-etch rate is slightly lower than the deposition rate on the mirror surface. This allows pits or depressions in the mirror surface to fill in quickly

because the grazing-incidence ion beam does not have a view factor to sputter-etch these areas which are receiving near-normal incident vapor or sputter deposition. At the same time, protrusions, bumps, and other convex surface asperities have a sputter-etch rate higher than surrounding smooth flat surfaces. This is due to the relative angles at which the sputter-etching ions and the deposition material arrive.

Figure 2 depicts the processes of simultaneous ion sputter, polishing, and deposition. The process leads to a smooth deposited and polished surface in a similar manner analogous to the macroscopic process of multiple painting and sanding operations for wood finishing. The net deposition resulting quickly becomes a smooth mirror-surface deposit that slowly builds up free from surface irregularities, such as defects, voids, or protrusions. The process is stopped when the desired deposit thickness is achieved. Both the ion-beam sputter polishing and the deposition should be stopped simultaneously when the desired coating thickness is achieved.

Eleven other adaptations to the process are the following:

1. The mirror material can be metals, metal carbides, metal oxides, certain polymers, and most inorganic compounds.
2. The deposition can be produced by vapor deposition from electron-

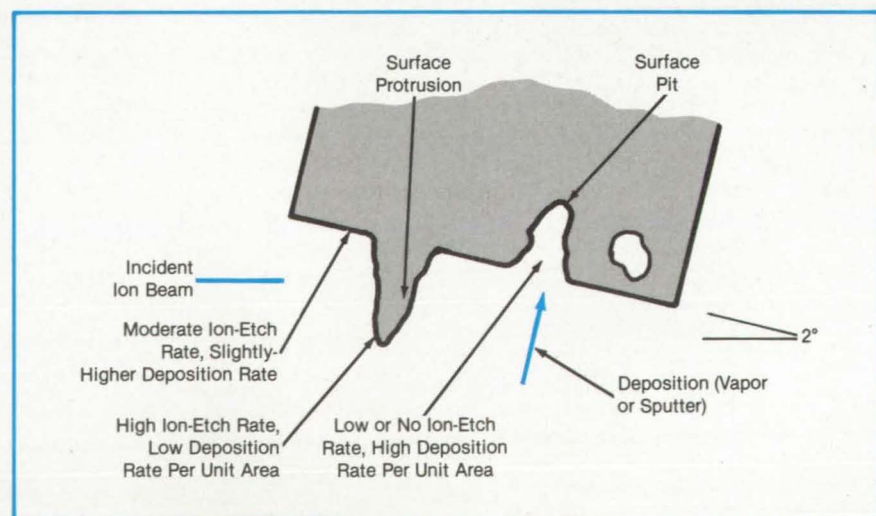


Figure 1. **Grazing-Incidence Ion Polishing** is conducted simultaneously with deposition by normally incident vapor or a sputtering beam.

beam evaporators, heated boats, filaments, or by ion-beam, dc or RF sputtering from the same or another deposition system.

3. The substrate surface angle θ can be varied from 0° to $\approx 10^\circ$ with respect to the incident ions, depending on the degree of polishing desired.
4. The surface can be cooled or heated as desired to improve the quality of the coating.
5. The ion energy can be varied from a few hundred to a few thousand electronvolts.
6. The sputtering ions can be a variety of gas species, such as Ar, Xe, Ne, and N.
7. The duration of initial sputter-etch cleaning can be varied from seconds to hours, depending upon the thickness desired.
8. The ion beam can be of various diameters, from centimeters to meters, depending upon the substrate diameter.
9. The deposited coating can be a variety of materials, such as metals, metal oxides, and metal nitrides. The deposited materials can also be a different material than the substrate.
10. The rotation rate of the substrate can be varied as desired to produce the best-quality surface coating.
11. Further coatings can be applied by the same process if one wants to switch materials for the outer substrate surface.

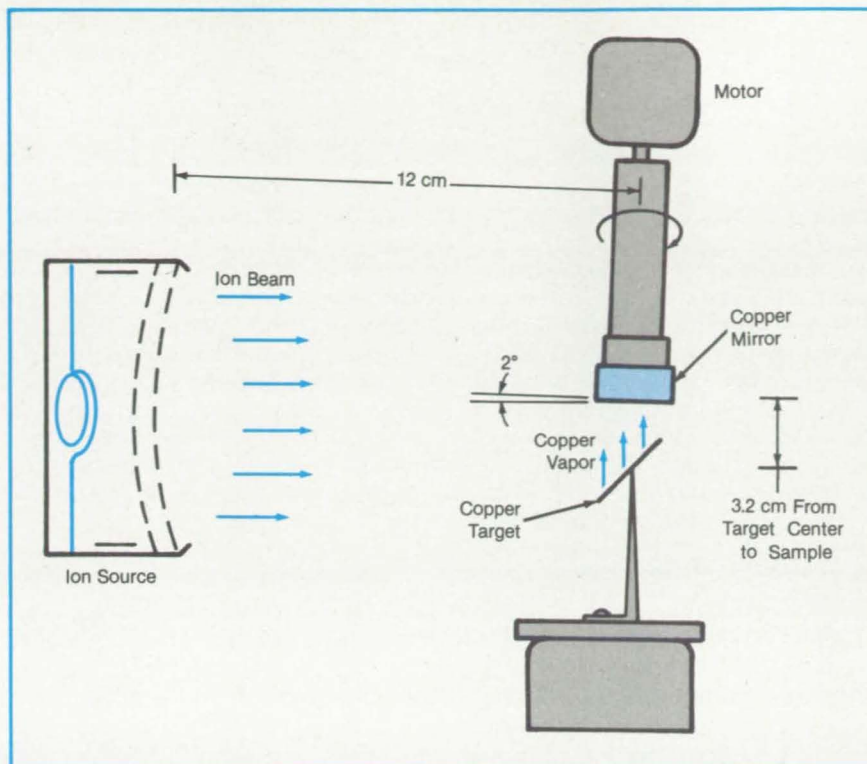


Figure 2. **Ion Sputter Polishing** and deposition give a smooth deposited and polished surface, in a manner analogous to that of the repeated painting and sanding of wood.

The process is particularly adaptable to the polishing of various substrates for optical or esthetic purposes.

This work was done by Bruce A. Banks of **Lewis Research Center**. Further information may be found in NASA

TM-81679 [N81-19278/NSP], "Simultaneous Ion Sputter Polishing and Deposition" [\$7]. A copy may be purchased [prepayment required] from the National Technical Information Service, Springfield, Virginia 22161. LEW-13545

Heat Bonding of Irradiated Ethylene Vinyl Acetate

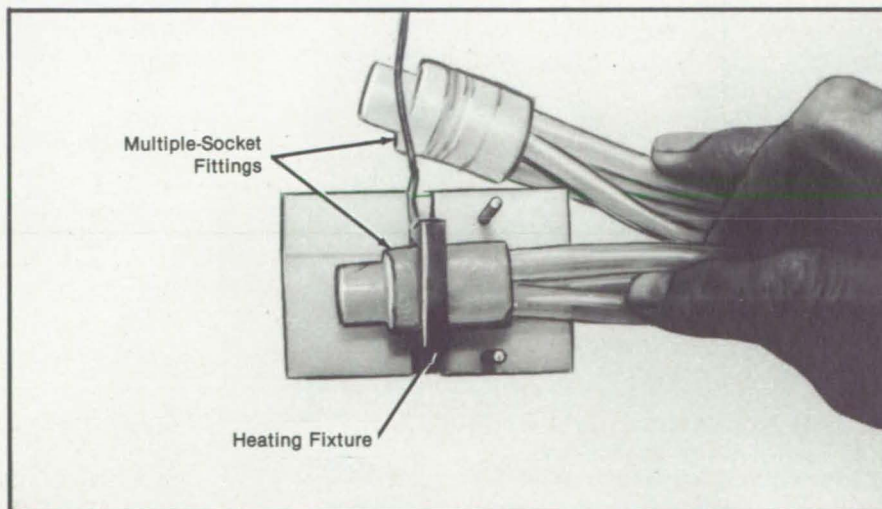
A reliable method is now available for joining parts of this difficult-to-bond material.

Lyndon B. Johnson Space Center, Houston, Texas

Tubing and fittings of irradiated ethylene vinyl acetate (EVA) are joined to each other with a new heat-bonding technique to form reliable, leak-free junctions. EVA tubing is useful as a conduit for cooling water because contaminants are not leached out of it by the water. The use of EVA was previously inhibited by the difficulty of joining this material to itself.

The new technique takes advantage of a characteristic of irradiated EVA: the migration of residual non-cross-linked oligomers to the surface when heated. The resulting exudate is tacky while hot. When a tube and socket are put together and heated, the exudate from the heated tubing mingles with that from the socket and forms a bond upon cooling.

The first step in the bonding process



A **Heating Fixture** encircles an ethylene vinyl acetate multiple-socket part, providing heat to it and to the tubes inserted in it. Fixtures are specially designed to match the parts to be bonded.

is to cut the tube end perpendicularly to the bore. The end is then cleaned with acetone and inserted in the socket. [If the tubing has a diameter less than one-eighth inch (about 3 millimeters), a stiffener, such as polytetrafluoroethylene-coated wire, will prevent the tube from distorting or collapsing.] A heating fixture, specially shaped to conform to the parts, is installed around the area to be heated (see figure).

Power is applied to the heating fixture while its temperature is monitored with thermocouples. The bond area is heated to 220 °F (104 °C) and held there for 4 minutes. The parts are allowed to cool naturally for 3 minutes and are then further cooled by forced air. The assembly can be handled when the temperature

drops below 113 °F (45 °C) since the bond will then have been formed. Stiffeners, if used, are removed at that point.

An important advantage of the method is that a joint can be separated and rebonded. The heating fixture is placed over the joint and heated gradually toward 400 °F (204 °C). Starting at 350 °F (177 °C) and while the temperature continues to rise, the tube is alternately stretched and released until it peels away from the socket. As soon as the tube is removed, a sizing tool is inserted in the socket to maintain its shape as it cools. Meanwhile, the tube is heated briefly so that it resumes its original shape. The tube and socket are then ready for rebonding.

The surfaces of the copper heating fixture must be treated before use with a high-temperature mold release to prevent sticking. If sticking occurs in spite of this precaution, the tool should be reheated to soften the EVA surface. When the fixture is removed in this way, however, it does not leave a smooth surface.

Tube-and-socket bonds made with this technique were subjected to tensile tests. Bond strengths of 50 percent that of the base material were obtained consistently.

This work was done by David H. Slack of ILC Dover for Johnson Space Center. For further information, Circle 68 on the TSP Request Card.
MSC-20320

Thermoplastic Composites for Research-Model Components

Oriented unidirectional prepreg tapes are formed in ceramic molds.

Langley Research Center, Hampton, Virginia

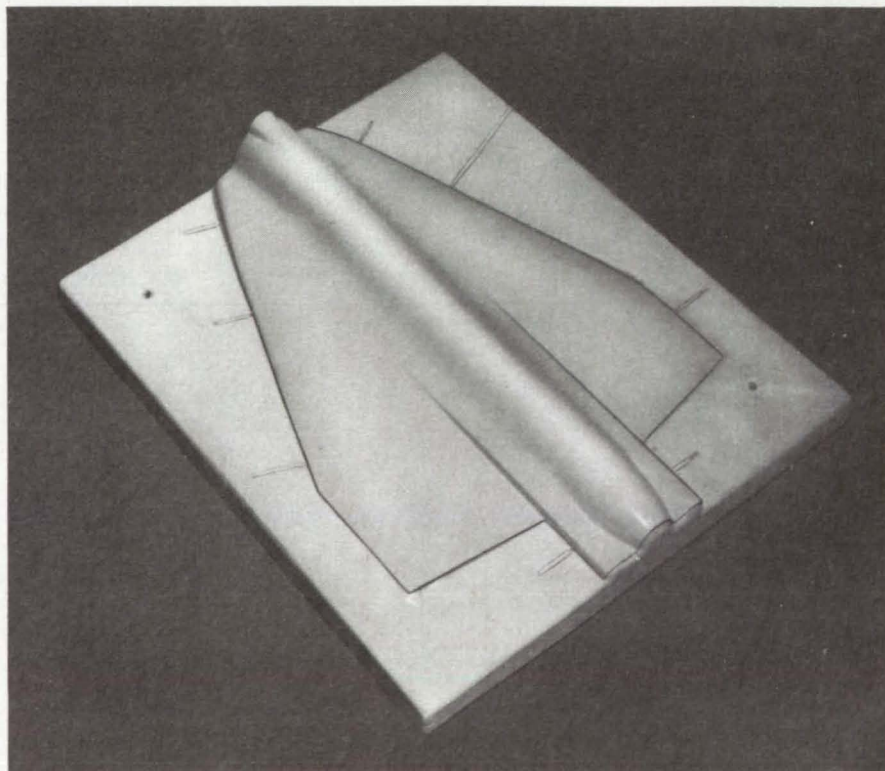
The construction of stiffer aircraft structures generally results from the use of graphite/epoxy or graphite/thermoplastic composites. Advanced wing designs take advantage of this stiffness by tailoring ply layout and ply orientation. To obtain the same scale effect in the construction of research models, the same materials must be used that are being developed for full-scale aircraft. Composite materials of graphite/epoxy are already being used in model fabrication. A new technique has been developed at Langley Research Center, using a ceramic mold for the fabrication of models from graphite/thermoplastic materials.

The remelt capability of thermoplastics allowed the proper ply orientation of the unidirectional graphite. The prepregs were tacked together during layup with a soldering iron, thus ensuring the desired ply orientation during the curing cycle. Ceramic materials were used for the mold because they can withstand the high temperatures and pressures of the thermoplastic-resin curing cycle and can be fabricated more quickly and economically than metal molds.

The upper surface of a model, which includes the wings and fuselage of an advanced fighter aircraft, was selected to be fabricated from the thermoplastic preimpregnated material and to be used as the mold pattern (see figure). The unidirectional, continuous-filament graphite material was preimpregnated with a high-temperature thermoplastic

resin. The layup method involved preforming the shape to minimize bulk, thereby allowing the fiber orientation to remain constant and preventing excessive pressure on the molds.

The correct length of prepreg was stripped, inserted manually into the mold, and successive strips were tacked together to acquire the shape of the mold and, ultimately, the component.



The Upper Surface of the Wings and Fuselage of an advanced airplane was selected as a shape to test the fabrication technique. The technique is well suited for other complex shapes as well.

This layup method is vital in the fabrication of complexly shaped pieces. Each layer of an eight-ply layup was made in this manner. A quasi-isotropic layup equal in all four directions was selected for tests (0° , 90° , $\pm 45^\circ$, $\pm 45^\circ$, 90° , 0°).

The ceramic mold was preheated to 800°F (430°C), then opened, and the preformed layup was placed between

the mold halves. The mold was then closed and placed in a heated press. A thermocouple attached to the mold recorded the temperature. Once the mold reached 800°F (430°C), a pressure of 700 psi (4.8 MN/m^2) was applied for 10 min. The press was allowed to cool under pressure till it reached 700°F (370°C), at which point the pressure was gradually reduced.

The component was removed when the press reached room temperature. The thermoplastic composite was found to be easily workable with normal shop equipment and could be painted and repaired by all of the standard methods.

This work was done by Benjamin F. Guenther and Peter Vasquez of **Langle Research Center**. No further documentation is available. LAR-13348

Controlling Arc Length in Plasma Welding

A circuit maintains the arc length on irregularly shaped workpieces.

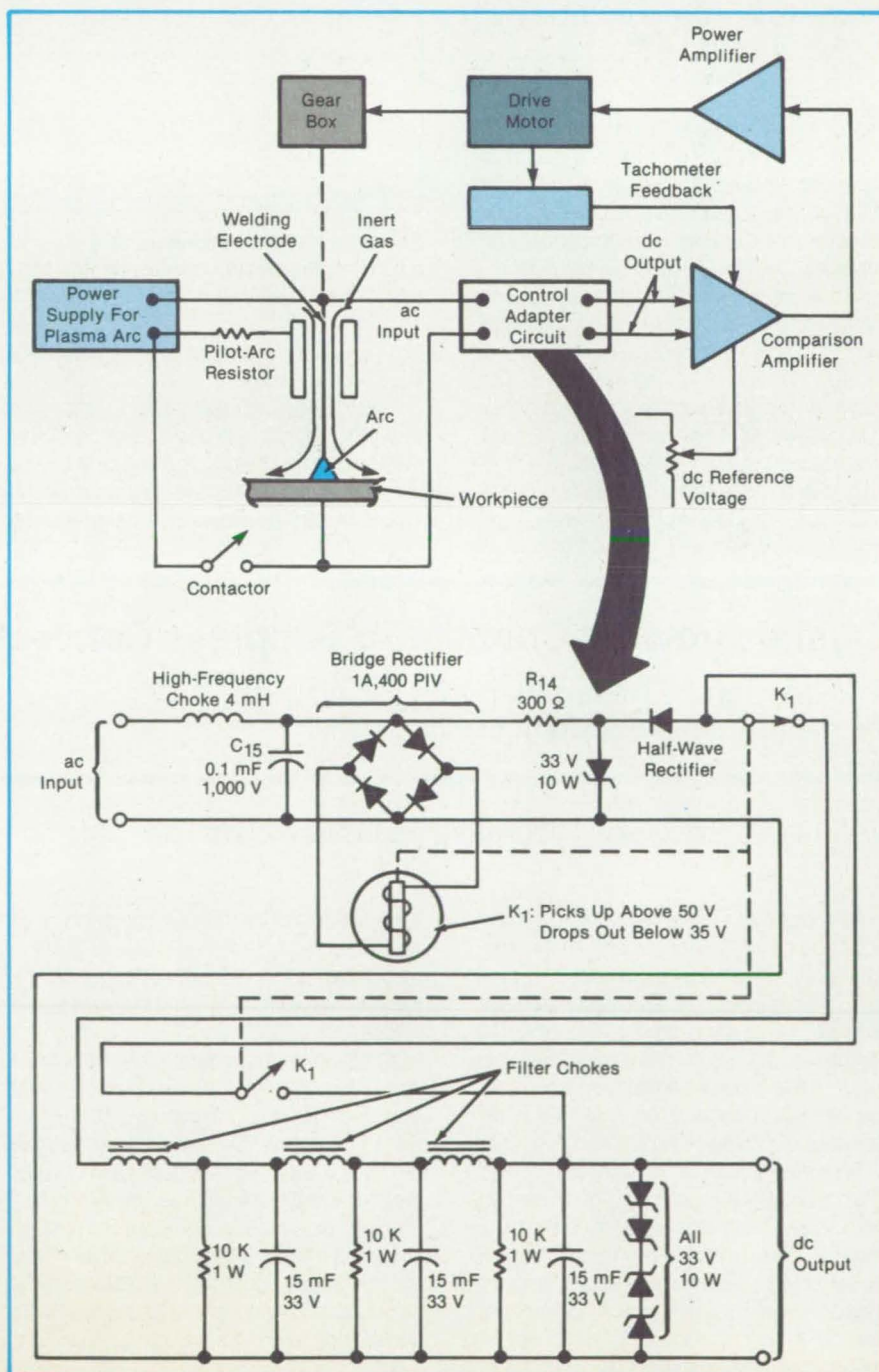
*Lyndon B. Johnson Space Center,
Houston, Texas*

A control adapter circuit maintains a constant arc length during plasma arc welding of irregularly contoured parts. The circuit can be added to plasma arc welding machines with just a few wiring changes. Welds made with the circuit are cleaner and require less rework than do welds made without it. The beads are smooth and free of inclusions.

The circuit (see figure) samples the ac arc voltage, then half-wave rectifies and filters it to reduce the ripple. The resulting dc measurement signal is applied to a comparison amplifier, which compares it to a reference voltage that represents the commanded arc length. The amplified comparison signal is applied to a power amplifier that drives a motor and gear train to adjust the electrode position and therefore the arc length.

This work was done by William F. Iceland of Rockwell International Corp. for **Johnson Space Center**. For further information, Circle 66 on the TSP Request Card.

Inquiries concerning rights for the commercial use of this invention should be addressed to the Patent Counsel, Johnson Space Center [see page 29]. Refer to MSC-20900.



The **Length of a Plasma Arc** is continuously adjusted by the control circuit to maintain the commanded value. After a pilot arc has been established, the contactor is closed and transfers the arc to the workpiece. The control circuit then half-wave rectifies the ac arc voltage to produce a dc control signal proportional to the arc length.

Optical Monitoring of Weld Penetration

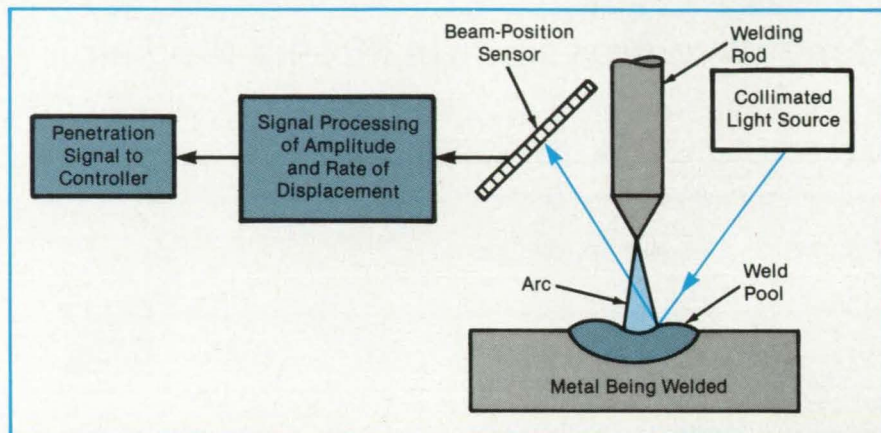
Robotic welding can be controlled by a reliable, relatively-noise-free optoelectronic unit.

Marshall Space Flight Center, Alabama

A system is being developed to monitor weld penetration optically and produce a signal for controlling an arc welder. The system is aimed for automatic welders, robot welders in particular. Made from small, low-cost components and utilizing optical fibers to conduct the signals, the system is immune to the electromagnetic interference that is common in industrial environments.

The monitor directs collimated light from a small diode laser at the molten pool of metal beneath the arc (see figure). A filter intercepts the reflected beam to suppress extraneous light, including light from the welding arc. A position-sensitive detector at a distance from the pool intercepts the beam reflected by the pool.

If the weld penetrates the workpiece completely, the curvature of the pool surface suddenly changes. This causes a sudden deflection of the reflected light beam, and consequently a displacement of the beam spot on the detector. Signal-processing circuitry determines the amplitude and rate of beam displacement to detect penetration and to generate con-



Bounding Off the Meniscus of a Pool of Molten Metal, a laser beam impinges on a position-sensitive photodetector. The beam diameter can be adjusted for the width of the weld. Optical filters screen out the light from the arc.

trol signals for the robot to regulate welding parameters.

The monitor is insensitive to changes in weld current, welder speed, and the thermal properties of the welded metal except as they affect weld penetration. The monitoring principle is adaptable to

other types of welding, including tungsten/inert-gas, laser, and electron-beam techniques.

This work was done by Jonathan Maram of Rockwell International Corp. for Marshall Space Flight Center. No further documentation is available.
MFS-29107

Crystal-Growing Crucible To Suppress Convection

A platform under the growth region can stabilize the melt for a more uniform crystal growth.

NASA's Jet Propulsion Laboratory, Pasadena, California

A proposed crucible for growing silicon webs or boules can suppress thermal convection near the solidification interface. Thermal convection must be suppressed because it causes nonuniform crystal growth. In the new crucible (see figure), there would be a platform just below the growth interface so that the melt would be too shallow to support convection.

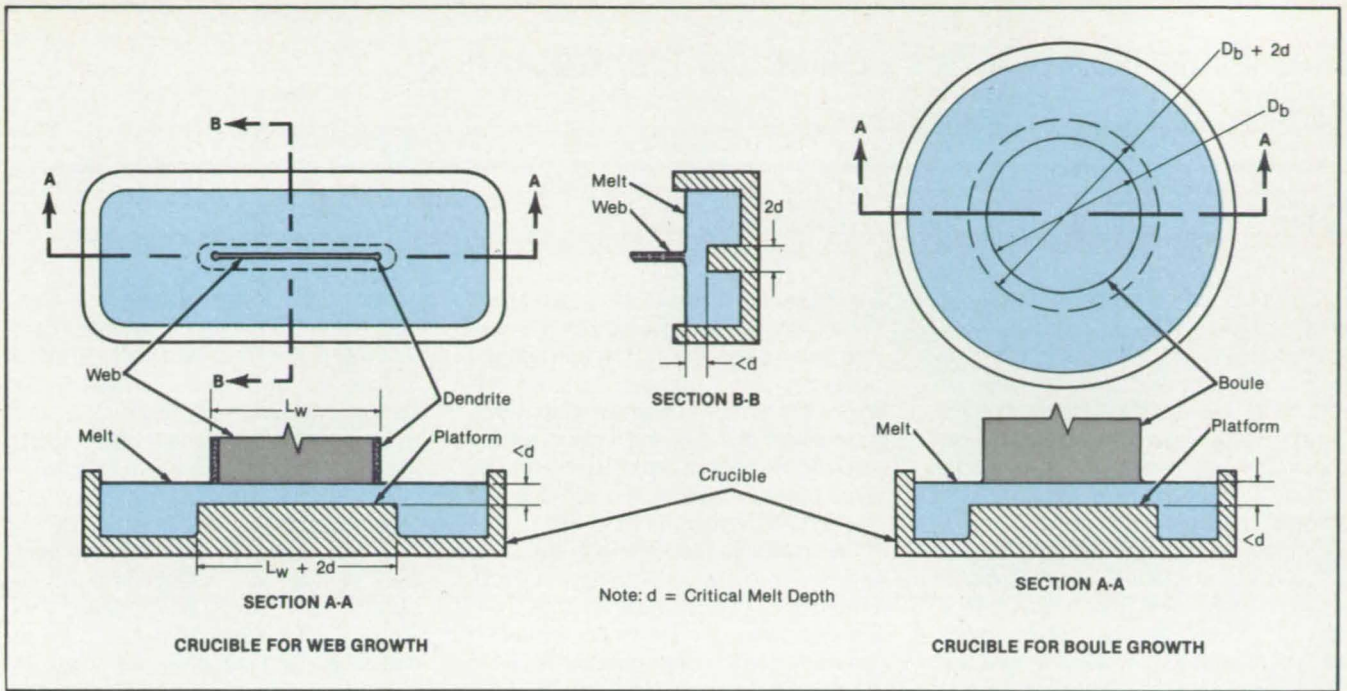
The new crucible design is derived from the theory of stability of a heated fluid. The instabilities that give rise to convection occur when the gravitational forces due to thermally induced density gradients exceed frictional forces in the fluid. The critical depth for the onset of the pertinent instability can be calculated

from the heat flux through the surface of the melt, the volume coefficient of thermal expansion, the thermal conductivity, the thermal diffusivity, and the kinematic viscosity.

All of these quantities except the heat flux are properties of the molten material and are available in standard reference works. The heat flux can be evaluated in terms of the system configuration and operating conditions. For example, if the crucible operates in a vacuum, the heat flux equals the net thermal radiation from the melt surface. If the operation is in a gaseous environment, conduction and convection also contribute to the heat flux.

The width of the platform is approximately the width of the crystal plus twice the critical depth. The platform height is such that the melt depth under the crystal-growth region is less than the critical depth. The thermal resistance of the quartz platform material is considerably greater than that of the molten silicon: This contributes further to stability by reducing the heat flux through the melt, thereby decreasing the thermal gradient that drives convection.

This work was done by Robert Richter of Caltech for NASA's Jet Propulsion Laboratory. For further information, Circle 8 on the TSP Request Card.
NPO-16597



The Improved Crucible for Growing Silicon Crystals would include a platform just below the growth interface.

Void-Free Lid for Food Packaging

A flexible cover eliminates air pockets in a sealed container.

Lyndon B. Johnson Space Center, Houston, Texas

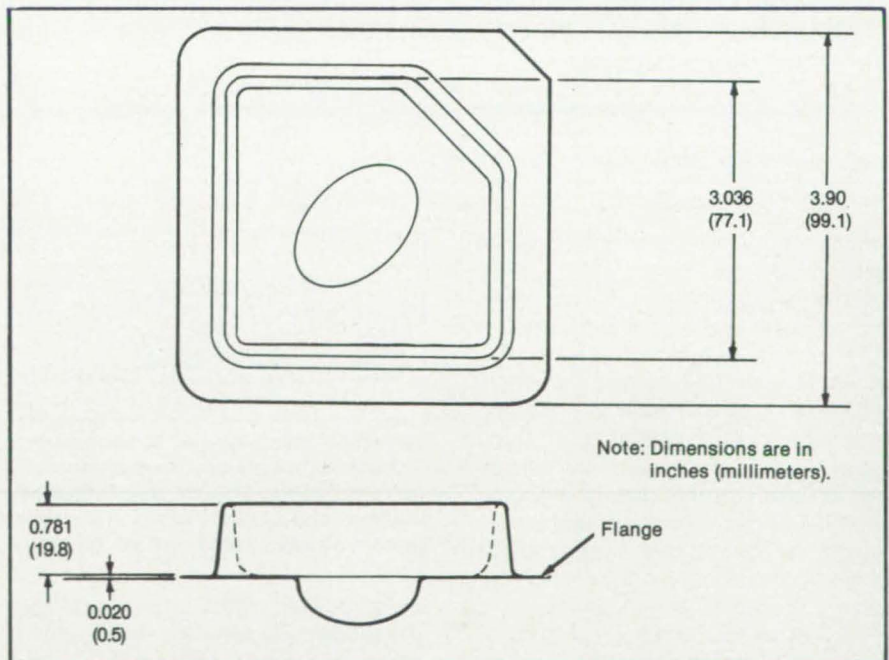
Containers holding varying, unpredictable levels of food are sealed at the precise fill level with the aid of a folding lid. The lid eliminates air or vacuum pockets above the food. It therefore keeps the food fresh, allows compact stacking of partially filled containers, and resists crushing.

The new lid was originally developed for packing dehydrated food for use in human consumption on the Space Shuttle missions. Other uses may include home canning and commercial food packaging.

The lid, made of folded, flexible plastic fits into a rigid plastic cup. The center of the lid is pushed into the cup to the top surface of the food. The lid unfolds as this is done and clings to the inside surface of the cup. The rim of the lid is then heat-sealed to the cup.

The new lid replaces an earlier model that, instead of having continuously variable depth, was available only in three fixed depths. That lid allowed voids when the container was filled to intermediate depths. It tended to crack and leak as a result and sometimes wrinkled, making it difficult to stack containers.

This work was done by Clyde D. NASA Tech Briefs, March/April 1986



The Universal Food-Package Lid is formed from flexible plastic. Shown here partially folded, the lid is unfolded by depressing the center portion: The height of the flat portion of the lid above the flange is thereby reduced. The pressure of the food against the central oval depression pops it out, forming a dome that provides a finger grip for mixing the contents with water or opening the lid.

Watson and William P. Farris of ESD Corp. for Johnson Space Center. For

further information, Circle 94 on the TSP Request Card. MSC-20661

Metalizing Solar Cells by Selective Electroplating

Contact patterns are traced by laser scanning.

NASA's Jet Propulsion Laboratory, Pasadena, California

Conductor paths have been deposited on silicon solar-cell wafers by laser irradiation followed by electroplating. The laser-assisted metalization technique offers better resolution and lower contact resistance than does conventional metalization by screen printing. At the same time, it is less expensive than metalization with masks and photolithography.

In preliminary experiments, a layer of Ti 1,500 Å thick was first evaporated onto a silicon wafer. This was followed by a layer of Pd 500 Å thick. (These layers were deposited to promote the adhesion of the metal to be deposited and to reduce diffusion between the metalization and the silicon substrate.) Twelve comb-shaped metalization patterns for solar cells were then written on the wafer by an argon laser.

The laser beam was focused to a diameter of 50 μm and was moved in a raster pattern over the wafer by scanning mirrors. Each comb consisted of five

9-mm-long horizontal teeth, 2 mm apart. The combs were connected by a 9-mm-long vertical line on which a contact pad measuring 1 by 2 mm was centered. The lines were written in a single scan with a laser power of 7.7 W and a beam spot of 20 cm/s. The contact pad was written at the same power with a scan speed of 0.2 cm/s and a scan overlap of 60 percent.

No marks corresponding to the laser scan were visible on the wafer surface, even under a high-power microscope. However, when the wafer was immersed in a silver cyanide electroplating bath with 10 mA of plating current, the hitherto-invisible contact pads plated instantly. The lines, which were written at higher speed, took longer to plate and become visible.

A subsequent experiment was performed with a uniform scanning speed of 0.2 cm/s for both pads and lines. After plating for 3 h, the Pd and Ti over the rest of the wafer were etched off. Since the etchant oxidized the surface of the silver

contact pattern, the oxide was removed in the plating solution, and the contact pattern was plated for an additional 30 min to restore the thickness. The final plated contact thickness was 25 μm.

Laser-written patterns on bare silicon and on silicon coated only with titanium were also plated selectively. It therefore seems likely that a laser-induced modification of the surface—laser-induced abrasion, for example—is responsible for the selectivity. On bare silicon, the plated silver did not adhere well. On the titanium-coated surface, however, the silver adhered well. This is an important finding because it means that it may be possible to reduce costs by doing away with the palladium layer.

This work was done by Subhendra Dutta and Patricia A. Palaschak of Westinghouse Electric Corp. for NASA's Jet Propulsion Laboratory. For further information, Circle 90 on the TSP Request Card. NPO-16600

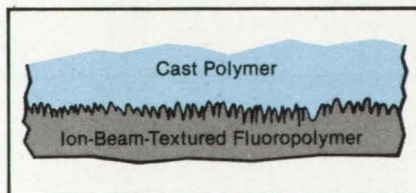
Transfer Casting From Ion-Beam-Textured Surfaces

Textured surfaces are created on metals, ceramics, and polymers.

Lewis Research Center, Cleveland, Ohio

A technique has been developed to generate precise, controllable, surface microstructures on metals, ceramics, and polymers. An electron-bombardment ion thruster is used as a neutralized-ion-beam source. The beam of directed, energetic ions can alter the surface chemistry and/or morphology of many materials. By adjusting the ion energy and ion-beam current density impinging upon the target, precise surface modifications can be obtained without risk of target-material melting or bulk decomposition.

A given ion-source operating condition results in a certain repeatable surface morphology for each material. Metals and ceramics generally can be sputtered at high ion-beam energies (1,000 to 2,000 eV), high ion-current densities (1 to 2 mA/cm²), and high surface temperatures (~500 °C). Metals sometimes require the use of a sputter-resistant



Transfer Casting is used to reproduce a surface with microscopic roughness: A polymer duplicate is cast on a fluoropolymer master, the surface of which has been given a texture by ion-beam sputtering.

material (seed), which is simultaneously sputter-deposited onto the metal surface during sputtering, to obtain a desired surface microstructure. The average separation between surface microstructures may range from less than 1 μm to 10 μm or more, and the average height of these features may range from less than 1 μm to 10 μm or more. Polymers generally require low ion-beam energies (~500 eV),

low ion-current densities (~0.1 mA/cm²), and low surface temperatures (<200 °C) to obtain a desired surface microstructure without thermal damage. The average surface-feature separation for polymers ranges from less than 1 μm to 10 μm or more, and the average height ranges from less than 1 μm to 100 μm or more.

To obtain a larger surface roughness on any material, a screen mesh may be superimposed on the target material during sputtering. The screen will prevent the sputtering of material directly beneath it, resulting in a surface with an array of holes of known dimensions. By varying the size of the screen apertures (present range is 14 μm to 200 μm.) and the ion-sputtering duration, different pit widths and depths can be obtained. The screen thickness limits the maximum pit depth.

The following list enumerates the limitations of ion-sputtered surface modifications:

1. Many hydrocarbon polymers do not develop a natural texture by beam sputtering.
2. Many polymers have very low sputtering yields; i.e., long ion-machining times to get a pit array.
3. A surface with pillars is very difficult to obtain.
4. Ion-beam sputtering alters the surface chemistry of most materials.

A method using a transfer-casting technique has been devised to overcome these shortcomings. As an example, ion-beam sputter texturing is used to develop a microscopically rough surface on a fluorocarbon polymer, such as polytetrafluoroethylene or fluoroethylenepropylene. These fluoropolymers easily develop surface texture by ion-beam sputtering.

The polymer to be surface-roughened is then cast over the textured fluoropolymer as shown in the figure. Other inorganic, organic, nonmetallic, and metallic

ion-beam-textured substrates can be used for the negative casting by sputtering a thin fluoropolymer coating over the texture to allow release of the cast polymer. A wide variety of polymers can be cast over the textured fluoropolymers, such as silicone rubbers, polyurethanes, polyolefins, and other low-elastic-modulus polymers.

There are many applications for these unique surface modifications. Natural-textured and seed-textured metals have high solar-absorptance values (0.97). The bonding strength of adhesive-bonded, natural-textured PTFE approaches that of the bulk material. In the biomedical area, ion-machined and natural-textured PTFE and polyoxymethylene enhance cellular attachment to soft tissue. Ion-machined metals increase the hard-tissue (bone) attachment to implants by as much as 10 times the attachment to smooth-surface implants. The fibrous capsule

thickness for natural-textured PTFE and polyoxymethylene implanted in soft tissue is less than the capsule thickness for smooth-surface implants.

This work was done by Bruce A. Banks, Albert J. Weigand, and James S. Sovey of Lewis Research Center. Further information may be found in NASA TM-81721 [N81-21129/NSP], "Ion Beam Applications Research — 1981 Survey of Lewis Research Center Programs." [\$10]. A copy may be purchased [prepayment required] from the National Technical Information Service, Springfield, Virginia 22161.

This invention has been patented by NASA [U.S. Patent No. 4,329,385]. Inquiries concerning nonexclusive or exclusive license for its commercial development should be addressed to the Patent Counsel, Lewis Research Center, [see page 29]. Refer to LEW-13120.

Books and Reports

These reports, studies, and handbooks are available from NASA as Technical Support Packages (TSP's) when a Request Card number is cited; otherwise they are available from the National Technical Information Service.

Making Latex Microspheres in Space

Equipment yields larger, more uniform particles.

Two NASA reports describe the first commercial product to be manufactured in space. The product is monodisperse latex, a suspension of spherical particles of essentially the same diameter. Carried aboard the Space Shuttle on its orbital missions, a monodisperse latex reactor (MLR) produces spheres of much larger size than is possible on Earth. Microspheres 30 μm in diameter have been produced, whereas 5 μm are the limit for Earthbound reactors. Microspheres as large as 100 μm are scheduled for production in the MLR.

The MLR-manufactured particles are highly uniform. The standard deviation in their diameter is less than 1.4 μm .

Latexes made on Earth lose their monodisperse character when the particle diameter gets much above 5 μm because the suspension starts to separate.

The reacting compounds float to the surface or drop to the bottom of the reactor under the influence of gravity, and particles of widely varying size result. Stirring the mixture does not help to maintain the suspension; it only coagulates the particles into an amorphous mass. In the nearly zero gravity of a Space Shuttle orbit, however, flotation and sedimentation do not occur, and particles can grow to larger sizes without losing their uniformity.

The monodisperse latexes from space are offered for sale by the National Bureau of Standards to research workers around the world as standards for microsphere size. They can be used for calibrating optical and electron microscopes, laser light-scattering apparatus, and many other kinds of laboratory equipment. They may also find use as probes for determining membrane pore size and as carriers for pharmaceuticals, tracer chemicals, or biological species in which particle volume and surface area must be accurately controlled.

The MLR consists of a boxlike support-electronics package and a drumlike experimental-apparatus container. The container holds four independent reactors, each of which produces a batch of 100 ml of latex during a flight by seeded-emulsion polymerization. The reactors are loaded before a launch with latex ingredients chosen to produce the requisite particle size. Once the Space Shuttle is in orbit, the crew turns on the reactors, and the reactions proceed automatically.

Each reactor is a small hollow steel cylinder with a stirrer at one end and a

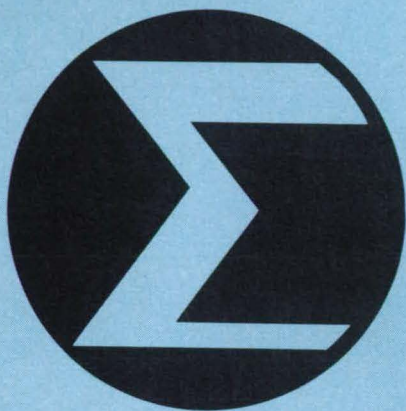
piston at the other. The piston moves to accommodate expansion and contraction of the contents as the reaction progresses. Heating tape wrapped around a reactor supplies heat in accordance with a temperature/time profile programed in a microprocessor controller. After 20 h, polymerization is complete, and the reactors turn themselves off. A linear variable-differential transformer on the piston and thermocouples on the heating tape send volume and temperature data to a recorder in the support-electronics package.

The reaction converts liquid styrene monomer into hard, colorless polystyrene spheres. The initiator is azobisisobutyronitrile (AIBN). When heated to 70° C, AIBN decomposes into two radicals plus a molecule of nitrogen gas. The secondary carbon atom in the radicals is highly reactive and adds a styrene molecule to itself. This composite molecule adds another styrene molecule and so forth, building a long, linear chain of styrene units. Growth stops when the chain meets another growing chain or a radical.

Billions of these long chains of polystyrene are formed inside latex seed particles introduced into the initiator. The particles thus swell to the required larger size.

This work was done by Dale M. Kornfeld of Marshall Space Flight Center and J. W. Vanderhoff, M. S. El-Aasser, F. J. Micala, E. D. Sudol, C. M. Tseng, and A. Silwanowicz of Lehigh University. To obtain copies of the report "Production of Large-Particle-Size Monodisperse Latexes," and "Monodisperse Latex Reactors," Circle 63 on the TSP Request Card. MFS-27085

Mathematics & Information Services



Hardware, Techniques, and Processes

146 Simplified Decoding of Convolutional Codes

Books & Reports

146 Report on Computer Programs for Robotic Vision

Computer Programs

106 Shaded-Color Picture Generation of Computer-Defined Arbitrary Shapes

Simplified Decoding of Convolutional Codes

Some complicated intermediate steps are shortened or eliminated.

NASA's Jet Propulsion Laboratory, Pasadena, California

The decoding of convolutional error-correcting digital codes is simplified by a new error-trellis syndrome technique. Existing decoding algorithms combined with new mathematical identities reduce the number of combinations of errors that have to be considered and enable the computation of the correction vector directly from the data and check bits as received.

In decoding a convolutional binary error-correcting code, the decoder must decide, on the basis of probabilities, whether the correct value of each digit received is zero or one. This decision is made according to an algorithm that operates on the sequence of a specified number of digits leading up to the present digit. Since the decision also had to be made and may yet have to be revised for each preceding digit in the sequence, the present assumed value can be represented as being connected to the previous values through a tree formed by the alternative decision paths.

Traditionally, the determination of the error pattern and the selection of the path through the decision tree have involved the intermediate step of computing a syndrome vector. The syndrome vector consists of all zeros if the assumed sequence satisfies the constraints of the code. If the syndrome vector is not zero, however, it

does not provide the correction vector (the sequence of correction digits) directly. Starting with the syndrome, it is still necessary to engage in a complicated search for the error locations in the tree.

In the new technique, the syndrome vector is not computed. Instead, advantage is taken of newly-derived mathematical identities that simplify the decision tree, folding it back on itself into a form called the "error trellis." This trellis is a graph of all path solutions of the syndrome equations. Each path through the trellis corresponds to a specific set of decisions as to the received digits.

The path for which the error pattern includes the minimum number of corrections to the previously-assumed digit sequence is considered to be the maximum-likelihood path through the trellis. The correction vector corresponding to the maximum-likelihood path is applied to the previously assumed sequence, and the result is adopted as the newly assumed sequence of digits; that is, the corrected version of the noisy received message.

This work was done by Trieu-Kie Truong and Irving S. Reed of Caltech for NASA's Jet Propulsion Laboratory. For further information, Circle 19 on the TSP Request Card.
NPO-16514

Books and Reports

These reports, studies, and handbooks are available from NASA as Technical Support Packages (TSP's) when a Request Card number is cited; otherwise they are available from the National Technical Information Service.

Report on Computer Programs for Robotic Vision

A collection of programs supports robotic research.

A report describes the computer-vision software library at NASA's Jet Propulsion Laboratory. The programs have evolved

during the past 10 years of research into robotics. The collection includes low- and high-level image-processing software that has been proved in applications ranging from factory automation to spacecraft tracking and grappling.

The programs fall into several overlapping categories. In the image utilities category are low-level routines that provide computer access to image data and some simple graphical capabilities for displaying the results of image processing. They include routines for the following:

- The input, output, and transfer of image data;
- Camera selection;
- Programming a pipeline image processor called the IMFEX (for Image Feature EXtractor);
- Cursor control; and
- Interactive manipulation or generation of image data.

In the feature-extraction category are routines that extract image features based solely on the two-dimensional data array:

- Clustering algorithms extract regions from images based on properties (for example, brightness) of neighboring picture elements.
- Convolution algorithms transform the image array (for example, to enhance contrasts) by performing the same set of operations on the picture elements in a small window centered on each picture element in the image.
- A stereo correlation algorithm obtains the three-dimensional coordinates of points.

A camera-calibration program, based on a standard perspective transformation, is used to make three-dimensional measurements. The stereoscopic cameras of the robotic system are calibrated empirically by viewing several known three-dimensional points and recording the coordinates of the corresponding image points. These data are then used to solve for the camera-model parameters using least-squares techniques.

Coordinate-transformation routines perform a variety of functions involving the camera calibration. The two basic functions are the computation of the image coordinates of a given three-dimensional point and the computation of the ray containing all the three-dimensional points that have a given pair of image coordinates. Additional functions are defined by imposing various three-dimensional constraints.

The programs for the acquisition and tracking of objects provide the visual-data feedback needed for robotic control in changing scenes. These include programs for correlating successive images, label tracking for remote-manipulator control, object tracking with trajectory prediction, and finding a known moving object to begin tracking it. Some applications include grasping moving objects with a robot arm, obstacle avoidance by an autonomous vehicle, landmark navigation, and spacecraft-docking maneuvers. The basic requirement in such applica-

tions is fast processing to keep up with the standard television frame rates of 30 Hz (interlaced) or 60 Hz (noninterlaced). This, in turn, requires powerful image-processing hardware and powerful pipeline processors like the IMFEX.

This work was done by Robert T. Cunningham and Edwin P. Kan of Caltech for NASA's Jet Propulsion Laboratory. To obtain a copy of the report, "JPL Robotics Laboratory Computer Vision Software Library," Circle 91 on the TSP Request Card.
NPO-16565

WHAT CORROSIVE ENVIRONMENTS DO TO SOME METALS, AN IVADIZER® COATING STOPS COLD.

The Ivadizer aluminum coating process, developed to protect critical parts of military aircraft, will plate complex metal parts of any size with a dense, adherent, protective aluminum coating of uniform thickness. It does so economically and without pollution problems.

With the Ivadizer process, ionized aluminum vapor bombards the part forming a tough, protective shield providing "sacrificial" corrosion resistance. A one mil coating protects steel for more than 7,500 hours in a neutral salt spray environment. In addition, there are no embrittlement problems, and the coating can be used at temperatures to 925° F.

For all the facts about the Ivadizer coating process, write to D.E. Muehlberger, McDonnell Aircraft Company, Dept. 357, P.O. Box 516, St. Louis, MO 63166. Or call (314) 232-5859.





Hardware, Techniques, and Processes

148 Visual-Accommodation Trainer/Tester

Books & Reports

149 Spring Small Grains Area Estimation

Visual-Accommodation Trainer/Tester

Ophthalmic instrument tests and helps develop focusing ability.

Ames Research Center, Moffett Field, California

An ophthalmic instrument provides four functions: (1) it measures the visual near and far points; (2) it provides a focus stimulus in vision research; (3) it measures the visual-accommodation resting position; and (4) it can be used to train for volitional control of a person's focus response.

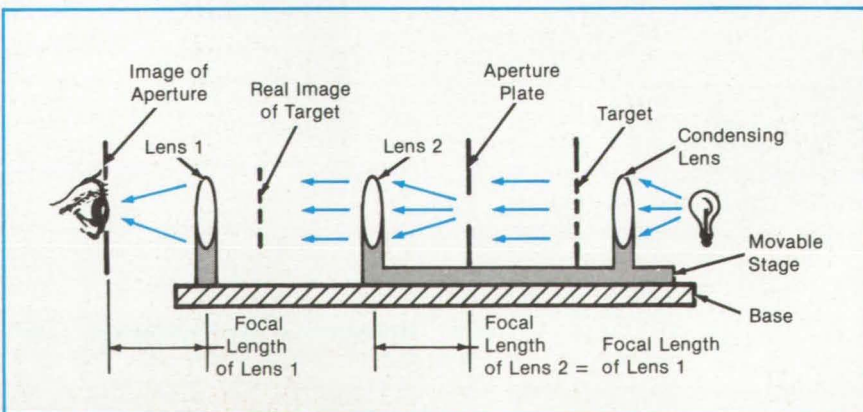
A pair of lenses, an aperture plate, a transparent target, and a target back-light source are mounted on a stage that can be moved along a baseplate (see figure). The aperture is at the focal plane of lens 2; therefore, the light rays from the aperture are collimated and impinge on lens 1 as a plane wave front. Lens 1 brings the image of the aperture to a focus at its left-hand focal plane. The subject's eye is positioned so that its entrance pupil is in this plane and coincident with the aperture image. This provides a nonintrusive artificial pupil of selectable size.

The target, a thin vertical luminous line on a dark background, is imaged a fixed distance to the left of lens 2. The image of the line is then the object for lens 1. Lens 1, with the eye at its second focal plane, forms a Badal subjective optometer. The dioptric power required by the eye is a linear function of the distance of the target image to the right of lens 1. Thus, to vary the power required at the eye, the movable stage is simply moved to the right and left. A dioptric scale is inscribed on the baseplate.

A mechanism is provided to quickly change aperture sizes. Three are selectable: (1) a wide-open, 8-mm circular hole, (2) a 0.3-mm circular hole, and (3) two 0.5-mm apertures placed side-by-side. The first is for using the system as a Badal optometer to measure and to stimulate the eye. The second is used to provide a large depth of focus (as in a pin-hole camera) and "open the accommodation loop." This provides a measurement of the resting position and allows the subject access to the control of his/her own focus. The third may be used in measurement as an alternate to the wide-open aperture. When the subject is not in the same focus as that of the trainer/tester, the image of the luminous line will be laterally split into two vertical, luminous lines by the two 0.5-mm apertures.

For the training application, apertures 2 and 3 are alternated. A defocused, split image is provided to the subject and he/she attempts to bring the images together without moving the stage. Aperture 2 can alternately be selected so the subject can practice, open loop, with brief returns to aperture 3 to check on progress in fusing the split images of the luminous line.

This work was done by Robert J. Randle, Jr., of Ames Research Center. For further information, Circle 24 on the TSP Request Card. ARC-11426



The **Movable Stage** on a fixed base permits adjustment of the effective target position as perceived by the subject. Various apertures can be used to perform tests and training procedures.

Books and Reports

These reports, studies, and handbooks are available from NASA as Technical Support Packages (TSP's) when a Request Card number is cited; otherwise they are available from the National Technical Information Service.

Spring Small Grains Area Estimation

SSG3 automatically estimates the acreage of spring small grains from Landsat data.

A report describes the development and testing of a computerized technique for using Landsat multispectral scanner (MSS) data to estimate the acreage of spring small grains (wheat, barley, and oats). The application of this technique to the analysis of four years of data from the United States and Canada yielded estimates of accuracy comparable to those obtained through procedures that rely on trained analysts. An analysis of errors showed that even higher accuracy is conceivable if the sample segments are assigned proper growing degree-day models so that the data acquisitions can be correctly designated.

The Landsat MSS data-analysis techniques of interest were developed during the Large Area Crop Inventory Experiment (LACIE), carried out during 1974-77. These techniques provided monthly harvest estimates that were within 10 percent of the U.S. Department of Agriculture crop estimates, with a confidence level of 90 percent. These results depended heavily on well-trained analysts and on an intricate system of quality assurance and teamwork.

A major goal of the Agriculture and Resources Inventory Surveys Through Aerospace Remote Sensing (AgRISTARS) program, initiated in 1980, was to ascertain whether the analysis procedure could be automated at a reduced cost, while the accuracy was maintained comparable to that reached in the analyst-intensive LACIE. Developed to meet this objective, the SSG3 is an expert system for the classification of remotely-sensed digital images.

The input data for this hierarchical procedure consists of from three to eight temporally spaced Landsat MSS acquisitions collected over a 5- by 6-nautical-mile (9.3- by 11.1-km) sample segment (177 lines, each containing 196 picture elements). The Kauth-Thomas transformation is applied to the four-channel MSS data before applying the procedural logic. The end products of this transformation are numerical values of greenness, brightness, yellowness, and nonesuch. The greenness value is stabilized by the subtraction of the greenness of bare soil from the greenness assigned to each picture element. The result is the green number, the temporal variation of which is used to determine the threshold values for the logic of the spring small grains used in the SSG3 procedure.

A systematic sample of 897 picture elements (every fifth line and sample) is selected from the segment for labeling. Samples are labeled by decision logic de-

signed to exploit the temporal behavior of picture elements. The inferences that lead to a label for each picture element are based on characteristic temporal/spectral patterns that were determined by expert analysts to be significant for distinguishing between the spring small grains and other classes of vegetation present in the scene.

This work was done by Wesley F. Palmer and Robert J. Mohler of Lockheed Engineering & Management Services Co., Inc., for Johnson Space Center. To obtain a copy of the report, "Test of an Automatic Procedure for Estimating Spring Small Grains Acreage from Landsat Data," Circle 43 on the TSP Request Card.

Inquiries concerning rights for the commercial use of this invention should be addressed to the Patent Counsel, Johnson Space Center [see page 29]. Refer to MSC-20973.

What's Your Angle?

Sperry's new AccuStar electronic clinometer is the low cost answer for your angle measurement applications. Not just another angle sensor, the AccuStar is a precise, gravity-referenced clinometer featuring:

- Outstanding performance – resolution to 1 arc sec., linearity within 1 percent.
- Simple integration – your choice of digital or analog I/O
- Economy – priced under \$100



Sperry Corporation
Aerospace & Marine Group
Sensing Systems
P.O. Box 21111
(MS DV-2)
Phoenix, AZ
85036-1111.
(800) 545-3243.

© SPERRY CORPORATION 1985

Subject Index

A

ACOUSTIC MEASUREMENT
Acoustic/magnetic stress sensor
page 112 LAR-13320

ADDITIVES
Heat- and radiation-resistant lubricants for metals
page 92 NPO-16341

AERODYNAMIC CHARACTERISTICS
Aerodynamic characteristics of NACA 16-series airfoils
page 104 LAR-13355

Predicting vortex shedding in supersonic flow
page 106 LAR-13375

AERODYNAMIC CONFIGURATIONS
Helicopter tail-boom strakes
page 132 LAR-13233

Second-order-potential analysis and optimization
page 107 LAR-13314

AERODYNAMICS
Nonconical relaxation for supersonic potential flow
page 102 LAR-13346

Predicting wall modifications for adaptive wind tunnels
page 106 LAR-13301

AERODYNAMICS INTERFERENCE
Wall interference in two-dimensional wind tunnels
page 104 LAR-13394

AGRISTARS PROJECT
Spring small grains area estimation
page 149 MSC-20973

AIR SAMPLING
Solid-sorbent air sampler
page 68 MSC-20653

AIR TRAFFIC CONTROL
Video processor for transponder pulses
page 42 KSC-11155

AIRCRAFT DESIGN
Shaded color picture generation of computer-defined arbitrary shapes
page 107 ARC-11496

AIRCRAFT LANDING
Aircraft takeoff and landing analysis
page 102 LAR-13390

AIRCRAFT MODELS
Thermoplastic composites for research-model components
page 140 LAR-13348

AIRFOILS
Aerodynamic characteristics of NACA 16-series airfoils
page 104 LAR-13355

ALLOYS
Fundamentals of alloy solidification
page 93 LEW-14229

AMMONIA
Detoxification of Halon fire-extinguishant products
page 82 MSC-20962

ANTENNAS
Cross-array antenna with switched steering
page 38 MSC-20889

ATOMIC BEAMS
High-flux atomic-oxygen source
page 66 NPO-16640

ATTITUDE GYROS
Blending gyro signals to improve control stability
page 55 MSC-20370

AUDIO EQUIPMENT
Adjustable headband for earphones
page 32 KSC-11322

B

BEVERAGES
Device for extracting flavors and fragrances
page 118 MSC-20761

BINARY CODES
Simplified decoding of convolutional codes
page 146 NPO-16514

BIREFRINGENCE
Electro-optical tuning of Fabry-Perot interferometers
page 72 GSC-12971

BODY-WING AND TAIL CONFIGURATIONS
Second-order-potential analysis and optimization
page 107 LAR-13314

BOLTS
Finite-element fracture analysis of pins and bolts
page 110 MFS-28061

BONDING
Heat bonding of irradiated ethylene vinyl acetate
page 139 MSC-20320

BOULES
Crystal-growing crucible to suppress convection
page 142 NPO-16597

BOUNDARY LAYER FLOW
Wall interference in two-dimensional wind tunnels
page 104 LAR-13394

BUBBLE MEMORY DEVICES
Fast initialization of bubble-memory systems
page 52 LAR-13357

C

CALIBRATING
Making latex microspheres in space
page 145 MFS-27085

CAMBER
Second-order-potential analysis and optimization
page 107 LAR-13314

CANNING
Void-free lid for food packaging
page 143 MSC-20661

CARBON FIBER REINFORCED PLASTICS
Thermoplastic composites for research-model components
page 140 LAR-13348

CARBON FIBERS
Carbon shields for intercalated fiber conductors
page 86 LEW-14063

CARBORANE
Phosphazene polymers containing carborane
page 83 ARC-11487

CASTING
Transfer casting from ion-beam-textured surfaces
page 144 LEW-13120

CERAMIC COATINGS
Impact-resistant ceramic coating
page 86 MSC-20829

CERAMICS
Composite refractory felt/ceramic material
page 93 LEW-14238

Si_3N_4 -based ceramic with greater hot strength
page 80 LEW-14193

CIRCUIT BOARDS
Ejection mechanism for circuit boards
page 46 MSC-20763

CLOSED CIRCUIT TELEVISION
Laser ranging system
page 59 MSC-20870

COAL LIQUEFACTION
Pressure-letdown machine for a coal reactor
page 131 NPO-15083

COATINGS
Anti-soiling coatings for solar-energy devices
page 90 NPO-16552

Impact-resistant ceramic coating
page 86 MSC-20829

COGENERATION
Pressure-letdown machine for a coal reactor
page 131 NPO-15083

COMBUSTION CHAMBERS
Composite refractory felt/ceramic material
page 93 LEW-14238

COMPOSITE MATERIALS
Intrapy hybrid composite design
page 94 LEW-14079

COMPRESSORS
Oil-free compressor
page 130 MSC-20860

COMPUTER GRAPHICS
Shaded color picture generation of computer-defined arbitrary shapes
page 107 ARC-11496

COMPUTER PROGRAMS
Rendezvous BET program
page 98 MSC-20785

COMPUTERIZED SIMULATION
Predicting vortex shedding in supersonic flow
page 106 LAR-13375

COMPUTERIZED DESIGN
Two programs for supersonic wing design and analysis
page 106 LAR-13239

CONDUCTIVE HEAT TRANSFER
Comparative thermal-conductivity test technique
page 75 MSC-20980

CONDUCTORS
Carbon shields for intercalated fiber conductors
page 86 LEW-14063

CONTROL EQUIPMENT
Controlling arc length in plasma welding
page 141 MSC-20900

COOLING SYSTEMS
Heat-pipe array for large-area cooling
page 64 MSC-20946

Oil-free compressor
page 130 MSC-20860

CRACK PROPAGATION
Fatigue-crack-growth structural analysis
page 102 LAR-13412

CROP INVENTORIES
Spring small grains area estimation
page 149 MSC-20973

CRYOGENIC WIND TUNNELS
Increasing the cryogenic toughness of steels
page 85 LAR-13376

CRYSTAL GROWTH
Crystal-growing crucible to suppress convection
page 142 NPO-16597

D

DAMPERS
Variable-force eddy-current damper
page 120 LEW-13717

DATA CONVERTERS
Digital signal combining for conference calling
page 50 KSC-11285

DATA RECORDING
Synchronization of data recorded on different tracks
page 56 NPO-16555

DATA STORAGE
Fast initialization of bubble-memory systems
page 52 LAR-13357

DECODING
Simplified decoding of convolutional codes
page 146 NPO-16514

DEHYDRATED FOOD
Void-free lid for food packaging
page 143 MSC-20661

DELAY CIRCUITS
Switched-multibeam antenna system
page 59 MSC-20873

DESIGN ANALYSIS
Programming structural synthesis system
page 100 LAR-13408

DIGITAL SIMULATION
Shaded color picture generation of computer-defined arbitrary shapes
page 107 ARC-11496

Simulation of PCM data
page 63 KSC-11239

DIRECT CURRENT
A 25-kW series-resonant power converter
page 49 LEW-14197

DIRECTIONAL ANTENNAS
Switched-multibeam antenna system
page 59 MSC-20873

DISTANCE MEASURING EQUIPMENT
Laser ranging system
page 59 MSC-20870

DRAG CHUTES
Stable ejection seat
page 109 MSC-20780

DYNAMIC PRESSURE
Dynamic pressure calibration standard
page 116 LAR-13443

DYNAMIC RESPONSE
Vibration-response analysis
page 100 LAR-13291

E

EARPHONES
Adjustable headband for earphones
page 32 KSC-11322

EARTH ORBITAL RENDEZVOUS
Rendezvous BET program
page 98 MSC-20785

EDDY CURRENTS
Variable-force eddy-current damper
page 120 LEW-13717

EJECTION SEATS
Stable ejection seat
page 109 MSC-20780

ELECTROMAGNETIC WAVE FILTERS
Electro-optical tuning of Fabry-Perot interferometers
page 72 GSC-12971

ELECTRON MICROSCOPES
Mapping the structure of heterogeneous materials
page 70 NPO-16487

ELECTRONIC PACKAGING
Ejection mechanism for circuit boards
page 46 MSC-20763

ELECTROPLATING
Metalizing solar cells by selective electroplating
page 144 NPO-16600

ERROR CORRECTING CODES
Simplified decoding of convolutional codes
page 146 NPO-16514

EVAPORATIVE COOLING
Heat-pipe array for large-area cooling
page 64 MSC-20946

F

FABRY-PEROT INTERFEROMETERS
Electro-optical tuning of Fabry-Perot interferometers
page 72 GSC-12971

FAILURE MODES
Compression-failure mechanisms in composite laminates
page 80 LAR-13345

FASTENERS
Quick-connect heavy-duty fastener
page 108 NPO-16370

FATIGUE (MATERIALS)
Fatigue-crack-growth structural analysis
page 102 LAR-13412

FIBER OPTICS
Optical monitoring of weld penetration
page 142 MFS-29107

FILM THICKNESS
Measuring water-layer thickness
page 115 LAR-13347

FINAL ELEMENT METHODS
Programming structural synthesis system
page 100 LAR-13408

FIRE EXTINGUISHERS
Detoxification of Halon fire-extinguishant products
page 82 MSC-20962

FLIGHT CONTROL
Blending gyro signals to improve control stability
page 55 MSC-20370

FLOW EQUATIONS
Nonconical relaxation for supersonic potential flow
page 102 LAR-13346

Predicting wall modifications for adaptive wind tunnels
page 106 LAR-13301

FLOW REGULATORS
Variable control port for fluidic control device
page 114 NPO-16603

FLUID JETS
Analysis of lubricant jet flow
page 104 LEW-14242

FLUIDICS
Variable control port for fluidic control device
page 114 NPO-16603

FLUOROPOLYMERS
Anti-soiling coatings for solar-energy devices
page 90 NPO-16552

FOCUSING
Visual-Accommodation Trainer/Tester
page 148 ARC-11426

FOURIER TRANSFORMATION
Three-dimensional radiative-transfer equation
page 76 NPO-16563

G

GAIN (AMPLIFICATION)
TV video-level controller
page 62 MSC-18578

GALLIUM ARSENIDE LASERS
Positive-index guiding in CDH-LOC lasers
page 40 LAR-13312

GAS ANALYSIS
Solid-sorbent air sampler
page 68 MSC-20653

GAS BEARINGS
Air-bearing table for machine shops
page 134 MFS-29035

GEARS
Analysis of lubricant jet flow
page 104 LEW-14242

GRAPHITE-EPOXY COMPOSITES
Compression-failure mechanisms in composite laminates
page 80 LAR-13345

H

HALOCARBONS
Detoxification of Halon fire-extinguishant products
page 82 MSC-20962

HEADSETS
Adjustable headband for earphones
page 32 KSC-11322

HEAT PIPES

Heat-pipe array for large-area cooling
page 64 MSC-20946

Variable-conductance heat pipes
page 100 LEW-14075

HEAT TRANSFER

Comparative thermal-conductivity test technique
page 75 MSC-20980

HEAT TREATMENT

Increasing the cryogenic toughness of steels
page 85 LAR-13376

HEATING

Shadowed space heating of sparse structures
page 98 LEW-13977

HELICOPTER DESIGN

Helicopter tail-boom strakes
page 132 LAR-13233

HIGH STRENGTH STEELS

Increasing the cryogenic toughness of steels
page 85 LAR-13376

HIGH TEMPERATURE LUBRICANTS

Heat- and radiation-resistant lubricants for metals
page 92 NPO-16341

HOLOGRAPHIC INTERFEROMETRY

Recording interferograms holographically
page 74 MFS-26024

I**IMAGE PROCESSING**

Report on computer programs for robotic vision
page 146 NPO-16565

IMPACT RESISTANCE

Impact-resistant ceramic coating
page 86 MSC-20829

INFRARED DETECTORS

Correcting for nonlinearity in a photodetector
page 47 NPO-16055

INSTRUMENT ORIENTATION

Ball-and-socket mount for instruments
page 78 MFS-28064

INSULATING MATERIALS

Impact-resistant ceramic coating
page 86 MSC-20829

INTERROGATION

Video processor for transponder pulses
page 42 KSC-11155

ION BEAMS

Partial-transmission scintillation detector for ions
page 68 NPO-16501

IRISES (MECHANICAL APERTURES)

TV video-level controller
page 62 MSC-18578

J**JET MIXING FLOW**

Mixer analysis of nacelle/nozzle flow
page 117 LEW-14073

JOINTS (JUNCTIONS)

Heat bonding of irradiated ethylene vinyl acetate
page 139 MSC-20320

K**KALMAN FILTERS**

Rendezvous BET program
page 98 MSC-20785

L**LABYRINTH SEALS**

Improved seal for NTF fan shaft
page 127 LAR-13218

LANDING SIMULATION

Aircraft takeoff and landing analysis
page 102 LAR-13390

LANDSAT SATELLITES

Spring small grains area estimation
page 149 MSC-20973

LASER INTERFEROMETRY

Recording interferograms holographically
page 74 MFS-26024

LASER RANGER/TRACKER

Laser ranging system
page 59 MSC-20870

LASERS

Positive-index guiding in CDH-LOC lasers
page 40 LAR-13312

LATEX

Making latex microspheres in space
page 145 MFS-27085

Producing large-particle monodisperse latexes
page 87 MFS-26026

LAYOUTS

Multipurpose scribing and drawing tool
page 119 MSC-20913

LEAKAGE

Wind-tunnel-model leak-checking system
page 58 LAR-13449

LINEAR CIRCUITS

Linear phase modulator
page 34 MSC-20555

LOADS (FORCES)

Three-axis load-cell assembly
page 111 MSC-20875

LOW GRAVITY MANUFACTURING

Device for extracting flavors and fragrances
page 118 MSC-20761

Fundamentals of alloy solidification
page 93 LEW-14229

LUBRICANTS

Heat- and radiation-resistant lubricants for metals
page 92 NPO-16341

LUBRICATION

Analysis of lubricant jet flow
page 104 LEW-14242

M**MACH-ZEHNDER INTERFEROMETERS**

Recording interferograms holographically
page 74 MFS-26024

MACHINING

Air-bearing table for machine shops
page 134 MFS-29035

MAGNETIC MEASUREMENT

Acoustic/magnetic stress sensor
page 112 LAR-13320

MAGNETIC TAPES

Synchronization of data recorded on different tracks
page 56 NPO-16555

MAGNETRON SPUTTERING

Room-temperature deposition of NBN superconducting films
page 84 NPO-16681

MANIPULATORS

Gentle end effector for robots
page 128 MFS-28119

MATERIALS HANDLING

Air-bearing table for machine shops
page 134 MFS-29035

Automated conduit unloading
page 129 NPO-16187

MATRICES (MATHEMATICS)

Three-dimensional radiative-transfer equation
page 76 NPO-16563

MEASURING INSTRUMENTS

Multipurpose scribing and drawing tool
page 119 MSC-20913

Three-axis load-cell assembly
page 111 MSC-20875

MECHANICAL MEASUREMENT

Matching vibration testing to "real world" conditions
page 113 MSC-20665

MECHANICAL PROPERTIES

Intrinsically hybrid composite design
page 94 LEW-14079

Si₃N₄-based ceramic with greater hot strength
page 80 LEW-14193

MERCURY CADMIUM TELLURIDES

Correcting for nonlinearity in a photodetector
page 47 NPO-16055

METALIZING

Metalizing solar cells by selective electroplating
page 144 NPO-16600

METALLOGRAPHY

Fundamentals of alloy solidification
page 93 LEW-14229

Microdensitometers Mapping the structure of heterogeneous materials
page 70 NPO-16487

Microstructure Transfer casting from ion-beam-textured surfaces
page 144 LEW-13120

Microwave antennas Switched-multibeam antenna system
page 59 MSC-20873

MISSILES

Predicting vortex shedding in supersonic flow
page 106 LAR-13375

Mixing Mixer analysis of nacelle/nozzle flow
page 117 LEW-14073

Modulation Linear phase modulator
page 34 MSC-20555

Moisture meters Measuring water-layer thickness
page 115 LAR-13347

Monitors Optical monitoring of weld penetration
page 142 MFS-29107

Mounting Ball-and-socket mount for instruments
page 78 MFS-28064

N**NONDESTRUCTIVE TESTS**

Mapping the structure of heterogeneous materials
page 70 NPO-16487

Nonflammable materials Phosphazene polymers containing carborane
page 83 ARC-11487

Nozzle flow Mixer analysis of nacelle/nozzle flow
page 117 LEW-14073

NUTS (FASTENERS)

Quick-connect heavy-duty fastener
page 108 NPO-16370

O**OPEN CIRCUIT VOLTAGE**

Improved high/low junction silicon solar cells
page 48 LEW-13618

OPHTHALMOLOGY

Visual-Accommodation Trainer/Tester
page 148 ARC-11426

OPTICAL DATA PROCESSING

Report on computer programs for robotic vision
page 146 NPO-16565

OPTICAL MEASUREMENT

Stress measurement by geometrical optics
page 114 LEW-14169

Optical waveguides Positive-index guiding in CDH-LOC lasers
page 40 LAR-13312

Orbital rendezvous Rendezvous BET program
page 98 MSC-20785

Oxygen atoms High-flux atomic-oxygen source
page 66 NPO-16640

P**PACKAGING**

Void-free lid for food packaging
page 143 MSC-20661

PARACHUTES

Stable ejection seat
page 109 MSC-20780

PARTICLES

Producing large-particle monodisperse latexes
page 87 MFS-26026

Phase modulation Linear phase modulator
page 34 MSC-20555

Phased arrays Cross-array antenna with switched steering
page 38 MSC-20889

PHOSPHORUS POLYMERS

Phosphazene polymers containing carborane
page 83 ARC-11487

Photoconductive cells Correcting for nonlinearity in a photodetector
page 47 NPO-16055

Photodetachment High-flux atomic-oxygen source
page 66 NPO-16640

Photoelastic analysis Compression-failure mechanisms in composite laminates
page 80 LAR-13345

Piezoelectric transducers Broadband ultrasonic transducers
page 47 NPO-16590

Pins Finite-element fracture analysis of pins and bolts
page 110 MFS-28061

Pipes (tubes) Automated conduit unloading
page 129 NPO-16187

Plasma arc welding Controlling arc length in plasma welding
page 141 MSC-20900

Plastics Heat bonding of irradiated ethylene vinyl acetate
page 139 MSC-20320

POLISHING

Ion-deposited polished coatings
page 138 LEW-13545

POWER SUPPLY CIRCUITS

A 25-kW series-resonant power converter
page 49 LEW-14197

Bidirectional dc-to-dc power converter
page 40 MFS-28095

Pressure sensors Dynamic pressure calibration standard
page 116 LAR-13443

Printed circuits Ejection mechanism for circuit boards
page 46 MSC-20763

Propeller efficiency Aerodynamic characteristics of NACA 16-series airfoils
page 104 LAR-13355

Propellers Electromechanical turboprop-pitch-control mechanism
page 134 LEW-14234

Protective coatings Carbon shields for intercalated fiber conductors
page 86 LEW-14063

Pulse code modulation Simulation of PCM data
page 63 KSC-11239

Q

Quartz transducers Dynamic pressure calibration standard
page 116 LAR-13443

R

Radiation hardening Lithium-counterdoped solar cells
page 43 LEW-14177

Radiation measuring instruments Partial-transmission scintillation detector for ions
page 68 NPO-16501

Radiative transfer Three-dimensional radiative-transfer equation
page 76 NPO-16563

Read-only memory devices Fast initialization of bubble-memory systems
page 52 LAR-13357

Reduced gravity Operating a remote manipulator in simulated low gravity
page 137 NPO-16477

Refractory coatings Composite refractory felt/ceramic material
page 93 LEW-14238

Refractory materials Si₃N₄-based ceramic with greater hot strength
page 80 LEW-14193

Refrigerating machinery Oil-free compressor
page 130 MSC-20860

Remote manipulator systems Operating a remote manipulator in simulated low gravity
page 137 NPO-16477

Robots Solid-sorbent air sampler
page 68 MSC-20653

Space manufacturing Making latex microspheres in space
page 145 MFS-27085

Spacecraft power supplies Lithium-counterdoped solar cells
page 43 LEW-14177

S**SATELLITE TEMPERATURE**

Shadowed space heating of sparse structures
page 98 LEW-13977

Scintillation counters Partial-transmission scintillation detector for ions
page 68 NPO-16501

Scoring Multipurpose scribing and drawing tool
page 119 MSC-20913

Seals (stoppers) Improved seal for NTF fan shaft
page 127 LAR-13218

Secondary emission A process produces low-secondary-electron-emission surfaces
page 88 LEW-14130

Semiconductor junctions Improved high/low junction silicon solar cells
page 48 LEW-13618

Servomechanisms Gentle end effector for robots
page 128 MFS-28119

Shafts Improved seal for NTF fan shaft
page 127 LAR-13218

Shakers Matching vibration testing to "real world" conditions
page 113 MSC-20665

Signal mixing Blending gyro signals to improve control stability
page 55 MSC-20370

Silicon Digital signal combining for conference calling
page 50 KSC-11285

Silicon Crystal-growing crucible to suppress convection
page 142 NPO-16597

Simulators Operating a remote manipulator in simulated low gravity
page 137 NPO-16477

Size determination Producing large-particle monodisperse latexes
page 87 MFS-26026

Solar cells Anti-soiling coatings for solar-energy devices
page 90 NPO-16552

Solar cells Improved high/low junction silicon solar cells
page 48 LEW-13618

Solar cells Lithium-counterdoped solar cells
page 43 LEW-14177

Solar cells Metalizing solar cells by selective electroplating
page 144 NPO-16600

Solar heating Shadowed space heating of sparse structures
page 98 LEW-13977

Solvent extraction Device for extracting flavors and fragrances
page 118 MSC-20761

Sonar Broadband ultrasonic transducers
page 47 NPO-16590

Sorbents Solid-sorbent air sampler
page 68 MSC-20653

Space manufacturing Making latex microspheres in space
page 145 MFS-27085

Spacecraft power supplies Lithium-counterdoped solar cells
page 43 LEW-14177

SPEECH RECOGNITION
Wind-tunnel-model leak-checking system
page 58 LAR-13449

SPHERES
Making latex microspheres in space
page 145 MFS-27085

SPUTTERING
A process produces low-secondary-electron-emission surfaces
page 88 LEW-14130

Ion-deposited polished coatings
page 138 LEW-13545

Transfer casting from ion-beam-textured surfaces
page 144 LEW-13120

STATIC LOADS
Analyzing static loading of complex structures
page 98 MSC-20896

STEERABLE ANTENNAS
Cross-array antenna with switched steering
page 38 MSC-20889

STRAKES
Helicopter tail-boom strakes
page 132 LAR-13233

STRESS ANALYSIS
Analyzing static loading of complex structures
page 98 MSC-20896

Finite-element fracture analysis of pins and bolts
page 110 MFS-28061

STRESS MEASUREMENT
Acoustic/magnetic stress sensor
page 112 LAR-13320

Stress measurement by geometrical optics
page 114 LEW-14169

STRUCTURAL ANALYSIS
Analyzing static loading of complex structures
page 98 MSC-20896

Fatigue-crack-growth structural analysis
page 102 LAR-13412

Mapping the structure of heterogeneous materials
page 70 NPO-16487

STRUCTURAL DESIGN CRITERIA
Programming structural synthesis system
page 100 LAR-13408

STRUCTURAL VIBRATION
Vibration-response analysis
page 100 LAR-13291

SUPERCONDUCTORS
Room-temperature deposition of NbN superconducting films
page 84 NPO-16681

SUPERSONIC AIRFOILS
Two programs for supersonic wing design and analysis
page 106 LAR-13339

SUPERSONIC FLOW
Nonconical relaxation for supersonic potential flow
page 102 LAR-13346

Predicting vortex shedding in supersonic flow
page 106 LAR-13375

Predicting wall modifications for adaptive wind tunnels
page 106 LAR-13301

SUPPORTS
Ball-and-socket mount for instruments
page 78 MFS-28064

SYNCHRONISM
Synchronization of data recorded on different tracks
page 56 NPO-16555

TAKEOFF
Aircraft takeoff and landing analysis
page 102 LAR-13390

TELECOMMUNICATION
Simulation of PCM data
page 63 KSC-11239

TELEPHONY
Digital signal combining for conference calling
page 50 KSC-11285

TELEVISION CAMERAS
TV video-level controller
page 62 MSC-18578

TEMPERATURE CONTROL
Variable-conductance heat pipes
page 100 LEW-14075

THERMAL CONDUCTIVITY
Comparative thermal-conductivity test technique
page 75 MSC-20980

THERMAL CONDUCTORS
Variable-conductance heat pipes
page 100 LEW-14075

THERMODYNAMIC PROPERTIES
Intrinsically hybrid composite design
page 94 LEW-14079

THERMOPLASTIC RESINS
Thermoplastic composites for research-model components
page 140 LAR-13348

THIN FILMS
Stress measurement by geometrical optics
page 114 LEW-14169

THREADS
Quick-connect heavy-duty fastener
page 108 NPO-16370

THROTTLING
Variable control port for fluidic control device
page 114 NPO-16603

THYRISTORS
Bidirectional dc-to-dc power converter
page 40 MFS-28095

TRANSITION TEMPERATURE
Room-temperature deposition of NbN superconducting films
page 84 NPO-16681

TRANSONIC FLOW
Predicting wall modifications for adaptive wind tunnels
page 106 LAR-13301

TRANSPONDERS
Video processor for transponder pulses
page 42 KSC-11155

TRAVELING WAVE TUBES
A process produces low-secondary-electron-emission surfaces
page 88 LEW-14130

TURBOPROP ENGINES
Aerodynamic characteristics of NACA 16-series airfoils
page 104 LAR-13355

Electromechanical turboprop-pitch-control mechanism
page 134 LEW-14234

ULTRASONIC WAVE TRANSDUCERS
Broadband ultrasonic transducers
page 47 NPO-16590

UNLOADING
Automated conduit unloading
page 129 NPO-16187

VAPOR DEPOSITION
Ion-deposited polished coatings
page 138 LEW-13545

VARIABLE PITCH PROPELLERS
Electromechanical turboprop-pitch-control mechanism
page 134 LEW-14234

VIBRATION DAMPING
Variable-force eddy-current damper
page 120 LEW-13717

VIBRATION TESTS
Matching vibration testing to "real world" conditions
page 113 MSC-20665

VIBRATORY LOADS
Vibration-response analysis
page 100 LAR-13291

VISUAL ACCOMMODATION
Visual-Accommodation Trainer/Tester
page 148 ARC-11426

VOLTAGE CONVERTERS (DC TO DC)
A 25-kW series-resonant power converter
page 49 LEW-14197

Bidirectional dc-to-dc power converter
page 40 MFS-28095

WASTE ENERGY UTILIZATION
Pressure-letdown machine for a coal reactor
page 131 NPO-15083

WATER DEPTH
Measuring water-layer thickness
page 115 LAR-13347

WELDING
Controlling arc length in plasma welding
page 141 MSC-20900

WELDING MACHINES
Optical monitoring of weld penetration
page 142 MFS-29107

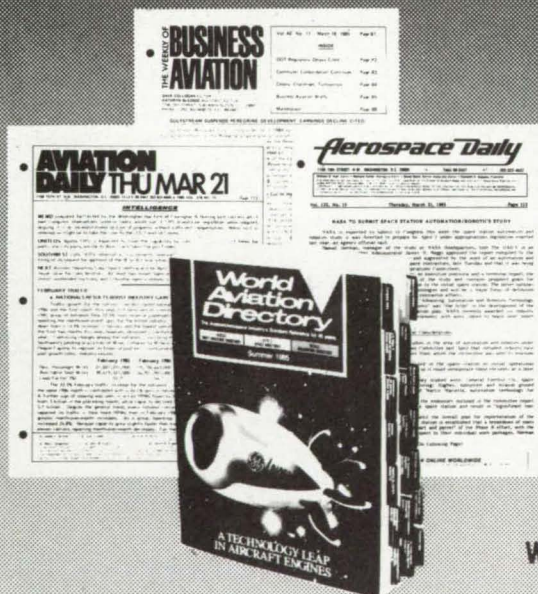
WIND TUNNEL MODELS
Wind-tunnel-model leak-checking system
page 58 LAR-13449

WIND TUNNEL WALLS
Predicting wall modifications for adaptive wind tunnels
page 106 LAR-13301

Wall interference in two-dimensional wind tunnels
page 104 LAR-13394

WINGS
Two programs for supersonic wing design and analysis
page 106 LAR-13239

X-RAY ANALYSIS
Mapping the structure of heterogeneous materials
page 70 NPO-16487



Are You a Subscriber?

The most relied-upon
"intelligence/communications"
network serving the
aviation/aerospace industry
worldwide.

Write on company letterhead or call for FREE trial subscriptions:

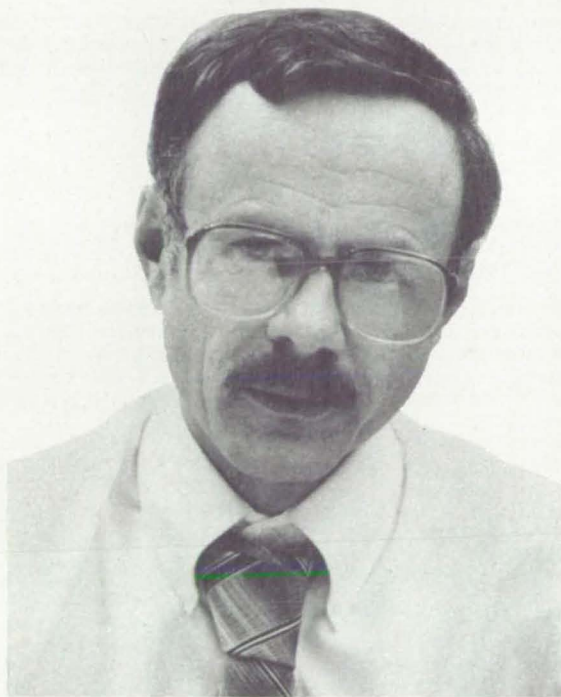
- 3 weeks of Aerospace Daily*
- 3 weeks of Aviation Daily
- 4 weeks of Business Aviation
- 30 day inspection of World Aviation Directory

*Aerospace Daily is now on-line as part of a comprehensive network of electronic databases called **Aerospace Online**. Call 202-822-4691 for a one month test at only a nominal cost.

Murdoch Magazines • 1156 15th St., NW • Washington, DC 20005 • 202-822-4600

Boundary-Breakers in Radar Systems Development

“Write to me directly. I want to tell you how you can enhance your expertise with broader systems responsibility and involvement.”



Lee Owen
Radar Systems Development Manager

“Don’t miss this opportunity to discover firsthand—right from me—why you should join Norden. I can give you the facts about what’s going on here and what you will be doing to further our systems advances.

Norden has exciting and amply-funded programs that extend well into the next decade. We’re currently involved in major projects in synthetic aperture radar, integrated displays, multimode radar, digital electronics, radar interfaces and millimeter wave systems. Our newest program award is Joint STARS . . . and the radar we develop will draw on our expertise in high-resolution, state-of-the-art radar technologies. The radar will be capable of operation from extreme standoff ranges, with higher reliability, maintainability, and supportability.

With us you’ll assume a key role in developing new architecture to meet new performance demands. You’ll work on translating broad concepts and directions of radar systems into specific functional requirements. Our total system approach from concept, development, integration and sophisticated built-in testing offers you entire system involvement. If you’re ready to go beyond established technical boundaries and have expertise in •Interface Design •Antenna Drive & Servo Control •System Requirements Definition or •System Integration & Test, let me give you a personal briefing. Contact me directly and send me your resume and salary information.

Let’s talk about our attractive location in the heart of Fairfield County, Connecticut, one of the nation’s most desirable areas . . . and our relocation package tailored to your needs.”

Send your resume in strictest confidence to: Lee Owen, Norden Systems, Inc., 350 Norden Place, P.O. Box 5300, Norwalk, CT 06856.



**UNITED
TECHNOLOGIES
NORDEN
SYSTEMS**

An Equal Opportunity Employer.
U.S. Citizenship Required.

MICROSECOND RESPONSE THERMOCOUPLES

For surface temperature applications, such as:

Internal Surface Temperatures • Pressure Vessels • Re-entry Heat Shields • Ablation Studies • Shock Tubes • Wind Tunnels • Rocket Nozzles • Bearings • Rotating Shafts • Drums, etc. • Piston Ring Temperatures • Gun Barrels • Internal Combustion Engine Walls • Materials Evaluation • Heat Transfer • Hot Moving Wires and Rods • Metal Extrusions • Stampings • Plastic Extrusion • Injection Molds • Friction Tests • Boundary Layers • Automotive Brake Bands • Glass Molding • Zinc Die Casting • High Velocity Gases •

Complete details in Section E of our Handbook. Ask for it. It's FREE!

FREE TEMPERATURE MEASUREMENT HANDBOOK/CATALOG

• Over 225 pages • More than 9000 products • Complete ANSI Calibration tables • 16 pages of application notes • 7 technical articles on transient Temperature Applications and Heat Transfer • Industrial Research and Aerospace Data Included •

Call Mass. (617) 872-4811 or TELEX 951711 for FREE Handbook

NANMAC CORPORATION
Foremost in Temperature Measurement

526 South H St., Lake Worth, FL 33460-USA
9-11 Mayhew St., Framingham Ctr., MA 01701-USA



Letters

The "Letters" column is designed to encourage a wide exchange of ideas among NASA Tech Briefs readers. To contribute a request for information or to respond to such a request, use the feedback cards in this issue, or write or call: Manager/Technology Transfer Division, P.O. Box 8757, Baltimore/Washington International Airport, MD 21240; (301) 859-5300. While we can print only a small number of letters, we will endeavor to select those that are of varied and wide interest.

FAST AND FREE

Just finished becoming exposed to your fine magazine. I was surprised to see how well written the articles were (i.e., easy for me to understand!) and how much research obviously accompanies each article.

As you know, pilots are among the most well-read citizens, due to many hours at airports waiting on our 500 m.p.h. transportation.

I also tested your publication at dispatch: I layed it down in plain view; elapsed time before it was stolen away by another line pilot—1 min., 17 sec.

Thanks for the best reading I've enjoyed in years.

John S. Cole
Line Pilot
Connie Kalitta Services
Ypsilanti, MI

STRAIGHT TALK

I object to your subscription qualification questions. You are not just another trade journal. You are an information dissemination service to your owners—the American people. No objection to advertising to offset costs, but any interested person should qualify. The emphasis on business (i.e., asking for address) is uncalled for.

Great magazine and service though!

Peter Collins
Senior Engineer
Computer Automation
Tucson, AZ

Your TSP request form instructions are not clear! They imply that since I am a subscriber I have to fill out the entire form on both sides simply to request a TSP! That is ridiculous!

Charles H. Loch
Independent Testing Labs
Boulder, CO

A number of readers have asked about the NASA Tech Briefs Subscription/Address Change/Technical Support Package Request Form. By design, the form has multi-purpose functions, but not all of them come into play each time you make a request.

Here are some guidelines to make it easier for you to make requests using the form, and easier for us to process them:

• **New Subscribers:** Complete the form in its entirety and don't forget to sign and date it.

• **Existing Subscribers:** If you request Technical Support Packages or an address change, you do not have to complete the entire form. However, indicating your T-number from your mailing label aids in the rapid processing of your request.

• **Non-Subscribers:** If you only wish to request Technical Support Packages, you do not have to complete the bottom of the form. However, all address information requested on the top of the form, down to and including a telephone number, is necessary. By indicating your T-number from the mailing label of previous requests, you can help speed the processing of your request.

• **Subscribers:** You must complete the form in its entirety once a year in order to continue to receive NASA Tech Briefs. Do this whenever you remember, at any time during the year, even if you do it more than once. This updates your subscription for another year, effective at that time. A completely filled-out form will always be processed.

There are two reasons why we request the information we do. One of them fulfills NASA's policy requirements and the other fulfills audit qualification requirements for a subscription to a commercial publication.

ARAC Finds Answers To Questions You Never Knew You Had!!

1. **IMAGINE** A resource that could provide total access to disclosed technology data worldwide.
2. **IMAGINE** That this resource is staffed with the finest scientific and engineering minds to assist you in acquiring these data.

An ARAC Technology Transfer Process Provides:

- An edited search of all relevant published technologies.
- Full texts highlighting the most significant information.
- Contacts with identified technical experts.
- Overall analysis and discussion of key findings by experienced ARAC engineers.

3. **UTILIZE ARAC** services and find the best possible answers to your technical questions at the best possible prices.

For Those Answers Contact:

Ms. Chris Schell
ARAC
611 N. Capitol Avenue
Indianapolis, IN 46204
317/262-5003

A NASA Supported Industrial Applications Center

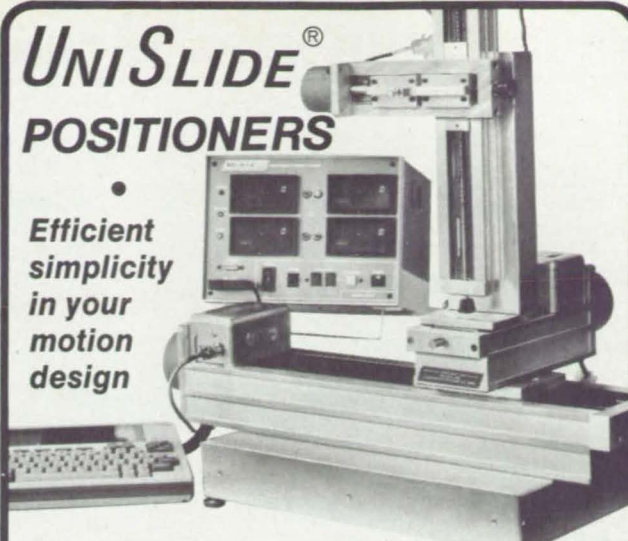
Advertiser's Index

Advanced Purification Systems, Inc.	(RAC* 434)	26
Aerospace Research Applications Center	(RAC 437)	154
Allied Corporation Synthetic		
Crystal Products	(RAC 435)	67
Andus Corporation	(RAC 436)	91
A.O. Smith Data Systems, Inc.	(RAC 426)	51
Astro-Med, Inc.	(RAC 424)	57
A T & T Technologies		36-37
Aurora Bearings	(RAC 413)	6
BEI Motion Systems, KIMCO Div.	(RAC 312)	16
Bell Helicopter Textron Inc.		133
Boeing Electronics Company	(RAC 414)	33
Brimrose Corporation of America	(RAC 415)	69
Celerity Computing	(RAC 352)	15
Collins Industrial GPS Products.		
Rockwell International	(RAC 354)	39
Control Data Corporation		
Government Systems	(RAC 439)	101
Custom Scientific Instruments, Inc.		
/subsidiary Atlas Electric Devices	(RAC 438)	155
Data General Corporation	(RAC 353)	99
Data Precision	(RAC 432, 433)	35
Du Pont-KAPTON	(RAC 399,400,401)	81, 83, 85
Eastman Kodak-Government		
Systems Division	(RAC 339)	23
EcoTech, Inc. Computer Systems	(RAC 440)	103
E G & G Electro-Optic	(RAC 431)	75
EMR Photoelectric	(RAC 356)	65
Express Systems Inc.	(RAC 346)	77
Fairchild Control Systems Co.	(RAC 357)	17
Fairchild Weston Systems, Inc.	(RAC 441)	19
Fiberite	(RAC 307)	44-45
GAF Corporation	(RAC 359)	87
General Motors Corporation		7-9
General Systems Corporation	(RAC 306)	95
Greene, Tweed & Co.	(RAC 328)	137
Grumman Data Systems	(RAC 363)	4-5
Harris Aerospace	(RAC 410)	20-21
Honeywell Inc. Space and		
Strategic Avionics Division	(RAC 364)	158, Cov III
Hughes Aircraft Company.		
Semiconductor Div.	(RAC 449)	41
IBM Information Systems	(RAC 390)	12-13
IFR Inc.	(RAC 317)	71
IMSL	(RAC 300)	30
Inland Motor,		
Specialty Products Group	(RAC 423)	135
ITT Electro-Optical Products	(RAC 403)	63
Jet Propulsion Laboratory	(RAC 442)	16
Kinetic Systems	(RAC 316)	157
Klinger Scientific Corp.	(RAC 368)	73
Leader Instruments	(RAC 443, 444)	27
Martin Marietta		Cov II-1
McDonnell Douglas Corp.	(RAC 372, 374)	147, Cov IV
Motorola Inc.,		
Government Electronics Group	(RAC 375)	61
Nanmac Corporation	(RAC 405)	154
Norden Systems Inc.		153
Pacific Scientific	(RAC 301)	25
Power Technology, Inc.	(RAC 320)	24
Pressure Systems, Incorporated	(RAC 378)	10
Racal-Dana Instruments, Inc.	(RAC 445)	53
Scanivalve Corporation	(RAC 381)	31
Schott Glass Technologies Inc.	(RAC 383)	79
Sperry Corp. Aerospace & Marine		
Group Sensing Systems	(RAC 409)	149
Symbolics	(RAC 446)	96-97
3 M Federal Systems	(RAC 422)	11
Velmex, Inc.	(RAC 447)	155
Vitro Corporation	(RAC 394)	2
World Aviation Directory		152
Wyle Laboratories Scientific		
Services & Systems Group	(RAC 396)	89
Yellow Springs Instrument Co.	(RAC 448)	117
Zenith Data Systems	(RAC 349)	105

*RAC stands for Reader Action Card. For further information on these advertisers, please circle the RAC number on the Reader Action Card elsewhere in this issue. This index has been compiled as a service to our readers and advertisers. Every precaution is taken to ensure its accuracy, but the publisher assumes no liability for errors or omissions.

UNISLIDE® POSITIONERS

Efficient
simplicity
in your
motion
design



The UniSlide system of motorized linear and rotary positioners offers versatility in automated production and quality control at a moderate cost. The modular components are easily assembled into XY, XYZ or angular configurations.

UniSlide assemblies can be equipped with AC induction or DC shunt wound motors, steppers, gear motors, speed controls, automatic reversing circuits, translators & indexers. Motorized UniSlide assemblies are made in 4 cross-sections; from 2½" x 1½" up to 9" x 3½", in lengths to 90".

VELMEX PROGRAMMABLE STEPPING MOTOR CONTROLS

Velmex Series 8300 Stepping Motor Drivers function as preset indexers with an RS-232C interface. A single intelligent control operates up to 4 motors. Where the RS-232 is not required, the low cost Series 8200 Translator/Driver can be used.

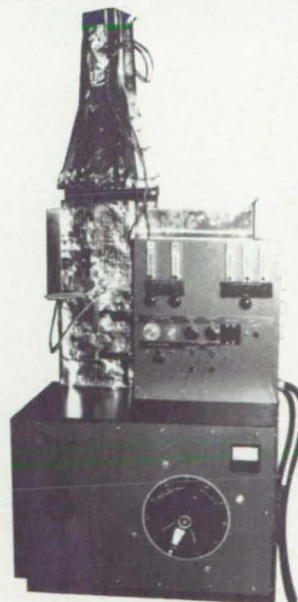
Custom Modifications to your Specifications
For more information request UniSlide Catalog M-86.

VELMEX, INC.

P.O. BOX 38
E. BLOOMFIELD, NY 14443
Telephone 716/657-6151

Circle Reader Action No. 447

Heat Release



Heat Release Rate Apparatus

The CSI Release Rate Apparatus used for testing aircraft cabin materials is one of more than thirty flammability testers manufactured by CSI. Check the **CSI catalog** for instruments to test for flame spread, ignition, smoke, etc., that meet ASTM, industry, and government standards.



CSI Custom Scientific Instruments, Inc.
A Subsidiary of Atlas Electric Devices Co.

13 Wing Drive, Cedar Knolls, New Jersey 07927 U.S.A. Phone: (201) 538-8500 Telex: 25-4328

Specialists in Material Testing Instrumentation

Circle Reader Action No. 438

ABOUT THE NASA TECHNOLOGY UTILIZATION PROGRAM

Thumb Index



NASA TU Services



New Product Ideas



Electronic Components and Circuits



Electronic Systems



Physical Sciences



Materials



Computer Programs



Mechanics



Machinery



Fabrication Technology



Mathematics and Information Sciences



Life Sciences



Subject Index

This document was prepared under the sponsorship of the National Aeronautics and Space Administration. NASA Tech Briefs is published quarterly and is free to engineers in U.S. industry and and to other domestic technology transfer agents. It is both a current-awareness medium and a problem-solving tool. Potential products... industrial processes... basic and applied research... shop and lab techniques... computer software... new sources of technical data... concepts... can be found here. The short section on New Product Ideas highlights a few of the potential new products contained in this issue. The remainder of the volume is organized by technical category to help you quickly review new developments in your areas of interest. Finally, a subject index makes each issue a convenient reference file.

Further information on innovations—Although some new technology announcements are complete in themselves, most are backed up by Technical Support Packages (TSP's). TSP's are available without charge and may be ordered by simply completing a TSP Request Card, found at the back of this volume. Further information on some innovations is available for a nominal fee from other sources, as indicated. In addition, Technology Utilization Officers at NASA Field Centers will often be able to lend necessary guidance and assistance.

Patent Licenses—Patents have been issued to NASA on some of the inventions described, and patent applications have been submitted on others. Each announcement indicates patent status and availability of patent licenses if applicable.

Other Technology Utilization Services—To assist engineers, industrial researchers, business executives, Government officials, and other potential users in applying space technology to their problems, NASA sponsors Industrial Applications Centers. Their services are described on pages 28-29. In addition, an extensive library of computer programs is available through COSMIC, the Technology Utilization Program's outlet for NASA-developed software. See special section on computer programs on page 94.

Applications Program—NASA conducts applications engineering projects to help solve public-sector problems in such areas as safety, health, transportation, and environmental protection. Two applications teams, staffed by professionals from a variety of disciplines, assist in this effort by working with Federal agencies and health organizations to identify critical problems amenable to solution by the application of existing NASA technology.

Reader Feedback—We hope you find the information in *NASA Tech Briefs* useful. A reader-feedback card has been included because we want your comments and suggestions on how we can further help you apply NASA innovations and technology to your needs. Please use it; or if you need more space, write to the Manager, Technology Transfer Division, P.O. Box 8757, Baltimore/Washington International Airport, Maryland 21240.

Advertising Reader Service—Reader Action Card (RAC): For further information on the advertisers, please circle the RAC number on the separate Reader Action Card in this issue.

Change of Address—If you wish to have *NASA Tech Briefs* forwarded to your new address, use the Subscription Card enclosed at the back of this volume of *NASA Tech Briefs*. Be sure to check the appropriate box indicating change of address, and also fill in your identification number (T number) in the space indicated.

This document was prepared under the sponsorship of the National Aeronautics and Space Administration. Neither Associated Business Publications, Inc., nor anyone acting on behalf of Associated Business Publications, Inc., nor the United States Government nor any person acting on behalf of the United States Government assumes any liability resulting from the use of the information contained in this document, or warrants that such use will be free from privately owned rights. The U.S. Government does not endorse any commercial product, process, or activity identified in this publication.

Mission **A**ccomplished

Through the technology transfer process, many of the systems, methods and products pioneered by NASA are re-applied in the private sector, obviating duplicate research and making a broad range of new products and services available to the public.

The serene and self-sustaining nature of aquatic life is a subject rarely associated with technology, and in a manner of speaking, the two are diametrically opposed: one represents the natural world and the other, the artificial. Not so with the EcoSphere®, a system that synthesizes the natural and artificial in an aesthetically-pleasing way.

The EcoSphere concept was originally developed by Joe N. Hanson, a scientist at Jet Propulsion Laboratory, as part of a NASA program researching bioregenerative systems capable of sustaining life in the space environment. After investigating the dynamics of microbial ecosystems, Hanson determined that such systems, sealed in one-liter flasks and exposed to light for extended periods, could survive for more than 15 years, a period comparable to that of the same ecosystem in a natural environment.

Eventually, Hanson was able to extend the range of the system to include crustacea and macroalgae. He added tiny shrimp and clusters of algae to his microbial soup, enclosing the entire system in a glass flask.

Loren Acker, president of Engineering and Research Associates, Inc. of Tucson, Arizona, saw one of the prototype flasks during a business visit with a NASA official. He obtained a license for the technology and began producing the EcoSphere in 1983. To date, nearly 4000 EcoSpheres have been produced as a sideline by the company, which also manufactures medical instruments.

In essence, the EcoSphere is a self-



The art of science lives in the EcoSphere.

sustaining aquarium. Its only outside need is a source of light. The algae in the EcoSphere produce oxygen for the six shrimp, who feed on the algae and bacteria. The shrimp, in turn, excrete organic wastes that sustain the bacteria. Finally, the bacteria provide the carbon dioxide and inorganic chemicals that, when combined with light, sustain the algae.

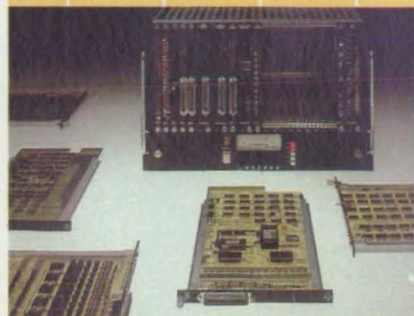
Engineering and Research Associates has isolated a particularly light-tolerant algae for use in its EcoSpheres. Previously, they gathered part of the algae from the wild. "With that," says Acker, "we got all kinds of microscopic creepy crawlers that we couldn't control, so we isolated a specific strain and we grow it in a semi-sterile container.

"What we've basically added beyond the NASA technology," Acker says, "is what we call a synthetic system, that is the ingredients are quite highly predictable and, if you will, recipitated." Recipe in hand, scientists and technicians have succeeded in synthesizing a naturally self-sustaining system in an artificial environment.

It's been said that art imitates life. Perched atop its pedestal, the elegant EcoSphere evokes the art of sculpture, not only imitating life, but sustaining it as well. □

CAMAC

(IEEE-583)



Your Standard Tools for Data Acquisition and Control

For 15 years, KSC has been supplying users in laboratories, plants, and R & D facilities with practical CAMAC (IEEE-583) hardware and software tools for automation. The reason is simple. CAMAC, the international standard for Computer Automated Measurement And Control, provides modular real-time data acquisition and control solutions that can be implemented a step at a time.

CAMAC features . . .

Full Standardization. Specified by the IEEE, ANSI, and IEC.

Open-end Architecture. Start as small as you like and expand when and how you want.

Multicomputer Support. Interfaces for a wide range of computers, such as DEC, CDC, MODCOMP, Gould/SYSTEMS, and Hewlett-Packard.

High Data Rates. Data transfer rates to 348,000 bytes per second with DMA interfaces.

Unsurpassed Selection of Process I/O Modules. From A/D and D/A converters and signal multiplexers to event counters and transient recorders.

Powerful Distributed Systems. Peak block rates up to three million data bytes per second over a fiber optic serial highway to as many as 62 remote stations.

Supporting Software. Easy to use CAMAC handlers, software drivers, and Process Control/Data Base System software packages.

Field-proven System Design. Used in such facilities as Boeing, Nalco Chemical, Kimberley-Clark, Digital, NASA, Bell Labs, Martin Marietta, DuPont, and General Electric.

Join the growing list of users who are specifying our CAMAC tools for their system development. Call us today.

Kinetic Systems Corporation

11 Maryknoll Dr., Lockport, IL 60441
(815) 838-0005
TWX: 910 635 2831





Zero defects at zero gravity.

When you're working on America's first space station, the requirement is zero defects at zero gravity.

Which is why NASA depends on Honeywell Reliability to make advanced space concepts a reality.

Honeywell has played a major role in every one of NASA's manned space missions, from the X15 through Gemini and Apollo, to SkyLab and the Space Shuttle. And now we're working with other leaders in the aerospace industry to engineer critical control systems for life support, power distribution as well as guidance and navigation for NASA's first space station, scheduled for deployment in the mid-1990s.

Honeywell combines advanced technology with reliable performance to ensure America's space program will succeed well into the 21st century—and beyond.

Honeywell Reliability

Together, we can find the answers.

Honeywell

Circle Reader Action No. 364

©1986 Honeywell Inc.

U.S.



PAM EARNS NEW ASTRONAUT WINGS WITH THE U.S. AIR FORCE

The U.S. Air Force Space Division has contracted for 28 McDonnell Douglas PAMs (Payload Assist Modules) to launch a series of Navstar Global Positioning System satellites from the space shuttle.

PAM development began in 1976 as a privately funded commercial venture. It has launched numerous commercial satellites, first from our Delta rocket and more recently from the space shuttle. The PAM-D11 chosen by the Air Force is a new-generation booster with an improved motor capable of lifting a 4200-pound satellite to geosynchronous orbit altitude. The first Air Force PAM-D11 launch is set for 1986 from Kennedy Space Center.

The Navstar satellite system will allow land, sea and air forces from the U.S. and NATO nations to obtain instant three-dimensional navigation information from any point on Earth. Navigation information also will be available for worldwide commercial and private operations such as air traffic control, commercial shipping, and search and rescue.

For more information, write PAM Marketing,
McDonnell Douglas Astronautics Company,
5301 Bolsa Ave., Huntington Beach, CA 92647.

**MCDONNELL
DOUGLAS**